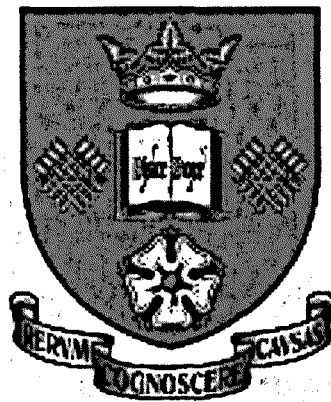


Investigating Spontaneous Sister Chromatid Exchange in Uveal Melanoma

A thesis submitted to the University of Sheffield for the degree of
Doctor of Philosophy



Polly Laura Gravells

Institute for Cancer Studies
School of Medicine and Biomedical Sciences
University of Sheffield

October 2010

**I hereby declare that no part of this thesis has previously been
submitted for any degree or qualification at this, or any other
University or Institute of Learning**

Acknowledgements

Firstly I would like to thank my supervisor Dr. Helen Bryant for her constant support and invaluable advice and guidance for which I am eternally grateful. I would also like to thank Prof. Mark Meuth for his advice and interest in this work. A big thank you goes to all the technicians at ICS particularly, Sarah Bottomley, Janet White, Sheila Blizard for their assistance and friendship, Andy Platts for his help with technical issues and finding my way home, and finally Gary Rodgers for his help with immunofluorescence and the banter!

I would also like to thank everyone who works at ICS past and present but particularly the members of my group, Katie, Rachel and Catherine. Thank you for making my PhD such an enjoyable experience, being there for me through the bad times and laughing with me through the good.

Thank you to all my family for their continued support both financially and emotionally without which this wouldn't have been possible. Mum, thank you for the constant guidance and for having confidence in me when I needed it most. Thank you to all my friends, particularly Hannah, Danielle and Laura; I wouldn't know what to do without you. Finally, I would like to thank Neil for being the constant source of love and support that has got me through over the years. Thank you for putting up with me over the last few months and always believing in me; my success is because of you.

Abstract

Sister chromatid exchange (SCE) occurs during S-phase of the cell cycle and is the physical exchange of genetic information between two sister chromatids. Although it has been used for many years as a marker of mutagenesis and genetic instability, the exact mechanism of SCE formation remains to be elucidated. However, it is known to be an end product of the DSB repair pathway, homologous recombination (HR), and defects in various repair proteins have been associated with altered levels of SCE, we therefore investigated the DNA damage repair response in uveal melanoma, using these cells as a model system for SCE formation.

Uveal melanoma is a rare but aggressive cancer that arises in the uveal tract of the eye affecting the iris, ciliary body and choroid. It is characterised by non-random chromosomal alterations such as monosomy of chromosome 3 that is associated with metastasis and a poor prognosis. However, random chromosomal aberrations are rare suggesting that these tumours have low genetic instability. In addition these tumours have been found to have reduced levels of spontaneous SCE, which is also consistent with low genetic instability. In general, cancer is associated with high genetic instability and high SCE; this is therefore the only disease state known to date to exhibit this low SCE phenotype.

Here, we have found that uveal melanoma cells have high levels of spontaneous DNA damage consistent with a defect in repair. Furthermore, endogenous HR is reduced and we postulate that it is caused by a reduction in the expression of the FA protein FANCD2, and that this defect causes the reduced SCE frequency in these cells. Consistent with this, complementing uveal melanoma cell lines with FANCD2 restores the spontaneous levels of SCE.

In addition, we have shown that the high chemo-resistance of uveal melanoma to interstrand cross-link inducing agents such as Mitomycin C is due to a defect in metabolism rather than a defect in DNA repair.

Abbreviations

A	Adenine
ADP	Adenosine Diphosphate
APH	Aphidicolin
APS	Ammonium Persulphate
AP site	Apurinic or Apyrimidinic site
ATM	Ataxia Telangiectasia Mutated
ATP	Adenosine Triphosphate
ATR	ATM and Rad3 Related
BACH1	BRCA1 Associated C-terminal Helicase 1
BER	Base Excision Repair
BLAP75	Bloom Associated Protein of 75 kDa
BLM	Bloom
bp	Base Pairs
BRCA1/2	Breast Cancer Susceptibility gene 1 or 2
BrdU	5-bromodeoxyuridine
BRIP1	BRCA1 Interacting Protein 1
BS	Bloom's Syndrome
BSA	Bovine Serum Albumin
C	Cytosine
CDK4/6	Cyclin Dependent Kinase 4 or 6
cDNA	Complementary DNA
Chk1	Checkpoint Protein 1
CHO	Chinese Hamster Ovary
CIS	Cisplatin
CPDs	Cyclobutane Pyrimidine Dimers
CpG site	Cytosine and Guanine Bases Separated by a Phosphate
CPT	Camptothecin
CSA	Cockayne's syndrome complementation group A
CSB	Cockayne's syndrome complementation group B
CtIP	Retinoblastoma Binding Protein 8
CY3	Fluorochrome Excitation 554 nm, Emission 568 nm (Red)

Cyclin D	Cell Cycle Regulator Encoded by <i>CCND1</i> Gene
CYP450R	Cytochrome P450 Reductase
DAPI	4',6-diamidino-2-phenylindole excitation 350 nm, emission 470 nm
dATP	Deoxyadenosine Triphosphate
dCTP	Deoxycytidine Triphosphate
ddH₂O	Double Distilled Water
DEPC	Diethylpyrocarbonate
dGTP	Deoxyguanosine Triphosphate
D-Loop	Heteroduplex Structure formed during HR
DMEM	Dulbecco's Modified Eagle Medium
DMSO	Dimethyl Sulphoxide
DNA	Deoxyribonucleic Acid
DNA-PK	DNA-Dependent Protein Kinase
DNA-PK_{cs}	DNA-Dependent Protein Kinase Catalytic Subunit
dNTP	Deoxyribonucleotide Triphosphate
DOC	Sodium Deoxycholate
DSB	Double-Strand Break
DSBR	Double-Strand Break Repair
dsDNA	Double-stranded DNA
dT	Thymidine
DTD	DT-Diaphorase (also known as NQO1)
DTT	Dithiothreitol
dTTP	Deoxythymidine Triphosphate
E1	Ubiquitin-activating enzyme
E2	Ubiquitin-conjugating enzyme
E2F	E2 Transcription Factor
E3	Ubiquitin protein ligase
<i>E. coli</i>	<i>Escherichia coli</i>
ECL	Enhanced Chemiluminescence
EDTA	Ethylene-Diamine-Tetra-acetic Acid
EME1	Essential Meiotic Endonuclease 1 Homolog 1

ERCC1	Excision repair cross-complementing rodent repair deficiency, complementation group 1
ES cells	Embryonic Stem Cells
Exo1	Exonuclease 1
FA	Fanconi Anaemia
FAAP24	Fanconi Anaemia Associated Protein 24 kDa
FAAP100	Fanconi Anaemia Associated Protein 100 kDa
FACS	Fluorescence-Activated Cell Sorting Analysis
FANCA/B/C	Fanconi Anaemia Complementation Group A, B or C
FANCD1/D2	Fanconi Anaemia Complementation Group D1 or D2
FANCD2S/L	FANCD2 Short (155 kDa) or Long (166 kDa) Isoforms
FANCE/F/G	Fanconi Anaemia Complementation Group E, F or G
FANCI/J	Fanconi Anaemia Complementation Group I or J
FANCM/N	Fanconi Anaemia Complementation Group M or N
FCS	Foetal Calf Serum
FEN1	Flap Endonuclease 1
FHIT	Fragile Histidine Triad
FISH	Fluorescent <i>In Situ</i> Hybridisation
FITC	Fluorescein Isothiocyanate, excitation 490 nm, emission 525 nm
g	Gram
G	Guanine
G1	Gap 1 Phase
G2	Gap 2 Phase
G418	Geneticin®
GAPDH	Glyceraldehyde 3-Phosphate Dehydrogenase
GEN1	Gen Homolog 1, Endonuclease
GG-NER	Global Genome Nucleotide Excision Repair
GMP	Guanine Monophosphate
GTP	Guanine Triphosphate
GY	Grays
h	Hours
H₂A.X	H2A Histone Family, Member X

H₂O₂	Hydrogen Peroxide
HCl	Hydrogen Chloride
hHR23B	Human RAD23 Yeast Homolog, B
HO[•]	Hydroxyl Radicals
HPRT	Hypoxanthine-guanine Phosphoribosyltransferase
HR	Homologous Recombination
HRP	Horseradish Peroxidase
HU	Hydroxyurea
ICL	Interstrand Cross-Link
IF	Immunofluorescence
IgG	Immunoglobulin
IR	Ionising Radiation
J/M²	Joules per Metre squared
K	Lysine Residue
Kb	Kilobases
KCl	Potassium Chloride
kDa	Kilodaltons
KU70	Ku Autoantigen p70 Subunit
KU80	Ku Autoantigen p80 Subunit
L	Litre
L32	Ribosomal Protein L32
LIGI	DNA Ligase I
LIGIII	DNA Ligase III
LIGIV	DNA Ligase IV
min	Minute
M	Molar
mA	Milliamps
MCRA	Bacterial MMC Resistance Associated Protein
MEFs	Mouse Embryonic Fibroblasts
mg	Milligrams
MgCl₂	Magnesium Chloride
MgSO₄	Magnesium Sulphate

ml	Millilitres
MLH1	MutL Homolog 1
mm	Millimetres
mM	Millimolars
MMC	Mitomycin C
MMR	Mismatch Repair
MMS	Methyl-methanesulfonate
M Phase	Mitosis Phase
MRE11	Meiotic Recombination 11 Homologue A
MRN	MRE11-Rad50-NBS1 Complex
mRNA	Messenger RNA
MSH2/3/6	MutS Homolog 2, 3 or 6
MTT	3-[4, 5-Dimethylthiazol-2-yl]-2, 5-Diphenyltetrazolium Bromide
MUS81	MUS81 Endonuclease Homolog
MutS	DNA Mismatch Repair Protein MutS
MutL	DNA Mismatch Repair Protein MutL
Na₂Ca₃	Sodium Carbonate
NaCl	Sodium Chloride
NAD(H)	Nicotinamide Adenine Dinucleotide
NADPH	Nicotinamide Adenine Dinucleotide Phosphate
NBS1	Nijmegen Breakage Syndrome 1
NER	Nucleotide Excision Repair
ng	Nanograms
NHEJ	Non-Homologous End-Joining
nm	Nanometres
nM	Nanomolars
nt	Nucleotide Length
NQO1	NAD(P)H Dehydrogenase, Quinone 1 (also known as DT-Diaphorase)
O₂⁻	Superoxide
OD	Optical Density
P	Passage
P16	Cyclin-Dependent Kinase Inhibitor p16

P53	Tumour Protein p53
PAGE	Polyacrylamide Gel Electrophoresis
PAHs	Polycyclic Aromatic Hydrocarbons
PALB2	Partner and Localizer of BRCA2
PARP-1	Poly [ADP-ribose] Polymerase 1
PBS	Phosphate Buffered Saline
PCNA	Proliferating Cell Nuclear Antigen
PCR	Polymerase Chain Reaction
PFA	Paraformaldehyde
pg	Picograms
pH	Potentiometric Hydrogen Ion Concentration
PHD	Plant Homeo Domain
PI	Propidium Iodine
PIP	PCNA-Interacting-Protein
PLK1	Polo-Like Kinase 1
PMS1/2	Postmeiotic Segregation Increased 1 or 2
PMSF	Phenylmethylsulfonyl Fluoride
POL	DNA Polymerase
pRb	Retinoblastoma Protein
PRPP	Phosphoribosyl Pyrophosphate
p.s.i	Pound-Force per Square Inch
RAD6/18	Radiation Sensitive Protein 6 & 18
RAD50/51	Radiation Sensitive Protein 50 & 51
RAD51B/C/D	RAD51 Homolog B, C or D
RAD52/54	Radiation Sensitive Protein 52 or 54
RASSF1	Ras Association Domain-Containing Protein 1
REV1/3/7	Deoxycytidyl Transferase 1, 3 or 7
RNA	Ribonucleic Acid
RNase	Ribonuclease
rNTPs	Ribonucleotide Triphosphates
ROS	Reactive Oxygen Species
RPA	Replication Protein A

rpm	Revolutions per Minute
RT	Reverse Transcriptase
RTEL	Regulator of Telomere Elongation Helicase 1
S	Second
S-Phase	DNA Synthesis Phase
SCE	Sister Chromatid Exchange
<i>S. cerevisiae</i>	<i>Saccharomyces cerevisiae</i>
SDS	Sodium Dodecyl Sulphate
SiRNA	Short-interfering RNA
<i>S. pombe</i>	<i>Schizosaccharomyces pombe</i>
SOB	Super Optimal Broth
SSA	Single-Strand Annealing
SSB	Single-Strand Break
SSBR	Single-Strand Break Repair
ssDNA	Single-Stranded DNA
T	Thymine
TBE	Tris/Borate/EDTA
TBS	Tris-Buffered Saline
TC-NER	Transcription-Coupled Nucleotide Excision Repair
TdT	Terminal Deoxynucleotidyltransferase
TE Buffer	Tris-EDTA Buffer
TEMED	N,N,N,N -Tetramethyl-Ethylenediamine
TFIIH	Transcription Factor IIH
TLS	Translesion Synthesis
TM	Tail Moment
U	Uracil
UAF1	Usp1 Associated Factor 1
UBE2T	Ubiquitin-Conjugating Enzyme E2 T
USP1	Ubiquitin Carboxyl-Terminal Hydrolase 1
UTP	Uridine Triphosphate
UV	Ultra-Violet
VSV-G	Vesicular Stomatitis Virus G

XPA/B/C	Xeroderma Pigmentosum Group A, B or C
XPD/F/G	Xeroderma Pigmentosum Group D, F or G
XRCC1/2/3/4	X-ray Cross-Complementating 1, 2, 3 or 4
µg	Micrograms
µl	Microlitres
µM	Micromolars
2,7,DAM	2, 7-diaminomitose
6-TG	6-Thioguanine
8-oxoG	7,8-dihydro-8-oxoguanine
8-OH-dG	8-hydroxydeoxyguanosine

Contents Page

Chapter 1 – Introduction.....	1
1.1 Introduction.....	3
1.2 DNA Damage.....	3
1.3 DNA Repair Pathways.....	6
1.4 Sister Chromatid Exchange.....	30
1.5 Uveal Melanoma.....	43
1.6 Aims of this Study.....	47
Chapter 2 – Materials and Methods.....	49
2.1 Materials.....	53
2.2 Methods.....	65
Chapter 3 – Characterisation of Uveal Melanoma Cell Lines.....	100
3.1 Introduction.....	102
3.2 Differences in proliferation rate are not responsible for the reduced spontaneous SCE frequency in uveal melanoma.....	103
3.3 Uveal melanoma cell lines have increased levels of endogenous DNA damage indicative of a defect in DNA repair.....	105
3.4 Endogenous levels of HR are reduced in uveal melanoma cell lines....	108
3.5 TLS and MMR are not upregulated in uveal melanoma cell lines.....	110
3.6 Uveal melanoma cell lines have reduced <i>FANCD2</i> gene and protein expression.....	111
3.7 Uveal melanoma cell lines have reduced LIGIV protein expression.....	120
3.8 Discussion.....	121

Chapter 4 – Complementation of FANCD2 in a uveal melanoma cell line corrects the reduced SCE phenotype.....	125
4.1 Introduction.....	127
4.2 Generation of a uveal melanoma cell line complemented with pMMP-FANCD2.....	128
4.3 Complementation of a uveal melanoma with FANCD2 increases spontaneous levels of SCE.....	131
4.4 Endogenous HR is increased in a uveal melanoma cell line complemented with FANCD2.....	134
4.5 Complementation of the uveal melanoma cell line, 196b with FANCD2 reduces the level of endogenous DNA damage.....	136
4.6 Observation: Following long-term culture, uveal melanoma cell lines gain FANCD2 expression and exhibit increased levels of spontaneous SCE.....	138
4.7 Discussion.....	140
Chapter 5 – Characterisation of the induced DNA damage response in uveal melanoma.....	142
5.1 Introduction.....	144
5.2 Uveal melanoma cell lines have increased resistance to thymidine and the ICL-inducing agents MMC and cisplatin.....	145
5.3 FANCD2 is activated at a lower level in response to MMC induced damage.....	150
5.4 HR is induced at a lower level in response to MMC induced damage in uveal melanoma cell lines.....	154
5.5 MMC induces less DNA damage in uveal melanoma cell lines compared to WM793 and MRC5VA control cell lines.....	158
5.6 MMC induces fewer DNA ICLs in uveal melanoma cell lines.....	161
5.7 CYP450R required for MMC metabolism is reduced in uveal melanoma cell lines, thus causing the observed resistance to MMC.....	164

5.8 The defect in FANCD2 in uveal melanoma is not associated with the resistance to MMC.....	166
5.9 Discussion.....	172
Chapter 6 – Discussion.....	175
6.1 Introduction.....	176
6.2 Decreased FANCD2 is associated with decreased spontaneous SCE frequency in uveal melanoma.....	176
6.3 Decreased levels of endogenous HR may be associated with decreased spontaneous SCE through the role of FANCD2 in the repair of endogenous damage.....	177
6.4 Types of endogenous DNA damage in uveal melanoma.....	180
6.5 Postulated involvement of NHEJ in the repair of endogenous DNA damage in uveal melanoma.....	181
6.6 Resistance to ICL-inducing agents in uveal melanoma is caused by a lack of CYP450R.....	183
6.7 Methylation events in uveal melanoma.....	186
6.8 How do uveal melanoma cells survive?.....	189
References.....	192
Appendix 1.....	216
Appendix 2.....	217
Appendix 3.....	218
Appendix 4.....	219

Chapter 1 – Introduction

1.1	Introduction	3
1.2	DNA Damage	3
1.2.1	Endogenous Damage.....	3
1.2.2	Exogenous Damage.....	5
1.3	DNA Repair Pathways	6
1.3.1	Repair of Base Damage.....	6
1.3.1.A	Base Excision Repair (BER).....	6
1.3.1.B	Nucleotide Excision Repair (NER).....	7
1.3.1.C	Mismatch Repair (MMR).....	8
1.3.1.D	Translesion Synthesis (TLS).....	10
1.3.2	Double Strand Break Repair (DSBR)	11
1.3.2.A	Non-Homologous End-Joining (NHEJ).....	12
1.3.2.A.1	PARP-1 Dependent End-Joining (Alternative NHEJ)	14
1.3.2.B	Homologous Recombination (HR)	14
1.3.2.B.1	Two-Ended Repair	15
1.3.2.B.2	Single Strand Annealing (SSA).....	17
1.3.2.B.3	One-Ended Repair	18
1.3.3	Fanconi Anaemia (FA) Pathway.....	19
1.3.3.A	Regulation of the FA Pathway	22
1.3.3.B	Activation of the FA Pathway.....	23
1.3.3.C	FANCD2 and Cancer	25
1.3.4	Interstrand Cross-link (ICL) Repair	25
1.3.5	MMC Metabolism.....	29
1.4	Sister Chromatid Exchange (SCE).....	30
1.4.1	DNA Repair Proteins and SCE	37
1.4.2	SCE and Disease	40
1.4.2.A	Fanconi Anaemia (FA).....	40
1.4.2.B	Bloom Syndrome (BS).....	41
1.4.2.C	Cancer Predisposition.....	41
1.5	Uveal Melanoma	43

1.5.1	Uveal Melanoma as a Model System for SCE.....	44
1.5.1.A	Established Uveal Melanoma Cell Lines	47
1.5.1.B	Short-Term Cultures (Primary Samples).....	47
1.6	Aims of this Study	47

List of Figures

Figure 1.1	Model of the NHEJ repair pathway for the repair of DSBs.....	13
Figure 1.2	Models of HR for the repair of two-ended DSBs.....	17
Figure 1.3	HR at a collapsed replication fork (one-ended repair).....	19
Figure 1.4	The structure of the FA pathway.....	22
Figure 1.5	Model of mammalian ICL repair.....	28
Figure 1.6	SCE detection by BrdU incorporation and Hoescht 33 258 staining.....	32
Figure 1.7	Replication bypass model by Shafer (1977).....	33
Figure 1.8	DNA topoisomerase II subunit exchange model by Pommier et al. (1985)..	35
Figure 1.9	Recombinational model of SCE formation by Kato (1977).....	36
Figure 1.10	Replication model of SCE formation by Ishii and Bender (1980) and Painter (1980).....	37
Figure 1.11	Representative image of the number of spontaneous SCE in a primary uveal melanoma tumour and matched patient blood sample.....	46

List of Tables

Table 1.1	Comparison of SCE frequencies in different human cell types taken from the literature.....	30
Table 1.2	The induction of SCEs by various DNA damaging agents.....	31
Table 1.3	Repair proteins involved in altered spontaneous SCE frequencies taken from the literature.....	38
Table 1.4	SCE frequencies in human sporadic and hereditary cancers.....	42
Table 1.5	SCE frequencies in established uveal melanoma cell lines.....	45
Table 1.6	SCE frequencies in primary uveal melanoma tumour and matched patient blood samples.....	45

1.1 Introduction

Genomic stability is essential for cell survival. DNA is constantly exposed to endogenous and exogenous sources of DNA damage, so the cell employs numerous repair processes to deal with this damage and ensure that faithful replication and transcription of the genome continues. Genomic instability is a consequence of inefficient DNA repair and is a hallmark of tumourigenesis. It is characterised by increased chromosomal aberrations and sister chromatid exchanges (SCEs) in many types of cancer. SCE is the physical exchange of genetic information between two sister chromatids during replication. Although SCE can be used as a marker of mutagenic potential and chromosome stability, the mechanism of SCE formation is largely unknown. This chapter will discuss the theories of SCE formation, the cellular DNA repair responses to endogenous and exogenous DNA damage and the use of uveal melanoma as a model system for studying SCE formation.

1.2 DNA Damage

1.2.1 Endogenous Damage

Within the cell, DNA continually reacts with the surrounding oxygen and water giving rise to spontaneous DNA lesions. Without the DNA repair processes, these lesions would be lethal to the cell, by causing replication and transcription blockage. Although all the primary components of DNA are susceptible to oxidative and hydrolytic reactions, the majority of spontaneous lesions arise from the deamination, modification and hydrolysis, leading to the loss of the DNA bases; all of which will be discussed below.

The deamination of the bases cytosine, adenine, guanine and 5-methylcytosine to uracil, hypoxanthine, xanthine and thymine respectively is the most prevalent endogenous DNA lesion (Lindahl, 1993). Deamination of 5-methylcytosine produces thymine and results in the formation of T·G mispairs. Similarly, hypoxanthine can pair with cytosine during DNA replication causing A·T - G·C transitions (Lindahl, 1979). Cytosine can also be deaminated to uracil, a common component of RNA that is easily identified as foreign in DNA. Such damage would induce DNA repair pathways such as base excision repair (BER), mismatch repair (MMR) and translesion synthesis (TLS), thus these pathways are essential to ensure cell survival.

In addition to deamination processes, base modifications are a common source of endogenous DNA damage. Reactive oxygen species (ROS) such as hydrogen peroxide (H_2O_2), superoxide (O_2^-) and hydroxyl radicals (HO^\bullet) are constantly generated as by-products of normal cellular metabolism and are a major source of damage to all intracellular macromolecules especially nucleic acids, proteins and lipids. ROS attack on the sugar residues of DNA can lead to single strand breaks (SSBs) (Mello Filho and Meneghini, 1984) and base modifications. Guanine is particularly susceptible to modification by ROS, producing 7,8-dihydro-8-oxoguanine (8-oxoG) that causes mispairing with adenine (Cadet et al., 2003). During replication persistent SSBs can also be converted to double-strand breaks (DSBs) and thus, as well as the SSB repair pathways, ROS can also induce homologous recombination (HR) and potentially non-homologous end-joining (NHEJ), although this is a rare event (Lindahl, 1993).

ROS can also cause modification of the DNA bases through its attack on unsaturated lipids generating lipid hydroperoxides such as malondialdehyde. Malondialdehyde can react with DNA, resulting in the formation of bulky adducts to adenine, cytosine and guanine, and can lead to the generation of DNA-protein cross-links and interstrand cross-links (ICLs) between cytosine and guanine residues on opposite strands of the DNA duplex (Nair et al., 1986; Niedernhofer et al., 2003). Although this type of endogenous damage is rare, they are highly toxic and may require the coordination of a number of DNA repair pathways such as nucleotide excision repair (NER), the Fanconi Anaemia (FA) pathway, HR and TLS for efficient repair.

Finally, hydrolytic reactions can cause loss of the DNA bases that are primarily recognised and repaired by BER. The cellular environment and structural composition of DNA make it a common substrate for hydrolytic reactions. A common site for such reactions is the N-glycosyl bond between the sugar-phosphate backbone and the DNA bases. The hydrolytic cleavage of the N-glycosyl bond leaves the sugar-phosphate backbone intact, but results in the loss of the DNA base. Although all bases can be lost, it more commonly occurs at purine sites. The loss of the base produces either an apurine or apyrimidine abasic (AP) site, the consequences of which have obvious genetic implications.

Finally, in addition to DNA modifications, endogenous DNA damage can result from errors that occur during replication. Replication slippage during the replication of repetitive sequences or during recombination causes DNA polymerases to mispair nucleotides. In this case the cell employs MMR to remove the affected base and ensure continued replication.

1.2.2 Exogenous Damage

As well as the constant attack on DNA from endogenous cellular metabolism and replication errors, damage can be induced by a wide variety of environmental mutagens, to which we are constantly exposed. These exogenous sources of DNA damage can cause a number of different lesions that are repaired by specific DNA repair pathways. Firstly, similarly to endogenous damage, DNA can be altered through the induction of oxidative damage induced from exogenous sources. UVB (290-320 nm) and the less carcinogenic UVA (320-400 nm) components of ultra-violet (UV) light for example, can induce DNA damage by the generation of active oxygen species (Kuluncsics et al., 1999). Furthermore, it is thought that cytotoxic chemicals such as Benzo[α]pyrene in cigarette smoke and Aflatoxin B₁, a toxic fungal metabolite found in foodstuffs such as cereal, spices, nuts and dried fruit, can modify DNA (Asami et al., 1997; Shen et al., 1996). Finally, ionising radiation (IR) can alter DNA structure through the interaction of DNA with hydroxyl radicals. IR occurs naturally within the environment as cosmic rays from the solar system and radioactive material within the Earth's crust. Furthermore, manmade products such as X-rays and CT scanners emit IR. SSBs, base lesions, sugar modifications and AP sites can all be produced from exposure to IR.

As well as inducing oxidative damage, IR can directly ionise DNA causing DSBs. The ability of cells to repair DSBs induced by IR decreases with the density of the ionising radiation (Jenner et al., 1993), thus IR can lead to chromosome aberrations, cell death and cancer.

Finally, DNA intra- and interstrand cross-links can be induced from a range of environmental mutagens. DNA intra-strand cross-links are highly stable lesions that can disrupt both transcription and replication, thus promoting cancer if left unrepaired

(Mitchell et al., 1985). These lesions cause a covalent link between proximal pyrimidines, most commonly thymine bases, on the same DNA strand. The most common source of such lesions comes from the everyday exposure to UV radiation (sunlight) although polycyclic aromatic hydrocarbons (PAHs) found in food can also result in these lesions. In addition to intra-strand cross-links, ICLs can also be induced. These lesions are the most toxic of all DNA lesions as they produce a covalent link between the two strands of the DNA duplex blocking replication and transcription and thus the agents that induce such lesions have been used successfully as chemotherapeutics to induce cell death. The natural anti-tumour antibiotic mitomycin C (MMC) and the platinum-based compound cisplatin are two such agents that have been used extensively as chemotherapeutics for many years. MMC generates ICLs between cytosine and guanine residues on opposite strands of the DNA duplex, whereas cisplatin forms ICLs between two guanine residues. In addition to these ICLs, these compounds also form intra-strand cross-links between guanine residues on the same strand, DNA adducts by monofunctional alkylation and DNA-protein cross-links (Fichtinger-Schepman et al., 1985; Tomasz et al., 1987). Although ICL-inducing agents are highly effective chemotherapeutics, any cytotoxic chemical that can induce DNA damage and cause replication inhibition has the potential to be used as a chemotherapeutic agent.

1.3 DNA Repair Pathways

1.3.1 Repair of Base Damage

SSBs can arise from a wide range of endogenous and exogenous sources that cause damage to one of the DNA strands either by altering DNA structure or through replication errors. If unrepaired, SSBs can block transcription and replication, and persist to be converted into potentially lethal DSBs during replication (see Section 1.3.2). There are therefore a number of repair pathways that deal with the specific lesions that arise from this type of DNA damage.

1.3.1.A Base Excision Repair (BER)

BER is probably the most frequently used DNA repair pathway and guards against the many types of damage that can alter DNA base structures. This type of damage arises mainly from the by-products of many endogenous cellular processes such as

deamination, methylation and hydroxylation but can also arise from exogenous sources such as IR and some induced oxidative damage.

The excision of the damaged base is initiated by a variety of DNA glycosylases, specific to the type of lesion. The relevant glycosylase catalyses the hydrolysis of the N-glycosyl bond holding the chemically altered base to the deoxyribose-phosphate backbone (Cunningham, 1997). The removal of these bases generates AP sites that are then recognised specifically by AP endonucleases. These endonucleases produce an incision at the AP site through the hydrolysis of the phosphodiester bond 5' to the affected base, resulting in the formation of a 5' terminal deoxyribose-phosphate residue that is subsequently removed by a DNA-deoxyribosephosphodiesterase (dRpase) to form a single nucleotide gap. In addition, some DNA glycosylases possess AP lyase activity that can cleave DNA 3' to the AP site and require a 3' phosphodiesterase to generate the single nucleotide gap (Hazra et al., 1998).

Subsequent repair of the resulting single nucleotide gap involves DNA synthesis and ligation of the DNA backbone. DNA polymerase β (Pol β) is the main polymerase in mammalian cells to incorporate a newly synthesised base into the nucleotide gap (Sobol et al., 1996). Following this, the remaining nick is ligated by either DNA Ligase (Lig) I or III. This mechanism of action is known as short patch repair and is the most dominant BER pathway in mammalian cells. Long-patch repair can also occur, and involves the additional proteins Pol δ , Pol ϵ and PCNA to synthesise several nucleotides at the single nucleotide gap. Strand displacement results, and this is removed by the flap endonuclease Fen1. The utilisation of either the short-patch or long-patch repair pathway is influenced by a number of factors, including the particular DNA glycosylase activity and the type of initial lesion (Fortini et al., 1999).

1.3.1.B Nucleotide Excision Repair (NER)

NER deals with the wide variety of helix distorting lesions that can disrupt base pairing and inhibit transcription. Many of these lesions arise from exogenous sources such as UV-induced cyclobutane pyrimidine dimers (CPDs) and PAHs found in food but they can also arise endogenously from oxidative damage. Furthermore, it is postulated that

NER has a role in the initial stages of ICL repair that involves the excision of the cross-link prior to repair by other repair pathways (see Section 1.3.4).

NER can be split into two subpathways that differ only in the way in which the lesion is initially recognised, Global Genome NER (GG-NER) and Transcription Coupled NER (TC-NER). In humans, GG-NER recognises lesions that arise in non-transcribed DNA by the GG-NER specific complex XPC-hHR23B that binds to regions of distorted DNA and recognises disrupted base pairing (Sugasawa et al., 2001). The XPB and XPD helicases of the multi-subunit transcription factor TFIIH subsequently unwind the DNA for approximately 30 bp surrounding the damaged site, creating a bubble-like structure (Evans et al., 1997). This structure is stabilised by the binding of the single stranded binding protein RPA to the undamaged DNA strand (Wang et al., 2000). The two endonucleases XPG and ERCC1/XPF are recruited to the damaged site by XPA where they cleave 3' and 5' of the opened structure respectively, creating a 24 – 32 base oligonucleotide containing the damaged bases (de Laat et al., 1998). Once removed, the resulting gap is filled by the DNA polymerases POL δ and POL ϵ , stabilised by PCNA. Finally, the nick between the newly synthesised and existing DNA strand is joined by Lig I (de Laat et al., 1999) or Lig III (Moser et al., 2007).

TC-NER differs from GG-NER in that it recognises lesions in actively transcribed DNA. Therefore any lesion in the transcribed strand that blocks RNA polymerase II can activate this pathway and thus the XPC-hHR23B complex is not required (van Hoffen et al., 1995). The proteins CSB and CSA displace the stalled polymerase allowing repair to take place through the same downstream mechanism as described for GG-NER (Le Page et al., 2000).

1.3.1.C Mismatch Repair (MMR)

MMR is a highly conserved DNA repair pathway that has an important role in maintaining genomic stability hence defects in this repair pathway are a common factor in promoting oncogenesis. MMR removes nucleotides that have been mispaired by DNA polymerases either as a result of DNA replication slippage of repetitive sequences or during recombination. As MMR is highly conserved between species, mammalian MMR involves multi-member families of the *Escherichia coli* (*E. coli*) prototype factors

MutS and MutL (Kolodner and Marsischky, 1999). In humans, mismatch recognition is carried out by the MSH2 protein that forms a heterodimer with either MSH6 (hMutS α) or MSH3 (hMutS β) depending on whether base to base mismatches (MSH6) or insertion/deletion loops (MSH3) are to be repaired (Drummond et al., 1995; Palombo et al., 1996). Biochemical studies have shown that mismatched DNA produces ATP. This induces a conformational change in the MSH2/MSH6 complex that converts it into a sliding clamp that is capable of moving along the DNA backbone (Gradia et al., 1999). Whilst ATP binding and hydrolysis is dispensable for mismatch recognition, it may facilitate subsequent protein-protein interactions (Blackwell et al., 1998). Upon a second ATP dependent step the MutL homolog, MLH1 forms heterodimers with both PMS1 (MutL α) and PMS2 (MutL β) and interacts with the MSH complexes allowing translocation along the DNA bidirectionally and the subsequent recognition of mismatching events (Genschel and Modrich, 2003).

Once the mismatch event has been identified it is excised by the 5' to 3' exonuclease Exo1, shown in *Saccharomyces cerevisiae* (*S. cerevisiae*) to interact with Msh2 (Sancar and Hearst, 1993). The resulting single strand gap is stabilised by RPA (Ramilo et al., 2002) allowing the resynthesis of the excised strand by Pol δ stabilised by PCNA. In human cells it has been found that in addition to resynthesis, PCNA interacts with both MutS and MutL homologs (Gu et al., 1998). Furthermore, mutations in PCNA in yeast increase frameshift mutations in repeated sequences through MMR (Kokoska et al., 1999), suggesting a role for PCNA in the recognition of the initial mismatching event prior to the excision step.

In addition to replication errors, base mismatching can also arise as a result of the pairing of non-complementary sequences during HR and can lead to translocations and deletions, potentially causing cancer. The MMR proteins therefore have a role in the suppression of HR, when these mismatches occur, to ensure that HR is an error-free process. HR involves the pairing of complementary single strands, from two different duplexes, resulting in a heteroduplex structure that can then be resolved to form either a SCE or gene conversion event (see Section 1.3.2.B). It is mismatches in this heteroduplex intermediate resulting from non-complementary sequences that can be recognised and processed by the MMR proteins. Studies in prokaryotic and lower

eukaryotic systems have shown that MutS and MutL homologs are involved in a mechanism to reverse strand exchange in the presence of low levels of complementation (Surtees et al., 2004). In humans, MLH1 complexes are involved in the fidelity control of divergent DNA sequences during recombinational processes (Siehler et al., 2009).

1.3.1.D Translesion Synthesis (TLS)

TLS is a post-replicative repair pathway that ensures the continuation of DNA synthesis in the presence of DNA damage. DNA damage that alters base structure such as CPDs and endogenous modifications block the progression of the replication fork, as DNA polymerases are unable to replicate past the lesion. To overcome this, the cell utilises specialised low fidelity DNA polymerases to bypass the lesion and restart replication. Using this system the lesion is not actually repaired, the damage is simply tolerated, ensuring the continual replication of the genome.

The DNA polymerases utilised in TLS belong to the Y-family polymerases which, in contrast to replicative polymerases, have low processivity with low fidelity. Due to the open structure of their active sites, they can bind to altered DNA bases and complete the synthesis opposite the affected base. The unspecific nature of these polymerases results in less stringent base pairing and thus this process often results in point mutations and increased mutagenesis. There are two Y-family polymerases in *E. coli* (polIV and polV), two in *S. cerevisiae* (Pol η and Rev1) and four in mammalian cells (Pol η , Pol ι , Pol κ and Rev1). In addition, the B-family polymerase Pol ζ has been implicated in TLS in eukaryotes. The diverse range of TLS polymerases ensures the bypass of the many different types of lesions that can disrupt replication. In eukaryotes, it has also been postulated that they have a further role in the repair of DNA ICLs (See Section 1.3.4).

TLS was first observed in *E. coli* where it was found that a NER mutant produced gaps in the nascent strand opposite UV-induced thymine dimers, suggesting that replication was able to restart downstream of the lesion (Bridges and Sedgwick, 1974). This process was subsequently found to be dependent on the bacterial SOS response (Radman, 1975) whereby the expression of both the *DinB* and *UmuDC* operon encoding the two TLS polymerases PolIV and PolV respectively were induced.

In eukaryotes, TLS has been extensively studied in the budding yeast *S. cerevisiae* and has been found to be mediated by the *RAD* genes. Rad6 forms a stable complex with Rad18 (Bailly et al., 1994), that displays ubiquitin conjugation, single-stranded DNA (ssDNA) binding, ATPase activities (Bailly et al., 1997) and physically interacts with Pol30 (PCNA) (Hoege et al., 2002). There are two subpathways of the Rad6-Rad18 pathway, an error-prone pathway involving the *REV* genes that encode the non-essential DNA polymerases (Pol η and Rev1) to bypass replication blocks (polymerase switching), and an error-free process involving the Mms2-Ubc13-Rad5 complex that is capable of restarting replication further downstream of the blocking lesion, using recombinational repair (strand exchange) to complete the synthesis of the resulting gap (template switching) (Broomfield et al., 2001). The ubiquitination of PCNA has an essential role in the control of these two sub-pathways. The TLS polymerases colocalise with PCNA during normal replication and following DNA damage that stalls replication forks, PCNA is monoubiquitinated by the ubiquitin-conjugating activity of the Rad6-Rad18 complex (Hoege et al., 2002). Additional ubiquitination can then occur through the ubiquitin activity of the Mms2-Ubc13-Rad5 complex. It was therefore postulated that monoubiquitination of PCNA promotes polymerase switching whereas polyubiquitination results in template switching and error-free bypass (Hoege et al., 2002). These results have been paralleled in mammalian and human cells (Kannouche and Lehmann, 2004; Watanabe et al., 2004) although the process is less well understood and is likely to be more complex.

1.3.2 Double Strand Break Repair (DSBR)

DSBs are a common form of DNA damage that can arise from any exogenous or endogenous source that is able to break both strands of the DNA duplex. Endogenously, metabolic products and ROS can cause a DSB; exogenously they can be induced by IR causing clusters of ROS that in turn create a DSB. Furthermore, during replication unrepaired SSBs can persist, collapsing the replication fork and generating a DSB. In eukaryotes, there are two major pathways for the repair of DSBs, HR and NHEJ. HR is primarily active during late S and G2 phase of the cell cycle when a sister chromatid is readily available for recombinational repair, whereas NHEJ predominantly occurs throughout G1. The exact factors that govern the use of each pathway remain to be elucidated, although cell cycle status is thought to have a major influence, controlled by

CtIP phosphorylation. In humans it has been found that mammalian CtIP becomes phosphorylated during S-phase and that this phosphorylation is required for the initial resectioning of the DSB during HR (Yun and Hiom, 2009). As CtIP is not required for NHEJ, it has been proposed that the phosphorylation of CtIP governs the initiation of HR during S/G2 phase and thus the use of each DSB pathway in a cell-cycle dependent manner (Yun and Hiom, 2009).

1.3.2.A Non-Homologous End-Joining (NHEJ)

NHEJ involves the binding and re-ligation of two broken DNA ends that often results in the loss of genetic information hence it is a fast but often error-prone mechanism of repair. Within seconds of a DSB being introduced, the KU70/80 heterodimer migrates to the site of damage and binds to the two broken DNA ends (Mari et al., 2006; Mimori and Hardin, 1986). Its high abundance within the cell and its high affinity for DNA through its open-ring structure contributes towards this quick response (Walker et al., 2001). The binding of the DNA end with this protein complex acts as a scaffold to facilitate the binding of the DNA-dependent protein kinase catalytic subunit (DNA-PK_{CS}). Once bound, DNA-PK_{CS} forms a synaptic complex that bridges the gap across the DSB, bringing the two broken DNA ends together. In its unphosphorylated form, DNA-PK_{CS} blocks premature degradation and ligation until the DNA ends have been brought together (Calsou et al., 1999; Weterings et al., 2003). Autophosphorylation of DNA-PK_{CS} is required to induce a conformational change that allows processing enzymes and ligases access to the break site, essential to the downstream NHEJ events (Meek et al., 2007).

The subsequent steps in NHEJ depend upon the type of DSB. In its simplest form a DSB consists of two compatible blunt ends that can be immediately ligated back together. More commonly however, the induction of a DSB generates heterogeneous incompatible ends producing a 3' or 5' single stranded DNA (ssDNA) overhang at one or both of the DNA ends. This overhang must be removed either by resynthesis of the DNA strand using the nucleotide sequence of the overhang as a template (gap filling), or by resection before ligation can occur. In mammalian cells, a family of DNA polymerases μ , λ and terminal deoxynucleotidyltransferase (TdT) are all involved in the resynthesis of the DNA strand (Lee et al., 2004; Mahajan et al., 1999; Mahajan et

al., 2002), whereas a conformational change in the Artemis protein, phosphorylated by DNA-PK_{CS}, allows it to function as a 5' or 3' endonuclease to remove the overhang (Ma et al., 2002). Once processed, the resulting compatible ends can be ligated by the DNA LIGIV/XRCC4 complex, recruited to the synaptic complex by the KU70/80 heterodimer (Costantini et al., 2007). LIGIV can ligate double-stranded DNA that have compatible overhangs or blunt ends (Grawunder et al., 1997), the efficiency of which is increased by XRCC4 that acts to stabilise the interaction between the DNA helix and LIGIV (Grawunder et al., 1997; Modesti et al., 1999).

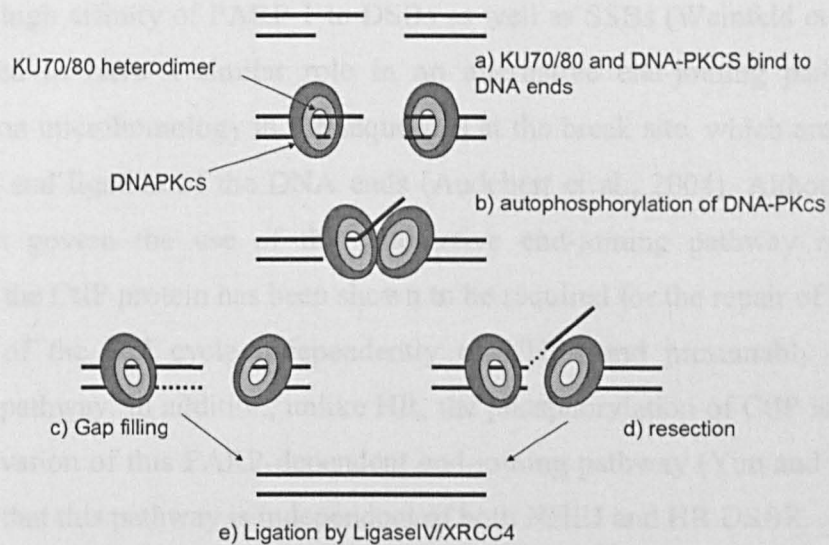


Figure 1.1 Model of the NHEJ repair pathway for the repair of DSBs

a) The KU70/80 heterodimer binds to the broken DNA ends of the DSB allowing the recruitment of DNA-PK_{CS}, forming a synaptic complex across the break site. b) Autophosphorylation of DNA-PK_{CS} allows processing enzymes to perform either c) gap filling or d) resection, before e) ligation is carried out on compatible ends by the DNA LIGIV/XRCC4 complex, adapted from Weterings (2008).

1.3.2.A.1 PARP-1 Dependent End-Joining (Alternative NHEJ)

In addition to NHEJ evidence from both *in vivo* and *in vitro* studies suggests an alternative end-joining pathway exists to repair DSBs that is independent of DNA-PK_{CS} but dependent on PARP-1 (Audebert et al., 2004). Chicken DT40 cells deficient in essential NHEJ and HR proteins exhibit sensitivity to IR-induced DSBs but are still capable of repairing the DSBs by a more slowly activated pathway (Wang et al., 2001). PARP-1 is a major protein of SSBR that catalyses the covalent transfer of successive ADP-ribose polymers from NAD to itself and other repair proteins upon binding at the break site. Using a yeast two hybrid system it was shown that PARP-1 interacts with XRCC1 at the break site, which then acts as a scaffold protein allowing POL β and LIGIII to resynthesise and ligate the DNA ends accordingly (Caldecott et al., 1996). Due to the high affinity of PARP-1 to DSBs as well as SSBs (Weinfeld et al., 1997), it is postulated to have a similar role in an alternative end-joining pathway that is dependent on microhomology in the sequences at the break site, which are used for the resynthesis and ligation of the DNA ends (Audebert et al., 2004). Although the exact factors that govern the use of this alternative end-joining pathway remain to be elucidated, the CtIP protein has been shown to be required for the repair of DSBs during G1 phase of the cell cycle independently of NHEJ and presumably through this alternative pathway. In addition, unlike HR, the phosphorylation of CtIP is not required for the activation of this PARP-dependent end-joining pathway (Yun and Hiom, 2009) suggesting that this pathway is independent of both NHEJ and HR DSBR.

1.3.2.B Homologous Recombination (HR)

HR is an error-free conservative process that repairs DSBs through a homology mediated mechanism. During late S or G2 phase, a sister chromatid becomes available to be used as a homologous template for the faithful repair of a DSB. Like NHEJ, HR can repair classic DSBs that produce two free DNA ends as substrates for repair (Fuller and Painter, 1988), however this type of DSB is comparatively rare and is primarily repaired by NHEJ (Sargent et al., 1997). Another role of HR is therefore postulated to be the repair of DSBs that arise during replication. Persistent SSBs that occur during S-phase are converted to DSBs at collapsed replication forks leaving only one-end of the DNA strand free for repair (Arnaudeau et al., 2001).

1.3.2.B.1 Two-Ended Repair

During mammalian HR, DSBs are initially recognised and bound by the Mre11/Rad50/Nbs1 (MRN) protein complex recruiting the ataxia-telangiectasia mutated (ATM) checkpoint kinase to the damage site (Paull and Lee, 2005). The MRN complex is also thought to have a role in the processing of the free DNA ends to generate 3' ssDNA ends due to its exonuclease as well as endonuclease activity (Carney et al., 1998; Paull and Gellert, 1998). In humans, the CtIP protein has been found to interact with BRCA1 to promote the resection of ssDNA tail ends at the break site (Yu and Chen, 2004). The resected 3' ssDNA overhang is coated with RPA due to its high affinity to ssDNA. Strand invasion is initiated by the displacement of RPA by Rad51 forming a presynaptic filament on the ssDNA overhang (Baumann and West, 1998) (Figure 1.2). *In vitro*, RPA inhibits the nucleation of Rad51 filaments on ssDNA; the process of displacement is therefore promoted by a number of mediator proteins such as Rad52 and the Rad51 paralogs, Xrcc2, Xrcc3, Rad51B, C and D. Although the exact function of these mediator proteins remains to be elucidated, all are required for Rad51 nucleoprotein filament formation (Yonetani et al., 2005). In humans, BRCA2/FANCD1 has also been shown to bind to RAD51 and facilitate nucleoprotein filament formation, and is essential for efficient HR repair (Chen et al., 1998). Stimulated by Rad54, the Rad51 nucleoprotein filament invades an aligned homologous DNA duplex and displaces the resident strand to create a heteroduplex structure known as a D-loop (Petukhova et al., 1998) (Figure 1.2). DNA polymerases are then recruited to the site and synthesis occurs past the original DSB using the sister chromatid as a homologous template.

A Holliday junction will form at the site of invasion and it is the direction in which branch migration takes place that determines the subsequent steps of the process. If the Holliday junction migrates in the direction of replication, the invasion will be reversed and the invading ssDNA will re-anneal with the 3' end of the original DSB. This synthesis-dependent single strand annealing (SDSSA) is error-free unlike normal SSA (see Section 1.3.2.B.2), and results in gene conversion (non-crossover event) (Figure 1.2). Alternatively, the ssDNA end may be repaired by synthesis-dependent NHEJ resulting in a tandem duplication at the site of the DSB and hence mutation (Richardson

and Jasin, 2000). Finally, the free end of the original duplex may invade the same homologous sister chromatid facilitated by Rad52 and RPA known as second end capture (Nimonkar et al., 2009; Sugiyama et al., 1998). Subsequent branch migration facilitated by Rad54 results in the formation of a double Holliday junction. This structure can either be dissolved by topoisomerase III α and BLM through convergent branch migration forming non-crossover events, or alternatively, it can be resolved by resolvases to result in either crossover (SCE) or non crossover (gene conversion) products. In humans, the MUS81/EME1 complex has been shown to cleave Holliday junctions however this cleavage results in non-ligatable ends (Ciccia et al., 2003). More recently, GEN1 has been identified as a resolvase of Holliday junctions in humans that results in ligatable ends (Ip et al., 2008). It is the direction of the resolution that determines the end product of HR. If the cleavage of the Holliday junction occurs in the same plane no crossovers will result (gene conversion). However, cleavage can also occur in opposite planes resulting in crossover between the two sister chromatids, thus a SCE is produced (Figure 1.2).

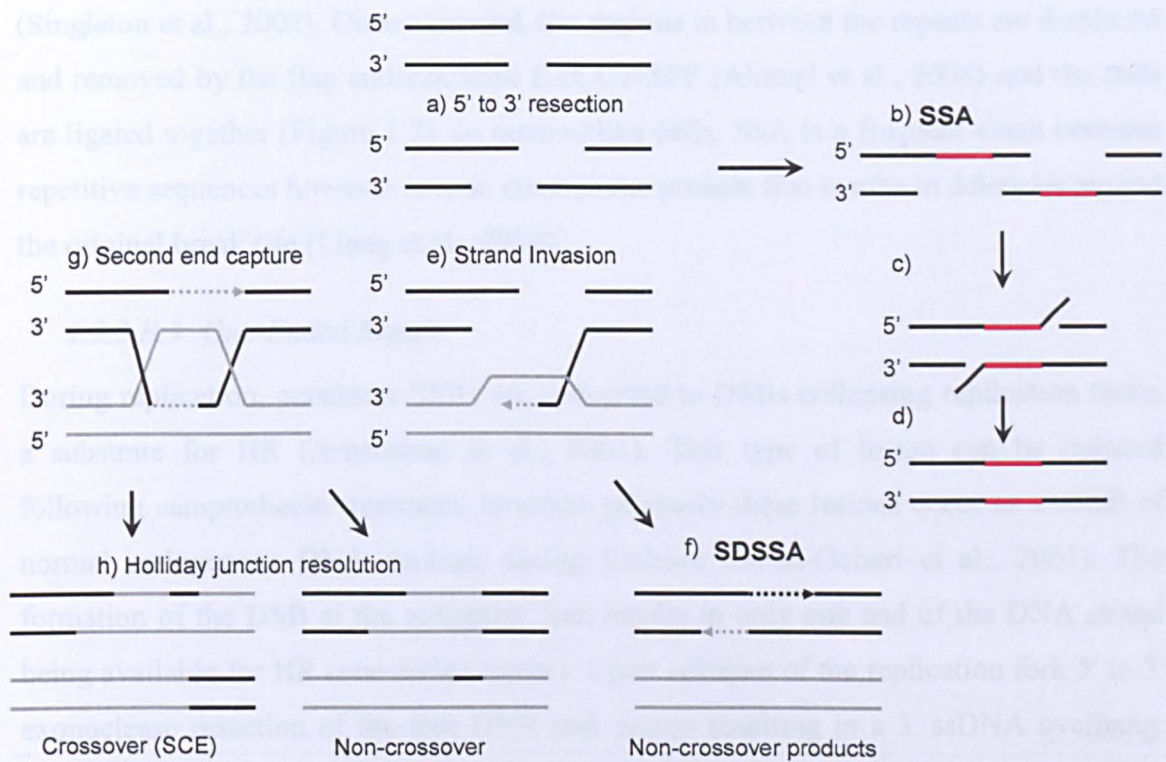


Figure 1.2 Models of HR for the repair of two-ended DSBs

a) The initial step of all HR sub-pathways is the 5' to 3' resectioning of the DSB to generate 3' ssDNA overhangs. If sequences of homology are revealed, b) SSA takes place annealing the complementary ssDNA. c) The strands are displaced and excised by ERCC1/XPF. d) Single strand gaps are filled and the strands are ligated back together. Alternatively, e) strand invasion can occur initiated by Rad51 which results in either f) synthesis-dependent SSA, where the invading strand anneals to the original strand and the gaps are filled resulting in non crossover products, or g) second end capture occurs forming a double Holliday junction and allowing synthesis to continue. h) The way in which the double Holliday junction is resolved results in non-crossover (gene conversion) or crossover products (SCE), adapted from Mimitou and Symington (2009).

1.3.2.B.2 Single Strand Annealing (SSA)

SSA is a repair mechanism similar to HR in that it utilises homologous sequences to facilitate the repair of a two-ended DSB. The 5' to 3' resection at the break site occurs in the same way as in HR however if repeated sequences are revealed within the 3' ssDNA overhangs, SSA will be initiated by the annealing of RPA coated ssDNA by Rad52

(Singleton et al., 2002). Once annealed, the regions in between the repeats are displaced and removed by the flap endonuclease ERCC1/XPF (Ahmad et al., 2008) and the ends are ligated together (Figure 1.2). In mammalian cells, SSA is a frequent event between repetitive sequences however it is an error-prone process that results in deletions around the original break site (Liang et al., 1998).

1.3.2.B.3 One-Ended Repair

During replication, persistent SSBs are converted to DSBs collapsing replication forks, a substrate for HR (Arnaudeau et al., 2001). This type of lesion can be induced following camptothecin treatment, however primarily these lesions occur as a result of normal endogenous DNA damage during S-phase (Saleh-Gohari et al., 2005). The formation of the DSB at the collapsed fork results in only one end of the DNA strand being available for HR (one-ended repair). Upon collapse of the replication fork 5' to 3' exonuclease resection of the free DNA end occurs resulting in a 3' ssDNA overhang. The resulting single strand gap on the template DNA is filled resulting in an intact sister chromatid template (Figure 1.3). In a similar process as described for two-ended repair (Section 1.3.2.B.1), strand invasion occurs allowing the leading strand synthesis to continue, re-establishing the replication fork. As only a single Holliday junction is left behind the replicating fork it can only be resolved in one way to result in an SCE (Figure 1.3).

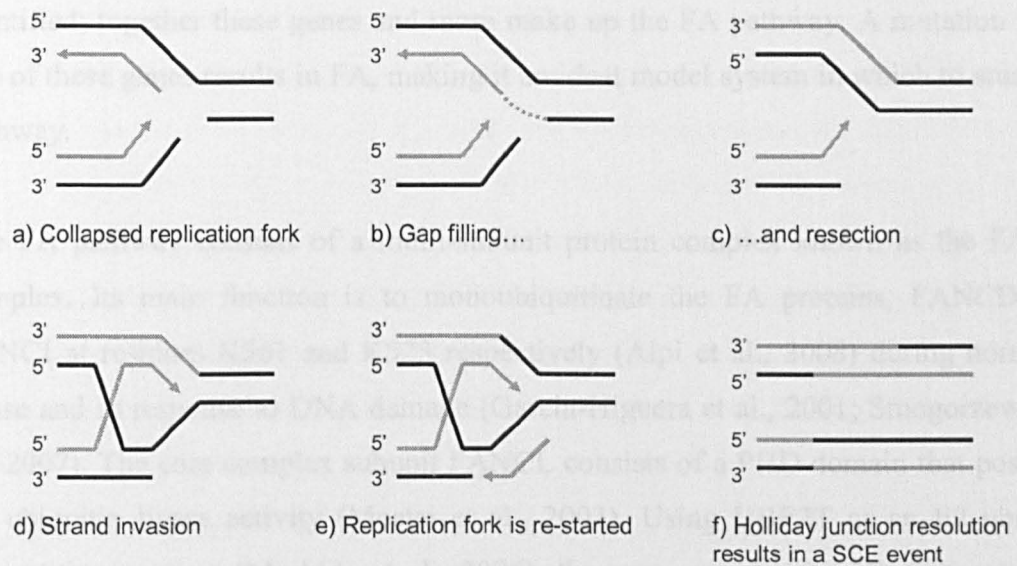


Figure 1.3 HR at a collapsed replication fork (one-ended repair)

a) A SSB is converted to a DSB collapsing the replication fork. b) Gap filling joins the single strand gap on the template DNA forming an intact sister chromatid. This is followed by c) 5' to 3' resection resulting in a 3' ssDNA overhang. The overhang is coated in Rad51 amongst other proteins to facilitate d) strand invasion. e) The displaced template strand is then used for DNA synthesis and the replication fork is re-established. f) Formation of a single Holliday junction behind the replicating fork leads to its resolution in only one direction producing a SCE event. Adapted from Helleday (2003).

1.3.3 Fanconi Anaemia (FA) Pathway

FA is a rare genetic instability disorder that is usually an autosomal recessive disease but in some cases can be X-linked (FANCB patients). FA causes acute myeloid leukaemia, bone marrow failure, congenital abnormalities and a predisposition to cancer. Cells from FA patients are characterised by increased chromosomal fragility leading to increased chromosomal aberrations and a hypersensitivity to DNA ICL-inducing agents such as MMC, which is used for its clinical diagnosis. Although a genomic instability disorder, unlike BLM and many cancers (see Section 1.4.2), FA patient cells exhibit normal levels of spontaneous SCE. They do however display a reduced induction of SCE in response to ICL damage (Latt et al., 1975), consistent with an inability to repair this damage and thus their hypersensitivity to ICL-inducing agents. To date there have been thirteen complementation groups and their corresponding genes

identified; together these genes and more make up the FA pathway. A mutation in any one of these genes results in FA, making it an ideal model system in which to study this pathway.

The FA pathway consists of a multi-subunit protein complex known as the FA core complex. Its main function is to monoubiquitinate the FA proteins, FANCD2 and FANCI at residues K561 and K523 respectively (Alpi et al., 2008) during normal S-phase and in response to DNA damage (Garcia-Higuera et al., 2001; Smogorzewska et al., 2007). The core complex subunit FANCL consists of a PHD domain that possesses E3 ubiquitin ligase activity (Meetei et al., 2003). Using UBE2T as an E2 ubiquitin conjugating enzyme (Machida et al., 2006), the core complex is able to regulate the monoubiquitination of FANCD2 and FANCI through this essential catalytic subunit. This modification of FANCD2 and FANCI allows their localisation to chromatin foci where they interact with other repair proteins during normal S-phase and following DNA damage to promote repair, although their exact function at these foci sites remains to be elucidated.

The FA core complex is composed of the FA proteins FANCA, B, C, E, F, G, L and M all of which have been linked to the FA phenotype. FAAP24 and FAAP100 are also members of the FA core complex but have not been associated with the disease (Ciccia et al., 2007; Ling et al., 2007). Each member of the complex is essential for the monoubiquitination of FANCD2 as determined by the lack of FANCD2 monoubiquitination in each of the FA patient subtypes (Garcia-Higuera et al., 2001). FANCA and FANCG form a subcomplex within the core complex, as do FANCB, L and FAAP100, and FANCC, E and F (Medhurst et al., 2006) however the functional significance of these remains to be elucidated.

FANCM and FAAP24, although a part of the core complex, have a separate function. FANCM and FAAP24 were first identified by Meetei et al. (2005) and Ciccia et al. (2007) respectively, and are both members of the XPF endonuclease family. FANCM contains DNA helicase motifs that have been shown *in vitro* to be involved in the translocation of Holliday junctions and fork reversal (Meetei et al., 2005). FAAP24, in a complex with FANCM, has also been shown to bind to ssDNA and branched DNA

structures (Ciccia et al., 2007). As FANCM and FAAP24 are constantly bound to the chromatin during the cell cycle, it is suggested that in response to DNA damage, FANCM and FAAP24 recognise and bind to stalled replication forks and recruit the FA core complex to the chromatin (Kim et al., 2008). During S phase however, it is the reduction in the phosphorylation of FANCM that allows the recruitment of the core complex to the chromatin and thus FANCD2 monoubiquitination (Kim et al., 2008). Conversely, it has been shown that upon hyperphosphorylation of FANCM by the polo-like kinase PLK1 regulator, the core complex is released from the chromatin (Kee et al., 2009).

The final three FA proteins, FANCD1, FANCI and FANCD3 are not required for the monoubiquitination of FANCD2 and function downstream of this modification. FANCI also known as BRIP1 or BACH1 possesses 5' to 3' helicase activity, interacts with BRCA1 and localises to repair foci with BRCA2 and RPA; its function at these foci is currently unknown (Gupta et al., 2007). FANCD3 also known as PALB2, is a binding partner of BRCA2 and is required for the localisation of BRCA2 to chromatin to promote HR (Xia et al., 2006). Lastly FANCD1, better known as the tumour suppressor BRCA2, facilitates the formation of RAD51 filaments and is essential for HR (Yang et al., 2002). FANCD2 functionally interacts with BRCA2/FANCD1, promoting its loading into chromatin complexes that are essential to HR (Wang et al., 2004).

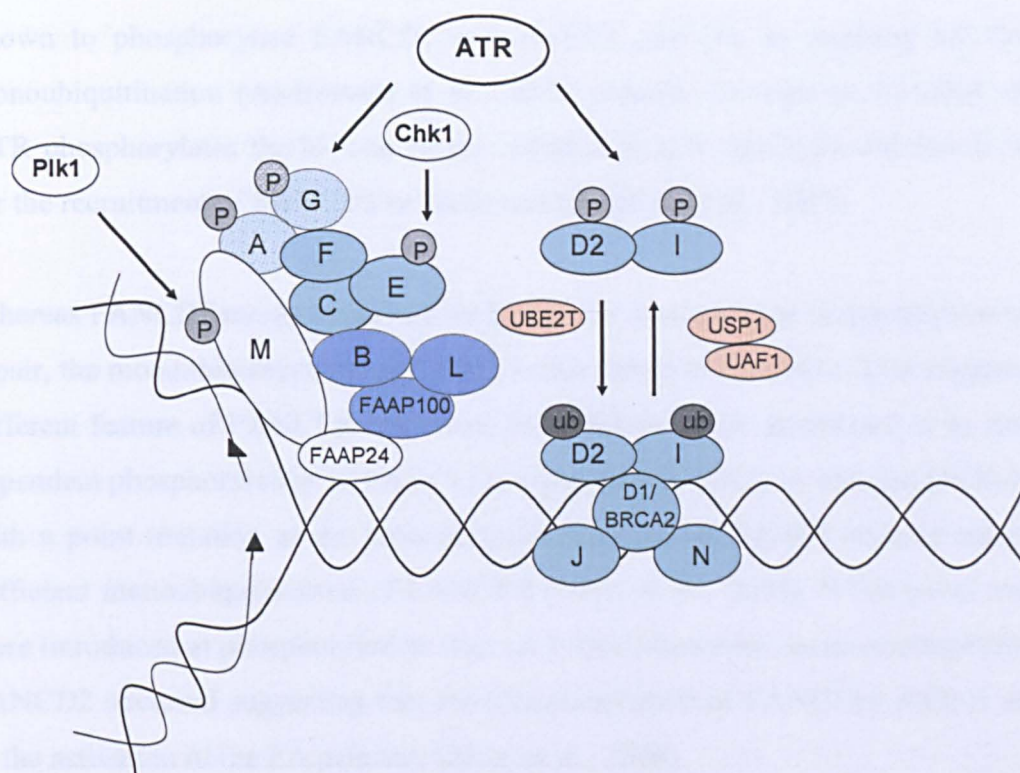


Figure 1.4 The structure of the FA pathway

FANCM and FAAP24 are constantly bound to the chromatin and recruit the FA core complex to the chromatin during S-phase and in response to DNA damage. The three subunits, FANCA and G (blue with grey outline), FANCC, E and F (blue with black outline) and FANCB, L and FAAP100 (dark blue) make up the FA core complex. The FA core complex monoubiquitinates FANCD2 and FANCI which then localises to DNA repair foci along with the downstream FA proteins FANCD1/BRCA2, FANCI and FANCN to facilitate repair, adapted from Moldovan and D'Andrea (2009).

1.3.3.A Regulation of the FA Pathway

The ATR checkpoint kinase is the major upstream regulator of the FA pathway and has been shown to phosphorylate a number of FA proteins either directly or by its effector kinase Chk1 to ensure efficient repair during S-phase (Pichierri and Rosselli, 2004). FANCA and FANCG are phosphorylated directly by ATR and this is required for the nuclear localisation of the FA core complex (Collins et al., 2009; Qiao et al., 2004). FANCE however is degraded following phosphorylation by CHK1 required for the regulation of the ubiquitin ligase activity of the core complex rather than its chromatin association (Wang et al., 2007). Independently of the FA core complex, ATR is also

known to phosphorylate FANCD2 and FANCI, and this is essential for FANCD2 monoubiquitination (Andreassen et al., 2004). Finally, in response to DNA damage, ATR phosphorylates the histone family member H₂A.X (γ H₂A.X) and this is required for the recruitment of FANCD2 to chromatin (Bogliolo et al., 2007).

Whereas FANCD2 monoubiquitination by the FA core complex is essential for efficient repair, the monoubiquitination of FANCI is not (Ishiai et al., 2008). This suggests that a different feature of FANCI is important for efficient repair, postulated to be the ATR-dependent phosphorylation of FANCI (Smogorzewska, 2007). A chicken DT40 cell line with a point mutation at the monoubiquitination site of FANCI showed reduced but sufficient monoubiquitination of FANCD2 (Ishiai et al., 2008). When point mutations were introduced at phosphorylation sites on FANCI however, no monoubiquitination of FANCD2 occurred suggesting that the phosphorylation of FANCI by ATR is essential to the activation of the FA pathway (Ishiai et al., 2008).

Another mechanism of regulating the FA pathway occurs through the removal of ubiquitin from FANCD2 and FANCI by the deubiquitinating enzyme USP1 and its activator UAF1 (Nijman et al., 2005). In the absence of DNA damage, USP1 and UAF1 constantly act to deubiquitinate FANCD2 and FANCI however, upon DNA damage, *USP1* gene transcription is switched off and the protein is quickly degraded. This allows a build up of monoubiquitinated FANCD2 and FANCI leading to the formation of foci and efficient repair (Nijman et al., 2005).

1.3.3.B Activation of the FA Pathway

As FA patient cells are hypersensitive to ICL-inducing agents, it was proposed that the FA pathway has an important role in the repair of DNA ICLs and this was confirmed by complementation studies, showing that the hypersensitivity to ICL-inducing agents could be corrected by the complementation of the mutated FA proteins in FA patient cells (Strathdee et al., 1992). The many interactions of FANCD2 with other repair proteins involved in NER, TLS and HR suggests a pivotal role for the FA pathway in the coordination of a number of repair pathways to deal with the highly toxic ICL lesion (Mirchandani and D'Andrea, 2006) (see Section 1.3.4). Inactivation of FANCD2 however, not only sensitises cells to ICL-inducing agents but also to oxidative stress

(Willers et al., 2008) therefore, although it is clear that the FA pathway is involved in ICL repair, evidence suggests that this pathway is not linear and that the FA proteins, particularly FANCD2, have a broader role in the response to spontaneous as well as induced DNA repair.

The FA pathway can be activated (as measured by the monoubiquitination of FANCD2) by a wide range of exogenous and endogenous damage (Garcia-Higuera et al., 2001; Taniguchi et al., 2002). FANCD2 monoubiquitination is required for the normal cell cycle progression through S-phase and thus forms nuclear foci both spontaneously (Taniguchi et al., 2002) and in response to DNA damage induced by a variety of agents such as IR, MMC, and replication stress induced by Aphidicolin (APH) and Hydroxyurea (HU) (Howlett et al., 2005). Once monoubiquitinated, FANCD2 (and FANCI) form discrete nuclear foci and co-localise with the repair proteins BRCA1, RAD51 (Garcia-Higuera et al., 2001; Taniguchi et al., 2002) and the DNA polymerase processivity factor, PCNA (Howlett et al., 2005; Hussain et al., 2004). The co-localisation of FANCD2 with BRCA1 and RAD51 is S-phase specific and occurs not only following the induction of DNA damage from exogenous sources but also endogenously through the replication associated repair by HR (Taniguchi et al., 2002). Recently, it has also been shown that FANCD2 functionally interacts with PCNA through a highly conserved putative PCNA interaction motif (PIP-box) (Howlett et al., 2009). Mutation in the PIP box of FANCD2 abrogates monoubiquitination both spontaneously and in response to DNA damage. ATR phosphorylation of FANCD2 however can still occur thus, FANCD2 is able to localise to chromatin but does not form nuclear foci (Howlett et al., 2009). It is therefore postulated that PCNA acts as a platform to facilitate the recruitment of monoubiquitinated FANCD2 to the chromatin at stalled replication forks following endogenous or induced replication stress (Howlett et al., 2009).

Although monoubiquitinated FANCD2 is recruited to stalled replication forks its exact function at these sites remains to be elucidated. A role for the FA pathway and thus FANCD2 in the restart of collapsed replication forks has been proposed (Wang et al., 2008). Replication fork restart was measured by radioactive nucleotide incorporation following the induction of damage in *Xenopus* egg extracts. Using camptothecin to

create replication-dependent DSBs and thus collapsed replication forks, it was found that *fancd2*-depleted extracts were deficient in the restart of replication. The replication restart of stalled forks induced by APH (an inhibitor of DNA polymerase) however was not affected by the depletion of *fancd2* (Wang et al., 2008). This suggests that the FA pathway has a role in the replication restart of collapsed but not stalled forks, irrespective of the presence of a DNA ICL.

1.3.3.C FANCD2 and Cancer

The *FANCD2* complementation group accounts for just 2% of all FA patient cells but generally causes a more severe phenotype (Timmers et al., 2001). Interestingly, like other proteins of the FA pathway such as the well characterised FANCD1/BRCA2 protein, FANCD2 defects have also been associated with sporadic and hereditary breast cancers in different mammalian systems (Moldovan and D'Andrea, 2009). Firstly, *Fancd2* knockout mice have been shown to develop ovarian and epithelial breast cancers (Houghtaling et al., 2003) whilst in humans, polymorphisms on *FANCD2* have been associated with increased sporadic breast cancer risk (Barroso et al., 2006) and FANCD2 expression has been found to be absent in 10 – 20% of sporadic and BRCA1-related breast cancers (van der Groep et al., 2008). Recently it was found that 19/20 malignant breast carcinomas had negative nuclear immunocytochemical staining of FANCD2 whereas cytoplasmic staining was normal (Rudland et al., 2010). One possible explanation for this is that FANCD2 is not being activated in these cells, causing a defect in repair that may promote tumour growth. In addition, a further reduction in cytoplasmic FANCD2 staining was correlated with positive staining for metastatic-inducing proteins such as osteopontin and thus was correlated with decreased patient survival and metastatic disease (Rudland et al., 2010). Taken together these data suggest that deregulation of *FANCD2* transcription and protein expression may be important in promoting breast and other human cancers (Hoskins et al., 2008).

1.3.4 Interstrand Cross-link (ICL) Repair

ICLs are the most cytotoxic of all DNA lesions covalently linking both strands of the DNA duplex, thus preventing unwinding of the DNA and therefore blocking essential cellular processes such as replication and transcription. Many ICL-inducing agents such as MMC and cisplatin are widely used as chemotherapeutic drugs, however ICLs can

also arise endogenously from metabolic by-products such as the lipid peroxidation product malondialdehyde (Niedernhofer et al., 2003). The ICL repair mechanism has been well defined in *E. coli* and involves the NER complex *UvrABC*, the recombination repair pathway or DNA polymerase II-dependent TLS (Berardini et al., 1999; Cole, 1973). Similarly in *S. cerevisiae*, ICL repair requires the NER and HR mechanisms (Jachymczyk et al., 1981). The exact repair mechanism in mammalian cells however remains to be elucidated. From the evidence in bacteria and yeast, it has been proposed that a cascade of repair proteins from several repair pathways; namely NER, HR and TLS, and coordinated by the FA pathway, are involved in the repair of this type of lesion (Mirchandani and D'Andrea, 2006).

The initial step of mammalian ICL repair involves a double incision either side of the ICL on one strand resulting in the unhooking of the DNA crosslink. The NER heterodimer MUS81-EME1 has 3' endonuclease activity and is able to incise DNA at ICLs (Hanada et al., 2006). Similarly, the heterodimer ERCC1/XPF has 5' endonuclease activity and can incise DNA near to the crosslink both *in vitro* and *in vivo* (Fisher et al., 2008; Kumaresan et al., 2002). Mammalian cells deficient in ERCC1/XPF exhibit extreme sensitivity to ICL-inducing agents (De Silva et al., 2000), similarly mouse ES cells deficient in either Mus81 or Emel show hypersensitivity to ICL damage (Abraham et al., 2003; McPherson et al., 2004).

The repair of ICLs primarily takes place during replication (Akkari et al., 2000). Therefore, the unhooking of the DNA crosslink is postulated to generate a SSB which, during replication, can be converted to a DSB leading to replication fork collapse and repair by HR. Evidence for the involvement of HR following an ICL-induced DSB in mammalian cells was determined by complementing the ICL hypersensitive *irs1* and *irs1SF* hamster cell lines (Caldecott and Jeggo, 1991) with human HR proteins XRCC2 and XRCC3 respectively. This corrects the hypersensitivity to ICL-inducing agents in these cells (De Silva et al., 2000). Furthermore, NHEJ defective CHO cell lines (Ku80 knockouts) were still capable of repairing DSBs produced by ICL-inducing agents, whereas the HR-deficient *irs1* and *irs1SF* cell lines were impaired (De Silva et al., 2000).

The excision of the initial ICL only removes the crosslink from one of the parental strands, allowing it to be flipped out (unhooked). The presence of the ICL on the opposite parental strand still affects the base structure at this site and therefore must be bypassed or repaired. It is postulated that TLS is employed to bypass the affected base generating an intact sister chromatid that can be used in the subsequent strand invasion step of HR (Figure 1.5). Firstly, Rev3 mutant MEFs are hypersensitive to ICL damage (Zander and Bemark, 2004) and in the *Xenopus* biochemical system the DNA polymerase pol ζ is required for the completion of ICL repair (Raschle et al., 2008). Furthermore, DT40 chicken cells deficient in Rev3 or Rev7 do not form SCEs in response to ICL damage. As SCE is an end product of HR it was postulated that TLS and HR act in a sequential manner to repair ICL damage (Niedzwiedz et al., 2004).

Similarly to the hypersensitivity of ICL-inducing agents in HR deficient cell lines, FA patient cells also show hypersensitivity to ICL-inducing agents. This phenotype therefore suggests that the FA pathway has a role in ICL repair; postulated to be the coordination of NER, HR and TLS to repair this type of damage (Mirchandani and D'Andrea, 2006). Firstly, FANCM has been implicated in the initial recognition of an ICL as it recruits the FA core complex to the site of the cross-linked DNA in chromatin following ICL damage (Mosedale et al., 2005). FANCI/BRIP1 has also been implicated in the initial processing of this lesion due to its ability to bind and unwind DNA strands at forked duplexes (Gupta et al., 2005). Recently, ERCC1 has been shown to interact with FANCD2 and is required for FANCD2 foci formation following ICL damage (McCabe et al., 2008). Furthermore, ICL-induced FANCD2 foci formation is significantly reduced in ERCC1/XPF deficient cells suggesting that the initial unhooking of the ICL by ERCC1/XPF is essential for the localisation of FANCD2 to chromatin (Bhagwat et al., 2009).

The FA pathway is known to promote HR through the interactions of FANCD2 and the HR proteins BRCA2/FANCD1, BRCA1 and RAD51 during S-phase or following exogenous DNA damage (see Section 1.3.3.B). A similar role is therefore postulated to promote HR in the repair of an ICL-generated DSB as indicated by studies in DT40 chicken cell lines where knocking out *Fancc* impaired HR following ICL damage (Niedzwiedz et al., 2004). Furthermore, recently it was found that the newly identified

DNA polymerase POLN physically interacts with FANCD2 and that knocking out POLN caused a 50% reduction in HR following MMC-induced damage (Moldovan et al., 2010).

Finally, interactions between the FA pathway and the TLS polymerases have been reported. FA patient cells have reduced point mutations suggesting that TLS pathways are suppressed in these cells (Hinz et al., 2006). Furthermore in human cells, REV1 interacts with the FA core complex and is required in conjunction with PCNA for REV1 foci formation following ICL induced damage (Mirchandani et al., 2008).

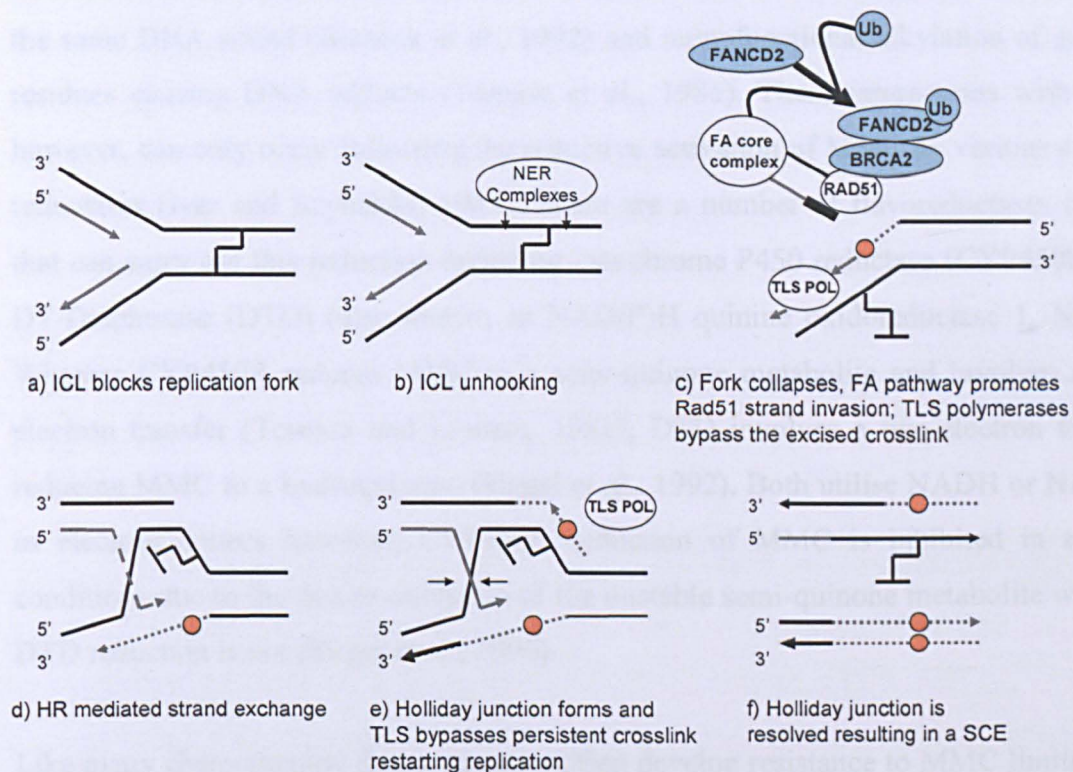


Figure 1.5 Model of mammalian ICL repair

a) An ICL occurs blocking replication and stalling the replication fork. The NER complexes ERCC1/XPF and MUS81-EME1 unhook the ICL from one of the parental strands at 3' and 5' to the ICL b). The resulting SSB is converted to a DSB collapsing the replication fork. c) The FA pathway coordinates the HR proteins RAD51 and BRCA2 to bind to the collapsed replication fork to promote strand invasion. TLS DNA polymerases bypass the affected base (orange circle) on the opposite parental strand generating an intact sister chromatid to be used for d) HR-mediated strand exchange. e) Holliday junction is formed and TLS polymerases bypass the persisting crosslink site allowing synthesis to continue. f) Progression of the fork continues resulting in a SCE. Adapted from Thompson (2005).

1.3.5 MMC Metabolism

MMC is a potent inducer of ICLs and has been used extensively in the study of the FA pathway. In the present study, MMC has also been used and so here its metabolism will be considered in detail.

MMC is a natural anti-tumour antibiotic used for many years for cancer chemotherapy. It is used to damage the DNA of tumour cells by generating primarily ICLs between guanine residues on opposite strands of the DNA duplex (Iyer and Szybalski, 1963). In addition to ICLs, MMC also forms intra-strand cross-links between guanine residues on the same DNA strand (Bizanek et al., 1992) and monofunctional alkylation of guanine residues causing DNA adducts (Tomasz et al., 1986). These interactions with DNA however, can only occur following the reductive activation of MMC by various cellular reductases (Iyer and Szybalski, 1963). There are a number of flavoreductases *in vivo* that can carry out this reduction including cytochrome P450 reductase (CYP450R) and DT-Diaphorase (DTD) (also known as NAD(P)H quinine oxidoreductase 1, NQO1). Whereas CYP450R reduces MMC to a semi-quinone metabolite and involves a one-electron transfer (Tomasz and Lipman, 1981), DTD involves a two-electron transfer reducing MMC to a hydroquinone (Siegel et al., 1992). Both utilise NADH or NADPH as electron donors however, CYP450R reduction of MMC is inhibited in aerobic conditions due to the fast re-oxidation of the unstable semi-quinone metabolite whereas DTD reduction is not (Siegel et al., 1990).

Like many chemotherapy drugs, tumours often develop resistance to MMC limiting the clinical utility of these agents. The CYP450R and DTD reductases play a major role in the anti-cancer activity of MMC, thus the expression of these enzymes and their activation has been the subject of a number of studies investigating chemo-resistance. Firstly, using CHO cells expressing the bacterial MMC resistance-associated (MCRA) protein, it was found that the resistance to MMC could be reduced significantly by the overexpression of DTD and CYP450R (Baumann et al., 2001). Similarly, in human bladder tumours, the expression of DTD and CYP450R was positively correlated with MMC sensitivity in these tumours (Gan et al., 2001). Taken together, this suggests that

chemo-resistance to ICL-inducing agents could be the result of a defect in cellular metabolism and not just a result of defects in the DNA repair machinery.

1.4 Sister Chromatid Exchange (SCE)

During S-phase, as part of the normal cell cycle, DNA is replicated and chromosomes are copied resulting in two closely associated sister chromatids joined together at the centromere. Following the normal cycle of mitosis, these sister chromatids then segregate resulting in two daughter cells. SCE is the process of the physical exchange of chromatid regions resulting from the breaking and rejoining of two sister chromatids. SCE usually occur naturally within the cell at a rate that varies between cell types, from 6 SCE events per cell in human lymphocytes to 10 SCE per cell in human fibroblasts (Table 1.1). These spontaneous SCEs are considered to be a product of normal DNA replication or endogenous DNA damage. Alternatively, SCE can be induced by a variety of DNA damaging agents. DNA ICL-inducing agents such as MMC are potent SCE inducers (Nagasawa et al., 1983) whereas IR and UV both induce SCE but to a lesser extent (Wojcik et al., 2004). It is postulated however, that any agent capable of initiating the DNA damage response by collapsing replication forks has the potential to cause the induction of a SCE event (Nagasawa et al., 1983) (Table 1.2).

Cell Type	SCE Frequency	Reference
Peripheral blood lymphocytes	6.7 ± 0.145	(Miranda et al., 1997)
Fibroblasts	9.48 ± 1.74	(Jung et al., 1986)
Amniotic fluid cells	8.56 ± 0.28	(Goyanes et al., 1994)
Human skin fibroblasts	9.9	(Wolff et al., 1975)
Embryonic lung fibroblasts	3.8	(Kato and Stich, 1976)

Table 1.1 Comparison of SCE frequencies in different human cell types taken from the literature

Values shown for spontaneous SCE frequency are the average SCE per cell with standard deviations (where available) taken from the reference indicated.

DNA Damaging Agent (and Concentration)	Cell Type	Fold Induction	Reference
Benzo[α]pyrene (0.1 mM)	Lymphocytes	2 fold	(Lindahl-Kiessling et al., 1989)
Camptothecin (10 nM)	Lymphocytes	6 fold	(Degrassi et al., 1989)
Hydroxyurea (0.25 mM)	CHO cells	3.4 fold	(Ishii and Bender, 1980)
MMC (100 nM)	CHO cells	10.4 fold	(Perry and Evans, 1975)
UV light - UV-A (225 J/M ²), UV-B (150 J/M ²)	Fibroblasts	1.8 fold	(Knees-Matzen et al., 1991)
X-rays (4 GY)	CHO cells	2 fold	(Perry and Evans, 1975)

Table 1.2 The induction of SCEs by various DNA damaging agents

A selection of DNA damaging agents found to induce SCE in various cell types taken from the reference indicated. The difference shown is the fold difference compared to the spontaneous rate in each of the individual references.

SCEs were first observed by Taylor (1958) using tritium labelled chromosomes and autoradiography. Methods for the detection of these SCEs were not further developed until the mid 1970's when it was found that a chromatid that has replicated twice in the presence of the thymine analogue 5-bromodeoxyuridine (BrdU), has reduced fluorescence detected by the fluorochrome 33 258 Hoechst (Latt, 1973). Methods based on this principle, but without the need for fluorescent microscopy soon followed (Korenberg and Freedlender, 1974; Perry and Wolff, 1974) and it is these methods that are still widely used today (Figure 1.6).

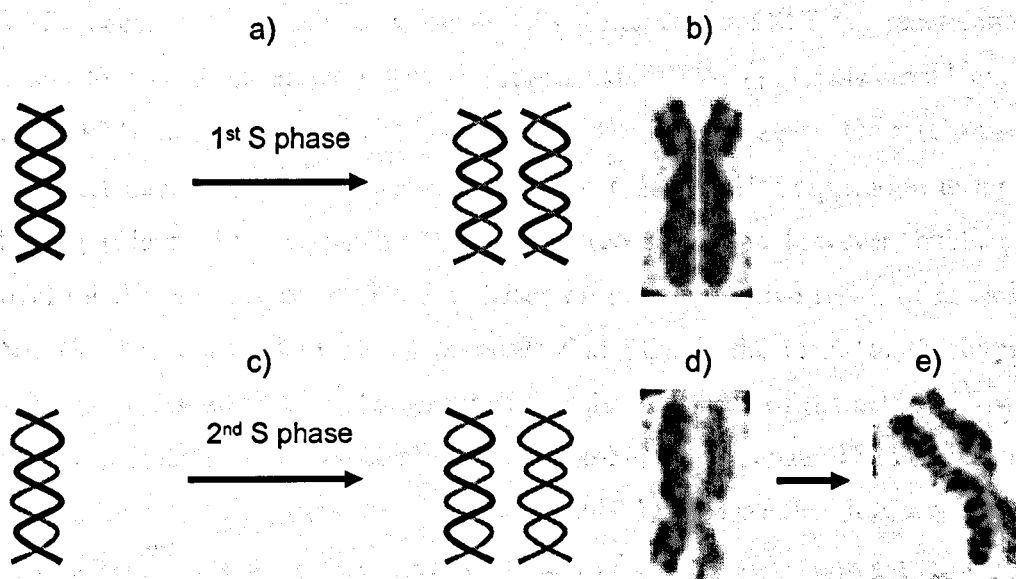


Figure 1.6 SCE detection by BrdU incorporation and Hoechst 33 258 staining

Parental DNA undergoes two rounds of replication in the presence of BrdU. a) During the first S phase BrdU is incorporated into the DNA in place of thymine. The two resulting daughter chromatids contain one strand with no incorporation (black) and one with full BrdU labelling (grey). b) Sister chromatids can not be distinguished using Hoechst 33 258 staining as both chromatids appear dark. c) Following a second round of replication, one daughter chromatid contains one strand with BrdU incorporation and one without, and the other daughter chromatid contains both strands with BrdU incorporation. d) The sister chromatids can now be distinguished using Hoechst 33 258 staining as the chromatid containing full BrdU incorporation in both strands appears light whereas the chromatid with incorporation in only one strand remains dark. e) Areas where SCEs have occurred can now be distinguished using this method. Adapted from Meschini et al. (1996), images from Hoh, unpublished data (2007).

The ability to visualise SCEs led to two important concepts. Firstly, it was assumed that the process of SCE must involve DNA breakage and hence, that it could be used as a measure of DNA damage and repair (Kato, 1973). Secondly, a correlation between the ability of agents to induce SCEs and their mutagenic and carcinogenic properties was observed (Latt and Schreck, 1980) and thus SCEs could be used extensively as a genetic indicator of potential mutagens. Since then, and despite the widespread use of SCE as a mutagenic screen, there is still very little known about the mechanism of SCE.

As SCE occurs during S-phase, it was initially postulated that SCE is a recombinational process that involves either single (Bender et al., 1974) or double-strand exchange (Kato, 1974). Single strand exchange was soon dismissed as a possible mechanism due to the fact that SCE is not observed during the first round of replication using BrdU labelling (Figure 1.6). Opposing the idea of recombination however, another early model for the mechanism of SCE was based on post-replicative repair of cross-linked DNA (Shafer, 1977). This model proposes that SCE is the result of the bypass of irreparable DNA cross-links that occur during the G1 phase of the cell cycle, when a homologous chromatid is not available for recombinational repair. The model suggests that SCE is a two step process whereby the parental strands are first displaced at the site of the cross-link and then rejoined downstream of the damage, allowing replication to continue. The polarity and alignment of the parental strands forms two duplexes which have undergone SCE (Figure 1.7). Although this theory could be used to explain the affects of the ICL-inducing agents on SCE, it does not explain the induction of SCE by other non-ICL-inducing agents and the earlier postulated involvement of recombination (Kato, 1974).

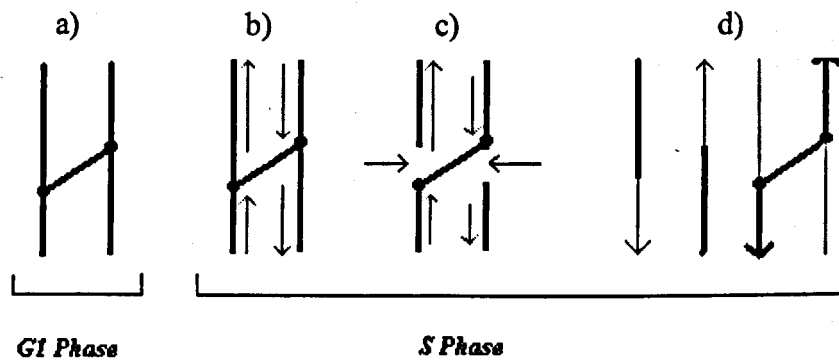


Figure 1.7 Replication bypass model by Shafer (1977)

a) A single DNA duplex in G1 phase of the cell cycle showing an ICL. b) Bidirectional replication begins (S-phase). The advancing nascent strands (grey arrows) cannot replicate further than the ICL therefore the corresponding complementary region is back-filled with Okazaki fragments. c) The advancing nascent strands cause stress at the cross-link site on the parental strands causing breaks to occur (thin black arrows). d) Duplexes are displaced and the upper left strand aligns with the lower right, and the upper right aligns with the lower left. The continued presence of the cross-link maintains structural continuity. Back-filling by Okazaki fragments and the final ligation of the presenting gap occurs resulting in the DNA forming two continuous double helices and SCE, adapted from Stetka (1979).

There were two major models suggested for the idea that SCE is a recombinational event involving double strand exchange. The first proposes that DNA topoisomerase II causes transient DSBs during replication, the proximity of which on the sister chromatid, results in aberrant rejoining thus resulting in a SCE (Figure 1.8) (Dillehay et al., 1989; Pommier et al., 1985). During replication, DNA topoisomerases I and II, catalyze the unwinding of the double helical structure of DNA by forming cleavable complexes with the DNA strands and creating transient DNA strand breaks (Liu et al., 1983). DNA topoisomerases also have the ability to ligate these DNA strands following replication (Liu et al., 1983). The biochemical properties of topoisomerase II therefore support its role in this model of SCE formation. However, the DNA topoisomerase II inhibitors ICRF-193 and Bufalin had a little or no effect respectively, on the SCE frequency in both wild type and BER-deficient cells (which display elevated spontaneous SCE events). This suggests that topoisomerase II is not involved in SCE formation although the inhibition of such enzymes during replication cannot be ruled out as having an effect on SCE frequency (Dominguez et al., 2001).

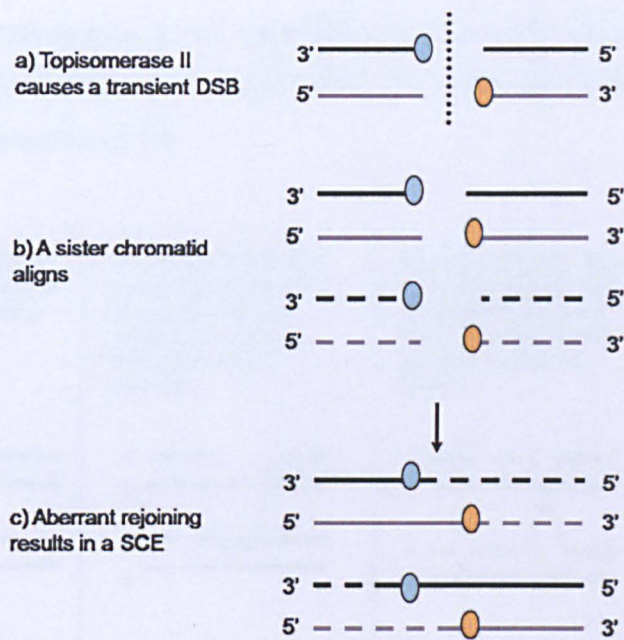


Figure 1.8 DNA topoisomerase II subunit exchange model by Pommier et al. (1985)

a) During replication, topoisomerase II causes a transient DSB, the subunits of which form covalent bonds at the 3' end of the break (blue and orange circles). b) A sister chromatid aligns containing another transient DSB in close proximity to the initial break caused by the action of topoisomerase II. c) Aberrant rejoining occurs. The topoisomerase II subunit at the 3' end of the break on the parental strand of the original chromatid ligates to the 5' end of the parental strand on the sister chromatid, and the subunit at the 3' end on the parental strand of the sister chromatid ligates to the 5' end of the parental strand of the original chromatid and vice versa for the remaining subunits on the nascent strands. This results in a SCE event, adapted from Dillehay et al. (1989).

The second major recombinational model of SCE formation is that SCE is mediated by homologous recombination (HR). The idea that SCE is a result of a DNA repair mechanism was first described by Kato (1977) and although no speculation was made as to what that mechanism might be, it was suggested that SCE formation may arise from various DNA repair pathways dependent on the type of initial lesion (Kato, 1977). It is postulated further that a SCE can arise from two initial processes. The first is a SSB that allows the free end of the SSB to bind to the complementary sequence of the DNA duplex in the sister chromatid (strand invasion) generating a heteroduplex (Holliday junction) (Figure 1.9). The second is by the formation of two single-strand discontinuities, one in the parental strand and one as the gap in the growing nascent

strand, again generating a heteroduplex; a prerequisite for SCE (Kato, 1977). The resulting heteroduplexes were postulated to be resolved by an unknown mechanism which today is known as HR.

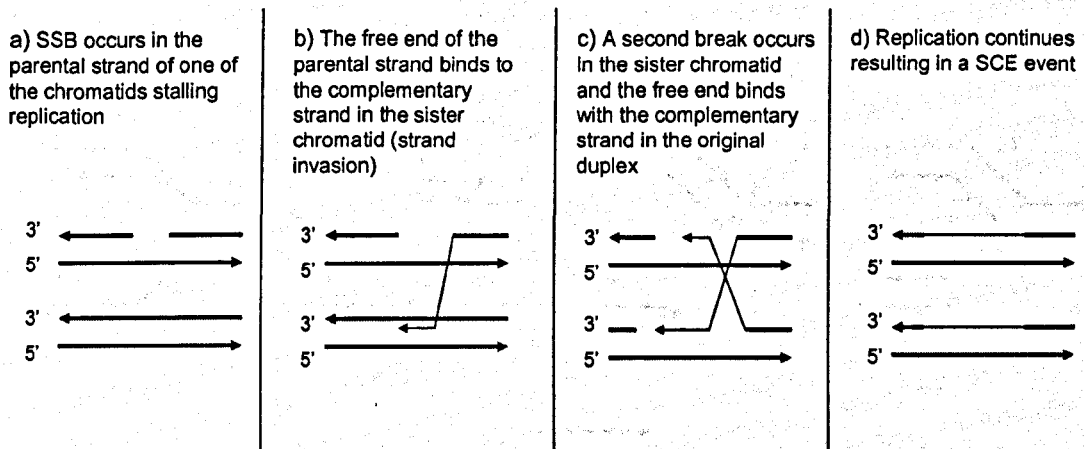


Figure 1.9 Recombinational model of SCE formation by Kato (1977)

a) A SSB occurs in the parental strand of the initial chromatid. b) The resulting free end invades the sister chromatid, binding to the complementary strand. c) This causes a second SSB to occur in the sister chromatid initiating a second 'strand invasion', binding to the complementary strand of the original chromatid. d) A SCE results from the continued replication of the opposite chromatids, adapted from Kato (1977).

A second conflicting theory to the involvement of recombination in SCE formation was based on aberrant replication caused by DNA damage (Ishii and Bender, 1980; Painter, 1980). Although it was agreed that a SCE event was the result of a double strand exchange, they postulated that this was due to collapsed replication forks resulting in the aberrant breaking and rejoining of the DNA strands. In this model, a SCE results from the occurrence of nicks (SSBs) at the replication fork (Ishii and Bender, 1980). These nicks can occur spontaneously or result from the presence of DNA damage such as UV dimers. It is postulated that a nick occurs in the parental strand near to the damage site allowing the free end to incorrectly bind with the newly synthesised daughter strand (Figure 1.10). A second nick in the parental strand near the end of the daughter strand then occurs resulting in the ligation of this daughter strand with the parental strand containing the initial damage (Figure 1.10). For this model, no details were given about the process of the breaking and rejoining of the DNA strands, however it was postulated

that topoisomerases may be involved (Ishii and Bender, 1980), or that the aberrant ligation of the DNA strands could be due to a defect in DNA repair (Painter, 1980).

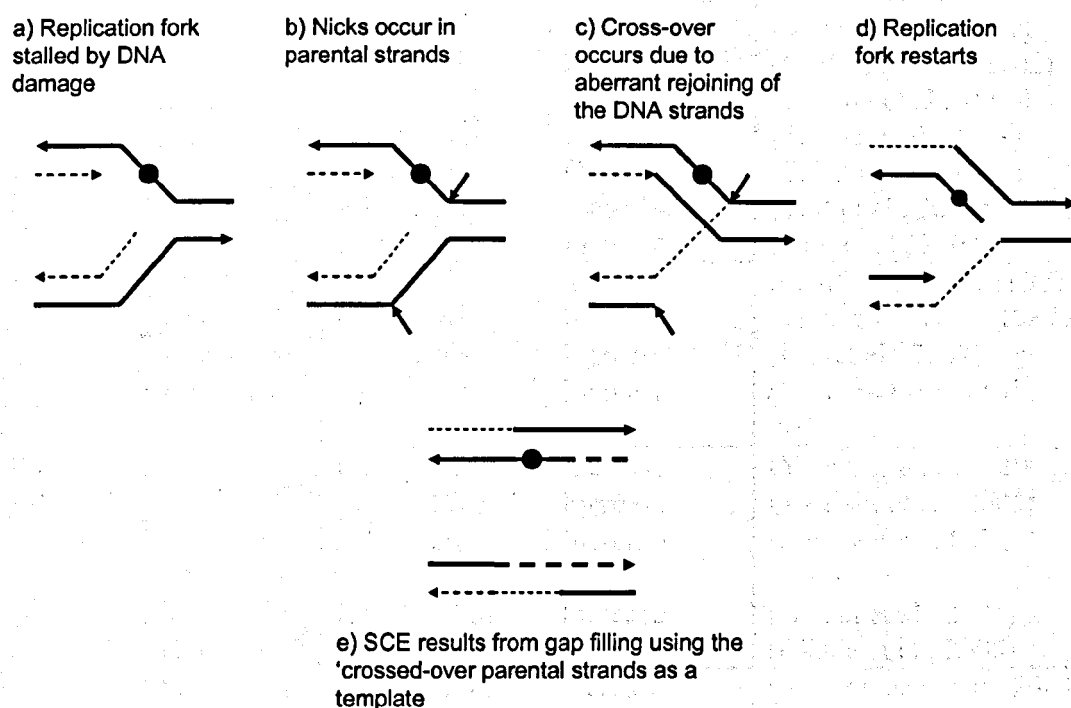


Figure 1.10 Replication model of SCE formation by Ishii and Bender (1980) and Painter (1980)

a) DNA damage causes a replication fork (black circle) to stall. b) Two nicks occur in each of the parental strands, one near to the damage site and one near the end of the daughter strand in the opposite parental strand (sites indicated by arrows). c) The free ends of the strand breaks incorrectly rejoin with the newly synthesised daughter strands in the opposite duplex. d) The replication fork can restart as the damage has been bypassed. e) Gap filling finishes the SCE formation using the crossed-over parental strands as templates for synthesis. Adapted from Ishii and Bender (1980).

1.4.1 DNA Repair Proteins and SCE

More recently, further evidence implicating DNA repair, particularly HR, in SCE formation has been identified by studying the association between defective DNA repair proteins and SCE levels in a number of different systems (Table 1.3).

Repair pathway	Protein	Cellular System	Affect on SCE	Reference
HR	BLM	Humans	Increase	(Chaganti et al., 1974)
	Rad54	DT40 cell lines	Decrease	(Sonoda et al., 1999)
	Rad51	DT40 cell lines	Decrease	(Sonoda et al., 1999)
	Rad51b	DT40 cell lines	Decrease	(Sonoda et al., 1999)
	Rad51c	DT40 cell lines	Decrease	(Sonoda et al., 1999)
		CHO cells	Decrease	(Godthelp et al., 2002)
	Rad51d	DT40 cell lines	Decrease	(Sonoda et al., 1999)
	Xrcc2	CHO cells	Decrease	(Takata et al., 2001)
	Xrcc3	CHO cells	Decrease	(Takata et al., 2001)
	Brca2	Mouse ES cells	Decrease	(Tutt et al., 2001)
	BRCA2	Humans	Increase	(Kim et al., 2004)
SSBR	Parp1	CHO cells	Increase	(de Murcia et al., 1997)
	Xrcc1	CHO cells	Increase	(Thompson et al., 1982)
	XRCC1	HeLa cells	Increase	(Fan et al., 2007)
	LigaseIII	CHO cells	Increase	(Puebla-Osorio et al., 2006)
TLS	Rad18	DT40 cell lines	Increase	(Yamashita et al., 2002)
		Mouse ES cells	Increase	(Tateishi et al., 2003)
	Rev1	DT40 cell lines	Increase	(Simpson and Sale, 2003)
	Rev3	DT40 cell lines	Increase	(Okada et al., 2005)
	Rev7	DT40 cell lines	Increase	(Okada et al., 2005)
FA pathway	Fance	DT40 cell lines	Increase	(Niedzwiedz et al., 2004)
	Fancd2	DT40 cell lines	Increase	(Yamamoto et al., 2005)
	FA Proteins	Humans	Normal	(Latt et al., 1975)
Replisome component	Timeless	MEFs	Increase	(Urtishak et al., 2009)

Table 1.3 Repair proteins involved in altered spontaneous SCE frequencies taken from the literature

Numerous DNA repair proteins have been associated with altered spontaneous SCE levels. Both the pathway and system used to study the affects are shown as well as the effect observed. The relevant reference is also indicated.

Firstly, in the chicken DT40 cell lines, HR defective mutants such as *Rad51*, *Rad54* and the *Rad51* paralogs, *Rad51B*, *C* and *D*, all show a marked reduction in both spontaneous and MMC-induced SCE. *Ku70/80* knockouts (NHEJ defective mutants) however, showed no alteration in SCE frequency further supporting the role of HR rather than NHEJ in SCE formation (Sonoda et al., 1999). In mammalian cells, the same effects

have not been observed. Neither isogenic *Rad51D* mutant CHO or mouse fibroblast cell lines show a reduction in spontaneous SCE levels (Smiraldo et al., 2005). In addition, *Rad54* knockout mice do not exhibit a reduction in spontaneous SCE, but do show a marked reduction in MMC-induced SCE (Dronkert et al., 2000). *Rad51C* however, has been shown to be important for SCE formation as CHO cells deficient in *Rad51C* show decreased spontaneous and MMC-induced SCE frequencies (Godthelp et al., 2002). Furthermore, knocking out *Brca2* in mouse ES cell lines reduces spontaneous SCE (Tutt et al., 2001). Finally, a deficiency in the replisome component Timeless (Tim), required for normal DNA replication, causes an increase in spontaneous SCE in MEF cells. An increase in Rad51 and Rad52 foci formation was also observed suggesting that the increase in SCE is a result of an increase in the reliance of HR for normal DNA synthesis in these cells (Urtishak et al., 2009). In humans, most evidence has arisen from the study of genomic instability disorders (see Section 1.4.2). Bloom syndrome, characterised by increased levels of spontaneous SCE, is caused by a mutation in the *BLM* gene that encodes for the BLM helicase involved in HR (Ellis et al., 1995). Furthermore, carriers of the heterozygous *BRCA2* germline mutation exhibit an elevated frequency of spontaneous SCE (Kim et al., 2004).

Knockout mutations in proteins involved in TLS have also been associated with SCE levels in chicken DT40 cell lines. Mutants of the E3 ligase Rad18 and the polymerases Rev1 and Pol ζ result in increased spontaneous SCE levels (Okada et al., 2005; Simpson and Sale, 2003; Yamashita et al., 2002). This is consistent with mouse ES cells deficient in Rad18 that exhibit a two-fold increase in spontaneous SCE (Tateishi et al., 2003), however Rev1 mutant mouse ES cells show no change in spontaneous SCE (Jansen et al., 2005). A defect in TLS may lead to increased SCE through the increased capacity of HR to repair persistent lesions that would ordinarily be bypassed by TLS.

The proteins of the FA pathway have also been implicated in varying SCE levels. Chicken DT40 cells mutant in the *Fance* and *Fancd2* genes show elevated SCE levels (Niedzwiedz et al., 2004; Yamamoto et al., 2005), whereas isogenic *Fancg* CHO cell lines do not exhibit increased spontaneous SCE (Tebbs et al., 2005). In human FA patient cells, SCE levels are normal but these cells are characterised by an decrease in MMC-induced SCE (Latt et al., 1975) (see Section 1.4.2.A).

Finally, in mammalian cells, proteins involved in SSBR have been associated with increased levels of SCE. CHO cell lines deficient in *Xrcc1* exhibit elevated levels of SCE (Thompson et al., 1982). This is consistent with XRCC1 down regulation in human fibroblasts and HeLa cell lines that also show elevated SCE levels (Fan et al., 2007). Similarly, *Parp-1* deficient mice and *LigIII* knockout mice also show high levels of SCE (de Murcia et al., 1997; Puebla-Osorio et al., 2006). The implication of defective proteins involved in SSBR can be explained through the repair mechanism of persistent SSBs. An irreparable SSB leads to DSB formation and replication fork collapse, and is repaired by HR (Arnaudeau et al., 2001), thus resulting in a SCE event (see Section 1.3.2.B.3).

The disparity of results from the different study systems suggests that the molecular mechanism of SCE formation and the implication of DNA repair may differ between lower vertebrate and mammalian cells. In humans, it is even less clear. However, the different effect of defective repair proteins on spontaneous and induced SCE suggests that there may be more than one mechanism involved in the formation of SCE in higher eukaryotes.

1.4.2 SCE and Disease

The cellular response to DNA damage employs a number of DNA repair mechanisms that work efficiently and conservatively to ensure cellular survival through the control of mutations arising within our DNA. Failure to control efficient DNA repair can result in various genetic instability disorders and cancer. As SCE is an end product of DNA repair and a marker of DNA damage, SCE frequency has been heavily associated with these types of diseases and in some cases is used as a diagnostic tool.

1.4.2.A Fanconi Anaemia (FA)

FA (as mentioned in Section 1.3.3) is a rare cancer predisposition disorder that at the genetic level is associated with chromosome instability, an increase in chromosomal breaks and hypersensitivity to DNA ICL-inducing agents such as MMC. Cells from FA patients exhibit normal levels of spontaneous SCE but show a marked reduction in the number of SCE events induced by MMC. As FA is caused by mutations in the FA genes of the FA pathway, the role of which is thought to be to promote HR both endogenously

and after ICL damage, it is presumably through this association with HR that the SCE frequency in these cells is altered, although the exact causal mechanism is unknown.

1.4.2.B Bloom Syndrome (BS)

BS, like FA, is a rare human autosomal recessive disorder which is characterised by genetic instability including an elevated baseline mutation rate, an increase in neoplasia and a pre-disposition to a wide range of cancers including leukaemia and skin cancer due to sun-sensitive skin. Cells from BS patients are characterised by many cytogenetic abnormalities including a ten-fold increase in the spontaneous SCE frequency, also used for its diagnosis (Chaganti et al., 1974). BS is caused by mutations in both copies of the *BLM* gene, cells are therefore defective in the BLM helicase that is a prominent protein involved in HR. BLM is a member of the Rec-Q helicase sub-family that possesses 3' to 5' helicase activity (Ellis et al., 1995). *In vitro*, BLM can dissociate D-loop intermediates and promotes branch migration of Holliday junctions in conjunction with topoisomerase III α and BLAP75 to yield non-crossover events (gene conversion) (Karow et al., 2000; Wu and Hickson, 2003). Thus, a defect in BLM may result in a higher frequency of cross-over events (SCE) as seen in BS patient cells. Finally, BLM accumulates at stalled replication forks following DNA damage and can promote fork regression aiding repair at stalled forks (Ralf et al., 2006). From this evidence, it is postulated that the increase in SCE in BS cells is a hallmark of aberrant HR caused by the defect in the BLM protein.

1.4.2.C Cancer Predisposition

Genomic instability and dysfunctional genes involved in DNA repair and recombination are associated with neoplastic development and cancer (Hoeijmakers, 2001). Although SCE cannot be used as a predictive biomarker for this disease (Norppa et al., 2006), it can be used as a marker of chromosome stability (Carrano et al., 1978) and thus has been found to be elevated in a number of patients with sporadic and hereditary cancers (Table 1.4). Firstly, patients with Hodgkins disease have a higher level of spontaneous SCE events compared to a control group (Caggana and Kelsey, 1991). Patients with sporadic malignant melanoma also have increased levels of SCE compared to their relatives and control lymphocytes (Illeni et al., 1991). In the same study, patients with familial malignant melanoma also had a similar increase in SCE compared to controls.

UNIVERSITY
OF SHEFFIELD
LIBRARY

The peripheral blood lymphocytes of patients with early stage breast cancer have high SCE (Aristei et al., 2009). In addition, varying degrees of elevated SCE frequencies have been reported in lymphocytes of patients with various cancers including hereditary breast cancer, carcinoma of the cervix uteri and ovarian cancer (Baltaci et al., 2002; Cortes-Gutierrez et al., 2000; Roy et al., 2000). Furthermore, heterozygous carriers of germ-line mutations of the *BRCA2* breast cancer susceptibility gene demonstrate an average 65% increase in spontaneous SCEs compared to wild-type family members (Kim et al., 2004). *BRCA2* is an essential protein of HR (Davies et al., 2001) and is therefore essential for chromosome stability. There is a clear association between mono-allelic *BRCA2* inactivation and increased SCE frequencies however this is not the case for all cancers with elevated SCEs. Indeed, it is more likely that different cancers have different defects in repair and therefore result in varying levels of SCE. Although SCE is a marker of chromosome stability, the exact association between SCE and cancer in general remains to be elucidated.

Patient Type	SCE Frequency	Reference
Early stage breast cancer	8.2 ± 0.913	(Aristei et al., 2009)
Control group	6.6 ± 0.6	
Hereditary breast cancer	11.01	(Roy et al., 2000)
Control group	7.67	
Hodgkins Disease	8.93 ± 1.86	(Caggana and Kelsey, 1991)
Control group	7.56 ± 1.95	
Cervical cancer	7.8 ± 1.05	(Cortes-Gutierrez et al., 2000)
Control group	6.98 ± 1.13	
Ovarian cancer	18.13	(Baltaci et al., 2002)
Control group	6.85	
Sporadic malignant melanoma	8.0 ± 0.3	(Illeni et al., 1991)
Patient Relatives	5.4 ± 0.1	
Control Lymphocytes	4.7 ± 0.2	
Familial malignant melanoma	8.4 ± 0.8	(Illeni et al., 1991)
Patient Relatives	5.4 ± 0.2	
Control Lymphocytes	4.7 ± 0.2	
<i>BRCA2</i> ^{+/-} carriers	6.6	(Kim et al., 2004)
<i>BRCA2</i> ^{+/+} carriers (controls)	4.04	

Table 1.4 SCE frequencies in human sporadic and hereditary cancers

Values shown for SCE frequency are mean SCE per cell with standard deviations (where available). All values are for peripheral blood lymphocytes from patients with or without disease (controls).

1.5 Uveal Melanoma

Uveal melanoma is the most common form of intraocular tumour in adults with a stable annual incidence of approximately 7 cases per million over the last 25 years (Singh and Topham, 2003a). The eye is the most common site for non-cutaneous melanoma, accounting for approximately 80% of such cases (Scotto et al., 1976). Ocular melanomas mainly arise from the uveal tract of the eye consisting of the iris, ciliary body and choroid. Current treatments involve enucleation of the affected eye, plaque radiotherapy and transpupillary thermotherapy. Chemotherapy has little effect on this tumour due to its high chemo-resistance (Albert et al., 1992). Despite advances in the initial diagnosis and treatment of the primary tumour, the 5 year mortality rate of uveal melanoma has not changed since 1973 (Singh and Topham, 2003b) with approximately 40% of patients developing metastatic melanoma to the liver within 10 years after the initial diagnosis and treatment (Virgili et al., 2008). The metastatic potential of these cells depends largely on the anatomical positioning of the tumours within the uveal tract. Posterior uveal melanoma affecting the ciliary body and choroid of the eye, are highly aggressive and frequently specifically metastasise to the liver and thus are associated with poor prognosis (Gragoudas et al., 1991). Conversely, iris melanomas have a good prognosis and rarely develop metastatic disease (Shields et al., 2001). Metastatic potential and thus prognosis, has been further characterised by cell type. Spindle cell uveal melanoma has the best prognosis whereas tumours containing epithelioid cells have the worst; a mixed cell melanoma has an intermediate prognosis (McLean et al., 1982). Furthermore, molecular classification using gene profiling studies indicated that uveal melanoma associated with high metastatic risk exhibited a broad down-regulation of neural crest/melanocytic genes and an up-regulation of epithelial genes (Onken et al., 2006). Finally, uveal melanoma have been well characterised by cytogenetic studies, particularly posterior uveal melanoma where recurrent chromosomal abnormalities have been associated with anatomical positioning and poor prognosis (Prescher et al., 1992).

Alterations of chromosomes 1, 3, 6, 8 and 11 have been found to be associated with posterior uveal melanoma. More specifically changes in chromosomes 1, 3 and 8 have been shown to characterise tumours of the ciliary body whereas alterations of chromosome 6 and 11 correlate to choroid melanoma (Sisley et al., 2000). The loss of

chromosome 3 and alterations of chromosome 8 (mostly extra copies of 8q) consistently occur together, specifically in ciliary body tumours. As these tumours are associated with a poor prognosis, this phenotype has been used to identify patients with reduced survival (Sisley et al., 1997). Furthermore, monosomy of chromosome 3 seen in over 50% of uveal melanomas has also been associated with a poor prognosis (Prescher et al., 1996).

As well as the loss or gain of entire chromosomes, small subsets of uveal melanoma tumours show only partial microdeletions on chromosome 3. Deletions of the short arm of chromosome 3 are common in other tumours whereas deletions of 3q are an infrequent event (Kok et al., 1997). In uveal melanoma however, the entire chromosome is subject to such deletions (Prescher et al., 1996). Deletion-mapping studies have identified the regions of 3p25, 3p11-14 and 3q24-26 as regions that are preferentially lost in uveal melanoma (Cross et al., 2006; Parrella et al., 2003; Tschentscher et al., 2001). This recurrent loss of chromosomal regions in uveal melanoma suggests these regions may indicate potential locations for tumour suppressor genes and, as the whole of chromosome 3 is subject to deletions, it is likely that multiple tumour suppressor genes exist (Prescher et al., 1996). Although potential candidates, including the Von Hippel-Lindau gene and FHIT (fragile histidine triad), have been identified on the 3p arm, none have been identified to date on the 3q arm, and no definite functional association has been found between the loss of these genes and the development of uveal melanoma.

1.5.1 Uveal Melanoma as a Model System for SCE

Although uveal melanoma cells exhibit a number of non-random chromosomal abnormalities, they do not demonstrate high levels of chromosomal aberrations (Sisley et al., 1990), which is a hallmark of many other types of tumours. Taking chromosomal aberrations as a marker of genetic instability, this phenotype would suggest that these tumours are stable in contrast to other forms of cancer. Furthermore, uveal melanoma cells have been found to have a reduced spontaneous SCE frequency in primary samples and in established cell lines. This is compared to matched patient blood samples (Table 1.6 and Figure 1.11), other human established cell lines and the cutaneous melanoma cell line WM793 (Table 1.5). Interestingly, in general, cancer has been associated with

increased levels of spontaneous SCE and indeed, uveal melanoma is the only disease state known to show decreased levels of SCE, thus this unique phenotype of uveal melanoma makes it an ideal system in which to study SCE formation.

Cell Line	Genotype	Average SCE	SCE Range
SOM 157	Established uveal melanoma cell line	3.1	1 – 8
SOM 196	Established uveal melanoma cell line	3.3	1 – 5
WM793	Established cutaneous melanoma cell line	10.3	3 – 23
MRC5VA	Transformed human fibroblast cell line	6.1	2 – 11
HCT116	Transformed human colon carcinoma cell line	12.5	6 – 24
SW480	Transformed human colorectal carcinoma cell line	6.9	2 – 11
Fibroblasts	Primary human fibroblasts	7.4	5 – 13

Table 1.5 SCE frequencies in established uveal melanoma cell lines

Established uveal melanoma cell lines exhibit a reduced SCE frequency compared to the controls. The SCE frequency is shown for two established uveal melanoma cell lines compared to a cutaneous melanoma cell line, primary human fibroblasts in culture and other human transformed cell lines. The range of SCE is shown as well as the average SCE per cell (Hoh, 2007, unpublished data).

Case Number	Uveal Melanoma Tumour		Matched Patient Blood	
	Average SCE	SCE Range	Average SCE	SCE Range
494	2	2 – 2	4.3	2 – 6
520	3.7	1 – 11	6.3	1 – 11
521	1.9	0 – 7	5.7	2 – 11
524	3.9	2 – 6	5.3	1 – 10
526	2.9	1 – 7	6.2	3 – 11
537	3.5	2 – 5	5.2	1 – 14
538	2.5	2 – 3	7.4	3 – 15
543	3.1	2 – 8	6.8	2 – 13
544	2.9	1 – 5	6.5	3 – 10
545	2.0	2 – 2	5.3	4 – 7
546	2.6	1 – 6	6.1	2 – 12
547	2.5	0 – 4	5.9	2 – 10
548	2.8	1 – 6	7.0	4 – 16
551	3.1	1 – 7	6.7	4 – 16

Table 1.6 SCE frequencies in primary uveal melanoma and matched patient blood samples

For all cases, the primary tumour samples exhibit a reduced SCE frequency compared to the matched patient blood. The SCE frequency is shown for primary uveal melanoma tumour samples and the matched patient blood samples isolated from the Ocular Oncology Unit at the Royal Hallamshire Hospital, Sheffield. The range of SCE is shown, as well as the average SCE per cell. (Hoh, 2007, unpublished data).

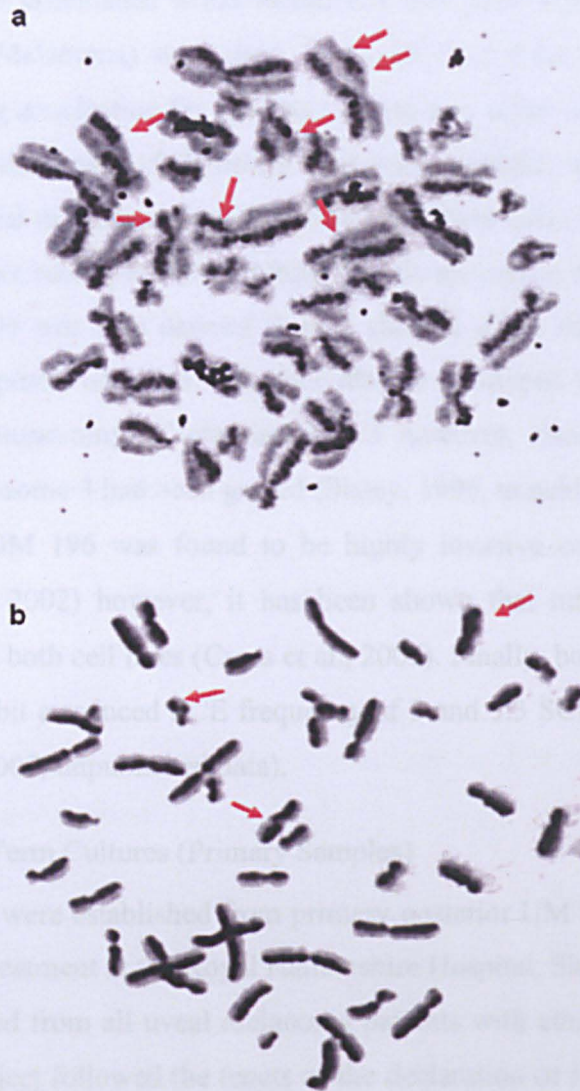


Figure 1.11 Representative image of the number of spontaneous SCE in a primary uveal melanoma tumour and matched patient blood sample

a) BrdU incorporation and Hoescht 33 258 staining showing the number of spontaneous SCE in the matched patient blood of Case Number 520. b) BrdU incorporation and Hoescht 33 258 staining showing the number of spontaneous SCE in the uveal melanoma tumour sample from Case Number 520. Images are representative of all cases showing that spontaneous SCE is reduced in uveal melanoma tumour samples compared to matched patient blood. Arrows depict regions where exchange has occurred (Hoh, 2007, unpublished data).

1.5.1.A Established Uveal Melanoma Cell Lines

For this study, the established uveal melanoma cell lines SOM 157 and SOM 196 (Sheffield Ocular Melanoma) were used. Both cell lines were established from male patients undergoing enucleation for treatment of primary uveal melanoma at the Ocular Oncology Unit at the Royal Hallamshire Hospital, Sheffield. SOM 157 was derived from a choroid uveal melanoma that contained epithelioid cells and showed metastatic potential. The patient subsequently died from hepatic metastatic disease 14 months after treatment. SOM 196 was also derived from a choroid uveal melanoma however this tumour contained spindle cells. No metastatic disease developed from this tumour. Both tumours showed monosomy of chromosome 3 however, once the cell lines were established, chromosome 3 had been gained (Sisley, 1996, unpublished data). In chemo-invasion assays SOM 196 was found to be highly invasive compared to SOM 157 (Woodward et al., 2002) however, it has been shown that numerous invasive sub-populations exist in both cell lines (Cross et al., 2005). Finally, both cell lines SOM 157 and SOM 196 exhibit a reduced SCE frequency of 3 and 3.3 SCE per cell respectively (Table 1.5) (Hoh, 2007, unpublished data).

1.5.1.B Short-Term Cultures (Primary Samples)

Short-term cultures were established from primary posterior UM biopsies from patients receiving surgical treatment at the Royal Hallamshire Hospital, Sheffield, UK. Informed consent was obtained from all uveal melanoma patients with ethical approval (SSREC 94/247) and the project followed the tenets of the declaration of Helsinki. A total of 14 primary uveal melanoma samples were analysed, for which paired blood samples were available in all cases. Unsuccessful analysis was also performed on a further 27 cases. The clinico-pathology details of the successfully analysed melanomas are presented in Appendix 1.

1.6 Aims of this Study

Although SCE has been used for many years as a marker of mutagenesis (Latt and Schreck, 1980) very little is known regarding the formation of this phenomenon in human cells. SCE is a known end-product of HR and it can be induced by a wide variety of DNA damaging agents. Furthermore, the frequency of SCE can be affected by defective proteins involved in DNA repair. Evidence therefore suggests that SCE occurs

as a consequence of DNA repair, although differences in the effect that defective DNA repair proteins have on spontaneous and induced SCE levels may suggest that different mechanisms exist for both.

Uveal melanoma is the only disease state known to date that exhibits reduced levels of spontaneous SCE. It is therefore an ideal model system in which to study the formation of SCE. In order to do this, the following was carried out:

- 1) Characterisation of uveal melanoma cell lines for defects in the endogenous DNA damage repair response.
- 2) The results of aim 1) were related to the observed reduction in spontaneous SCE frequency in uveal melanoma cell lines.
- 3) Characterisation of uveal melanoma cell lines for defects in the induced DNA damage repair response.

Chapter 2 – Materials and Methods

2.1	Materials.....	53
2.1.1	General Laboratory Equipment.....	53
2.1.2	Glassware, Plastics and Disposables.....	54
2.1.2.A	Purified Water	55
2.1.2.B	Sterilisation.....	55
2.1.3	Chemicals.....	56
2.1.4	Cytotoxic Agents.....	58
2.1.5	Selective Agents.....	59
2.1.6	Antibodies	59
2.1.7	Kits and Company Reagents	61
2.1.8	Cell Lines	62
2.1.9	Plasmids	62
2.1.10	Preparation of Standard Solutions.....	63
2.1.10.A	1x Phosphate Buffered Saline (PBS)	63
2.1.10.B	Tris-Buffered Saline (TBS).....	63
2.1.10.C	1 M Tris pH 6.8, 7.4 and 8	63
2.1.10.D	1.5 M Tris pH 8.8.....	63
2.1.10.E	Ethidium bromide	63
2.1.10.F	0.5 M EDTA	64
2.1.10.G	SOB medium and agar	64
2.1.11	Tissue Culture Reagents.....	64
2.1.11.A	Foetal Calf Serum (FCS).....	64
2.1.11.B	DMEM.....	64
2.1.11.C	Trypsin and Versene/EDTA.....	64
2.1.11.D	DiMethyl Sulphoxide (DMSO).....	65
2.1.11.E	Presept	65
2.2	Methods	65
2.2.1	Bacterial Studies.....	65
2.2.1.A	Transformations	65

2.2.1.A.1	One Shot® TOP10 Chemically Competent <i>Escherichia coli</i> (<i>E. coli</i>).....	65
2.2.1.A.2	MAX Efficiency® <i>Stbl2</i> Chemically Competent Cells.....	65
2.2.1.B	Bacterial Culture	66
2.2.2	DNA Studies	66
2.2.2.A	Plasmid purification using the Endofree® Plasmid Purification Maxi Kit.....	66
2.2.2.B	DNA extraction using the GenElute™ Mammalian Genomic DNA Miniprep Kit.....	66
2.2.2.C	Quantification.....	67
2.2.3	Methylation Studies	67
2.2.3.A	Bisulphite modification using the CpGenome™ DNA Modification Kit.....	67
2.2.3.B	The Polymerase Chain Reaction (PCR).....	69
2.2.3.C	Primer Design	70
2.2.3.D	PCR set up using Platinum® <i>Taq</i> DNA Polymerase.....	70
2.2.3.E	PCR Conditions.....	71
2.2.3.F	Agarose Gel Electrophoresis.....	72
2.2.3.G	PCR product purification using the GenElute™ PCR Clean-Up Kit..	72
2.2.3.H	Sequencing.....	72
2.2.3.I	Genome-wide demethylation using 5-azacytidine treatment.....	73
2.2.4	Tissue Culture Studies	73
2.2.4.A	Maintenance, Storage and Passage of Cell Lines.....	73
2.2.4.B	Cryopreservation.....	73
2.2.4.C	Thawing of Cells.....	74
2.2.4.D	Counting Cells.....	74
2.2.4.E	Toxicity Assays.....	74
2.2.4.F	Colorimetric Assay using the Cell Proliferation Kit I (MTT).....	75
2.2.4.F.1	The proliferation of primary uveal melanoma tumour samples in the presence of MMC.....	75
2.2.4.F.2	MTT Proliferation Assay	76
2.2.4.G	Fluctuation Assay.....	76

2.2.4.H	Retroviral Complementation.....	78
2.2.4.H.1	Transfection using Lipofectamine™ 2000.....	79
2.2.4.H.2	Viral infection of the uveal melanoma cell line.....	80
2.2.5	Single cell gel electrophoresis assay using the Trevigen® CometAssay™ Reagent Kit.....	80
2.2.6	RNA Studies	82
2.2.6.A	RNA extraction using the GenElute™ Mammalian Total RNA Kit ..	82
2.2.6.B	cDNA Synthesis using Superscript™ II Reverse Transcriptase	82
2.2.6.C	Real Time PCR	83
2.2.6.C.1	Primer Design.....	83
2.2.6.C.2	Real Time PCR reaction set up	84
2.2.6.C.3	Testing primer efficiency.....	84
2.2.6.C.4	Quantification.....	85
2.2.6.D	Ribonuclease (RNase) Protection Assay.....	85
2.2.6.D.1	Multi-probe template set design.....	87
2.2.6.D.2	Probe Synthesis using the T7 MAXIscript® Kit	87
2.2.6.D.3	RNA Preparation and Hybridisation using the RPA III™ Kit.....	89
2.2.6.D.4	RNase Digestion and Precipitation of Probe/Target mRNA Protected Fragments.....	89
2.2.6.D.5	Separation of Protected Fragments using a Denaturing TBE-Urea Acrylamide Gel	90
2.2.6.D.6	Quantification.....	91
2.2.7	Western Blot Analysis.....	91
2.2.7.A	Protein Extraction and Quantification.....	91
2.2.7.A.1	Harvest by Trypsinisation	91
2.2.7.A.2	Harvest by Scraping into 2x RIPA Buffer to Maintain Phosphate Moieties.....	92
2.2.7.A.3	Quantification.....	92
2.2.7.B	Western Blot Procedure	92
2.2.7.B.1	Assembly of Casting Equipment.....	92
2.2.7.B.2	Casting of the Tris-Glycine SDS-Polyacrylamide Gels	92
2.2.7.B.3	Electrophoresis	94

2.2.7.B.4	Semi-Dry Transfer.....	94
2.2.7.B.5	Blocking the Membrane	95
2.2.7.B.6	Antibody Incubation.....	95
2.2.7.B.7	ECL Detection.....	95
2.2.8	Immunofluorescence	95
2.2.8.A	Sample Preparation	96
2.2.8.A.1	Spontaneous Foci Formation.....	96
2.2.8.A.2	Induced Foci Formation Following MMC Treatment	96
2.2.8.B	RAD51 Foci Formation	96
2.2.8.C	FANCD2 Foci Formation	97
2.2.8.D	γ H ₂ A.X Foci Formation	97
2.2.9	Fluorescence-Activated Cell Sorting (FACS) Analysis.....	98
2.2.9.A	Propidium Iodine (PI) Staining	98
2.2.9.B	BrdU Staining	99

List of Figures

Figure 2.1	Sodium bisulphite modification of DNA.....	68
Figure 2.2	The chemical process of deaminating cytosine to uracil by sodium bisulphite modification.....	69
Figure 2.3	Metabolism of yellow MTT to a purple formazan salt by viable cells.....	75
Figure 2.4	The HPRT mechanism of guanine metabolism for DNA synthesis.....	77
Figure 2.5	Method of retroviral complementation.....	79
Figure 2.6	Standard regression line showing the R ² values and thus the primer efficiency for the FANCD2 and β -ACTIN primer sets used in the Real Time PCR experiments.....	85
Figure 2.7	RNase protection assay procedure.....	86

2.1 Materials

2.1.1 General Laboratory Equipment

Item	Company
Agarose gel electrophoresis system	Geneflow
Balance	Precisa
Benchtop centrifuge – eppendorfs	Fisher Scientific
Biological safety cabinet	Gelman Sciences
Colony counter	Stuart Scientific
DNA Engine Peltier thermal cycler	BioRad
EasyjecT plus electroporation machine	Geneflow
Electrophoretic transfer cell	BioRad
FACScalibur	Becton Dickinson
Haemocytometer	Hawksley
Heat block	Grant Instruments
Hoefer SE250 mighty small II system	Amersham Biosciences
Hoefer SE250 miniVE vertical electrophoresis unit	Amersham Biosciences
Ice machine	Scotsman
Incubator – bacterial culture	Weiss Gallenkamp
Incubator – shaking	New Brunswick Scientific
Incubator – tissue culture	Weiss Gallenkamp
Irradiator IBL 437C, Source 51.5 TBq, Cs137	CIS Bio International
Light microscope	Olympus
Mid bench centrifuge – falcon tubes	Sanyo
Nanodrop 2000 system	ThermoScientific
OmniPAGE Maxi vertical gel electrophoresis unit	Geneflow
pH meter	BDH Laboratory Supplies
PhosphorImager system	Molecular Dynamics
Pipette aid	Drummond
Pipettes	Gilson
Plate reader	Anthos Labtec

Item (Continued)	Company
Power pack	BioRad
Savant speedvac concentrator	ThermoScientific
Shaking platform	Stovall Life Science
UGenius gel imaging system	Geneflow
UV transilluminator	BDH Laboratory Supplies
Vacuum air dryer	Fisherband
Vortex	Fisons Scientific Equipment
Water baths	Grant Instruments

2.1.2 Glassware, Plastics and Disposables

Item	Company
0.22 μ m Millex GP filter unit	Millipore
Bacterial culture dish	Sterilin
Cell scraper	Sarstedt
Centrifuge tubes – 15 ml	Sarstedt
Centrifuge tubes – 30 ml	Corning
Coverglass – 22 x 22 mm	Scientific Laboratory Supplies
Cryovials – 1.2 ml	Nalgene
Culture plates - 12, 24 and 96 well	Corning
Culture plates - 6 well	Griener Bio One
Electroporation cuvettes	Geneflow
Eppendorfs - 0.2 ml, 0.5 ml and 1.5 ml	Sarstedt
Glass bottles	Fisher Scientific
Microlance needles	Becton Dickinson
Microscope slides	Scientific Laboratory Supplies
Non-sterile FACs tubes	Elkay
Plastic pipettes - 5 ml, 10 ml and 25 ml	Costar
Pyrex Glassware	Fisher Scientific
Refill tips	Sarstedt

Item (<i>Continued</i>)	Company
RNAse free barrier tips (1 – 200 µl)	Sorenson, BioScience, Inc.
RNAse free filter tips (200 - 1000 µl)	Axygen Inc.
Sterile syringes	Becton Dickinson
Tissue culture dish	Griener Bio One
Tissue culture flasks - T25 and T75	Nunc
Universal vials	Sarstedt

2.1.2.A Purified Water

Ultra-pure deionised water (ddH₂O) was produced via a Purite Prestige Labwater 250 purification system. Water > 18 MΩ was obtained from a Purite Neptune Labwater system.

2.1.2.B Sterilisation

Glassware was washed in RBS detergent and rinsed in cold water followed by ddH₂O before being dried in a hot air oven at 80 °C. Glassware was then either hot air sterilised at 180 °C or sterilised by autoclaving in a MP24 Rodwell autoclaver supplied by Scientific Laboratory Supplies. Solutions requiring sterilisation were also autoclaved. Autoclaving was carried out at 15 p.s.i and 120 °C for 15min.

Filter sterilisation was used to sterilise solutions used in tissue culture and this was carried out using sterile syringe filters (0.22 µm pore size) or bottle top filter units (0.2 µm) depending on the volume to be sterilised.

2.1.3 Chemicals

Item	Company
AccuGel™ acrylamide (40%)	National Diagnostics
Agar	Fisher Scientific
Ammonium persulphate (APS)	BDH laboratory supplies
5-Azacytidine	Sigma-Aldrich
β-mercaptoethanol	Sigma-Aldrich
Boric Acid	Fisher Scientific
Bovine serum albumin (BSA)	Sigma-Aldrich
Bromodeoxyuridine (BrdU)	Sigma-Aldrich
Bromophenol blue	Sigma-Aldrich
Deoxynucleoside triphosphate set, PCR grade	Roche
Diethylpyrocarbonate (DEPC)	Sigma-Aldrich
DNA loading dye (5x)	Bioline
EDTA	Fisher Scientific
Ethanol	Fisher Scientific
Ethidium bromide	Sigma-Aldrich
Glacial acetic acid	Fisher Scientific
Glycerol	Fisher Scientific
Glycine	Fisher Scientific
Goat serum donor herd	Sigma-Aldrich
Hydrochloric acid (HCl)	Fisher Scientific
Hyperladder I	Bioline
Industrial methylated spirit	Adams
Isoproponal	Fisher Scientific
Magnesium chloride (MgCl ₂)	Fisher Scientific
Magnesium sulphate (MgSO ₄)	Fisher Scientific
Methanol	Fisher Scientific
Methylene blue	Sigma-Aldrich
NP40 alternative	Calbiochem
Paraformaldehyde	BDH Laboratory Supplies
Phenol:chloroform:isoamyl alcohol (25:24:1)	Sigma-Aldrich

Item (Continued)	Company
Phosphatase inhibitors	Sigma-Aldrich
PMSF	Sigma-Aldrich
Polybrene (hexadimethrine bromide)	Sigma-Aldrich
Potassium chloride (KCl)	BDH Laboratory Supplies
Power SYBR [®] green PCR master mix (2x)	Applied Biosystems
Protease inhibitors	Sigma-Aldrich
Propidium iodide (PI)	Sigma-Aldrich
RNaseA	Sigma-Aldrich
SeaKem [®] LE agarose	Cambrex
Sodium carbonate (Na ₂ CO ₃)	Fisher Scientific
Sodium chloride (NaCl)	Fisher Scientific
Sodium deoxycholate (DOC)	Sigma-Aldrich
Sodium dodecyl sulphate (SDS)	BDH Laboratory Supplies
Sodium hydroxide pellets	Fisher Scientific
SYBR safe [™] DNA gel stain	Invitrogen
TEMED	Sigma-Aldrich
Tris-base	Fisher Scientific
TritonX-100	Sigma-Aldrich
Tryptone	Fisher Scientific
Tween 20	Sigma-Aldrich
Ultra pure protogel acrylamide (30%)	National Diagnostics
Universal developer	Ilford Hypam
Universal fixer	Ilford Hypam
Yeast extract	Oxoid

2.1.4 Cytotoxic Agents

All chemicals were obtained from Sigma-Aldrich

Cytotoxic Agent	Mechanism of Action	Diluent	Standard Doses (24 h unless otherwise stated)
Camptothecin (CPT)	Stabilises topoisomerase I bound to DNA preventing DNA re-ligation	DMSO	10 nM
Cisplatin (CIS)	Forms intra- and interstrand DNA cross-links (ICLs)	Dissolved in DMSO then diluted in growth medium	Up to 2 μ M for continuous exposure
Hydroxyurea (HU)	Inhibits ribonucleotide reductase	Growth Medium	0.5 mM
Hydrogen Peroxide (H ₂ O ₂)	Causes oxidative stress	N/A	100 μ M
Ionising radiation (IR)	Causes double strand breaks	N/A	10 Gy delivered 2 h prior to experimentation
Methyl methanesulfonate (MMS)	Alkylating agent that leads to methylation damage	DMSO	0.5 mM for 30 min
Mitomycin C (MMC)	Alkylating agent that leads to the formation of inter-strand DNA cross-links (ICLs)	Growth Medium	90 nM for 24 h or 500 ng/ml (15 μ M) for 1 h
Thymidine (dT)	Suppresses synthesis of dCTP	Growth Medium	10 mM
Ultraviolet irradiation (UV) (254 nm)	Leads to the formation of intra-strand DNA cross-links	N/A	40 J/M ² delivered 5 h prior to experimentation

2.1.5 Selective Agents

Selective agent	Company	Diluent	Standard doses
Ampicillin	Sigma-Aldrich	Sterile, ddH ₂ O	100 µg/ml
G418	Melford	PBS	300 µg/ml
6-Thioguanine	Sigma-Aldrich	1% Sodium carbonate	5 µg/ml
Puromycin	Calbiochem	PBS	2 - 3 µg/ml
Tetracycline	Fisher Scientific	PBS	1 µg/ml

2.1.6 Antibodies

Primary Antibody	Raised In	Company	Protein Size	Dilution Factor	
				WB	IF
ATM	Mouse	Santa Cruz Biotechnology	370 kDa	1:1000	
β-ACTIN	Rabbit	Sigma-Aldrich	37 kDa	1:2000	
BrdU	Mouse	Dako Cytomation	-	-	-
CYP450R	Rabbit	Abcam	78 kDa	1:1000	
DNA-PK _{CS}	Rabbit	Santa Cruz Biotechnology	460 kDa	1:1000	
ERCC1	Mouse	Neomarkers	36 kDa	1:1000	
FANCD2	Rabbit	Novus Biologicals	155 kDa 166kDa	1:10,000	
FANCD2	Mouse	Santa Cruz Biotechnology	155 kDa 166 kDa	-	1:1000
FEN1	Rabbit	Cell Signalling	42 kDa	1:2500	
KU70	Rabbit	Genetex Inc.	70 kDa	1:2000	
LIGIII	Rabbit	Genetex Inc.	100 kDa	1:1000	
LIGIV	Rabbit	Abcam	104 kDa	1:1000	
MLH1	Mouse	Calbiochem	85 kDa	1:1000	
MRE11	Rabbit	Calbiochem	85 kDa	1:1000	
MSH2	Mouse	Calbiochem	100 kDa	1:1000	
NBS1	Rabbit	Cell Signalling Technology	95 kDa	1:1000	
NQO1	Goat	Abcam	30 kDa	1:1000	

Primary Antibody (continued)	Raised In	Company	Protein Size	Dilution Factor	
				WB	IF
P53	Goat	Santa Cruz Biotechnology	53 kDa	1:1000	
PARP-1	Mouse	Santa Cruz Biotechnology	100 kDa	1:1000	
RAD50	Rabbit	Bethyl Laboratories Inc.	150 kDa	1:1000	
RAD51	Rabbit	Santa Cruz Biotechnology	37 kDa	1:1000	1:500
RAD51C	Mouse	Novus Biologicals	42 kDa	1:1000	
RAD51D	Mouse	Novus Biologicals	40 kDa	1:1000	
RPA-70	Mouse	Fisher Scientific	70 kDa	1:1000	
RTEL	Rabbit	Abcam	152 kDa	1:1000	
γ H ₂ A.X	Rabbit	Cell Signalling	15 kDa	-	1:500
XRCC1	Rabbit	Novus Biologicals	90 kDa	1:2000	
XRCC3	Mouse	Novus Biologicals	38 kDa	1:1000	

Secondary Antibody	Company	Dilution Factor	
		WB	IF
Alexa-fluor 488 [®] goat anti-mouse IgG FITC conjugate	Invitrogen		1:1000
Anti-rabbit IgG, HRP-linked	Cell Signalling Technology	1:2000	
Anti-mouse IgG, HRP-linked	Cell Signalling Technology	1:2000	
Anti-goat IgG, HRP-linked	Santa Cruz Biotechnology	1:2000	
FITC-conjugated goat anti-mouse	Dako Cytomation	-	-
Zymax Cy3 conjugated goat anti-rabbit IgG	Invitrogen		1:500

2.1.7 Kits and Company Reagents

Kit	Company
Cell Proliferation Kit I (MTT)	Roche
CometAssay TM Reagent Kit	Trevigen [®]
CpGenome TM DNA Modification Kit	Chemicon [®] International
Endofree [®] Plasmid Purification Maxi Kit	Qiagen
GenElute TM Mammalian Genomic DNA Miniprep Kit	Sigma-Aldrich
GenElute TM Mammalian Total RNA Kit	Sigma-Aldrich
GenElute TM PCR Clean-Up Kit	Sigma-Aldrich
Lipofectamine TM 2000 Transfection Reagent	Invitrogen
MAX Efficiency [®] Stbl2 Competent Cells	Invitrogen
One-Shot [®] TOP10 Competent E.coli	Invitrogen
Platinum [®] Taq DNA Polymerase	Invitrogen
RiboQuant TM Multiprobe Template Sets	Pharmingen
RPA III TM Kit	Ambion
Superscript TM Reverse Transcriptase	Invitrogen
T7 MAXIscript TM Kit	Ambion

2.1.8 Cell Lines

Cell Line	Genotype	Reference
MRC5VA	Transformed human fibroblast cell line	(Jacobs et al., 1970)
U2OS	Transformed human osteocarcinoma cell line	(Ponten and Saksela, 1967)
HCT116	Transformed human colon carcinoma cell line. Has mutant MRE11 and is mismatch repair deficient	(Brattain et al., 1981)
SW480	Transformed human colorectal carcinoma cell line	(Mohindra et al., 2002)
WM793	Cutaneous melanoma cell line established from the vertical growth phase of a primary melanoma lesion of a 39 year old male, caucasian patient	(Hsu, 1999)
SOM 157	Uveal melanoma cell line established from a choroid tumour containing epithelioid cells	Ocular Oncology Unit, Sheffield
SOM 196	Uveal melanoma cell line established from a choroid tumour containing spindle cells	Ocular Oncology Unit, Sheffield
293-GPG	Retro-viral packaging cell line derived from the transformed human kidney cell line HEK293 (Graham et al., 1977)	(Ory et al., 1996)
PD20	FANCD2 deficient immortalised fibroblast cell line, derived from a FA patient	(Timmers et al., 2001)
PD20-D2	PD20 immortalised fibroblast cell line retrovirally complemented with pMMP-FANCD2	(Timmers et al., 2001)

2.1.9 Plasmids

- The pMMP-empty vector and the pMMP-FANCD2 vector were both kind gifts from Dr. Alan D'Andrea at the Dana-Farber Cancer Institute, in Boston, Massachusetts (Appendix 2).

- The pEF-P450R-IRES-P vector was a kind gift from Dr. Kaye Williams at the School of Pharmacy and Pharmaceutical Sciences, University of Manchester, Manchester (Appendix 3).

2.1.10 Preparation of Standard Solutions

2.1.10.A 1x Phosphate Buffered Saline (PBS)

1x PBS was produced by dissolving 1 Oxoid PBS tablet in 100 ml of ddH₂O. This was autoclaved and stored at room temperature.

2.1.10.B Tris-Buffered Saline (TBS)

10x TBS was made by dissolving 24.2 g of Tris base and 80 g of NaCl in a small volume of ddH₂O. The solution was then adjusted to pH 7.6 using HCl before adding sufficient ddH₂O to make the total volume 1 L. The 10x stock was autoclaved and kept at room temperature.

2.1.10.C 1 M Tris pH 6.8, 7.4 and 8

121.14 g of tris(hydroxymethyl)aminomethane was dissolved in 700 ml of ddH₂O. The solution was adjusted to the required pH using HCl and sufficient ddH₂O was added to achieve a total volume of 1 L. The solutions were autoclaved before being stored at room temperature.

2.1.10.D 1.5 M Tris pH 8.8

1.5 M Tris was made by dissolving 181.71 g of tris(hydroxymethyl)aminomethane in 700 ml of ddH₂O and the solution was adjusted to pH 8.8 using HCl. Sufficient ddH₂O was added to achieve a total volume of 1 L and the solution was autoclaved before being stored at room temperature.

2.1.10.E Ethidium bromide

A 100 mg tablet was dissolved in 20 ml of ddH₂O to produce a 5 mg/ml stock of ethidium bromide. The stock was foil-wrapped and stored at room temperature. The working concentration was 0.5 µg/ml.

2.1.10.F 0.5 M EDTA

186.1 g disodium ethylene diamine tetra-acetate was added to 750 ml of ddH₂O. The pH was adjusted as required by the addition of solid sodium hydroxide pellets. The volume was then adjusted to 1 L with ddH₂O and the solution was stored at room temperature.

2.1.10.G SOB medium and agar

SOB medium was made up of 10 mM NaCl, 2.5 mM KCl, 10 mM MgCl₂, 10 mM MgSO₄, 2% Tryptone and 0.5% Yeast extract in ddH₂O. This suspension was autoclaved and stored at room temperature. Prior to use 100 µg/ml of ampicillin was added to the medium as the selective marker. For solid culture medium, 1.5% agar was added to the above solution prior to autoclaving.

2.1.11 Tissue Culture Reagents

2.1.11.A Foetal Calf Serum (FCS)

Foetal Calf Serum was purchased from Biosera that had previously been screened for virus, endotoxin and mycoplasma, and filter sterilised before use. Aliquots of which were stored at -20 °C.

2.1.11.B DMEM

All cell lines were cultured in Dulbecco's modified Eagle's medium (DMEM) purchased from Lonza containing 4.5 g/L glucose with glutamine. 500 ml DMEM was supplemented with 10% FCS. Medium was stored at 4 °C, heating to 37 °C before use.

2.1.11.C Trypsin and Versene/EDTA

A sterile 2.5% solution of trypsin was supplied by Invitrogen and stored at 4 °C. The working concentration of trypsin was 0.025%. Versene/EDTA was supplied by VWR. A stock solution was made by dissolving 0.2 g in 1 L of phosphate buffered saline (PBS) and this was stored as 10 ml aliquots at 4 °C. The working concentration of Versene/EDTA was 0.02%.

2.1.11.D DiMethyl Sulphoxide (DMSO)

DMSO prevents crystal formation within the cells that minimises the disruption of cell membranes and general damage to the cells whilst stored at -80 °C. DMSO was purchased from BDH Laboratory Supplies and used as a 10% supplement of growth medium in the cryopreservation of cells.

2.1.11.E Presept

Presept was supplied by Johnson and Johnson Medical Ltd and was prepared by dissolving 20 tablets in 2 L of tap water. This solution was stored at room temperature.

2.2 Methods

2.2.1 Bacterial Studies

2.2.1.A Transformations

2.2.1.A.1 *One Shot*[®] *TOP10 Chemically Competent Escherichia coli (E. coli)*

2 µl (~ 10 pg) of plasmid DNA was added to one vial of *One Shot*[®] *TOP10* chemically competent *E. coli* (Invitrogen) and then incubated on ice for 5 min. The cells were then heat shocked at 42 °C for 30 s without shaking and transferred back onto ice. 250 µl of SOB medium (10 mM NaCl, 2.5 mM KCl, 10 mM MgCl₂, 10 mM MgSO₄, 2% Tryptone and 0.5% Yeast extract in ddH₂O) without antibiotics, was added to the transformed cells and shaken horizontally at 37 °C for 1 h. 50 µl and 150 µl of bacteria were inoculated onto selective SOB-agar plates (SOB medium with 1.5% agar and 100 µg/ml ampicillin as selective agent) pre-warmed at 37 °C in the presence of a flame using a glass spreader, and incubated at 37 °C overnight to form single colonies.

2.2.1.A.2 *MAX Efficiency*[®] *Stbl2 Chemically Competent Cells*

The *MAX Efficiency*[®] *Stbl2* chemically competent cells (Invitrogen) were used for the transformation of the pMMP plasmids. These cells, unlike the *One Shot*[®] *TOP10* chemically competent *E. coli*, have a set of genetic markers that allow the stabilisation of unstable retroviral sequences. Thus, they were used here to reduce the risk of recombination, a common occurrence in pMMP plasmids. 1 µl (0.1 µg) of plasmid

DNA was added to 45 μ l of MAX Efficiency[®] *Stbl2* competent cells and incubated on ice for 30 m. The cells were then heat shocked at 42 °C for 25 s without shaking and transferred back onto ice for a further 2 m. 250 μ l of SOB medium without selection was added to the cells before shaking at 225 rpm at 30 °C for 90 m. Using a glass spreader, 50 μ l and 150 μ l of the bacterial suspension was spread onto pre-warmed selective SOB-agar plates (100 μ g/ml ampicillin) in the presence of a flame, and incubated at 30 °C for 24 h to form single colonies.

2.2.1.B Bacterial Culture

To expand the single colonies, individual colonies were picked from the SOB-agar plates using a pipette tip in the presence of a flame and placed in a universal vial containing 2 ml of selective SOB medium. Bacterial growth was then induced by shaking at 37 °C in a shaking incubator for 4 – 6 h. From this starter culture, 50 μ l was added to 50 ml of selective SOB medium in the presence of a flame and further incubated in a shaking incubator overnight at 37 °C.

2.2.2 DNA Studies

2.2.2.A Plasmid Purification using the Endofree[®] Plasmid Purification Maxi Kit

The Endofree[®] plasmid purification maxi kit (Qiagen) was used to purify plasmid DNA for use in subsequent transfections and was carried out according to the manufacturers' instructions. The kit uses a modified alkaline lysis procedure (Birnboim and Doly, 1979) followed by the binding of the plasmid DNA to the Qiagen Anion-Exchange Resin. The plasmid DNA was then washed in a medium-salt wash solution to remove cellular impurities such as RNA and protein and eluted into a high salt buffer. The salt was then removed and the DNA concentrated by the subsequent isopropanol precipitation.

2.2.2.B DNA extraction using the GenElute[™] Mammalian Genomic DNA Miniprep Kit

The GenElute[™] mammalian genomic DNA miniprep kit (Sigma-Aldrich) was used to extract pure genomic DNA from at least 1×10^7 cultured cells. The kit is based on silica binding and was carried out in accordance with the manufacturers' instructions. The

cells were first lysed in a chaotropic salt-containing solution to denature macromolecules. In the presence of ethanol, the DNA binds to a silica membrane when the lysate is spun through the membrane by centrifugation. The DNA was then washed to remove contaminants and eluted in 200 μ l of TE solution (10 mM Tris-HCl, 5 mM EDTA, pH 9.0).

2.2.2.C Quantification

Spectrophotometric analysis was carried out to quantify the resulting DNA from 2.2.2.A and 2.2.2.B. This was done using the Nanodrop 2000 system from ThermoScientific. Absorbance was measured at 260 nm and 280 nm to check for contaminants, where an absorbance of 1.0 at 260 nm corresponded to 50 μ g/ml of dsDNA.

2.2.3 Methylation Studies

Methylation of cytosines located 5' to guanosine (CpG sites) is known to have a profound effect on the expression of many eukaryotic genes (Bird, 1992). Although CG-rich regions called CpG islands are largely unmethylated, aberrant methylation of these areas is a frequent event and has been associated with transcriptional inactivation of many tumour suppressor genes in human cancer (Baylin et al., 2001; Robertson, 2002). Here, genomic DNA was first subjected to sodium bisulphite modification using the CpGenome™ DNA modification kit, followed by PCR amplification and DNA sequencing, to determine the methylation status of the *FANCD2* promoter in uveal melanoma cell lines compared to other human control cell lines.

2.2.3.A Bisulfite Modification using the CpGenome™ DNA Modification Kit

The CpGenome™ DNA modification kit from Chemicon® International was used for the sodium bisulphite modification of 1 μ g of genomic DNA and carried out in accordance with the manufacturers' instructions. In a sodium bisulphite reaction, all unmethylated cytosines are deaminated and sulfonated, converting them to uracils leaving methylated cytosines (5-methylcytosines) unchanged (Figure 2.1). The sequence of the treated DNA therefore differs from the untreated sequence depending on whether the CpG sites were originally methylated or unmethylated.

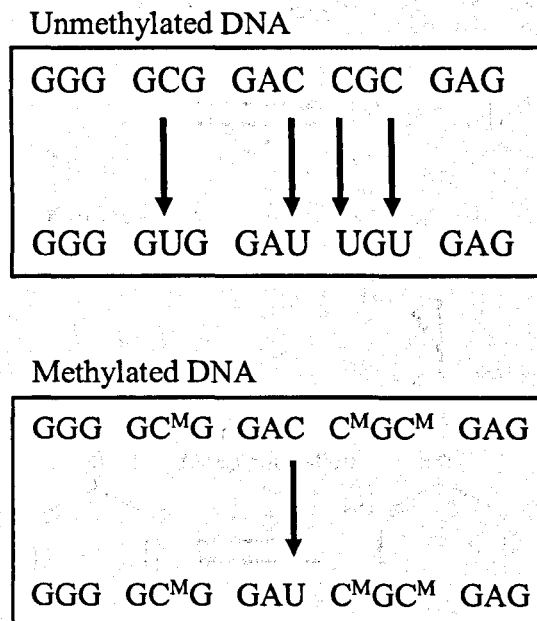


Figure 2.1 Sodium bisulphite modification of DNA

All unmethylated cytosines (C) are deaminated to uracils (U) whereas 5-methylcytosines (C^M) remain unchanged.

Using the CpGenome™ DNA modification kit for sodium bisulphite treatment, the DNA was first denatured to its single-stranded form to expose the bases using an alkaline pH at 50 °C. A sodium salt of bisulfite ion (HSO₃⁻) was then added, this causes unmethylated cytosines to be sulfonated and hydrolytically deaminated to produce a sulfonate intermediate (Figure 2.2). The DNA was then bound to a micro-particulate carrier in the presence of another salt, and then desalted by the addition of 70% ethanol. Alkaline desulfonation and desalting in 90% ethanol completes the conversion to uracil and the DNA was finally eluted in TE buffer.

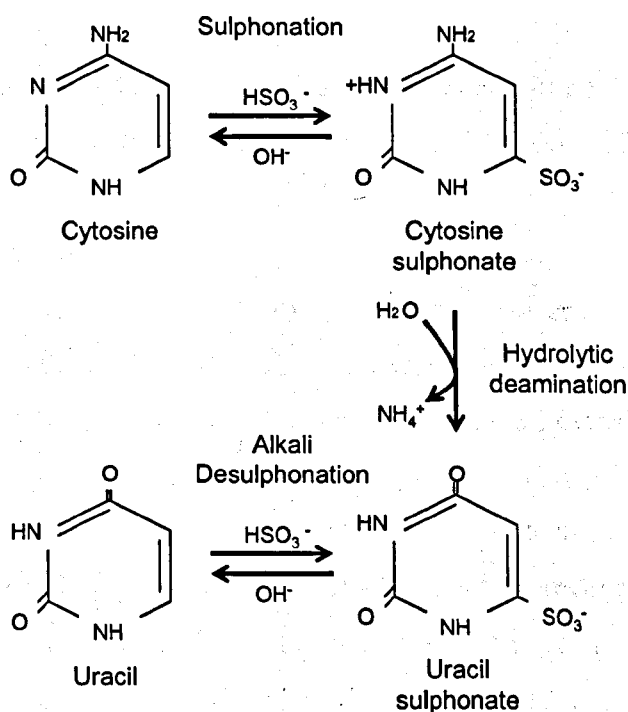


Figure 2.2 The chemical process of deaminating cytosine to uracil by sodium bisulphite modification

Cytosines are first sulfonated to cytosine sulphate and then hydrolytically deaminated to produce the sulphate intermediate, uracil sulphate. Alkaline desulphonation and desalting in 90% ethanol completes the conversion of cytosine to uracil.

2.2.3.B The Polymerase Chain Reaction (PCR)

PCR is an *in vitro* method for enzymatically synthesising defined sequences of DNA (Saiki et al., 1985). The reaction uses two pre-designed oligonucleotides known as primers that hybridise to, and flank either end of, a target sequence. The system consists of a number of phases of differing temperatures carried out in a thermocycler, which allows the exponential amplification of the DNA target sequence. The first step is a denaturation phase that separates the double helix structure of DNA. This is followed by primer annealing, where the primers bind to the separated strands of the DNA, flanking the target sequence. Finally, an extension phase is used to lengthen the primers according to the template DNA sequence using the thermo-stable enzyme *Taq* DNA polymerase.

2.2.3.C Primer Design

Primers were ordered from Invitrogen and designed to amplify a 1000 bp region of the human *FANCD2* promoter (GenBank accession number NG_007311). Three sets of overlapping primer pairs were designed for the amplification of the sodium bisulphite modified DNA. Following modification, DNA becomes fragmented and very unstable therefore three primer pairs were used to generate three shorter amplicons, spanning the whole 1000 bp promoter region. These primers were designed specifically for sodium bisulphite modified DNA. To do this, it was assumed that all cytosines not at CpG sites were converted to uracils by the modification process. The primer sequences were therefore designed so that thymines replaced all cytosines thus, during PCR amplification, uracil bases in the modified DNA would be recognised by the thymine bases in the primer sequences. CpG sites that may have been originally methylated before modification were avoided. The primers were designed as follows:

Primer Sets	Primer Sequence (5' to 3')	Size of Amplicon
Primer Set 1	Forward – TTTTATTTTAGGAAGGGAAATG Reverse – AGGATTATTTAGAGGTAGATGTTGGA	666 bp
Primer Set 2	Forward – TGATTTTTATTTGTTTATGAGGGAG Reverse – AGGATTATTTAGAGGTAGATGTTGGA	327 bp
Primer Set 3	Forward – TGGGTAGGATTATTTAGAGGTAGATG Reverse – TTTTTTGTGGTTTAATTTTAAGTT	408 bp

2.2.3.D PCR set up using Platinum[®] *Taq* DNA Polymerase

High background and low product yield can often result from the assembly of a PCR reaction at room temperature, due to the formation of unspecific primer annealing and primer dimer formation created by the premature activity of the *Taq* DNA polymerase. This is a particular problem with sodium bisulphite modified DNA due to its instability following the modification process. Using a polymerase antibody that blocks polymerase activity at ambient temperatures is therefore essential. Platinum[®] *Taq* DNA polymerase from Invitrogen is recombinant *Taq* DNA polymerase coupled with a proprietary antibody that blocks polymerase activity at ambient temperatures. The activity of the polymerase is restored after the initial denaturation step in PCR at 95 °C,

therefore allowing more convenient PCR set up at room temperature. Each PCR reaction was set up as follows:

Component	Volume	Final Concentration
10x PCR Buffer	5 μ l	1x
10 mM dNTP Mix	1 μ l	0.2 mM each
50 mM MgCl ₂	1.5 μ l	1.5 mM
10 μ M Forward Primer	1 μ l	0.2 μ M
10 μ M Reverse Primer	1 μ l	0.2 μ M
Template DNA	2 μ l	100 – 200 ng
Platinum [®] <i>Taq</i> DNA polymerase	0.2 μ l	1.0 unit*
Autoclaved, ddH ₂ O	To 50 μ l	N/A

* Where 1 Unit of Platinum[®] *Taq* polymerase incorporates 10 nmol of deoxyribonucleotide into acid-precipitable material in 30min at 74 °C.

2.2.3.E PCR Conditions

The PCR reactions were thermocycled in a DNA Engine Peltier thermal cycler from BioRad using the following conditions:

Denaturation	95 °C	4 min	}	5 cycles
Denaturation	95 °C	30 s		
Annealing	54 °C	90 s		
Extension	72 °C	2 min	}	25 cycles
Denaturation	95 °C	30 s		
Annealing	54 °C	90 s		
Extension	72 °C	90 s	}	
Extension	72 °C	4 min		

Due to the poor quality of sodium bisulphite modified DNA, a second round of PCR amplification was needed in order to yield enough target DNA for sequencing. Here, the second reaction was assembled as the first, but using 2 μ l of the first round PCR product

as template DNA. The second reaction was then thermocycled again using the same conditions as the first round.

2.2.3.F Agarose Gel Electrophoresis

Agarose gel electrophoresis was used to separate the target PCR product from non-specific amplicons for subsequent purification and sequencing. 1% agarose gels were made by adding 2 g SeaKem[®] LE agarose in 200 ml 1x TAE buffer (400 mM Tris base, 10 mM EDTA pH 8 and 1.1% Glacial Acetic Acid, pH 7.6 - 7.8 in ddH₂O) before heating the suspension in a microwave to dissolve the agarose. The solution was then left at room temperature to cool before adding 0.5 µg/ml ethidium bromide to visualise the DNA. The cooled agarose was poured into a mould containing a comb to produce wells and was left at room temperature to set. The comb was then removed and the gel immersed in 1x TAE in the gel tank. 20 µl of the PCR product was mixed with 5x DNA loading dye (Bioline) and loaded onto the gel alongside 5 µl of Hyperladder 1 DNA size ladder (Bioline). The gel was run at 80 V for 1 h to separate the bands of DNA. The gel was then visualised and documented using the UGenius gel imaging system (Geneflow).

2.2.3.G PCR product purification using the GenElute[™] PCR Clean-Up Kit

The GenElute[™] PCR clean-up kit (Sigma-Aldrich) was used to purify the PCR amplification products from the other components in the reaction such as excess primers, nucleotides, DNA polymerase, oils and salts. It is based on silica binding and was used following the manufacturers' instructions. Briefly, the DNA was bound onto a silica membrane by centrifugation and contaminants removed by an ethanol based wash solution. Finally, the bound DNA was eluted into TE buffer and quantified as in 2.2.2.C.

2.2.3.H Sequencing

Sequencing was carried out on 100 ng/µl samples by the Genetics Core Facility in the University of Sheffield Medical School. The same primers used for the amplification of the target sequence were used for sequencing at a concentration of 1 µM. Sequencing was carried out using an ABI 3730 capillary sequencer and data analysed using Sequencher[™]4.1.

2.2.3.I Genome-wide demethylation using 5-azacytidine treatment

5-azacytidine is an analogue of cytidine and thus becomes incorporated into the DNA at these sites. Due to its altered structure, methyl groups can no longer be covalently bound at these sites by DNA methyltransferase. Thus, 5-azacytidine treatment causes genome-wide demethylation of cytosine bases. To study the affects of genome-wide demethylation in uveal melanoma cell lines, cells were treated for 5 consecutive days with 5-azacytidine. Cells were seeded into T75 sterile flasks and then left under normal incubation conditions to adhere. The next day, 2.5 mM 5-azacytidine was added to the cells and the cells returned to normal incubation conditions. This was repeated for 5 consecutive days after which time toxicity assays and western blot analysis was carried out as in 2.2.4.E and 2.2.7, respectively.

2.2.4 Tissue Culture Studies

All work was carried out in containment 2 laboratory cabinets to maintain sterility and cabinets were cleaned with methanol before and after use. Cultured cells were grown in DMEM supplemented with 10% FCS (referred to as growth medium throughout), unless otherwise stated, and were incubated at 37 °C in a humid environment containing 5 – 10% CO₂.

2.2.4.A Maintenance, Storage and Passage of Cell Lines

Cells were grown in a monolayer on the surface of a T75 flask until seen to be 70 - 80% confluent under a light microscope. Passage of the cells involved removing the growth medium and washing twice with PBS. 1 ml Trypsin/Versene mix was then added and the cells placed in an incubator at 37 °C until the cells were seen to be free from the flask side. The cells were then fully resuspended in 9 ml growth medium by pipetting. The appropriate volume of cells for the dilution required (usually 1 in 3 to achieve confluence in 2 days) was placed into a new sterile T75 flask and fresh growth medium added to a total volume of 10 ml.

2.2.4.B Cryopreservation

Aliquots of each cell line were kept for long term storage at -80 °C. Cells were passaged as in 2.2.4.A except that the fully resuspended cells in 10 ml growth medium were placed in 15 ml falcon tubes and centrifuged at 2000 rpm for 3 m. The growth medium

was poured off and the pellet resuspended in 3 ml 10% DMSO in growth medium. Approximately 1 ml was aliquoted into two 1.2 ml cryovials and then placed at -80 °C.

2.2.4.C Thawing of Cells

Cells were thawed quickly in a 37 °C waterbath to minimise the toxic effects of DMSO and placed in a 15 ml falcon tube and centrifuged at 2000 rpm for 3 m. The medium was poured off and the pellet was resuspended in 5 ml PBS and centrifuged again. The pellet was then resuspended in 10 ml medium, placed in a T25 flask and incubated as normal at 37 °C.

2.2.4.D Counting Cells

Cells were counted using a Neubauer haemocytometer (Hawksley & Sons Ltd). Once cells were resuspended as in 2.2.4.A, 7 µl was placed under the cover slip of a haemocytometer and the average of 4 squares (5x 5 squares) was calculated. This value was then multiplied by 10,000 to give the number of cells/ml.

2.2.4.E Toxicity Assays

Toxicity assays were used to determine the cytotoxic response to various cytotoxic agents, of uveal melanoma cell lines compared to control cell lines. Cells that were less than 80% confluent were trypsinised and quantified as in 2.2.4.A and 2.2.4.D. 500 – 5000 cells were then plated in 10 ml growth medium on 100 mm plates. Cells were then placed under normal incubation conditions for 4 h to allow cells to adhere. After this time the cytotoxic agents were added to the medium in a range of 8 increasing doses. All treatments were continuous except for MMS that was removed after 30min and H₂O₂ that was removed after 2 h, and replaced with 10 ml fresh growth medium. Plates were then further incubated at 37 °C with 5% CO₂ for 15 days. After this time, the growth medium was removed from the plates and the viable colonies fixed and stained with methylene blue (4 g in 500 ml methanol) for 30 m. The stain was then removed using cold tap water and the plates left to dry before the colonies were counted using a colony counter. The survival fraction was calculated for each cell line by dividing the number of colonies at each dose by the number of colonies counted at dose zero. Only colonies with more than 50 cells were counted.

2.2.4.F Colorimetric Assay using the Cell Proliferation Kit I (MTT)

The colorimetric (MTT) assay kit from Roche was used as an alternative to the toxicity assays to study the viability of primary uveal melanoma tumour samples in the presence of MMC and to determine the proliferation rate of uveal melanoma cell lines compared to other established human cancer control cell lines. This kit allows the reliable quantification of viable cells as only metabolically active cells are able to cleave the yellow tetrazolium salt, MTT (3-[4, 5-dimethylthiazol-2-yl]-2, 5-diphenyltetrazolium bromide) to purple formazan crystals (Figure 2.3). The resulting crystals are then solubilised and the absorbance quantified using spectrophotometry. The absorbance directly correlates to the total metabolic activity in the sample and thus the number of viable cells within that same sample.

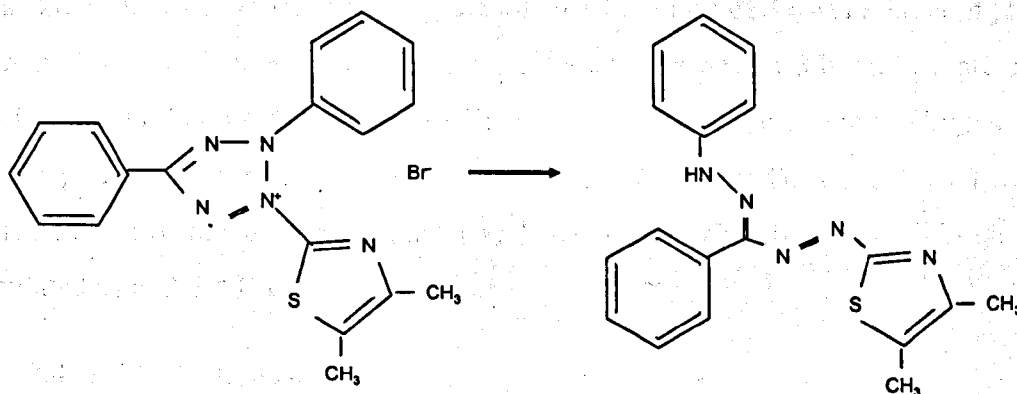


Figure 2.3 Metabolism of yellow MTT to a purple formazan salt by viable cells

Only viable cells can cleave the yellow tetrazolium salt, MTT to purple formazan salt and thus the absorbance can be quantified using spectrophotometry at OD 570 nm. This is directly proportional to the number of viable cells within a given sample.

2.2.4.F.1 The proliferation of primary uveal melanoma tumour samples in the presence of MMC

Cells were counted and plated in duplicate at a density of 500 cells/well of a 96-well plate for the primary uveal melanoma cells, and 250 cells/well for the established cell lines. The cells were then placed under normal incubation conditions for 4 h to allow cells to adhere. After this time, the cells were treated with increasing doses of MMC (0 – 50 μ M) and then left at 37 $^{\circ}$ C, under normal incubation conditions for 10 days. After

10 days, 1x MTT labelling reagent from the kit was added to each well at a dilution of 1 in 10. The cells were then placed back at 37 °C for 3 h, checking every 30min for the presence of purple formazan crystals. Once the crystals had formed, 100 µl of the 1x solubilisation solution from the kit was added and incubated overnight at 37 °C. The absorbance of each well was then measured at OD 570 nm on a plate reader and the relative absorbance (proliferation rate) calculated for each cell line by dividing the OD at each dose by the OD at dose zero.

2.2.4.F.2 MTT Proliferation Assay

Cells were counted and plated at a density of 250 cells/well of a 96-well plate in triplicate for each cell line. Cells were incubated under normal conditions for 4 h, 2 days, 4 days and 7 days, after which time a 1 in 10 dilution of the MTT labelling reagent from the kit was added to each well and incubated for a further 3 h until purple crystals had formed. Following this, 100 µl of 1x solubilisation solution from the kit was added and the plates were further incubated overnight at 37 °C. The OD of each well was then measured at 570 nm on a plate reader and the relative absorbance (proliferation rate) calculated as in 2.2.4.F.1.

2.2.4.G Fluctuation Assay

The fluctuation assay was used to determine the spontaneous mutation rate of the house-keeping gene *HPRT* in uveal melanoma cell lines. Within the cell, the nucleoside dGTP is catalysed from GMP (guanosine monophosphate) for use in DNA synthesis. There are two ways in which GMP can be formed either by *de novo* synthesis or by a functional *HPRT* gene. During *de novo* synthesis, GMP is catalysed from PRPP (phosphoribosyl pyrophosphate) using 10 different enzymatic steps. By using the *HPRT* enzyme however, GMP is formed from guanine and PRPP. The addition of the antimetabolite drug 6-Thioguanine (6-TG) to cells with a functional *HPRT* gene therefore causes cell death as it is incorporated into the DNA instead of guanine. Continual growth in 6-TG allows for the selection of cells with a *HPRT* gene that has mutated, as the 6-TG is no longer incorporated into the DNA allowing cells to survive (Figure 2.4). The rate at which this mutation occurs can then be calculated using the fluctuation test of Luria and Delbruck (Luria and Delbruck, 1943).

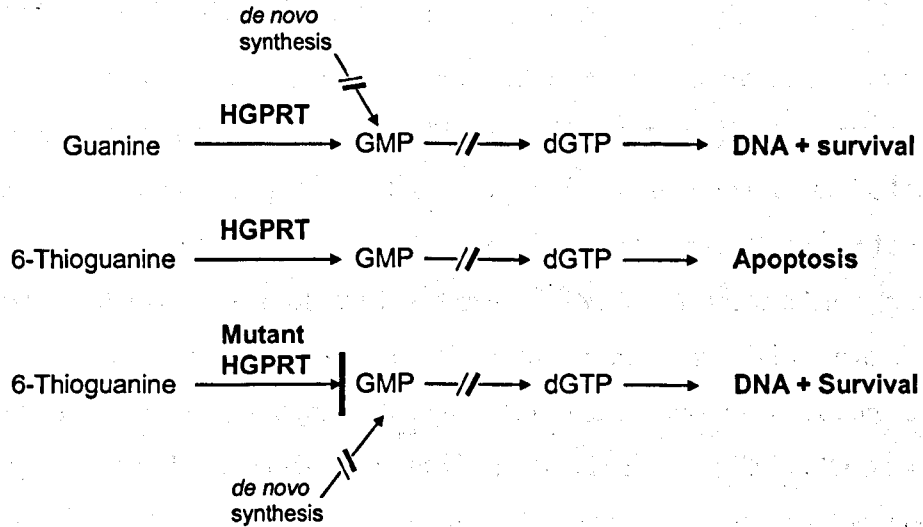


Figure 2.4 The *HPRT* mechanism of guanine metabolism for DNA synthesis

6-TG is incorporated into DNA by a functional *HPRT* gene instead of guanine causing cell death. A mutated *HPRT* gene results in survival as the drug can no longer become incorporated into the DNA through this mechanism. Guanine can now be incorporated by *de novo* synthesis and thus cells survive in the presence of 6-TG.

Cells were plated at a density of 1000 cells in 36 wells of 6-well plates and incubated under normal incubation conditions until 80 – 90% confluent. After this time, the cells were trypsinised, counted and replated 10 times at 1×10^5 cells/100 mm plate. 1 mg/ml of 6-TG was dissolved in 1% sodium carbonate and then 5 μ g/ml of this solution was added to the plates. The cells were then incubated for at least 15 days under normal incubation conditions before the colonies were stained and counted using methylene blue (4 g in 500 ml methanol) and a colony counter. The mutation rate was calculated using the Luria Delbruck method as follows:

$$\text{Rate of mutation} = \frac{\ln P_0}{N^\circ \text{ of cell generations}}$$

Where P_0 = the proportion of plates with no colonies

and the N° of cell generations =
$$\frac{(\text{the final } N^\circ \text{ of cells} - \text{the initial } N^\circ \text{ of cells})}{\ln 2}$$

2.2.4.H Retroviral Complementation

Retroviruses are used widely as an efficient method of complementing mammalian cells with new genetic material *in vitro* (Mulligan, 1993). Although retroviruses containing amphotropic envelope proteins have the ability to infect mammalian cells, human cells are relatively resistant to this infection (Emi et al., 1991). It was therefore found that by incorporating the vesicular stomatitis virus G (VSV-G) protein into amphotropic retrovirus vector particles, it was possible to create a retroviral pseudotype that possessed a wide host range, enhancing the efficiency of infection and hence complementation in human cells (Emi et al., 1991). The human 293GPG packaging cell line (Ory et al., 1996) can be used to create these retroviral pseudotypes as it continually expresses essential retroviral packaging proteins whilst providing large amounts of VSV-G by its inducible expression by tetracycline. Unlike other packaging cell lines that often lose their packaging efficiency through culture, 293GPG can be cultured in medium supplemented with 1 µg/ml tetracycline, 2 µg/ml puromycin and 300 µg/ml G418 to maintain the expression of these essential packaging proteins. Here, the pMMP-empty or pMMP-FANCD2 retroviral vector were first transfected into the 293GPG packaging cell line to produce the retroviral pseudotype, which could then be used to infect uveal melanoma cells to produce stable uveal melanoma cell lines complemented with FANCD2 (Figure 2.5).

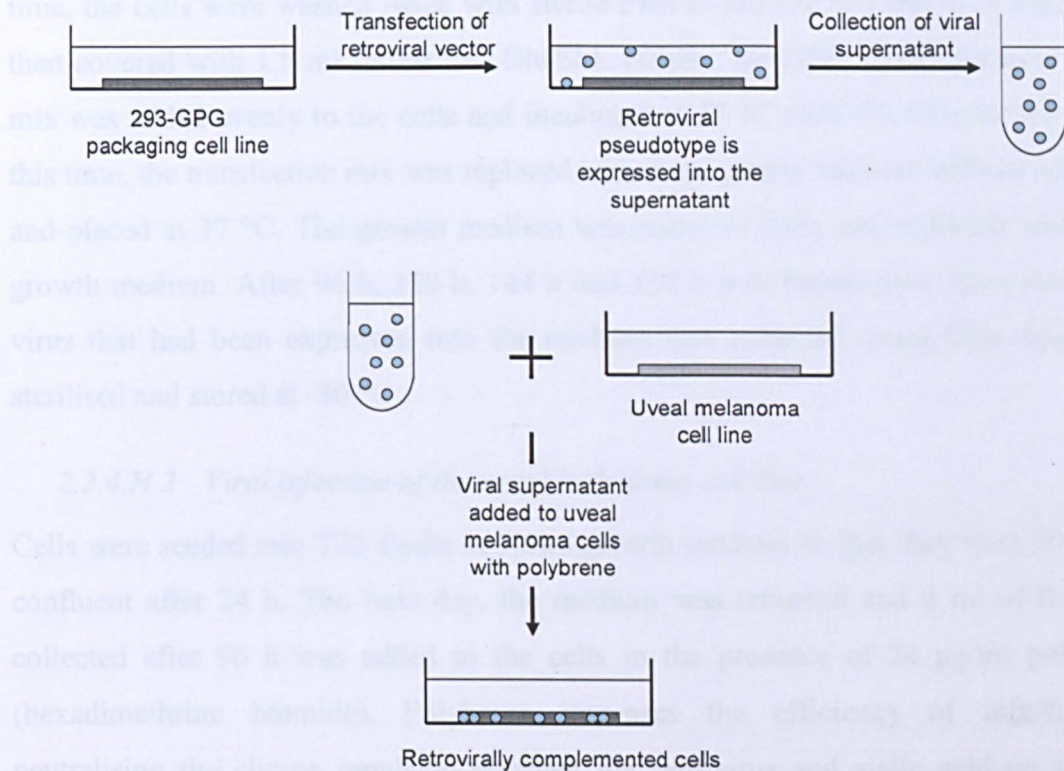


Figure 2.5 Method of retroviral complementation

The packaging cell line 293-GPG was first transfected with the retroviral vectors, pMMP-empty and pMMP-FANCD2, to produce the viral pseudotypes that were then collected from the medium 96, 120, 144 and 168 h post transfection. The collected pseudotypes were then used to infect the uveal melanoma cell line, SOM196b in the presence of polybrene to produce the complemented cell lines 196b-pMMP and 196b-D2.

2.2.4.H.1 Transfection using Lipofectamine™ 2000

Lipofectamine™ 2000 from Invitrogen was used to transfect the 293GPG packaging cell line with pMMP-empty and pMMP-FANCD2 retroviral vectors. Lipofectamine™ 2000 is a cationic lipid formulation commonly used for the delivery of plasmid DNA into eukaryotic cells. Cells were seeded in T25 flasks in 10 ml growth medium with selection so that they would be 90% confluent after 24 h. In a 1.5 ml sterile eppendorf tube, 5 µg of retroviral plasmid DNA was diluted in a total volume of 750 µl of serum free DMEM and left at room temperature for 15 m. In a second eppendorf tube, 10 µl of Lipofectamine™ 2000 was mixed with 750 µl serum free DMEM and then added to the first, mixed by inversion and left for another 15minat room temperature. During this

time, the cells were washed twice with sterile PBS to remove any traces of serum and then covered with 1.5 ml serum free DMEM. Finally, the DNA-lipofectamine™ 2000 mix was added evenly to the cells and incubated at 37 °C with 5% CO₂ for 6 h. After this time, the transfection mix was replaced with 5 ml growth medium without selection and placed at 37 °C. The growth medium was removed daily and replaced with fresh growth medium. After 96 h, 120 h, 144 h and 168 h post transfection, the pseudotype virus that had been expressed into the medium was collected using filter tips, filter sterilised and stored at -80 °C.

2.2.4.H.2 Viral infection of the uveal melanoma cell line

Cells were seeded into T25 flasks in 10 ml growth medium so that they were 80 - 90% confluent after 24 h. The next day, the medium was removed and 2 ml of the virus collected after 96 h was added to the cells in the presence of 24 µg/ml polybrene (hexadimethrine bromide). Polybrene increases the efficiency of infection by neutralising the charge repulsion between the retrovirus and sialic acid on the cell surface. The cells were placed back at 37 °C and the following day the viral containing medium was replaced with fresh growth medium. The cells were allowed 24 h to recover before the addition of the virus taken at 120 h. This procedure was repeated until all viral medium had been used. After the final viral containing medium had been washed off, cells were incubated in non-selective growth medium for 48 h. 3 µg/ml puromycin was then added to the medium to select for cells that had been successfully infected. Selection was maintained by continual growth in growth medium supplemented with 3 µg/ml puromycin.

2.2.5 Single cell gel electrophoresis assay using the Trevigen® CometAssay™ Reagent Kit

Alkaline single cell gel electrophoresis allows the evaluation of DNA damage in single cells based on the technique of microelectrophoresis (Ostling and Johanson, 1984; Singh et al., 1988). The assay is based on the principle that damaged, denatured DNA fragments have the ability to migrate out of the cell when an electric field is introduced whereas intact, supercoiled DNA migrates slower and therefore remains within the nucleus under the same conditions. Here, the CometAssay™ was used to evaluate the presence of DNA ICLs. Cells were first treated with MMC to allow the formation of

DNA ICLs. Following this, the cells were treated with IR to induce DSBs and to fragment the DNA. The induced ICLs hold the damaged DNA fragments together, causing them to move slower than non-crosslinked controls, and prevent them from migrating out of the cell under electrophoresis. Analysis was carried out using the average Tail Moment (TM) defined as the product of the amount of DNA in the tail and the mean distance of migration in the tail (Olive et al., 1990). From this, the MMC-induced percentage decrease in TM was calculated where the quantity of ICLs is proportional to the MMC-induced decrease in TM (Pichierri et al., 2002).

Cells were counted and plated at 1×10^6 cells/100 mm plate for each condition and incubated under normal conditions for 24 h. After this time, the cells were treated with $1 \mu\text{g/ml}$ MMC and returned to normal incubation conditions for 1 h. The cells were then scraped into 5 ml PBS using a cell scraper and centrifuged at 2000 rpm for 5 min at 4°C . The cells were then washed in PBS by centrifugation and resuspended in 3 ml PBS, and counted as in 2.2.4.D. 2×10^5 cells were transferred to a 1.5 ml eppendorf tube and treated with 10 GY IR. 25 μl of each cell sample was transferred to a 0.5 ml eppendorf tube and mixed with 250 μl of comet LMAgarose from the kit, which had previously been melted at 80°C for 10 min then kept molten at 37°C for at least 20 min before use. 75 μl of the agarose-cell mix was immediately transferred onto a CometSlide™ using the side of the pipette tip to ensure even coverage onto the sample area, and the slides incubated at 4°C for 20 min until set. The slides were immersed in prechilled Lysis solution from the kit (approx. 5 ml per slide) and incubated at 4°C for 1 h and then transferred to an alkaline solution $\text{pH} > 13$ (0.6 g NaOH pellets, 200 mM EDTA in 50 ml ddH₂O) for 1 h at room temperature in the dark. The slides were placed in a horizontal electrophoresis tank (Geneflow) equidistant from the electrodes, to which the alkaline electrophoresis buffer was carefully added (300 mM NaOH, 1 mM EDTA) until the slides were covered. The current was set to 20 V (1 Volt/cm) and the current set to 300 mA by the addition or removal of buffer. Electrophoresis was then carried out for 30 min at the controlled temperature of 4°C to reduce background damage and increase sample adherence. Following electrophoresis, the slides were carefully washed twice in ddH₂O for 5 min then immersed in 70% ethanol for 5 m. The slides were then left to dry at room temperature in the dark for approximately 20 min before adding 50

μl of 1x SYBR SafeTM DNA gel stain (1 μl of 10,000x SYBR SafeTM diluted in 10 ml TE buffer) onto each sample for 10 min and leaving at room temperature in the dark until dry. Samples were visualised using a Nikon TE200 inverted microscope and images recorded using a Hamamatsu C4742-95 digital camera. Analysis of the average TM from at least 100 cells was carried out using the TriTek CometScoreTM Freeware v1.5 software package. The MMC-induced percentage decrease in TM was then calculated using the formula set out below to determine the quantity of ICLs formed in each cell line (Pichierri et al., 2002).

$$\% \text{ decrease in TM} = 1 - \left(\frac{\text{TM of IR and MMC treated sample} - \text{TM of untreated sample}}{\text{TM of IR treated sample} - \text{TM of untreated sample}} \right) \times 100$$

2.2.6 RNA Studies

All RNA experimental work was carried out using filter tips, sterile eppendorf tubes and sterile ddH₂O that had been autoclaved so that it was known to be nuclease-free to stop the degradation of the RNA.

2.2.6.A RNA extraction using the GenEluteTM Mammalian Total RNA Kit

The GenEluteTM mammalian total RNA kit from Sigma-Aldrich was used to isolate total RNA from a flask containing 1×10^7 cells and was carried out according to the manufacturers' instructions. Briefly, cells were lysed in a buffer containing guanidine thiocyanate to ensure thorough denaturation of macromolecules and inactivation of RNases. Ethanol was then added to bind the RNA to a silica membrane during centrifugation. Contaminants were removed by washing and the RNA eluted in TE buffer. Quantification was carried out using the nanodrop system (2.2.2.C) measuring absorbance at 260 nm and 280 nm where an absorbance of 1.0 at 260 nm corresponds to 40 $\mu\text{g/ml}$ of RNA.

2.2.6.B cDNA Synthesis using SuperscriptTM II Reverse Transcriptase

For generating cDNA copies from total RNA extracts, SuperscriptTM II Reverse Transcriptase (Invitrogen) was used to reverse transcribe the RNA and was carried out

according to the manufacturers' instructions. Briefly, 1 μ l Oligo (dT)12-18 primer, 1 μ l dNTP Mix (10 mM each), and 1 μ g total RNA were added to a nuclease-free microcentrifuge tube and made up to a volume of 12 μ l with sterile ddH₂O then heated to 65 °C for 5 min and quickly chilled on ice. To this, 4 μ l 5x First-strand buffer and 2 μ l 0.1 M DTT from the kit was added. The contents were mixed gently then incubated at 42 °C for 2 min followed by the addition of 1 μ l Superscript™ II RT. The reaction was incubated at 42 °C for 50 min before being inactivated by incubating at 70 °C for 15 m.

2.2.6.C Real Time PCR

Real time PCR is a technique used to quantify sequence specific PCR products as they accumulate in 'real time' (Heid et al., 1996; Winer et al., 1999). Here, this technique was coupled with reverse transcription (2.2.6.B) to determine the amount of *FANCD2* mRNA in uveal melanoma cell lines. Using a fluorescent dye (SYBR Green I) that emits light and becomes excited when bound to newly synthesised DNA in the PCR reaction, the accumulation and quantification of the cDNA in the initial PCR reaction can be determined.

2.2.6.C.1 Primer Design

Forward and reverse primers were ordered from Invitrogen and were designed to amplify the longer *FANCD2* isoform a transcript sequence (GenBank accession number NM_033084). β -*ACTIN* primers were also used to amplify the β -*ACTIN* cDNA (GenBank accession number NM_001101) of each sample as a reference gene. The primer sequences were designed using the primer design software at www.genscript.com and excluded intronic regions to ensure genomic DNA was not amplified. The primers were designed as follows:

Target mRNA	Primer Sequence (5' to 3')	Primer positioning
<i>FANCD2</i>	Forward – CAT GGC TGT TCG AGA CTT CA Reverse – GAC ACA AGG CTG CTT CAT CA	3895 bp – 4078 bp
β - <i>ACTIN</i>	Forward – ACA CCC CAG CCA TGT ACG TAG CC Reverse – AAG AGC CTC AGG GCA ACG GAA CC	467 bp – 865 bp

2.2.6.C.2 Real Time PCR Reaction Set Up

Reactions were set up in triplicate for each cell line in a 384-well plate. For the number of reactions to be carried out, a master mix was made by mixing 5 μ l of 2x Power SYBR[®] Green PCR master mix with 0.3 μ l (per reaction) 10 μ M primers (forward and reverse) made up to a volume of 6 μ l per reaction. This was aliquoted into the appropriate wells, to which 4 μ l of cDNA was added. The plate was then covered with a clear plastic foil and centrifuged at 1000 rpm for 5 min to spin down any residual reaction mix. The plates were placed in the Applied Biosystems 7900HT fast real time PCR system and the samples were subjected to the following PCR conditions:

Stage 1	50 °C	2 min	} 40 cycles
Stage 2	95 °C	10 min	
Stage 3	95 °C	15 s	
	60 °C	1 min	

Images and data were documented using the SDS Enterprise Database software (Applied Biosystems).

2.2.6.C.3 Testing primer efficiency

Primer efficiency was determined using a standard curve and calculating the Coefficient of determination (R^2). Increasing dilutions of WM793 control cDNA (from 1:1 to 1: 50) were added in triplicate as in Section 2.2.6.C.2. Following the Real Time PCR procedure, CT values for FANCD2 and β -ACTIN were plotted against cDNA concentration to produce a regression line of efficiency (Figure 2.6). To determine how accurately this regression line approximated the real data points the coefficient of determination (R^2) was calculated for each set of primers. If primers are 100% efficient R^2 would equal 1. Here, both primers had a R^2 value of approximately 0.7 and thus are 70% efficient. As both primers had the same efficiency we were able to use the Comparative CT ($2^{-\Delta\Delta CT}$) method to compare the mRNA levels of FANCD2 to β -ACTIN in each cell line and then between uveal melanoma and the control cell lines (see Section 2.2.6.C.4).

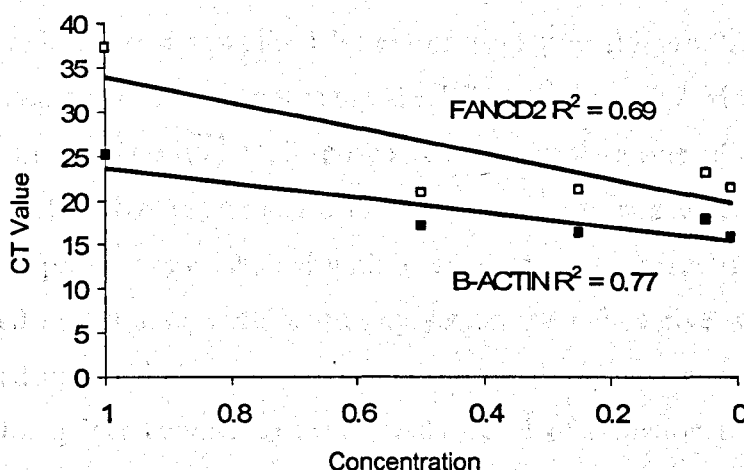


Figure 2.6 Standard regression lines showing the R^2 values and thus the primer efficiency for the FANCD2 and β -ACTIN primer sets used in the Real Time PCR experiments

CT values for the increasing concentrations of cDNA from the control cell line, WM793. Regression lines were produced for FANCD2 and β -ACTIN primers and the R^2 values determined to evaluate the efficiency of the primers. A R^2 value of 1 equals 100% primer efficiency.

2.2.6.C.4 Quantification

The real-time relative quantification of nucleic acids was determined using the Comparative CT ($2^{-\Delta\Delta CT}$) method (Livak and Schmittgen, 2001). Firstly, the average difference in cycling threshold of the gene of interest, in this case *FANCD2*, and the reference gene (*β -ACTIN*) was determined (ΔCT) for each cell line. The difference in these ΔCT values between cell lines was then calculated ($\Delta\Delta CT$) and the fold change in gene expression determined using the $2^{-\Delta\Delta CT}$ equation.

2.2.6.D Ribonuclease (RNase) Protection Assay

The ribonuclease (RNase) protection assay is a sensitive procedure that allows the detection and quantification of multiple target mRNA sequences in a total RNA sample (Friedberg et al., 1990). The technique involves the synthesis of a radioisotopically labelled RNA probe that is complementary to part of the target RNA sequences followed by hybridisation to the sample RNA. After hybridisation, the mixture is treated with RNase to degrade unhybridised probe. RNase only degrades single-stranded RNA, thus the probe bound to the target mRNA sequences protects them from degradation.

These protected fragments can then be separated on a denaturing TBE-urea polyacrylamide gel and visualised by autoradiography (Figure 2.7). Here, the RNase protection assay was carried out using the RPA IIITM and T7 MAXIscript[®] kits from Ambion with RiboQuantTM Multi-probe custom template sets (PharMingen) to detect and quantify 18 DNA repair genes in uveal melanoma and other human control cell lines. As the probes were labelled with a radioisotope for visualisation, all procedures were carried out in a separate laboratory set up for radioactive work. All procedures were carried out behind a perspex screen in the designated areas using a series 900 mini-monitor geiger counter to measure the level of radiation (beta particles) whilst conducting the experiment and to screen for contamination before and after the procedures had been completed. Laboratory coat and gloves were worn at all times.

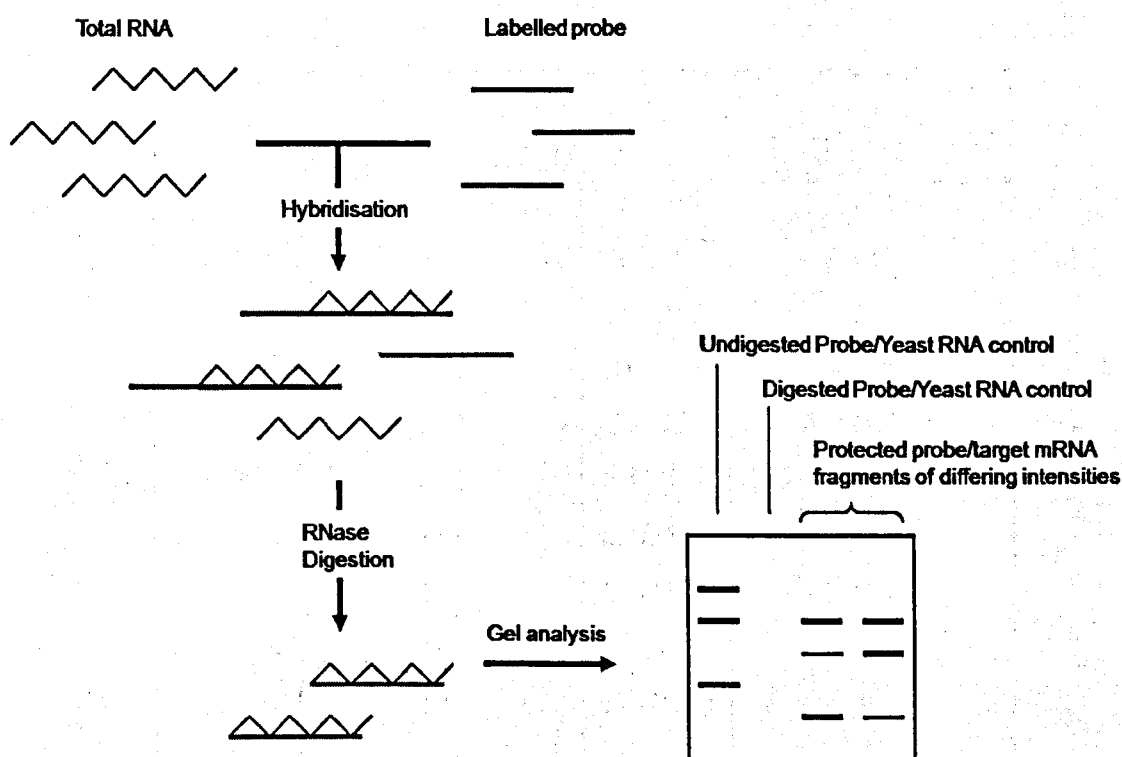


Figure 2.7 RNase protection assay procedure

The probe was synthesised by *in vitro* transcription using the T7 MAXIscript[®] kit, the hybridisation, digestion and precipitation were carried out using the RPATM III kit and the fragments separated on a denaturing TBE-urea polyacrylamide gel. The digested and undigested probes were made using the yeast RNA control provided in the kit. The intensity of the protected fragments was directly proportional to the quantity of mRNA in the original sample.

2.2.6.D.1 Multi-probe template set design

Multi-probe custom template sets were designed to detect the mRNA sequences of 18 different DNA repair genes and then purchased from PharMingen. In order to detect multiple mRNA sequences, all target sequences must differ in size sufficient for separation on a denaturing TBE-urea polyacrylamide gel (Hobbs et al., 1993). Thus repair genes were chosen depending not only on their previous published association with altered levels of SCE but also by the difference in fragment size between the genes of a template set to allow the detection and analysis of the target sequences. Two multi-probe template sets were made, each containing the housekeeping genes *L32* and *GAPDH* as internal controls. The two multi-probe template sets and the corresponding protected fragment size in nucleotide length (nt) of each target sequence are shown below:

Probe 1	Protected Fragment size (nt)	Probe 2	Protected Fragment size (nt)
<i>ATM</i>	404	<i>RAD50</i>	362
<i>NBS1</i>	362	<i>RAD54</i>	323
<i>XRCC4</i>	295	<i>RAD52</i>	297
<i>LIG4</i>	256	<i>MRE11</i>	258
<i>XRCC2</i>	227	<i>RAD51</i>	185
<i>XRCC3</i>	202	<i>RAD51B</i>	160
<i>FANCG</i>	181	<i>RAD51C</i>	148
<i>KU86</i>	161	<i>RAD51D</i>	127
<i>DNA-PK</i>	144	<i>L32</i>	113
<i>KU70</i>	127	<i>GAPDH</i>	96
<i>L32</i>	113		
<i>GAPDH</i>	96		

2.2.6.D.2 Probe Synthesis using the T7 MAXIscript[®] Kit

Radiolabelled probe synthesis was carried out by *in vitro* transcription using the T7 MAXIscript[®] kit from Ambion. Briefly, the multi-probe template sets contain a double-

stranded 19 – 23 base T7 promoter, upstream of the sequence to be transcribed. Under reaction conditions and in the presence of normal rNTPs and a radiolabelled rNTP, the T7 phage RNA polymerase binds to this promoter and using the 3' to 5' strand as a template, synthesises a complementary 5' to 3' strand at the end of the DNA template. All reagents were RNase-free and kept on ice. The transcription reaction was set up for each multi-probe template set as follows:

Component	Volume
RiboQuant multi-probe template set (5 ng/μl)	1 μl
10x Transcription buffer	2 μl
10 mM ATP	1 μl
10 mM CTP	1 μl
10 mM GTP	1 μl
[α ³² P]UTP*	5 μl
T7 RNA polymerase (15 U/μl)	2 μl
Nuclease-free dH ₂ O	To 20 μl

* radioisotopically labelled UTP (³²Phosphorus)

T7 RNA polymerase was added last, immediately before the reaction was incubated for 1 h at 37 °C. Following this incubation, 1 μl TURBO DNase 1 (from the kit) was added to the reaction to remove the template DNA and incubated for a further 30 min at 37 °C. The reaction mix was resuspended in 80 μl nuclease-free ddH₂O and then extracted with 100 μl phenol:chloroform:isoamyl alcohol (25:24:1) by mixing and removing the upper aqueous layer to a fresh RNase-free 1.5 ml eppendorf tube. 10 μl 5M sodium acetate (provided in the kit) and 275 μl 100% ethanol were added to precipitate the probe transcripts from the reaction mix. The samples were then incubated at -20 °C for 30 min followed by centrifugation at maximum speed at room temperature for 30 m. The supernatant was removed and the pellet resuspended in 50 μl nuclease-free ddH₂O. The probe was then stored at -20 °C until required.

2.2.6.D.3 RNA Preparation and Hybridisation using the Ambion RPA IIITM Kit

Total RNA was extracted from cells and measured as in 2.2.6.A. 10 µg total RNA was added to a RNase-free 0.5 ml eppendorf tube for each cell line and dried to completion using a Savant Speedvac concentrator with no heat (approximately 10 min for a 10 µl sample). Two tubes containing 2 µl (10 µg) yeast RNA were also included as controls. Once dry, the samples were resuspended in 8 µl RPA III hybridisation solution (provided in the kit) by vortexing and then 2 µl diluted probe from 2.2.6.D.2 was added to each sample and controls. The samples were then placed in a thermal cycler, heated to 95 °C for 3 min and then incubated overnight at 56 °C.

2.2.6.D.4 RNase Digestion and Precipitation of Probe/Target mRNA Protected Fragments

The RNase A/RNase T1 mix (provided in the kit) was diluted 1 in 1000 in RNase digestion III buffer (from the kit) and 100 µl of this solution was then added to the hybridised samples. One yeast RNA control was treated with RNase A in the same way as the samples and thus acted as a control for effective RNase treatment and to ensure that the probe was not protected in the absence of a complementary sequence. There should be no signal in this lane upon gel migration (Figure 2.6). The other yeast RNA control was not subjected to RNase treatment and thus only RNase digestion III buffer was added. This serves as a control for probe integrity to ensure no degradation or secondary structures exist. The full length probe was seen in this lane upon gel migration (Figure 2.6).

Following the addition of RNase, the samples were vortexed and incubated at 30 °C for 45 min to allow the digestion of unhybridised RNA and probe. 150 µl Inactivation/Precipitation III solution (from the kit) was added to each sample, vortexed and incubated at -20 °C for 30 m. The samples were then centrifuged at room temperature for 30 min and the supernatant removed. The samples were centrifuged again at room temperature for 15 min and the remaining supernatant removed by pipetting. The pellets were then air dried for 10 min at room temperature. The pellets were resuspended in 8 µl Gel loading buffer II (provided in the kit), and incubated at 95 °C for 3 min and place immediately on ice until loaded onto the gel.

2.2.6.D.5 Separation of Protected Fragments using a Denaturing TBE-Urea Acrylamide Gel

Electrophoresis was carried out using the OmniPAGE Maxi (20 x 20 cm) vertical gel electrophoresis unit from GeneFlow. To stop RNA contaminants, the kit was washed in 0.05% DEPC-treated ddH₂O (500 µl DEPC in 1 L of ddH₂O and left at room temperature for 2 h before autoclaving) prior to use and all reagents were made up with 0.05% DEPC-treated ddH₂O in RNase-free bottles and tubes, using RNase-free filter tips. DEPC-treated ddH₂O was made by adding 500 µl DEPC to 1 L ddH₂O, leaving at room temperature for 2 h before autoclaving. The gel apparatus was set up according to the manufacturers' instructions using the glass plates (one set with spacers attached) aligned to the edge on the silicone seal to stop leakage. A 5% acrylamide/8 M urea gel was cast to separate the protected probe/target mRNA fragments for a 16 x 17.5 cm x 0.75 mm gel as below:

Resolving Gel Components	
Urea	14.4 g
40% (w/v) 19:1 Acrylamide: Bis-acrylamide stock solution	3.8 ml
10 x TBE	3 ml
10% ammonium persulfate (APS)	240 µl
TEMED	32 µl
0.05% DEPC treated ddH ₂ O	to 30 ml

Before the addition of the 10% APS and TEMED, the gel solution was stirred at room temperature until the urea was completely dissolved. As it is the interaction between the 10% APS and TEMED that catalyses the polymerisation of the gel, following the addition of TEMED, the gel was poured immediately. A comb was then placed in the gel to create the loading wells and the gel was allowed to set at room temperature. Once set, the comb was removed, and the cast gel and glass plates were placed inside the vertical electrophoresis tank and covered with approximately 2 L 1x TBE running buffer (from a 10x stock of 0.9 M Tris base, 0.9 M Boric acid and 20 mM 0.5 M EDTA, made up to 1 L with 0.05% DEPC-treated ddH₂O). Prior to sample loading, urea was

rinsed from the wells of the gel by pipetting up and down with 1x TBE running buffer. The total volume of each sample (8 μ l) and probe controls were loaded into the wells. Electrophoresis was then carried out at 250 V for approximately 4 h or until the loading dye had run off the end of the gel.

2.2.6.D.6 *Quantification*

Following electrophoresis, the gel was removed from the tank and placed on to a piece of thick blotting paper. The gel was then covered in Cling film and placed in a vacuum pump air dryer (Fisherband) for 40 min at 70 °C until dry. The gel was then placed in a light proof cassette and exposed onto a storage phosphor screen for 1 h. The screen was then scanned using a PhosphorImager (FUJI Film FLA3000) and the intensities of the bands analysed using the ImageGauge V4.21 and ImageReader V1.8E software.

2.2.7 **Western Blot Analysis**

2.2.7.A Protein Extraction and Quantification

2.2.7.A.1 *Harvest by Trypsinisation*

Cells grown in a monolayer on T75 flasks until 70% confluent or at least 1×10^6 cells were present at the point of extraction. Cells were trypsinised using the protocol in 2.2.4.A and centrifuged at 2000 rpm at 4 °C for 5 m. The pellets were then washed in 3 ml cold PBS and centrifuged again at 2000 rpm at 4 °C for 5 m. This time the pellets were resuspended in 500 μ l of cold PBS, transferred to 1.5 ml eppendorf tubes and centrifuged again at 2000 rpm at 4 °C for 5 m. The PBS was then removed and the pellets lysed in 100 - 200 μ l of 1x RIPA buffer (0.75 M NaCl, 5% NP40, 2.5% DOC, 0.5% SDS and 0.25 M Tris pH 8 in ddH₂O) supplemented with 1x protease inhibitors and 1 mM PMSF. The extracts were incubated on ice for 30 min before being passed through a 25 G needle 5 times. The lysate was then spun at maximum speed (14,000 rpm) for 10 min at 4 °C to pellet the cell debris and the supernatant removed and stored at -20 °C.

2.2.7.A.2 Harvest by Scraping into 2x RIPA Buffer to Maintain Phosphate Moieties

Cells were seeded onto 100 mm plates so that at least 1×10^6 cells were present at the point of extraction and then incubated under normal conditions for 4 – 24 h before being treated as required. During the extraction procedure, the cells and reagents were kept cold on ice. Plates were washed 3 times in ice-cold PBS and residual PBS removed by pipetting. To the plates 100 μ l 2x RIPA buffer supplemented with 2x protease inhibitors, 2 mM PMSF and 2x phosphatase inhibitors (Sigma-Aldrich) was added and the cells detached from the plates using a cell scraper. The cells were then transferred to a 1.5 ml eppendorf tube and the extraction procedure followed as in 2.2.7.A.1.

2.2.7.A.3 Quantification

A range of standard solutions (1 μ g/ml to 20 μ g/ml) were made from a 10 mg/ml stock of BSA and used to generate a standard curve. For each protein extract, 2 μ l was added to 800 μ l ddH₂O before the addition of 200 μ l of BioRad Protein Assay Dye Reagent Concentrate. The solutions were mixed by vortexing and incubated at room temperature for 5 m. 200 μ l of each solution was then transferred to a 96-well plate and the OD measured at 595 nm using a plate reader. The protein concentration was calculated by comparing the sample OD to the standard curve generated.

2.2.7.B Western Blot Procedure

2.2.7.B.1 Assembly of Casting Equipment

Tris-glycine SDS-polyacrylamide gels were cast using the vertical Hoefer SE250 mighty small II system. The SE245 dual gel caster was assembled according to the manufacturers' instructions. Glass plates and spacers were washed with 70% ethanol prior to assembly and aligned to the edge of the caster to prevent leakage.

2.2.7.B.2 Casting of the Tris-Glycine SDS-Polyacrylamide Gels

The resolving gel was poured first. This gel allows the separation of proteins according to electrophoretic mobility. An 8, 10 or 12% gel was prepared as below depending on the size of the proteins to be analysed. It is the interaction of TEMED and APS that facilitates the polymerisation of acrylamide to produce a gel. Once poured, the gel was

immediately overlaid with approximately 1 ml H₂O to create an even surface. This was then left to set at room temperature. Once set the water overlay was removed and the stacking gel poured.

Resolving Gel Components	8 %	10 %	12 %
ddH ₂ O	2.3 ml	1.9 ml	1.6 ml
30% (w/v) acrylamide: 0.8% (w/v)			
Bis-Acyl-amide stock solution (37.5:1)	1.3 ml	1.7 ml	2.0 ml
1.5 M Tris (pH 8.8)	1.3 ml	1.3 ml	1.3 ml
10% SDS	50 µl	50 µl	50 µl
10% ammonium persulfate (APS)	50 µl	50 µl	50 µl
TEMED	6 µl	4 µl	4 µl

The stacking gel has a lower pH and acrylamide concentration than the resolving gel, which causes protein samples to compress at the interface between the gels. This produces better resolution and sharper protein bands. Once poured, a comb was immediately inserted into the gel to create wells. The composition of the stacking gel per gel cast is shown below:

Stacking Gel Components	
ddH ₂ O	1.4 ml
30% (w/v) acrylamide: 0.8% (w/v)	
Bis-Acyl-amide stock solution (37.5:1)	330 µl
1.5 M Tris (pH 6.8)	250 µl
10% SDS	20 µl
10% ammonium persulfate (APS)	20 µl
TEMED	2 µl

2.2.7.B.3 Electrophoresis

Once set, glass plates and spacers containing the gels were removed from the caster and washed with tap water before being assembled in the SE250 miniVE vertical electrophoresis unit. 1x SDS-PAGE running buffer was made from a 10x stock (250 mM Tris Base, 1.9 M Glycine dissolved in ddH₂O before the addition of 1% SDS) and then added to the chamber ensuring the gel was fully submerged and that the buffer was present in both sides of the chamber. Samples consisting of 20 – 30 µg of protein in 1x protein loading dye from a 5x stock (250 mM Tris pH 6.8, 10% SDS, 50% glycerol, 250 mM DTT and 0.02% bromophenol blue in ddH₂O) were first incubated at 100 °C for 10 min to denature the proteins before loading into the wells along with 5 µl of ColorBurst™ Electrophoresis Marker (Sigma-Aldrich). The gel was then subjected to an electrical current of 180 V at room temperature for approximately 1 h for all proteins except for larger proteins such as ATM and DNA-PK, which were run at 4 °C for approximately 4 h.

2.2.7.B.4 Semi-Dry Transfer

Following electrophoresis, the gel was removed from the glass plates and the stacking gel discarded. 1x Towbin transfer buffer was made from a 10x stock (250mM Tris Base and 1.9 M Glycine in ddH₂O) by adding 1 ml of 10% SDS to 100 ml of 10x Towbin transfer buffer and 700 ml of water before adding 200 ml of methanol. The remaining resolving gel was submerged in this buffer to remove any contaminating buffer salts from the electrophoresis. Two pieces of blotting paper were cut to the size of the gel, moistened in transfer buffer and placed onto the BioRad Trans-Blot SD Semi-dry Electrophoretic Transfer Cell. A piece of Protran nitrocellulose transfer membrane cut to the size of the gel and soaked in transfer buffer was then placed on top of this. The gel was then placed on top of the membrane ensuring that the surface was even, followed by the addition of two more pieces of moistened blotting paper. Transfer was then carried out at 10 V for 40 m. For larger proteins (>200 kDa), a 2x Towbin transfer buffer was used that contained twice the amount of 10x stock and 2 ml 10% SDS, and the transfer time was extended to 1.5 h.

2.2.7.B.5 Blocking the Membrane

To prevent non-specific binding of the antibodies and reduce background signal, following transfer, the membranes were incubated in 5% non-fat milk in PBS-T (0.1% Tween-20 in PBS) for 1 h at room temperature on a shaking platform.

2.2.7.B.6 Antibody Incubation

Following blocking, membranes were incubated with the appropriate primary antibody diluted in 5% non-fat milk in PBS-T to the correct dilution overnight at 4 °C on a shaking platform. After this time, the membranes were subjected to 3, 10 min washes with PBS-T (0.1% Tween-20 in PBS). After the washes, the membranes were incubated with the appropriate secondary antibody diluted in 5% non-fat milk in PBS-T for 1 h at room temperature on a shaking platform. Following this, the membranes were washed 3 times in PBS-T for 10 m.

2.2.7.B.7 ECL Detection

Proteins bound to the nitrocellulose membrane were visualised using Amersham ECL™ western blotting detection reagents. The ECL reagents are supplied as 2 solutions that were mixed in equal volumes according to the manufacturers' instructions before being added to the membranes for 1 min at room temperature. This incubation allows an oxidation reaction between the horseradish peroxidase conjugate to the secondary antibodies, and the luminol in the ECL reagents to take place, which leads to chemiluminescence. Excess ECL was removed and the membranes wrapped in Cling film avoiding any bubbles and placed in a light proof cassette. Under the safety red light, the membranes were incubated with Fujifilm Super RX medical x-ray film for between 20 s and 1 h in order for the light emitted from the chemiluminescence reaction to be recorded onto the light sensitive autoradiography film. To visualise this transfer, the film was placed in developing solution for 30 - 60 s, briefly washed in tap water, then placed in fixing solution for 2 min before finally washing once more with water.

2.2.8 Immunofluorescence

Immunofluorescence was used to visualise the nuclear distribution of specific proteins spontaneously and following treatment with MMC. All cells were visualised using a Nikon TE200 inverted microscope and images were recorded and analysed using a

Hamamatsu C4742-95 digital camera and the image analysis software Velocity version 3.61.

2.2.8.A Sample Preparation

2.2.8.A.1 *Spontaneous Foci Formation*

Coverslips were first sterilised by washing with 70% methanol then placed into individual wells on a 6-well plate. Cells were then trypsinised and quantified as in 2.2.4.A and 2.2.4.D, and 1×10^5 cells in 3 ml growth medium was added to each coverslip. Cells were incubated under normal conditions for 24 h after which time the growth medium was removed from the cells and the cells washed for 5 min in PBS followed by fixing.

2.2.8.A.2 *Induced Foci Formation Following MMC Treatment*

The DNA damage response in uveal melanoma cells compared to control cell lines following the induction of ICLs was determined by studying the induced foci formation at various time points after treatment with MMC. Cells were prepared in 6 well plates as described in 2.2.8.A.1. Each 6 well plate was used for one time point, ranging from 0 h - 48 h. The following day 500 ng/ml MMC (15 μ M) was added to the growth medium in each well and then returned to normal incubation conditions for 1 h, after which time the medium was removed and replaced with fresh growth medium. The cells for the 0 h time point were washed immediately with PBS for 5 min and then fixed. After fixing, cells were stored at 4 °C in either PBStx (0.15% BSA dissolved in PBS supplemented with 0.1% Triton X-100), Washing buffer (0.1% NP-40 in PBS) or 1% goat serum in TBS for RAD51, FANCD2 or γ H₂A.X foci formation respectively, until the final time point cells had been fixed. Each subsequent time point was fixed after the appropriate time using the described method.

2.2.8.B RAD51 Foci Formation

Cells were prepared as in either 2.2.8.A.1 or 2.2.8.A.2 and then fixed using 3% PFA (3g paraformaldehyde dissolved in 100 ml PBS by heating to 80 °C overnight on a stirring heat block) for 20 min at room temperature, after this time the PFA was removed and the cells washed 4 times in PBStx (0.15% BSA dissolved in PBS supplemented with

0.1% Triton X-100) for 15 min. Cells were incubated with the primary RAD51 antibody diluted 1 in 500 in 3% BSA in PBS and left overnight at 4 °C in a humidified chamber. The following day cells were washed 4 times in PBStx for 15 min at room temperature then incubated with the CY3 goat anti-rabbit secondary antibody at 1 in 500, diluted in 3% BSA in PBS for 1 h at room temperature in a dark humidified chamber. To stop fading of the fluorescently tagged secondary antibody, subsequent steps were carried out away from direct sunlight and the plates wrapped in foil. After incubation, the cells were washed two times in PBStx for 15 min followed by one wash for 5 min in PBS. Cells were mounted onto slides using mounting medium containing DAPI (Vectorshield) and stored in the dark at 4 °C until analysis. To quantify RAD51 foci formation, cells with greater than 10 foci/cell were scored as positive and at least 50 cells were counted/ condition on 3 separate occasions.

2.2.8.C FANCD2 Foci Formation

Cells were prepared as in either 2.2.8.A.1 or 2.2.8.A.2 and then fixed in 2% PFA in PBS (dissolved by heating to 80 °C overnight on a stirring heat block) for 20 min at room temperature. The PFA was then removed and the cells permeabilised in 0.3% Triton X-100 in PBS for 10 min at room temperature. Following this, the cells were incubated in blocking buffer (10% goat serum in PBS) for 1 h at room temperature and then incubated with the primary FANCD2 antibody diluted to 1 in 1000 in 3% goat serum in washing buffer (0.1% NP40 in PBS) overnight in a humidified chamber at 4 °C. After this time, the cells were washed 3 times in washing buffer for 10 min on a shaking platform and subsequently incubated with the secondary Alexa fluor 488[®] goat anti-mouse IgG (H+L) antibody diluted 1 in 1000 in 3% goat serum in washing buffer, for 1 hr at room temperature in the dark. The cells were subsequently washed 3 times in washing buffer for 10 min in low light and then mounted onto labelled microscope slides using mounting medium containing DAPI. The cells were visualised and the number of foci/cell quantified where cells with greater than 10 foci/cell were scored as positive. At least 50 cells were counted for each condition on 3 separate occasions.

2.2.8.D γ H₂A.X Foci Formation

Cells were prepared as in either 2.2.8.A.1 or 2.2.8.B.1 and then fixed in 3% PFA in PBS (dissolved by heating to 80 °C overnight on a stirring heat block) for 10 min at room

temperature. The cells were then permeabilised in 0.2% TritonX-100 in PBS for 5 min followed by washing 3 times in TBS for 10 min before the cells were incubated with blocking buffer (10% goat serum in TBS) for 1 h at room temperature. Following this incubation, the cells were washed twice in TBS for 10 min and subsequently incubated with the primary γ H₂A.X antibody diluted to 1 in 500 in 3% goat serum in TBS overnight in a humidified chamber at 4 °C. The cells were then washed 4 times in TBS for 10 min and incubated with the CY3 goat anti-rabbit secondary antibody at 1 in 500, diluted in 3% goat serum in TBS for 1 h in a dark humidified chamber at room temperature. Following this, the cells were washed 3 times in TBS for 5 min in low light and then mounted onto labelled microscope slides with mounting medium containing DAPI. The cells were visualised and the number of foci/cell quantified where cells with greater than 10 foci/cell were scored as positive. At least 50 cells were counted for each condition on 3 separate occasions.

2.2.9 Fluorescence-Activated Cell Sorting (FACS) Analysis

FACS analysis or flow cytometry is a technique that allows the simultaneous measurement of various cellular parameters, such as cell size and granularity. Fluorescently labelled cells are passed in a constant stream of fluid through a beam of light and the amount of fluorescence emitted as well as the amount of light scattered from the beam is measured.

2.2.9.A Propidium Iodine (PI) Staining

Cells were counted and plated at a concentration of 1×10^6 cells on 100 mm plates in 10 ml growth medium. For each cell line, one plate was used for no treatment and one for MMC treatment. The cells were left for 4 h to allow them to adhere before 100 nM MMC was added to the appropriate plate. After 24 h cells were trypsinised and washed twice in PBS by centrifugation at 2000 rpm for 3 min at 4 °C. The cells were then pelleted by centrifugation at 1000 rpm for 3 min at 4 °C. To fix the cells, 1 ml ice cold 70% ethanol was added drop-wise whilst vortexing the pellet to ensure full resuspension and the cells placed at -20 °C. The following day, the pellets were washed twice with PBS by centrifugation at 2000 rpm for 3 min at 4 °C and then resuspended in 100 μ g/ μ l RNase A (diluted in ddH₂O) and left on ice for 20 m. Following this, 500 μ l of 50 μ g/ml

PI (diluted in PBS) was added and the cells left in low light at 4 °C overnight. Analysis was performed the following day using FACS.

2.2.9.B BrdU Staining

BrdU is an analogue of thymine that competes with this base for uptake during DNA synthesis. As only actively synthesising cells at the time of BrdU addition will be positive for it, using an antibody specific to BrdU and co-staining with PI, the cell cycle status of a cell population can be determined.

Cells were counted and plated at a concentration of 1×10^6 cells on 100 mm plates in 10 ml growth medium. For each cell line, one plate was used for each of the time points 0 h, 4 h, 8 h, and 12 h. The following day 10 μ l of 10 mM stock of BrdU was added to each of the plates for 20 min then washed off with fresh growth medium. The 0 h time point plate was immediately trypsinised and then washed twice in PBS by centrifugation at 2000 rpm for 3 min at 4 °C. The cells were then pelleted by centrifugation at 1000 rpm for 3 min at 4 °C. To fix the cells, 1 ml ice cold 70% ethanol was added drop-wise whilst vortexing the pellet to ensure full resuspension and the cells placed at -20 °C. The subsequent plates for each time point were harvested and fixed as described and stored at -20°C until 24 h after the final time point plate had been fixed. After fixing, the alcohol was spun off by centrifugation at 2000 rpm at 4 °C for 5 min followed by washing twice in PBS by centrifugation. The subsequent pellet was resuspended in 2 M HCL and incubated for 30 min at room temperature. After this incubation, the acid was spun off by centrifugation at 2000 rpm at 4 °C for 5 min and the pellet washed 3 times in PBS followed by 1 wash in PBS-T (0.1% BSA, 0.2% Tween-20 in PBS pH 7.4) by centrifugation. The pellet was then resuspended in 10 μ l Dako Cytomation mouse anti-BrdU antibody diluted in PBS in equal volumes and incubated for 30 min at room temperature in the dark. Following this, the pellet was washed twice in PBS-T and then incubated with 50 μ l Dako Cytomation FITC-conjugated goat anti-mouse F(ab')₂ fragments antibody diluted to 1 in 10 in PBS for 20 min in the dark. The pellet was washed once in PBS and resuspended in 500 μ l of 50 μ g/ml PI and 100 μ g/ μ l RNase A for 30 min in the dark at room temperature followed by immediate analysis using FACS.

Chapter 3 – Characterisation of Uveal Melanoma Cell Lines

3.1	Introduction	102
3.2	Differences in proliferation rate are not responsible for the reduced spontaneous SCE frequency in uveal melanoma	103
3.3	Uveal melanoma cell lines have increased levels of endogenous DNA damage, indicative of a defect in DNA repair	105
3.4	Endogenous levels of HR are reduced in uveal melanoma cell lines	108
3.5	TLS and MMR are not upregulated in uveal melanoma cell lines	110
3.6	Uveal melanoma cell lines have reduced <i>FANCD2</i> gene and protein expression	111
3.6.1	<i>FANCD2</i> protein expression is altered following genome-wide demethylation	116
3.6.2	<i>FANCD2</i> transcription may be altered by aberrant methylation at a putative E2F transcriptional binding site within the <i>FANCD2</i> promoter	118
3.7	Uveal melanoma cell lines have reduced LIGIV protein expression.	120
3.8	Discussion.....	121

List of Figures

- Figure 3.1** Proliferation rates are similar in uveal melanoma and control cell lines and thus are not responsible for the reduced SCE phenotype.....104
- Figure 3.2** Cell cycle progression is similar in uveal melanoma and control cell lines and is not responsible for the reduced SCE phenotype.....105
- Figure 3.3** Uveal melanoma cell lines have increased levels of endogenous γ H₂A.X foci formation compared to WM793, MRC5VA and U2OS control cell lines.....107
- Figure 3.4** Endogenous RAD51 foci formation is reduced in uveal melanoma cell lines compared to control cell lines.....109
- Figure 3.5** Error-prone pathways are not upregulated in uveal melanoma.....111
- Figure 3.6** FANCD2 and LIGIV protein expression is reduced in uveal melanoma cell lines.....112
- Figure 3.7** Confirmation of the reduced levels of *FANCD2* gene and protein expression in uveal melanoma.....114
- Figure 3.8** FANCD2 protein expression is reduced further in uveal melanoma cell lines following genome-wide demethylation.....117
- Figure 3.9** A putative E2F transcriptional binding site in the FANCD2 promoter is altered in uveal melanoma cell lines.....119
- Figure 3.10** The mRNA levels of a range of genes in uveal melanoma cell lines compared to WM793 and other human control cell lines.....121

3.1 Introduction

Uveal melanoma affects the uveal tract of the eye and is the most common form of ocular melanoma in adults (Singh and Topham, 2003a). Previously, it has been found that uveal melanoma exhibit a reduced spontaneous SCE frequency compared to matched patient blood samples and other human cancer cell lines (Table 1.5 and 1.6) (Hoh, 2007, unpublished data). This is in contrast to many other types of sporadic tumours that have increased chromosomal aberrations and are associated with increased levels of spontaneous SCE, indicative of genetic instability. Uveal melanoma is therefore an ideal model system in which to study SCE formation.

SCE is the process of the physical exchange of chromatid regions resulting from the breaking and rejoining of two sister chromatids. SCE is a known end-product of HR and it can be induced by a wide variety of DNA damaging agents. Furthermore, the frequency of SCE can be affected by defective proteins involved in DNA repair (Table 1.3). Although very little is known about the mechanism of SCE formation, evidence therefore suggests that a SCE is formed as a consequence of DNA repair. For this reason, we characterised the DNA repair pathways in the uveal melanoma cell lines SOM 157d and SOM 196b (referred to as 157d and 196b respectively from here in) to understand the mechanism of SCE formation and investigate the underlying cause of the reduced spontaneous SCE phenotype.

As well as in disease states, spontaneous SCE frequency can vary between cell types (Table 1.1). It is possible then that the low SCE frequency in uveal melanoma is a consequence of cell type rather than a result of molecular defects. Ideally, to control for this, normal melanocytes from an unaffected uveal tract of a uveal melanoma patient would be investigated alongside the uveal melanoma cell lines and primary tumour samples. However, due to ethical issues this material is unavailable. Instead, we have used the cutaneous melanoma cell line, WM793 (Hsu, 1999). This cell line was established from the vertical growth phase of a primary cutaneous melanoma lesion of a 39 year old male caucasian patient and thus, although it does not originate from the uveal tract, it shares the same progenitor cell as uveal melanoma cells and thus is considered the best available control for the investigation of uveal melanoma cell lines.

In addition, we used a panel of standard cell lines used routinely in our laboratory to investigate DNA damage repair.

3.2 Differences in proliferation rate are not responsible for the reduced spontaneous SCE frequency in uveal melanoma

SCE is a recombinational event that occurs during S-phase of the cell cycle and thus is considered to be a result of normal DNA replication or repair of endogenous DNA damage. Altered spontaneous SCE frequency may therefore reflect changes in proliferation and cell cycle progression through S-phase. To investigate the association between SCE and S-phase in uveal melanoma, MTT proliferation assays (Figure 3.1) and cell cycle progression using BrdU incorporation and PI staining were carried out (Figure 3.2).

The proliferation rate of the uveal melanoma cell lines 157d and 196b were compared to the melanoma control cell line WM793 and the MRC5VA cell line over a 7 day period. There was no difference in the proliferation of both uveal melanoma cell lines compared to WM793 (Figure 3.1 a). Furthermore, there was no difference in the percentage of cells in S-phase as indicated by PI staining between these cell lines (Figure 3.1 b). Interestingly, both the uveal melanoma cell lines and WM793 proliferated at a significantly lower rate than the MRC5VA transformed fibroblast cell line ($p = 0.04$, $p = 0.008$ and $p = 0.02$ for 157d, 196b and WM793 respectively) (Figure 3.1 a). As the WM793 cell line has high SCE, uveal melanoma cell lines have low SCE and the MRC5VA cell line has an intermediate SCE frequency (Table 1.5), there appears to be no correlation between proliferation and spontaneous SCE.

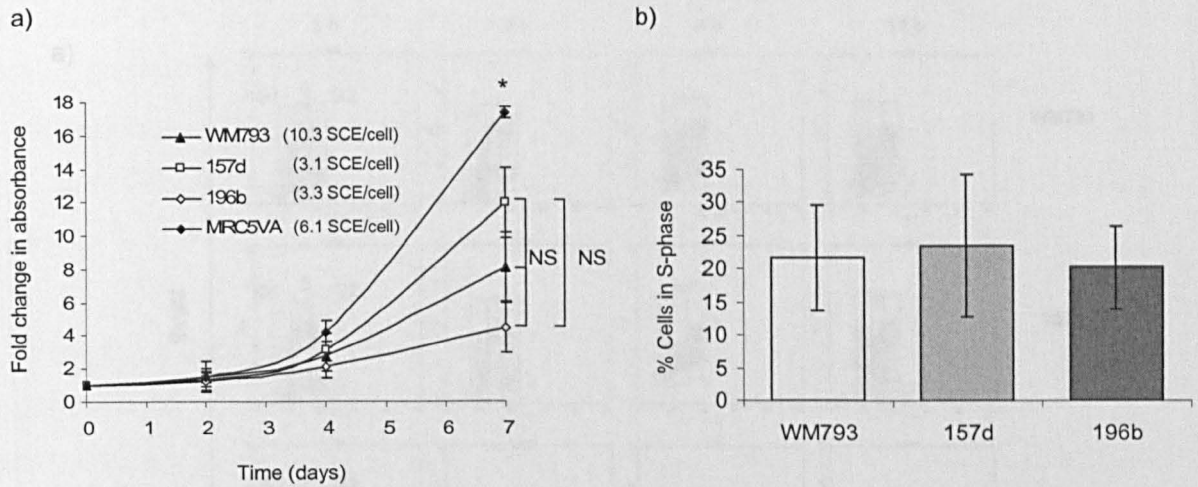


Figure 3.1 Proliferation rates are similar in uveal melanoma and control cell lines and thus are not responsible for the reduced SCE phenotype

a) Proliferation rates for the uveal melanoma cell lines 157d and 196b, and the WM793 and MRC5VA control cell lines shown by an MTT assay. Cells were allowed to grow for either 4 h (0 days), 2, 4 or 7 days after which time the number of viable cells was estimated from MTT reduction and measured using spectrophotometry (OD 570 nm). The fold change in absorbance was calculated relative to the absorbance measured on day 0. b) The % of cells in S-phase as indicated by PI staining in 157d, 196b and WM793. In each case, data represent the average of at least three separate experiments and error bars represent standard deviations. Statistical significance was calculated using the Student's T-test where $p < 0.05$ is indicated by *. Significance between samples is indicated by brackets and no significance is indicated by 'NS'.

To further confirm that uveal melanoma cell lines undergo normal cell cycle progression, BrdU staining was carried out (Figure 3.2). BrdU is incorporated into DNA during DNA synthesis thus, by staining with an antibody specific to BrdU and co-staining with PI, the cell cycle status, the percentage of cells actively replicating in the cell population and the speed at which the cells move through the cell cycle can all be determined using FACS. There was no difference in the cell cycle progression of both uveal melanoma cell lines compared to WM793 over a period of 12 h (Figure 3.2). The reduced level of spontaneous SCE is therefore not a consequence of aberrant cell cycle progression or a lack of proliferation in uveal melanoma cell lines.

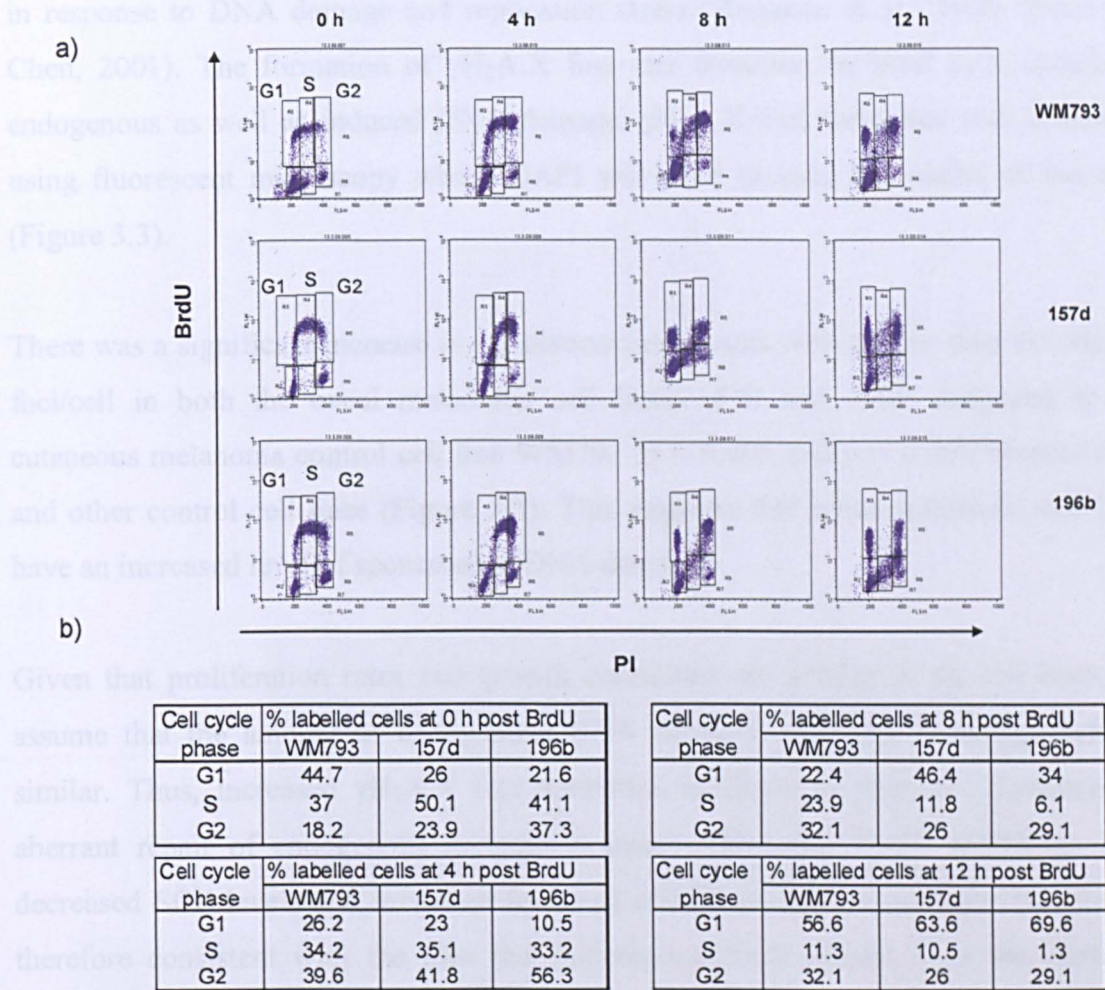


Figure 3.2 Cell cycle progression is similar in uveal melanoma and control cell lines and is not responsible for the reduced SCE phenotype

a) BrdU and PI staining in 157d, 196b and WM793 analysed using FACS. Cells were pulsed with BrdU for 20 minutes and then released for 0, 4, 8 or 12 h. BrdU positive cells were gated into G1, S and G2 phases, the quantification of which can be seen in b).

3.3 Uveal melanoma cell lines have increased levels of endogenous DNA damage, indicative of a defect in DNA repair

Once proliferation had been ruled out as a cause for reduced SCE frequency, we next investigated endogenous DNA damage. Differences in the levels of endogenous DNA damage in uveal melanoma cell lines may suggest defects in the response and repair of this damage. An early target of the DNA damage signalling pathway is histone H₂A.X. Both ATR and ATM are able to directly phosphorylate histone H₂A.X to form γ H₂A.X

in response to DNA damage and replication stress (Rogakou et al., 1998; Ward and Chen, 2001). The formation of $\gamma\text{H}_2\text{A.X}$ foci can therefore be used as a marker of endogenous as well as induced DNA damage. $\gamma\text{H}_2\text{A.X}$ foci formation was visualised using fluorescent microscopy where DAPI was used to stain the nuclei of the cells (Figure 3.3).

There was a significant increase in the percentage of cells with greater than 10 $\gamma\text{H}_2\text{A.X}$ foci/cell in both the uveal melanoma cell lines 157d and 196b compared to the cutaneous melanoma control cell line WM793 ($p = 0.005$ and $p = 0.003$, respectively) and other control cell lines (Figure 3.3). This suggests that uveal melanoma cell lines have an increased level of spontaneous DNA damage.

Given that proliferation rates and growth conditions are similar in all cell lines, we assume that the amount of endogenous DNA damage occurring in all cell lines is similar. Thus, increased $\gamma\text{H}_2\text{A.X}$ foci formation is likely to represent decreased or aberrant repair of endogenous damage in uveal melanoma. Uveal melanoma have decreased SCE levels and increased levels of endogenous DNA damage. This data is therefore consistent with the idea that spontaneous SCE results from the repair of endogenous DNA damage.

Interestingly, the increased level of $\gamma\text{H}_2\text{A.X}$ foci formation does not appear to affect cell cycle progression or proliferation (Figure 3.1 and 3.2) and furthermore, apoptosis levels are normal as shown by Annexin V staining (Appendix 4, Hoh, 2007, unpublished data). Together this data suggests that cell survival is not affected by increased $\gamma\text{H}_2\text{A.X}$ foci formation.

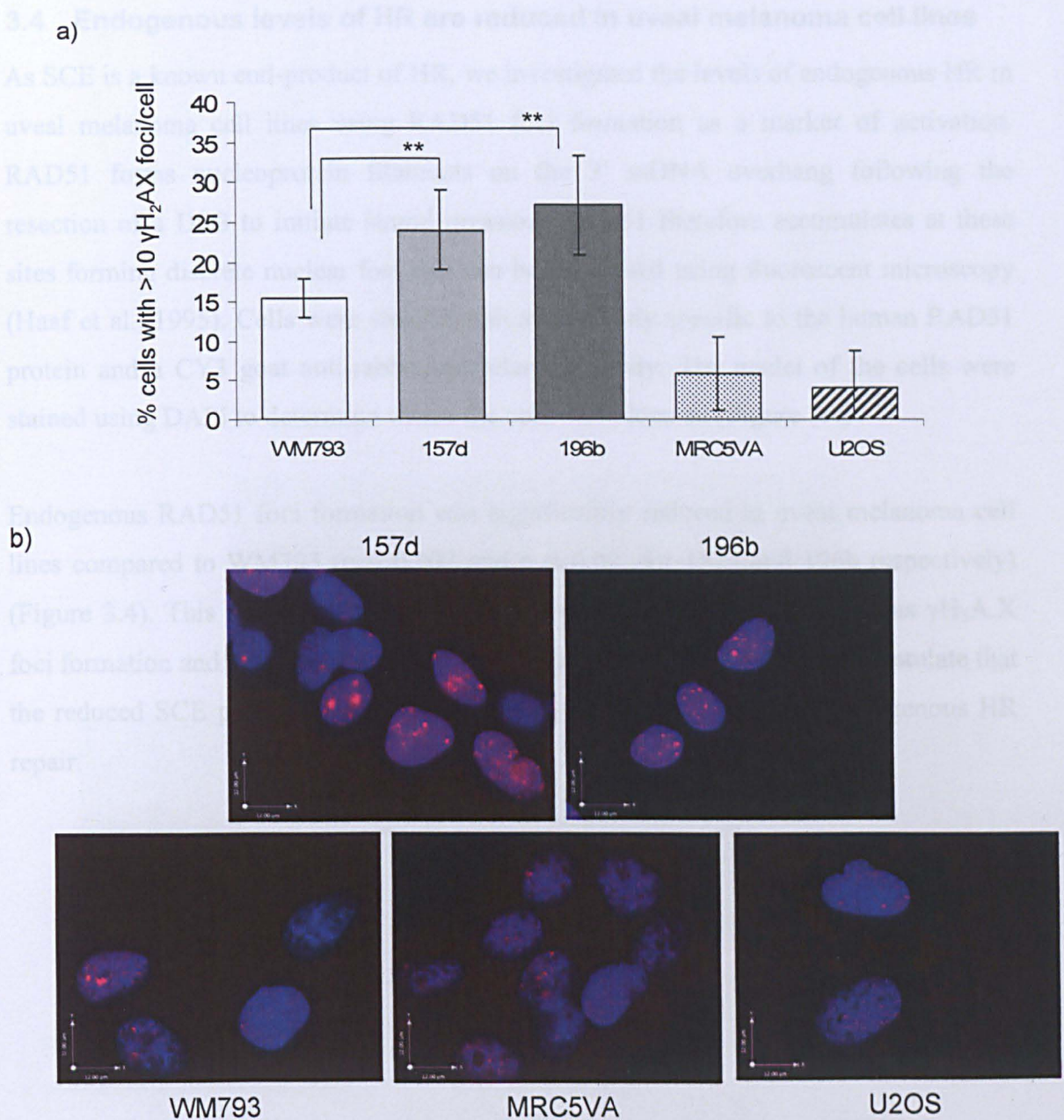


Figure 3.3 Uveal melanoma cell lines have increased levels of endogenous γ H₂A.X foci formation compared to WM793, MRC5VA and U2OS control cell lines

a) Endogenous γ H₂A.X foci formation visualised by fluorescent microscopy in the uveal melanoma cell lines, 157d and 196b, and in the WM793, MRC5VA and U2OS control cell lines. Cells were plated and left for 24 h before being fixed and stained. On each occasion, at least 50 cells were analysed and the % of cells with > 10 γ H₂A.X foci/cell was calculated. Data represents at least three separate experiments and error bars represent standard deviations. Statistical significance was calculated using the Student's T-test where $p < 0.01$ is indicated by **. Brackets indicate significance calculated between samples. b) Representative images of endogenous γ H₂A.X foci formation (red) in all cell lines studied, nuclei stained with DAPI (blue).

3.4 Endogenous levels of HR are reduced in uveal melanoma cell lines

As SCE is a known end-product of HR, we investigated the levels of endogenous HR in uveal melanoma cell lines using RAD51 foci formation as a marker of activation. RAD51 forms nucleoprotein filaments on the 3' ssDNA overhang following the resection of a DSB to initiate strand invasion. RAD51 therefore accumulates at these sites forming discrete nuclear foci that can be visualised using fluorescent microscopy (Haaf et al., 1995). Cells were stained with an antibody specific to the human RAD51 protein and a CY3 goat anti-rabbit secondary antibody. The nuclei of the cells were stained using DAPI to determine where the cells were located (Figure 3.4).

Endogenous RAD51 foci formation was significantly reduced in uveal melanoma cell lines compared to WM793 ($p = 0.002$ and $p = 0.02$, for 157d and 196b respectively) (Figure 3.4). This is consistent with both the increased levels of endogenous γ H₂A.X foci formation and the decreased levels of spontaneous SCE. We therefore postulate that the reduced SCE phenotype in uveal melanoma is due to a defect in endogenous HR repair.

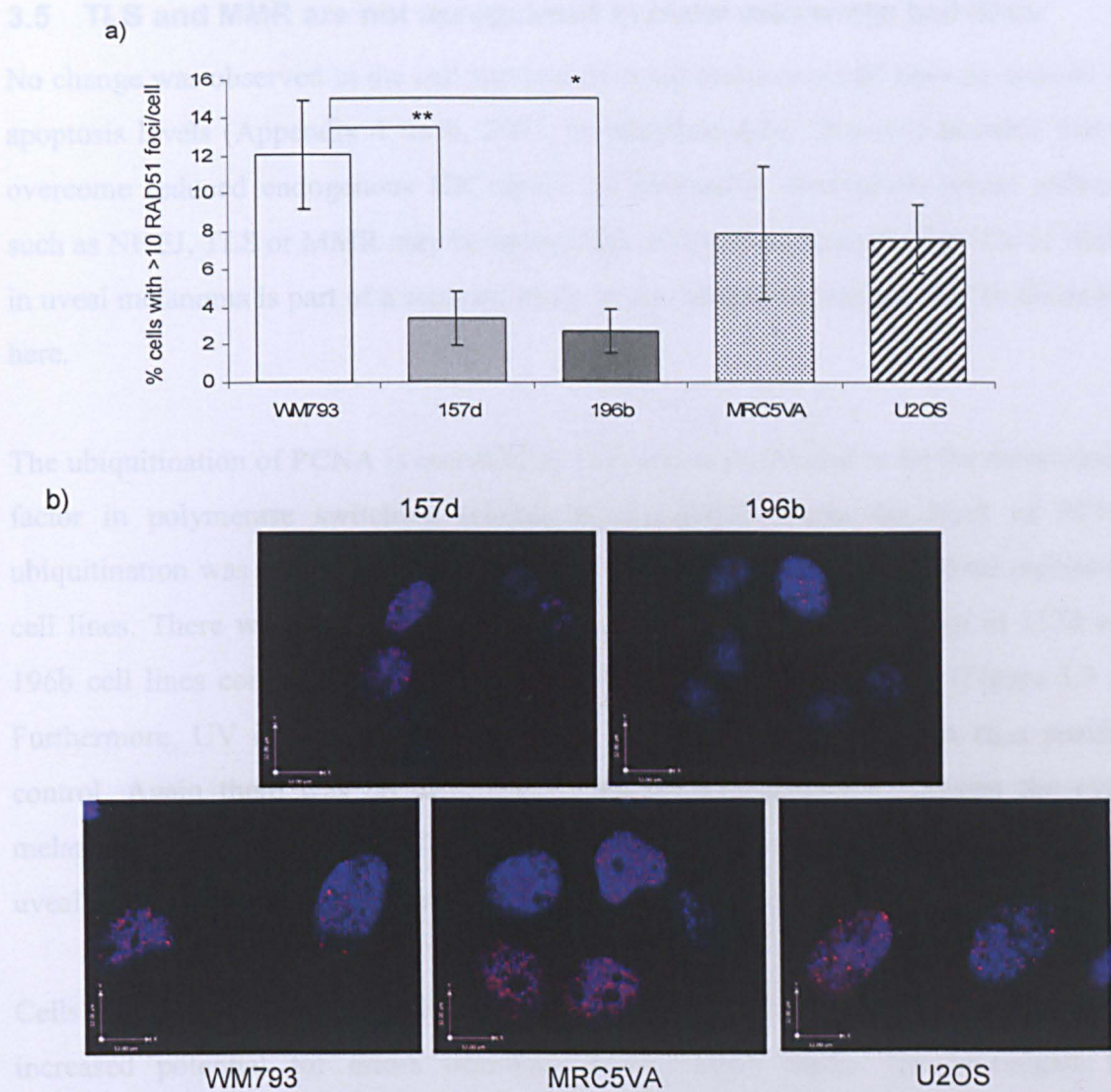


Figure 3.4 Endogenous RAD51 foci formation is reduced in uveal melanoma cell lines compared to control cell lines.

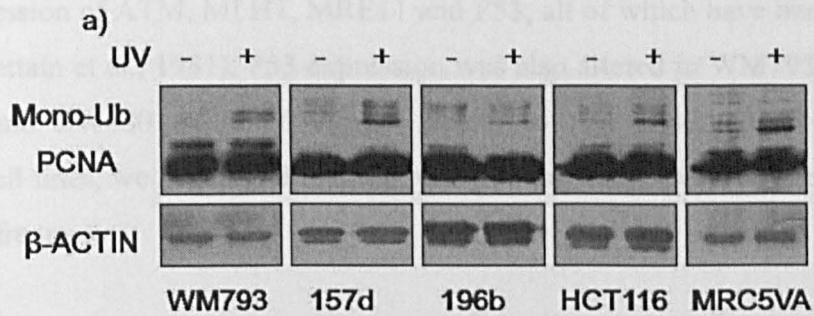
a) Endogenous RAD51 foci formation visualised by fluorescent microscopy in the uveal melanoma cell lines 157d and 196b, and in the WM793, MRC5VA and U2OS control cell lines. Cells were plated and left for 24 h before being fixed and stained. On each occasion, at least 50 cells were analysed and the % of cells with > 10 RAD51 foci/cell was calculated. Data shown is representative of at least two separate experiments and error bars represent the standard deviations. Statistical significance was calculated using the Student's T-test where $p < 0.05$ is indicated by * and $p < 0.01$ is indicated by **. Significance between samples is indicated by brackets. b) Representative images of endogenous RAD51 foci formation (red) in all cell lines studied, nuclei stained with DAPI (blue).

3.5 TLS and MMR are not upregulated in uveal melanoma cell lines

No change was observed in the cell survival of uveal melanoma cell lines as assayed by apoptosis levels (Appendix 4, Hoh, 2007, unpublished data) thus it is possible that to overcome reduced endogenous HR repair, an alternative error-prone repair pathway such as NHEJ, TLS or MMR may be upregulated in uveal melanoma. The role of NHEJ in uveal melanoma is part of a separate study in our laboratory and will not be discussed here.

The ubiquitination of PCNA is essential to TLS and is postulated to be the determining factor in polymerase switching (Hoegge et al., 2002). Here, the level of PCNA ubiquitination was used to determine the level of spontaneous TLS in uveal melanoma cell lines. There was no difference in spontaneous PCNA ubiquitination in 157d and 196b cell lines compared to WM793 and MRC5VA control cell lines (Figure 3.5 a). Furthermore, UV is known to induce TLS, and thus it was used here as a positive control. Again there was no difference in PCNA ubiquitination between the uveal melanoma cell lines and control cell lines suggesting that TLS activation is normal in uveal melanoma cell lines (Figure 3.5).

Cells that utilise error-prone pathways are associated with high mutation rates due to the increased potential for errors occurring during DNA repair. To investigate the spontaneous mutation rates in uveal melanoma cell lines, fluctuation assays were carried out (Figure 3.5 b). This technique is used to determine the spontaneous mutation rate of the house-keeping gene *HPRT* and it is the rate at which this mutation occurs that is calculated using the fluctuation test of Luria and Delbruck (Luria and Delbruck, 1943). There was no difference in the spontaneous mutation rate of the uveal melanoma cell lines 157d and 196b compared to WM793 and MRC5VA (Figure 3.5 b). The MMR deficient cell line, HCT116, is shown as a positive control and has a much higher mutation rate than any of the cell lines studied here. We therefore concluded that although uveal melanoma cell lines exhibit a reduction in error-free HR, error-prone repair is not upregulated to overcome this defect.



b)

Cell Line	Mutation Rate
WM793	6.6×10^{-9}
157d	1.0×10^{-8}
196b	4.0×10^{-8}
HCT116 *	1.5×10^{-5}
MRC5VA	2.8×10^{-8}

Figure 3.5 Error-prone pathways are not upregulated in uveal melanoma

a) PCNA ubiquitination shown by western blot analysis in the uveal melanoma cell lines 157d and 196b, and in the WM793 and MRC5VA control cell lines. Cells were either left untreated or treated with 40 J/M^2 UV with 5 h recovery before extracts were made. Images are representative of at least three separate experiments and β -ACTIN was used as a loading control where $30 \mu\text{g}$ of protein was added. b) Spontaneous mutation rates in the uveal melanoma cell lines 157d and 196b compared to the WM793 and MRC5VA control cell lines and the published data for the HCT116 cell line (Bhattacharyya et al., 1994) indicated by * using a fluctuation assay. Data represents the average mutation rates from two separate experiments calculated using the Luria Delbruck method (Luria and Delbruck, 1943).

3.6 Uveal melanoma cell lines have reduced *FANCD2* gene and protein expression

Western blot analysis was carried out on a range of potential candidate DNA repair proteins that may be associated with the observed defect in endogenous repair and decreased level of spontaneous SCE in uveal melanoma cell lines (Figure 3.6). Proteins were selected for the screen based on their previous association with altered levels of SCE in different mammalian systems (Table 1. 3). Only differences that were common to both uveal melanoma cell lines were classed as being altered and therefore subject to further study. In addition, the human cancer cell line HCT116 showed a reduction in

protein expression of ATM, MLH1, MRE11 and P53, all of which have been previously reported (Brattain et al., 1981). P53 expression was also altered in WM793, however as MRC5VA and SW480 exhibited similar levels to that observed for both uveal melanoma cell lines, we postulated that this was not associated with the defect in repair or low SCE frequency.

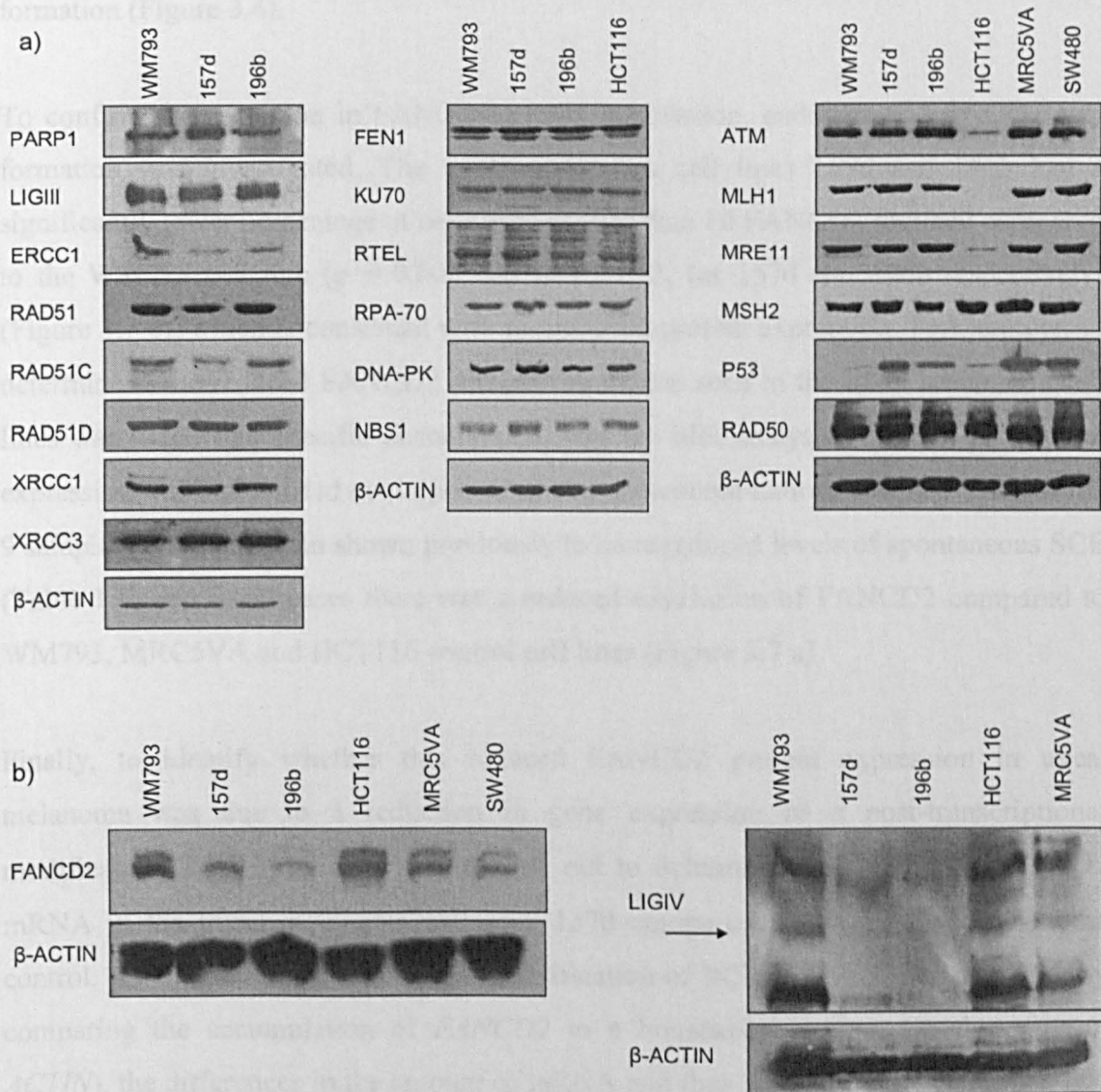


Figure 3.6 FANCD2 and LIGIV protein expression is reduced in uveal melanoma cell lines

a) Western blot screen showing the expression of a wide range of DNA repair proteins in the uveal melanoma cell lines 157d and 196b compared to the WM793, HCT116, MRC5VA and SW480 control cell lines. b) FANCD2 and LIGIV protein expression in uveal melanoma cell lines compared to controls. Images are representative of at least three separate experiments. β -ACTIN is shown as a loading control where 30 μ g of protein was loaded.

From this screen, it is clear that uveal melanoma cell lines have reduced protein expression of the FA protein, FANCD2 (Figure 3.6 b). FANCD2 is an essential protein of the FA pathway and is postulated to promote HR during S-phase and in response to DNA damage (Howlett et al., 2005; Taniguchi et al., 2002). The reduced expression of FANCD2 seen here is therefore consistent with the reduced levels of RAD51 foci formation (Figure 3.4).

To confirm the reduction in FANCD2 protein expression, endogenous FANCD2 foci formation was investigated. The uveal melanoma cell lines 157d and 196b had a significantly lower percentage of cells with greater than 10 FANCD2 foci/cell compared to the WM793 cell line ($p = 0.008$ and $p = 0.002$, for 157d and 196b respectively) (Figure 3.7 c), which is consistent with the reduced protein expression. Furthermore, to determine if the reduced FANCD2 protein expression seen in the uveal melanoma cell lines was a cell line specific phenomenon, western blot analysis of FANCD2 protein expression was also carried out in primary uveal melanoma tumour samples. Each of the 9 samples tested had been shown previously to have reduced levels of spontaneous SCE (Table 1.6) and in all cases there was a reduced expression of FANCD2 compared to WM793, MRC5VA and HCT116 control cell lines (Figure 3.7 a).

Finally, to identify whether this reduced FANCD2 protein expression in uveal melanoma was due to a reduction in gene expression or a post-transcriptional modification, Real Time PCR was carried out to determine the amount of *FANCD2* mRNA in the uveal melanoma cell line, 157d compared to the WM793 melanoma control. As this technique detects the amplification of PCR products in 'real time', by comparing the accumulation of *FANCD2* to a housekeeping gene (in this case β -*ACTIN*), the differences in the amount of mRNA and thus gene expression between two cell lines can be identified. Consistent with reduced protein expression, the uveal melanoma cell line, 157d showed a three-fold reduction in the level of *FANCD2* gene expression compared to the WM793 melanoma control (Figure 3.7 b).

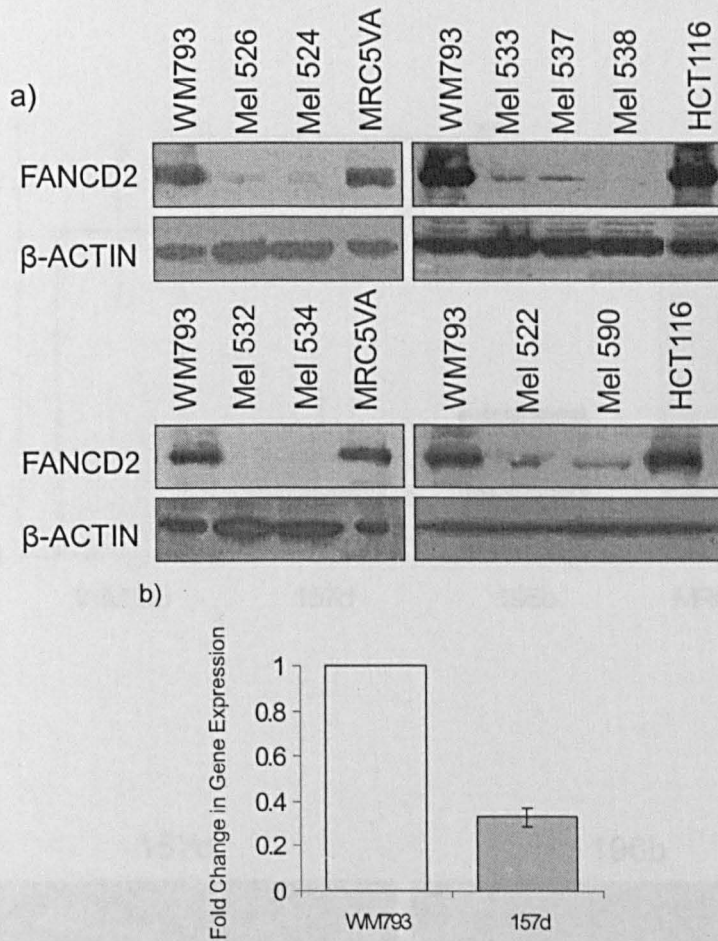
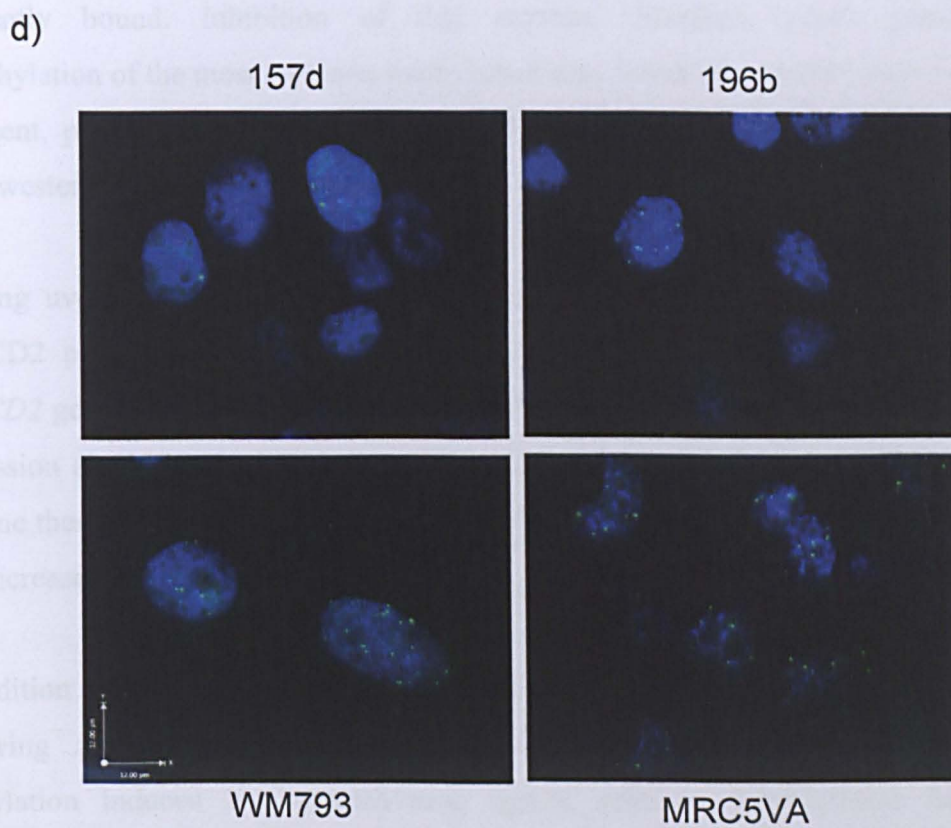
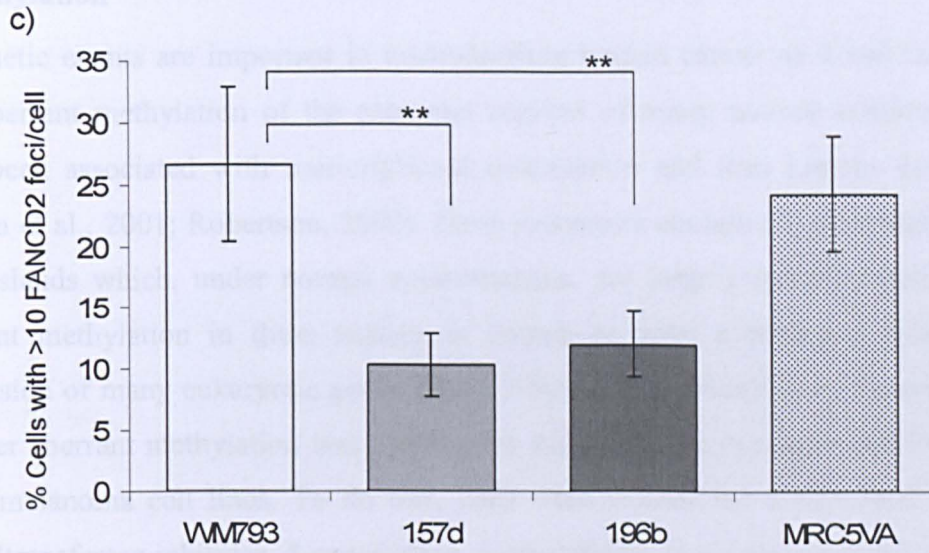


Figure 3.7 Confirmation of the reduced levels of *FANCD2* gene and protein expression in uveal melanoma

a) Western blot analysis for FANCD2 protein expression in 9 primary uveal melanoma tumour samples using WM793, HCT116 and MRC5VA as control cell lines. β -ACTIN is shown as a loading control where 30 μ g of protein was loaded. b) Fold change in *FANCD2* mRNA measured by Real-Time PCR in 157d and WM793 cell lines. The fold change in gene expression was calculated using the $2^{-\Delta\Delta CT}$ equation (Livak and Schmittgen, 2001) and represents two separate experiments. c) Endogenous FANCD2 foci formation visualised by fluorescent microscopy in the uveal melanoma cell lines 157d and 196b, and in the WM793 and MRC5VA control cell lines. Cells were plated for 24 h before being fixed and stained with an antibody specific to human FANCD2 protein and a goat anti-mouse FITC antibody. On each occasion at least 50 cells were analysed and the % of cells with > 10 FANCD2 foci/cell was calculated. Data shown is representative of at least three separate experiments and error bars represent standard deviations. Statistical significance was calculated using the Student's T-test where $p < 0.01$ is indicated by ** and brackets indicate significance between samples. d) Representative images of endogenous FANCD2 foci formation (green) for each of the cell lines studied, nuclei stained with DAPI (blue).



3.6.1 FANCD2 protein expression is altered following genome-wide demethylation

Epigenetic events are important in understanding human cancer as it has been shown that aberrant methylation of the promoter regions of many tumour suppressor genes have been associated with transcriptional inactivation and thus tumour development (Baylin et al., 2001; Robertson, 2002). Gene promoters contain CG-rich regions called CpG islands which, under normal circumstances, are largely unmethylated, however aberrant methylation in these regions is known to have a profound effect on the expression of many eukaryotic genes (Bird, 1992). It was therefore of interest to study whether aberrant methylation was causing the reduced gene expression of *FANCD2* in uveal melanoma cell lines. To do this, cells were treated for 5 days with the DNA methyltransferase inhibitor, 5-azacytidine. 5-azacytidine is an analogue of cytidine and thus becomes incorporated into DNA at these sites. Due to its altered structure, DNA methyltransferase can no longer bind to this base and thus methyl groups cannot be covalently bound. Inhibition of this enzyme therefore causes genome-wide demethylation of the most common methylation site, 5-methylcytosine bases. Following treatment, protein extracts were made and FANCD2 protein expression was studied using western blot analysis.

Treating uveal melanoma cell lines with 5-azacytidine caused a further decrease in FANCD2 protein expression (Figure 3.8 a) suggesting that methylation influences *FANCD2* gene expression. In the WM793 melanoma control cell line, FANCD2 protein expression also decreased with the addition of 5-azacytidine whereas in the HCT116 cell line there was no effect and in the MRC5VA cell line, FANCD2 protein expression was increased (Figure 3.8 b).

In addition to FANCD2 protein expression, spontaneous SCE was also investigated following genome-wide demethylation using BrdU incorporation. Changes in methylation induced by demethylating agents such as 5-azacytidine have been previously shown to affect SCE formation (Perticone et al., 1987), and thus differential methylation patterns could be responsible for the decreased level of spontaneous SCE in uveal melanoma. Here, the differences between spontaneous SCE frequency were compared between non-treated and 5-azacytidine treated cells. There was no difference

in the SCE frequency in any of the cell lines studied (Figure 3.8 b). Differences in global methylation therefore do not affect the SCE frequency in WM793, 157d and 196b cell lines and is unlikely to be the cause of the reduced SCE frequency in uveal melanoma cell lines.

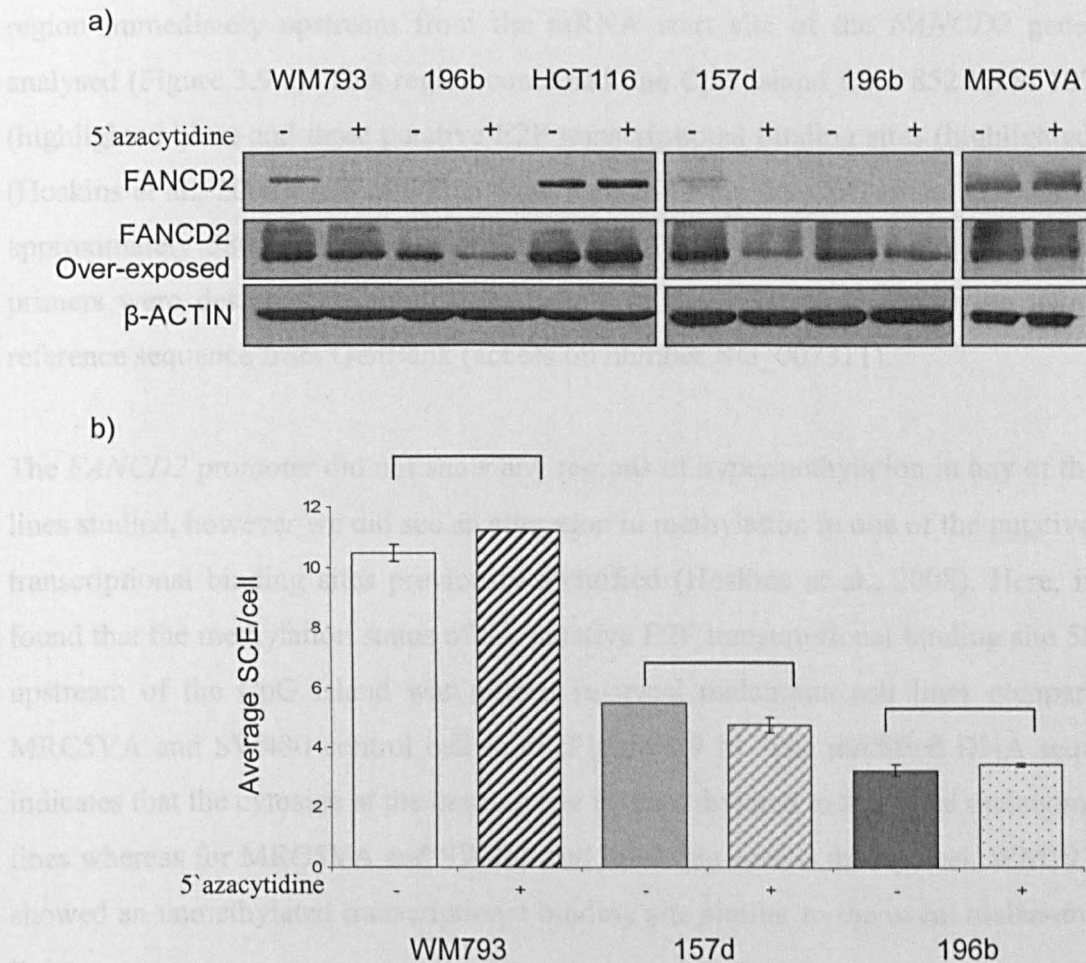


Figure 3.8 FANCD2 protein expression is reduced further in uveal melanoma cell lines following genome-wide demethylation

a) Western blot analysis for FANCD2 protein expression in the uveal melanoma cell lines 157d and 196b, and in the WM793, HCT116 and MRC5VA control cell lines following 5-azacytidine treatment. Cells were either left untreated or treated with 2.5 mM 5-azacytidine for 5 days before protein extracts were made. Images are representative of at least three separate experiments and β -ACTIN is shown as a loading control where 30 μ g of protein was loaded. b) The average spontaneous SCE/cell in WM793, 157d and 196b that were either left untreated or treated with 2.5 mM 5-azacytidine for 5 days, as determined using BrdU incorporation (Figure 1.6). Data represents the average from at least three experiments and the error bars represent the standard deviations. Statistical significance between non-treated and treated samples (as indicated by brackets) was calculated using the Student's T-test; no significance was obtained.

3.6.2 *FANCD2* transcription may be altered by aberrant methylation at a putative E2F transcriptional binding site within the *FANCD2* promoter

To further investigate the methylation status of the *FANCD2* promoter, sodium bisulphite modification of genomic DNA and direct sequencing was used. Here, a 1 kb region immediately upstream from the mRNA start site of the *FANCD2* gene was analysed (Figure 3.9 a). This region contained one CpG island from 852 bp to 1074 bp (highlighted blue) and three putative E2F transcriptional binding sites (highlighted red) (Hoskins et al., 2008), two of which were located inside the CpG island and one found approximately 580 bp further upstream of the CpG island. Three sets of methylated primers were designed to amplify the whole of the 1 kb promoter region using the reference sequence from GenBank (accession number NG_007311).

The *FANCD2* promoter did not show any regions of hypermethylation in any of the cell lines studied, however we did see an alteration in methylation in one of the putative E2F transcriptional binding sites previously identified (Hoskins et al., 2008). Here, it was found that the methylation status of the putative E2F transcriptional binding site 580 bp upstream of the CpG island was altered in uveal melanoma cell lines compared to MRC5VA and SW480 control cell lines (Figure 3.9 b). The modified DNA sequence indicates that the cytosine at the binding site is unmethylated in the uveal melanoma cell lines whereas for MRC5VA and SW480 cell lines this base is methylated. WM793 also showed an unmethylated transcriptional binding site similar to the uveal melanoma cell lines.



Figure 3.9 A putative E2F transcriptional binding site in the *FANCD2* promoter is altered in uveal melanoma cell lines

a) The methylation status of a 1 kb *FANCD2* promoter region in the uveal melanoma cell lines 157d and 196b, and in the WM793, MRC5VA and SW480 control cell lines. The sequence shown was obtained using GenBank (Accession number NG_007311) and indicated are the primer sets used, the three putative E2F transcriptional binding sites (red) (Hoskins et al., 2008) and the CpG island (blue). Region in b) is indicated by *. b) Genomic DNA modified using sodium bisulphite. The sequence shown is a 30 bp region containing the putative E2F transcriptional binding site at 580 bp upstream of the CpG island. Sequences of the uveal melanoma cell lines 157d and 196b were compared to the control cell lines and the modified and unmodified reference sequence from GenBank.

3.7 Uveal melanoma cell lines have reduced *LIGIV* protein expression

In Figure 3.6, we also demonstrated a reduced protein expression of *LIGIV*. As mentioned before, the role of NHEJ in uveal melanoma and spontaneous SCE is the subject of a different study however the finding that *LIGIV* is decreased suggests that the error-prone pathway NHEJ is not upregulated when HR is decreased.

To confirm this result, and to screen for other potential candidate genes that may be altered in uveal melanoma cell lines, a RNase protection assay was used to study the cellular mRNA levels in a panel of uveal melanoma and control cell lines (Figure 3.10). This is a sensitive method used to detect and quantify multiple mRNA transcripts from a single RNA sample. A RNA probe complementary to multiple gene sequences of interest was first synthesised and then hybridised to the target RNA sample. The binding of the probe to the target RNA produces a double-stranded molecule of the gene of interest and thus, it is not degraded following RNase treatment. The remaining probe/target fragments were then denatured on a TBE-urea polyacrylamide gel. The probe was radioactively labelled for visualisation where the intensity of the probe/target fragments is directly proportional to the quantity of mRNA to the gene of interest in the original sample.

Of the 18 DNA repair genes analysed, uveal melanoma cell lines had lower mRNA levels of *LIGIV* and *NBS1* compared to WM793, although other control cell lines also had less mRNA. This confirmed the reduced *LIGIV* protein result in uveal melanoma cell lines at the mRNA level (Figure 3.10) and although *NBS1* mRNA levels were reduced here, this was not seen at the protein level (Figure 3.6 and Figure 3.10)

Cell Line	ATM		DNA-PK	
	L32	GAPDH	L32	GAPDH
WM793	1.0±0.0	1.0±0.0	1.0±0.0	1.0±0.0
157d	0.7±0.1	0.8±0.1	1.1±0.3	1.2±0.6
196b	1.0±0.3	0.8±0.0	1.0±0.0	0.9±0.3
HCT116	0.5±0.2	0.7±0.1	0.9±0.1	1.3±0.5
MRC5VA	0.7±0.3	0.8±0.3	0.8±0.2	1.3±0.7
SW480	1.1±0.7	1.2±0.5	1.0±0.2	1.3±0.4

Cell Line	LIGASE IV		NBS1	
	L32	GAPDH	L32	GAPDH
WM793	1.0±0.0	1.0±0.0	1.0±0.0	1.0±0.0
157d	0.6±0.1	0.7±0.1	0.6±0.1	0.7±0.1
196b	0.8±0.1	0.7±0.1	0.7±0.2	0.6±0.2
HCT116	0.5±0.2	0.8±0.0	0.5±0.2	0.8±0.0
MRC5VA	0.6±0.1	0.7±0.3	0.5±0.2	0.7±0.3
SW480	0.8±0.4	0.9±0.2	0.8±0.4	0.9±0.2

Cell Line	XRCC3		XRCC4	
	L32	GAPDH	L32	GAPDH
WM793	1.0±0.0	1.0±0.0	1.0±0.0	1.0±0.0
157d	0.9±0.1	1.0±0.2	0.8±0.1	0.9±0.2
196b	1.0±0.2	0.9±0.2	1.0±0.2	1.0±0.1
HCT116	0.6±0.1	1.0±0.2	0.8±0.2	1.3±0.2
MRC5VA	0.9±0.1	1.1±0.4	0.7±0.2	1.0±0.4
SW480	1.3±0.4	1.5±0.0	1.1±0.6	1.3±0.2

Cell Line	XRCC2		XRCC2	
	L32	GAPDH	L32	GAPDH
WM793	1.0±0.0	1.0±0.0	1.0±0.0	1.0±0.0
157d	1.0±0.3	1.2±0.6	0.8±0.1	0.9±0.2
196b	0.8±0.1	0.8±0.3	0.8±0.2	0.7±0.3
HCT116	0.7±0.1	1.1±0.4	0.5±0.1	0.9±0.2
MRC5VA	0.8±0.3	1.4±0.7	0.7±0.1	0.9±0.4
SW480	1.0±0.1	1.1±0.4	1.1±0.3	1.2±0.0

Cell Line	MRE11		RAD50	
	L32	GAPDH	L32	GAPDH
WM793	1.0±0.0	1.0±0.0	1.0±0.0	1.0±0.0
157d	1.1±0.3	1.0±0.5	1.4±0.7	1.3±1.0
196b	1.1±0.2	0.8±0.5	1.2±0.2	0.9±0.6
HCT116	0.8±0.2	0.6±0.3	0.9±0.1	0.6±0.3
MRC5VA	1.4±0.4	2.0±1.2	1.1±0.4	1.7±1.1
SW480	1.0±0.2	1.3±0.5	0.7±0.2	0.9±0.4

Cell Line	RAD51		RAD51B	
	L32	GAPDH	L32	GAPDH
WM793	1.0±0.0	1.0±0.0	1.0±0.0	1.0±0.0
157d	0.9±0.2	0.8±0.4	1.2±0.2	1.1±0.4
196b	0.7±0.1	0.5±0.3	1.0±0.1	0.7±0.3
HCT116	0.9±0.1	0.6±0.3	1.1±0.1	0.6±0.3
MRC5VA	1.2±0.3	1.7±1.0	1.3±0.4	0.7±0.2
SW480	1.0±0.1	1.2±0.4	1.1±0.0	1.8±1.2

Cell Line	RAD51C		RAD51D	
	L32	GAPDH	L32	GAPDH
WM793	1.0±0.0	1.0±0.0	1.0±0.0	1.0±0.0
157d	1.0±0.3	1.4±0.9	1.0±0.2	0.9±0.4
196b	1.0±0.1	0.7±0.4	1.1±0.1	0.8±0.3
HCT116	1.3±0.3	0.8±0.1	1.4±0.1	0.9±0.2
MRC5VA	1.2±0.3	1.7±1.0	1.2±0.3	1.7±0.8
SW480	1.3±0.0	1.6±0.3	1.3±0.1	1.6±0.4

Cell Line	RAD52		RAD54	
	L32	GAPDH	L32	GAPDH
WM793	1.0±0.0	1.0±0.0	1.0±0.0	1.0±0.0
157d	1.5±0.6	1.5±0.9	1.1±0.2	0.9±0.5
196b	1.1±0.3	0.8±0.4	0.8±0.1	0.6±0.3
HCT116	1.2±0.3	0.8±0.4	1.0±0.0	0.7±0.2
MRC5VA	1.2±0.7	1.7±1.6	0.9±0.3	1.4±0.9
SW480	0.9±0.5	1.2±0.8	0.9±0.3	1.1±0.5

Figure 3.10 The mRNA levels of a range of genes in uveal melanoma cell lines compared to WM793 and other human control cell lines

The mRNA levels of 18 DNA repair genes in the uveal melanoma cell lines 157d and 196b, and in the WM793, HCT116, MRC5VA and SW480 control cell lines determined by RNase protection assays. The quantity of mRNA for each gene was first normalised to either L32 or GAPDH (housekeeping genes) and then calculated as the fold change in the amount of mRNA compared to WM793 for each cell line. Data shown is the average and standard deviations of at least two separate experiments. Differences in mRNA levels seen with both housekeeping genes are highlighted in grey compared to WM793.

3.8 Discussion

Both spontaneous SCE and *FANCD2* expression can be altered by cell cycle progression, however we ruled out reduced proliferation as the cause of the reduced spontaneous SCE phenotype. Here, we have found that there is a defect in both spontaneous HR (as indicated by reduced RAD51 foci formation) and *FANCD2* gene expression in uveal melanoma. We postulate that these events are linked to the low

spontaneous SCE phenotype. FANCD2 is an essential protein of the FA pathway and forms nuclear foci with BRCA2, BRCA1 and RAD51 both spontaneously and in response to DNA damage to promote HR repair (Taniguchi et al., 2002; Wang et al., 2004). Endogenous RAD51 foci formation was found to be decreased even though overall protein expression was normal. This suggests that RAD51 recruitment and activation, and thus HR, is reduced in response to endogenous DNA damage. FANCD2 and RAD51 have been shown to interact during S-phase and furthermore FANCD2 activation is required for the activation of RAD51 following DNA damage. Thus, it is likely that here the lack of FANCD2 prevents the formation of RAD51 foci at sites of endogenous DNA damage. In FANCD1/BRCA2 deficient cells, spontaneous and induced RAD51 foci formation is reduced, consistent with the known essential role of BRCA2 in HR (Godthelp et al., 2002). Although we have not fully ruled out a lack of FANCD1/BRCA2 as a possible cause of reduced spontaneous HR, in uveal melanoma cell lines, we observed normal levels of induced RAD51 foci formation suggesting that these cells have the ability to induce HR when required, but lack a response to endogenous DNA damage. It is unlikely then that uveal melanoma cells are deficient in an essential protein of HR such as FANCD1/BRCA2. Further analysis of the expression of FANCD1/BRCA2 in uveal melanoma is required to assess its full involvement if any, in the reduced endogenous HR observed here. As SCE is a known end product of HR and RAD51 foci formation is a marker of HR, we propose that the lack of FANCD2 protein expression is responsible for the reduced spontaneous SCE. This hypothesis will be tested in Chapter 4.

Uveal melanoma cell lines were found to have normal cell cycle progression suggesting that activation of FANCD2 still occurs at a level sufficient enough to allow normal replication or that an alternative repair pathway can take over, however as spontaneous mutation rates and TLS levels were normal and LIGIV was decreased, we cannot find any evidence for this. The increased level of endogenous DNA damage, as indicated by spontaneous γ H₂A.X foci formation, is consistent with a defect in the repair of endogenous DNA damage and is also consistent with the lack of upregulation of other types of repair.

The underlying cause of the reduced *FANCD2* gene expression remains to be elucidated. Here, we have shown that methylation may have a role in its regulation as genome-wide demethylation affects *FANCD2* protein expression. This was true of all cell lines studied however different affects were observed in each case. While it is clear that methylation changes effect *FANCD2* protein expression, it is possible that the *FANCD2* promoter may not be directly affected. Demethylation of genes encoding regulating proteins such as transcriptional binding factors may also cause the differences in protein expression. Furthermore, we cannot rule out point mutations in the *FANCD2* gene that may limit transcript stability and thus the decrease in protein expression.

The E2F transcriptional binding site upstream of the CpG island in the *FANCD2* promoter region was found to be altered in uveal melanoma cell lines compared to MRC5VA and SW480 cell lines (although not from the WM793 melanoma control). While it is unlikely that a single methylation change can cause an affect on protein expression, the alteration of the sequence of this transcriptional binding site cannot be ruled out as a cause for the decreased *FANCD2* expression in uveal melanoma. The recent finding that methylation events in the surrounding areas of CpG islands may be more important than alterations inside the islands (Irizarry et al., 2009) suggests that further investigation into the surrounding areas of the *FANCD2* promoter may provide additional insights into its regulation by methylation.

We have postulated that the unmethylated state of the E2F transcriptional binding site within the *FANCD2* promoter causes the decreased *FANCD2* expression in uveal melanoma and thus the decreased spontaneous SCE frequency. We have also shown that genome-wide demethylation causes a further decrease in *FANCD2* protein expression although this does not affect SCE frequency. In MRC5VA and SW480 control cell lines, the E2F transcriptional binding site is normally methylated and thus expression of *FANCD2* is normal. However, upon demethylation *FANCD2* protein expression is increased. This therefore contradicts our hypothesis that an unmethylated E2F transcriptional binding site causes a decrease in *FANCD2* expression, although this could be cell line or melanoma specific. Alternatively, it is possible that another gene unrelated to this single methylation change, upstream of *FANCD2* and E2F

transcriptional binding, is suppressed in uveal melanoma whereas in MRC5VA, it is activated by the loss of methylation. As there is no change in SCE frequency following demethylation, this suggests that this is unrelated to SCE frequency whereas the direct methylation change on the E2F binding site may still be related.

Finally, we cannot rule out cytogenetic causes for the reduced *FANCD2* expression. Monosomy of chromosome 3 is a common, non-random chromosomal alteration in uveal melanoma. *FANCD2* has been mapped to chromosome 3p25.3 and thus the reduced level of *FANCD2* could be due to this chromosomal loss. Both the uveal melanoma cell lines studied here were originally established from tumours with monosomy of chromosome 3, however in culture they both gained a copy of this chromosome. It is therefore unlikely that the lack of *FANCD2* is due to the entire loss of chromosome 3, however partial deletions can occur. Deletion-mapping studies have identified 3p25 as a region that is preferentially lost (Parrella et al., 2003) and thus this could be a possible cause of the reduced *FANCD2* protein expression in uveal melanoma.

Chapter 4 – Complementation of FANCD2 in a Uveal Melanoma Cell Line Corrects the Reduced SCE Phenotype

4.1	Introduction	127
4.2	Generation of a uveal melanoma cell line complemented with pMMP-FANCD2.....	128
4.3	Complementing a uveal melanoma cell line with FANCD2 increases the spontaneous levels of SCE.....	131
4.4	RAD51 foci formation is increased in a uveal melanoma cell line complemented with FANCD2.....	134
4.5	Complementing the uveal melanoma cell line, 196b with FANCD2 reduces the level of endogenous DNA damage.....	136
4.6	Observation: Following long-term culture, uveal melanoma cell lines gain FANCD2 expression and exhibit increased levels of spontaneous SCE.....	138
4.7	Discussion.....	140

List of Figures

Figure 4.1 Confirmation of the retroviral complementation of pMMP-empty and pMMP-FANCD2 in the uveal melanoma cell line, 196b.....	130
Figure 4.2 Spontaneous SCE frequency is increased in a uveal melanoma cell line complemented with FANCD2.....	131
Figure 4.3 Complementing the PD20 cell line with FANCD2 (PD20-D2 cell line) increases spontaneous SCE frequency.....	133
Figure 4.4 Endogenous RAD51 foci formation is increased in the uveal melanoma cell line 196b complemented with FANCD2.....	135
Figure 4.5 Complementing the uveal melanoma cell line 196b with FANCD2 decreases the level of endogenous γ H ₂ A.X foci formation.....	137
Figure 4.6 Long-term culture of the uveal melanoma cell lines led to a gain of FANCD2 expression and an increase in spontaneous SCE.....	139

4.1 Introduction

To date, uveal melanoma is the only disease state to exhibit reduced levels of spontaneous SCE (Hoh, 2007 unpublished data). In Chapter 3, it was found that the uveal melanoma cell lines and primary tumour samples also have reduced protein expression of FANCD2. As FANCD2 activation is required for normal cell cycle progression following exposure to MMC (Taniguchi et al., 2002) and it is a protein that promotes HR (Garcia-Higuera et al., 2001) it is a possible candidate for the reduced levels of spontaneous SCE in these cells. Furthermore, altered levels of both phenotypes have independently been associated with sporadic and hereditary cancer (Illeni et al., 1991; van der Groep et al., 2008).

Although a causal link has not been identified between *FANCD2* gene expression and SCE in humans, evidence suggests that there may be an association between the two. Firstly, it has been found that knocking out *Fancd2* in chicken DT40 cell lines causes an increase in spontaneous SCE frequency (Yamamoto et al., 2005). This is in contrast however to primary *FANCD2*^{-/-} patient cells that exhibit normal levels of spontaneous SCE but a reduced MMC-induced SCE frequency (Latt et al., 1975).

In Chapter 3, we postulated that the reduced FANCD2 protein expression in uveal melanoma is associated with the reduced level of spontaneous SCE observed in these cells. In this chapter, using retroviral complementation, an association if any, between the two will be investigated. As a control for this work, the *FANCD2*^{-/-} patient cell line, PD20 was also studied. The PD20 cell line is a *FANCD2* deficient immortalised fibroblast cell line, derived from a FA patient and exhibits the hallmark of FA patient cell lines, i.e. a hypersensitivity to ICL-inducing agents (Timmers et al., 2001). In addition, this cell line has been retrovirally complemented with FANCD2 to produce the functionally complemented cell line, PD20-D2 (Timmers et al., 2001). In this Chapter, the same retrovirus and technique was used to complement the uveal melanoma cell line, 196b. The PD20 cell line has been used widely in the literature, it is therefore of interest to compare the effects of the decrease in, and complementation of, FANCD2 in uveal melanoma cell lines compared to the WM793 control melanoma cell line, the PD20 (absent *FANCD2*) and PD20-D2 (retrovirally complemented FANCD2) cell line.

4.2 Generation of a uveal melanoma cell line complemented with pMMP-FANCD2

Using retroviral complementation, the uveal melanoma cell line 196b was complemented with the retroviral pMMP-empty and pMMP-FANCD2 vectors to create the two stable cell lines, 196b pMMP-empty and 196b pMMP-FANCD2 (referred to as 196b-pMMP and 196b-D2 from here in) (Figure 4.1). Retroviruses are used widely as an efficient method of stably complementing mammalian cells with new genetic material *in vitro* (Mulligan, 1993). Incorporating the vesicular stomatitis virus G (VSV-G) proteins (continually expressed by packaging cell lines) into the retroviral vector, creates a retroviral pseudotype with enhanced efficiency of infection in human cells (Emi et al., 1991). Here, the retroviral vectors were first transfected into the human packaging cell line 293GPG. As the retroviral pseudotype becomes expressed into the supernatant, this was removed and added to the uveal melanoma cell line 196b in the presence of polybrene to enhance infection (Figure 2.5). Cultures were maintained in 3 $\mu\text{g/ml}$ puromycin to select for cells containing the retroviral vector.

A western blot was carried out to ensure the vectors had been incorporated into the cells and that FANCD2 protein expression had been restored. Figure 4.1 a) shows that 196b-D2 cells were expressing FANCD2 protein at a similar level to that of WM793 and other controls, whereas the expression of FANCD2 remained low in the 196b and 196b-pMMP cell lines. Also shown, is the FANCD2 expression level in PD20 and PD20-D2 cell lines. As reported in the literature, PD20 cells show no expression of FANCD2 (Timmers et al., 2001), whereas the PD20-D2 cells, that are complemented using the same system as used here, show a similar level of FANCD2 expression as in the 196b-D2 cells and the other controls.

To further confirm that the 196b-D2 and 196b-pMMP cell lines had been complemented with FANCD2 and empty vector respectively, the level of endogenous FANCD2 foci formation in these cells was compared to 196b and WM793 (Figure 4.1 b and c). FANCD2 is monoubiquitinated by the FA core complex, allowing its localisation to chromatin foci where it interacts with other repair proteins such as BRCA2, BRCA1 and RAD51 to promote DNA repair (Taniguchi et al., 2002; Wang et al., 2004). As this

activation is required for the normal cell cycle progression through S-phase, FANCD2 forms nuclear foci spontaneously (Taniguchi et al., 2002). Here, these foci were visualised using fluorescent microscopy with an antibody specific to the human FANCD2 protein and a FITC conjugated goat anti-mouse secondary antibody. The nuclei were stained using DAPI to determine where the cells were located (Figure 4.1 b and c).

The 196b-D2 cell line showed an average of 30% of cells with greater than 10 FANCD2 foci/cell. This is consistent with the percentage of cells with greater than 10 FANCD2 foci/cell observed in WM793 (25%), MRC5VA (20%) and U2OS cell lines (26%) - shown previously in Chapter 3, and consistent with published data for endogenous levels of FANCD2 foci formation (Wang et al., 2004). It was also a significant increase from the levels observed in the parental 196b and 196b-pMMP cell lines ($p = 0.004$ and 0.02 respectively). Endogenous FANCD2 foci formation was not significantly different in 196b (11%) and 196b-pMMP cell lines (16%) (Figure 4.1 b and c). The significant increase of FANCD2 foci formation in the 196b-D2 cell line from the levels in 196b suggests that endogenous FANCD2 has been complemented in this uveal melanoma cell line. Together with the western blot analysis of FANCD2 protein expression, this data supports the system of complementation used here as an accurate way of developing stable cell lines expressing pMMP-FANCD2 and pMMP-empty vectors; in this case, to create the uveal melanoma cell line 196b-pMMP and 196b-D2 for use in subsequent studies.

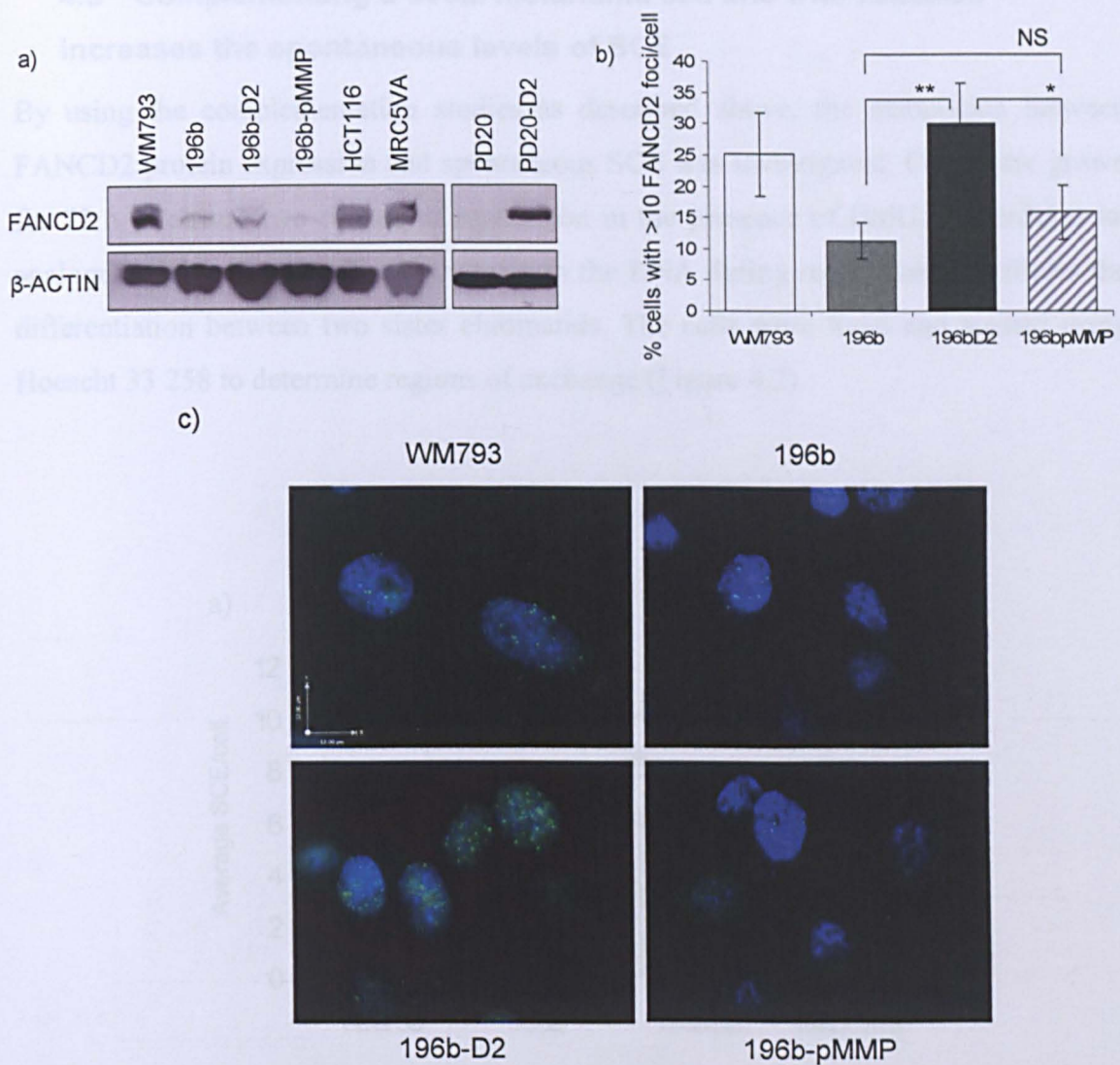


Figure 4.1 Confirmation of the retroviral complementation of pMMP-empty and pMMP-FANCD2 in the uveal melanoma cell line, 196b

a) Western blot analysis for the FANCD2 protein expression in the 196b-pMMP and 196b-D2 cell lines compared to the parental 196b cell line, PD20 and PD20-D2 cell lines, WM793 and other human control cell lines. β -ACTIN is shown as a loading control where 30 μ g of protein was loaded. b) Cells were fixed in 3% PFA and stained with anti-FANCD2 antibody and FITC goat anti-mouse antibody. On each occasion, more than 50 cells were analysed for each cell line and the % of cells with > 10 FANCD2 foci/cell was calculated. Data shown is the average of at least three experiments and error bars represent the standard deviations. Statistical significance was calculated using the Student's T-Test where $p < 0.05$ is indicated by * and $p < 0.01$ is indicated by **. P-values were calculated between the samples as indicated by brackets, where no significance is indicated by 'NS'. c) Representative images of endogenous FANCD2 foci formation (green) in all cell lines studied, nuclei stained with DAPI (blue).

4.3 Complementing a uveal melanoma cell line with FANCD2 increases the spontaneous levels of SCE

By using the complementation studies as described above, the association between FANCD2 protein expression and spontaneous SCE was investigated. Cells were grown for 72 h to ensure two rounds of replication in the presence of BrdU. As BrdU is an analogue of thymine, it is incorporated into the DNA during replication and allows the differentiation between two sister chromatids. The cells were fixed and stained using Hoescht 33 258 to determine regions of exchange (Figure 4.2).

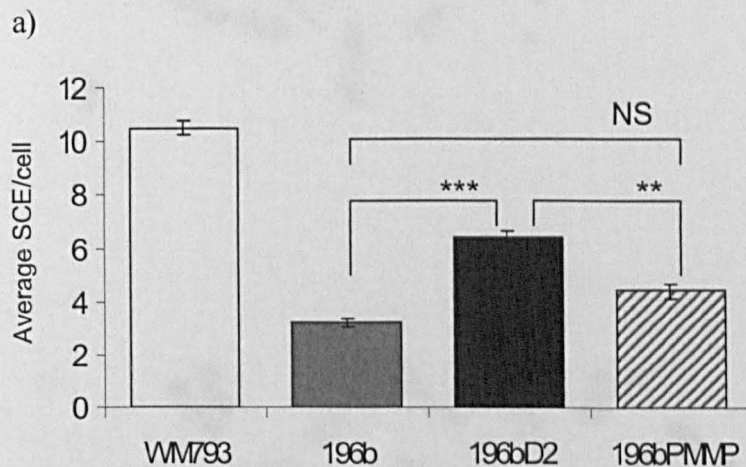
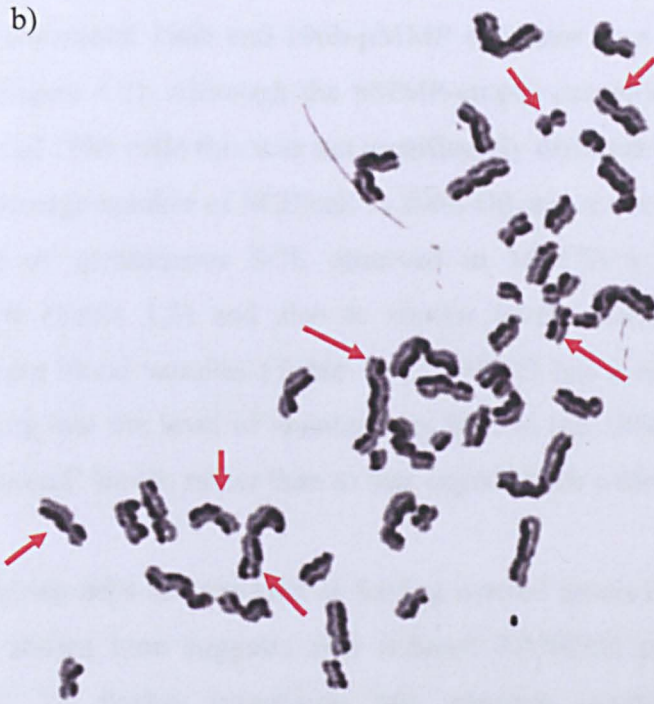


Figure 4.2 Spontaneous SCE frequency is increased in a uveal melanoma cell line complemented with FANCD2

a) Quantification of the spontaneous SCE levels in 196b-D2 compared to 196b, 196b-pMMP and WM793 cell lines. On each occasion, at least 30 cells were counted and the average SCE/cell represents three separate experiments. Error bars represent the standard deviations. Statistical significance was calculated using the Student's T-test where $p < 0.01$ is indicated by ** and $p < 0.001$ is indicated by ***. Significance between samples is indicated by brackets, where no significance is indicated by 'NS'. b) Representative image a typical metaphase spread showing the number of SCE/cell in 196bD2 compared to, c) the 196b cell line using BrdU incorporation and Hoescht 33 258 staining. Arrows indicate regions of SCE (Hoh, 2007, unpublished data).



The 196b-D2 cell line was found to have a significant increase in spontaneous SCE/cell compared to the parental 196b and 196b-pMMP cell lines ($p = 2 \times 10^{-4}$ and $p = 0.004$ respectively) (Figure 4.2). Although the pMMP-empty caused a slight increase in the SCE frequency of 196b cells this was not significantly different from the parental 196b cell line. The average number of SCE/cell in 196b-D2 was 6.4 ± 0.24 . This is consistent with the level of spontaneous SCE observed in MRC5VA (6.1), human primary fibroblasts (7.4) (Table 1.5) and also to similar levels observed in matched uveal melanoma patient blood samples (Table 1.6). WM793 has a higher average SCE/cell (10.5) suggesting that the level of spontaneous SCE in the 196b-D2 cell line has been corrected to ‘normal’ levels, rather than to that expected for a melanoma phenotype.

Primary FA patient cells are reported as having normal levels of spontaneous SCE. In contrast, data shown here suggests that reduced FANCD2 protein expression may decrease SCE. To further investigate this apparent contradiction, the level of spontaneous SCE was examined in PD20 and PD20-D2 cell lines (Figure 4.3).

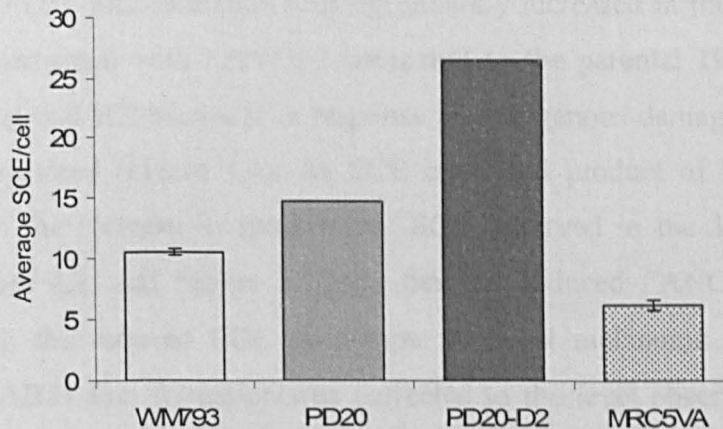


Figure 4.3 Complementing the PD20 cell line with FANCD2 (PD20-D2 cell line) increases spontaneous SCE frequency

Quantification of the spontaneous SCE levels in PD20 and PD20-D2 cell lines compared to MRC5VA and WM793 control cell lines. On each occasion, at least 30 cells were counted and the average SCE/cell represents three separate experiments in the controls. PD20 and PD20-D2 were only carried out once. Error bars represent the standard deviations.

Consistent with the uveal melanoma cell lines, complementation of the PD20 cell line with FANCD2 increased spontaneous SCE, supporting the hypothesis that FANCD2 plays a role in promoting spontaneous SCE frequency. Interestingly, compared with other cell lines tested here and published data (Table 1.5 and 1.6), the PD20 cell line did not have normal levels of SCE (Figure 4.3). This contradicts what has been reported for primary FA patient cells (Latt et al., 1975).

4.4 RAD51 foci formation is increased in a uveal melanoma cell line complemented with FANCD2

FANCD2 forms nuclear foci with RAD51 during S-phase, thus promoting HR (Taniguchi et al., 2002). It was therefore of interest to investigate the spontaneous formation of RAD51 foci in 196b-D2 compared to 196b and 196b-pMMP cell lines by fluorescent microscopy. Cells were fixed and stained with an antibody specific to the human RAD51 protein and a CY3 goat anti rabbit secondary antibody. DAPI was used to stain the nuclei of the cells (Figure 4.4).

Endogenous RAD51 foci formation was significantly increased in the uveal melanoma cell line complemented with FANCD2 compared to the parental 196b cell line ($p = 0.04$) suggesting that HR increases in response to endogenous damage when FANCD2 expression is restored (Figure 4.4). As SCE is an end product of HR, this result is consistent with the increase in spontaneous SCE observed in the 196b-D2 cell line, shown in Figure 4.2, and further suggests that the reduced FANCD2 expression is associated with the reduced SCE phenotype of uveal melanoma. This increase in endogenous RAD51 foci formation was corrected to the level observed in the control cell lines MRC5VA and U2OS. However, it was still lower than that seen in WM793 (Figure 4.4).

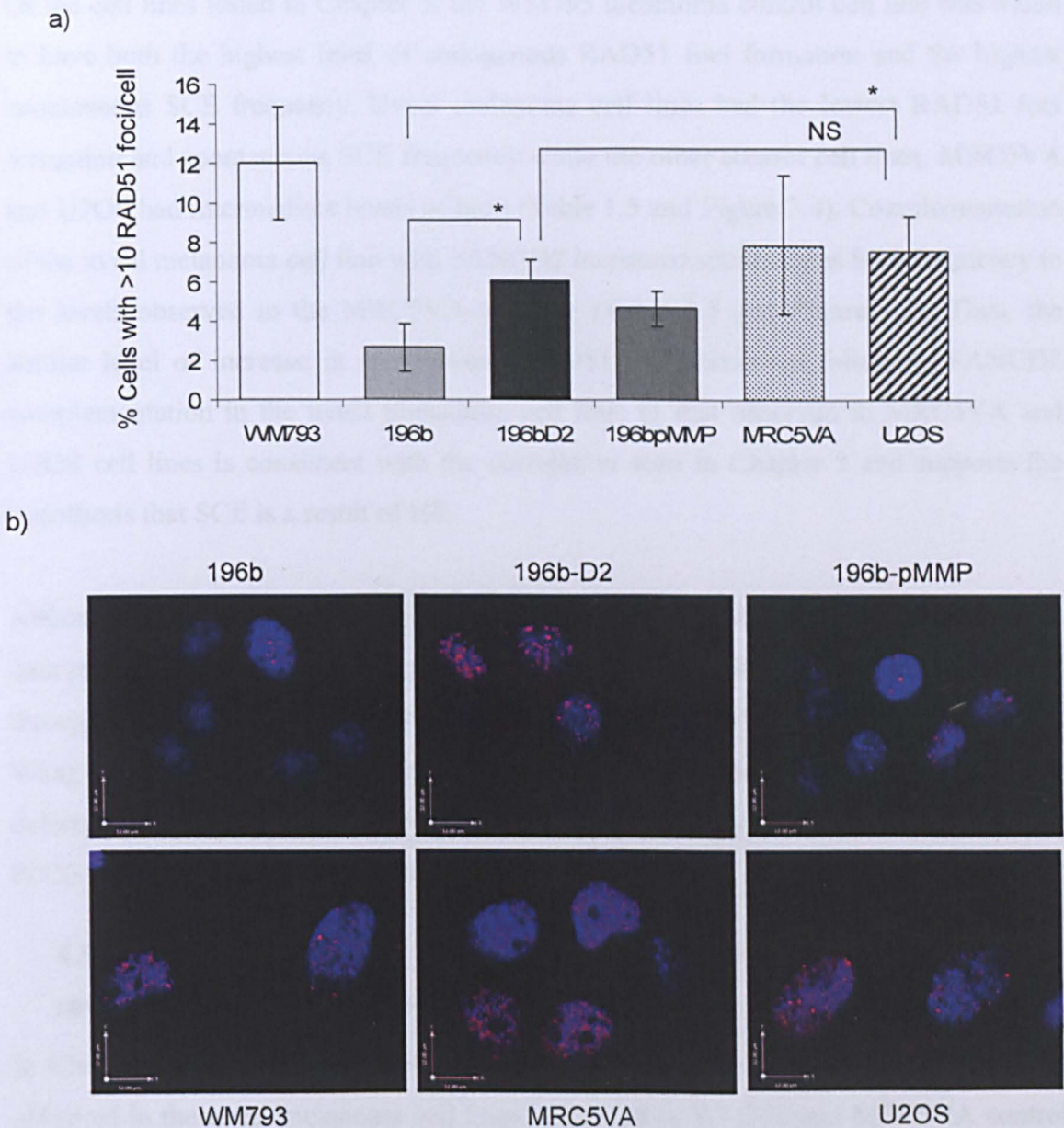


Figure 4.4 Endogenous RAD51 foci formation is increased in the uveal melanoma cell line 196b complemented with FANCD2

a) Endogenous RAD51 foci formation in 196b-D2 compared to 196b-pMMP and 196b uveal melanoma cell lines, and WM793, MRC5VA and U2OS control cell lines. On each occasion, at least 50 cells were analysed and the % of cells with > 10 RAD51 foci/cell was calculated. Data shown is the average of at least three experiments and the error bars represent the standard deviations. Significance was calculated using the Student's T-test and was calculated between samples as indicated by brackets where $p < 0.05$ is indicated by *. b) Representative images of endogenous RAD51 foci formation (red) in all cell lines studied, nuclei stained with DAPI (blue).

Of the cell lines tested in Chapter 3, the WM793 melanoma control cell line was found to have both the highest level of endogenous RAD51 foci formation and the highest spontaneous SCE frequency. Uveal melanoma cell lines had the lowest RAD51 foci formation and spontaneous SCE frequency while the other control cell lines, MRC5VA and U2OS had intermediate levels of both (Table 1.5 and Figure 3.4). Complementation of the uveal melanoma cell line with FANCD2 increased spontaneous SCE frequency to the levels observed in the MRC5VA cell line (Table 1.5 and Figure 4.2). Thus, the similar level of increase in spontaneous RAD51 foci formation following FANCD2 complementation in the uveal melanoma cell line, to that observed in MRC5VA and U2OS cell lines is consistent with the correlation seen in Chapter 3 and supports the hypothesis that SCE is a result of HR.

Although FANCD2 is not essential to RAD51 foci formation (Ohashi et al., 2005), the data presented here supports the postulated involvement of FANCD2 in promoting HR through its interactions with BRCA2, BRCA1 and RAD51 (Taniguchi et al., 2002; Wang et al., 2004). This also reflects published data where PD20 cell lines show defective formation of spontaneous RAD51 foci formation that is corrected in the PD20-D2 cell line (Wang et al., 2004).

4.5 ComPLEMENTING THE UVEAL MELANOMA CELL LINE, 196b WITH FANCD2 REDUCES THE LEVEL OF ENDOGENOUS DNA DAMAGE

In Chapter 3, a significant increase in the amount of endogenous DNA damage was observed in the uveal melanoma cell lines compared to WM793 and MRC5VA control cell lines, as indicated by the increased levels of spontaneous γ H₂A.X foci formation (Figure 3.3). H₂A.X is a member of the histone family and is phosphorylated upon DNA damage (Rogakou et al., 1998) and in response to replication stress (Ward and Chen, 2001) forming distinct nuclear foci at sites of DNA damage. Spontaneously formed γ H₂A.X foci are representative of unrepaired or aberrantly repaired spontaneous DNA damage. By studying the level of these foci in untreated cells, differences in the amount of endogenous DNA damage can be determined (Figure 4.5).

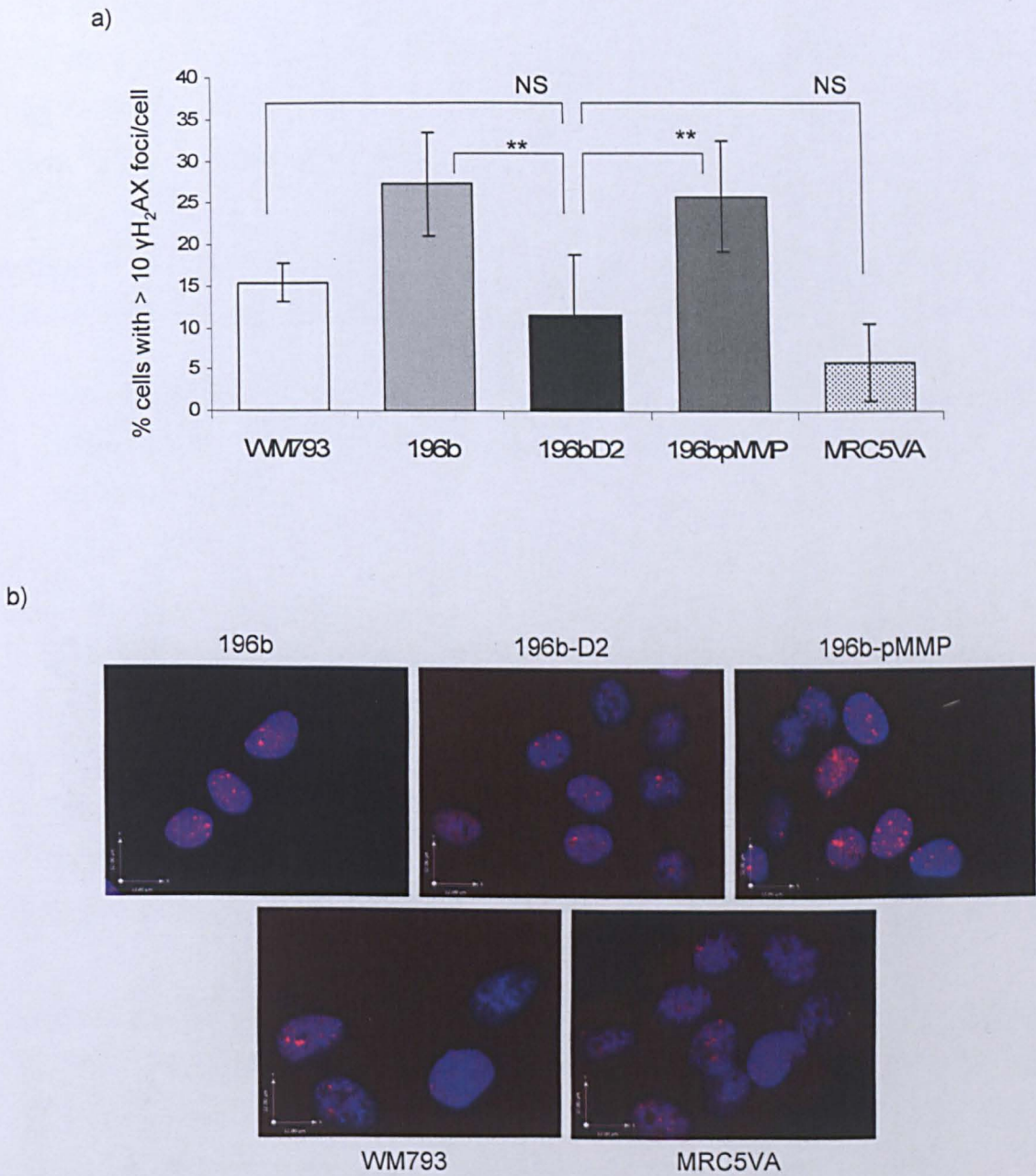


Figure 4.5 Complementing the uveal melanoma cell line 196b with FANCD2 decreases the level of endogenous $\gamma\text{H}_2\text{A.X}$ foci formation

a) Endogenous $\gamma\text{H}_2\text{A.X}$ foci formation in 196b-D2 compared to 196b-pMMP, 196b, WM793 and MRC5VA control cell lines. On each occasion, at least 50 cells were analysed and the % of cells with > 10 $\gamma\text{H}_2\text{A.X}$ foci/cell was calculated. Data shown is representative of at least three separate experiments and the error bars represent the standard deviations. Significance was calculated using the Student's T-test where $p < 0.01$ is indicated by **. Significance between samples is indicated by brackets, where no significance is indicated by 'NS'. b) Representative images of endogenous $\gamma\text{H}_2\text{A.X}$ foci formation (red) in all cell lines studied, nuclei stained with DAPI (blue).

The increased amount of endogenous $\gamma\text{H}_2\text{A.X}$ foci formation found in Chapter 3 is indicative of an increased level of endogenous DNA damage suggesting a defect in repair. Here, complementing the uveal melanoma cell line 196b with FANCD2 significantly decreased ($p = 0.007$) the level of endogenous $\gamma\text{H}_2\text{A.X}$ foci formation (Figure 4.5) suggesting endogenous DNA damage is no longer left unrepaired. The empty vector control did not alter the level of $\gamma\text{H}_2\text{A.X}$ foci formation (Figure 4.5). This is consistent with the restored HR activity seen in Section 4.4.

4.6 Observation: Following long-term culture, uveal melanoma cell lines gain FANCD2 expression and exhibit increased levels of spontaneous SCE

Further confirmation that there is an association between the lack of FANCD2 and reduced levels of spontaneous SCE in uveal melanoma came from an observation made whilst working with these cell lines. It was found that after the uveal melanoma cell lines 157d and 196b had been grown continuously for more than 20 – 30 passages, both cell lines started to express FANCD2 as determined by western blot analysis (Figure 4.6 a). At the same time we observed a decrease in spontaneous $\gamma\text{H}_2\text{A.X}$ foci formation, an increase in spontaneous RAD51 foci formation (data not shown) and interestingly, an increase in the level of spontaneous SCE frequency in these cells (Figure 4.6 b).

The uveal melanoma cell line 157d at a passage between P98 – P120, consistently showed a low average SCE/cell, however once over P150, the number of SCE/cell significantly increased to a similar level to that found in WM793 ($p = 3 \times 10^{-4}$). A similar observation was seen in 196b although at different passage numbers ($p = 3.1 \times 10^{-9}$) (Figure 4.6). Once this observation had been made, cells were checked every 10 passages for an increase in FANCD2 expression and an increase in SCE frequency. Once cells had ‘reverted’, new vials of these cell lines at a low passage were thawed and used for subsequent experiments. Experiments performed during the last 10 passages were ignored from data analysis. Studies are ongoing to identify the cause of this reversion that in turn may help understand the development of these genetic changes and tumourigenesis in uveal melanoma.

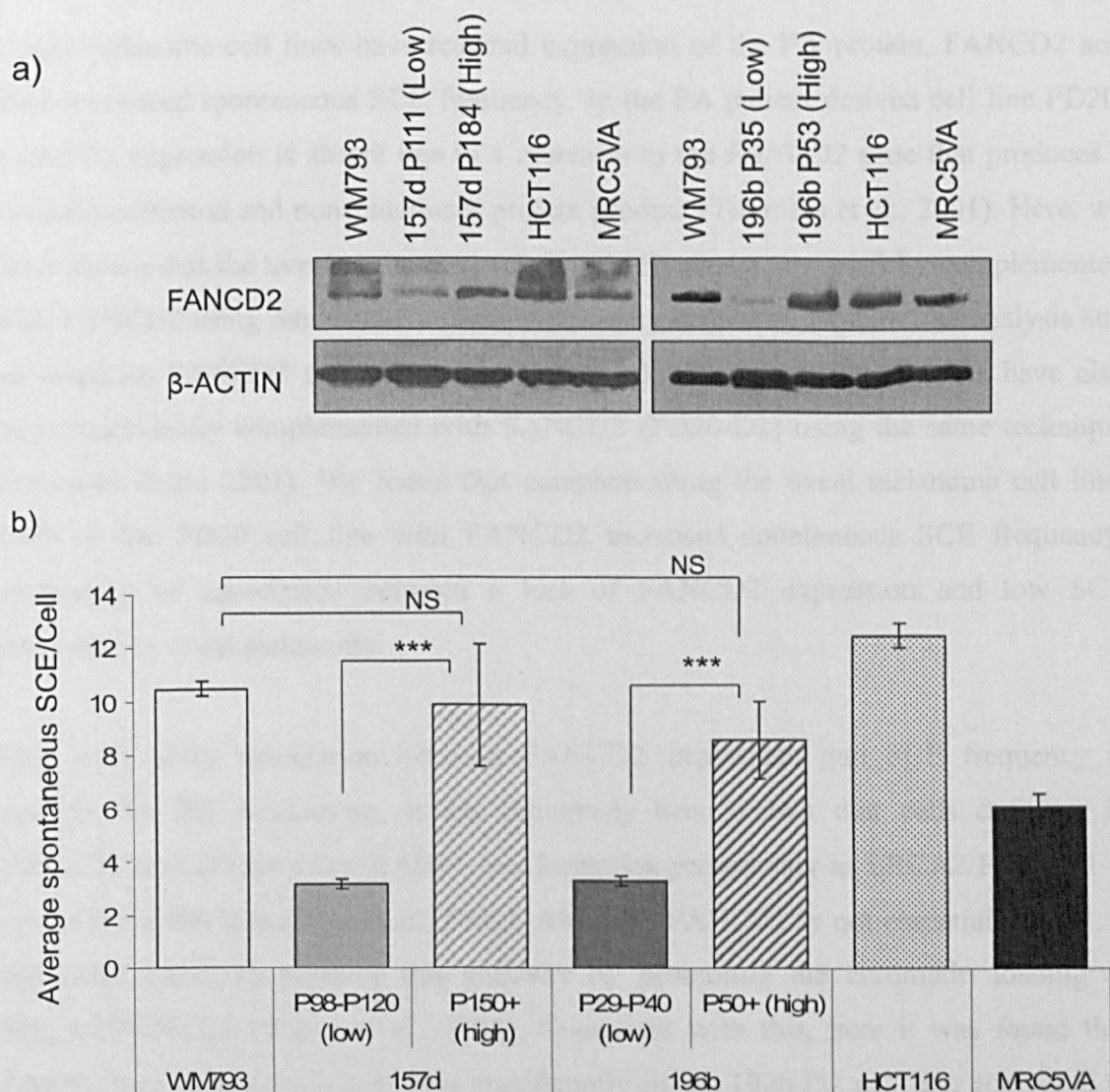


Figure 4.6 Long-term culture of the uveal melanoma cell lines led to a gain of FANCD2 expression and an increase in spontaneous SCE

a) Western blot analysis for the increase in FANCD2 protein expression in uveal melanoma cell lines following continuous passage. Image shown is representative of at least three separate experiments. β -ACTIN is shown as a loading control where 30 μ g protein was loaded. b) Quantification of the average number of SCE/cell showing the increase in spontaneous SCE in the uveal melanoma cell lines following continuous passage. On each occasion, at least 30 cells were counted and the average SCE/cell represents three separate experiments. Error bars represent the standard deviations. Statistical significance was calculated using the Student's T-test where $p < 0.001$ is indicated by ***. Significance between samples is indicated by brackets, where no significance is indicated by 'NS'.

4.7 Discussion

Uveal melanoma cell lines have reduced expression of the FA protein, FANCD2 and have a reduced spontaneous SCE frequency. In the FA patient derived cell line PD20, FANCD2 expression is absent due to a mutation in the *FANCD2* gene that produces a severely truncated and non-functional protein product (Timmers et al., 2001). Here, we have shown that the uveal melanoma cell line 196b can be successfully complemented with FANCD2 using retroviral complementation confirmed by western blot analysis and spontaneous FANCD2 foci formation (Figure 4.1). Previously, PD20 cells have also been functionally complemented with FANCD2 (PD20-D2) using the same technique (Timmers et al., 2001). We found that complementing the uveal melanoma cell line, 196b or the PD20 cell line with FANCD2 increased spontaneous SCE frequency, supporting an association between a loss of FANCD2 expression and low SCE frequency in uveal melanoma.

The most likely association between FANCD2 expression and SCE frequency is through the HR mechanism. It has previously been shown that cells deficient in BRCA2/FANCD1 have low RAD51 foci formation presumably as BRCA2/FANCD1 is essential for HR (Godthelp et al., 2002). Although FANCD2 is not essential for HR, it has been shown to promote this pathway by promoting the chromatin loading of BRCA2/FANCD1 (Wang et al., 2004). Consistent with this, here it was found that RAD51 foci formation is increased significantly in the 196b-D2 cell line compared to the parental 196b cell line and thus it is postulated that in uveal melanoma, increasing FANCD2 protein expression increases the response of HR to endogenous DNA damage and that this causes the increase in spontaneous SCE frequency.

Complementing the 196b cell line with FANCD2 also decreased the high level of spontaneous γ H₂A.X foci formation observed in the uveal melanoma cell lines. γ H₂A.X foci formation is a marker of DNA damage and thus, spontaneously formed γ H₂A.X foci are representative of unrepaired or aberrant repair of endogenous DNA damage. The reduction of γ H₂A.X foci formation therefore suggests that the defect in repair has been corrected by complementing the cells with FANCD2, presumably by the promotion of HR.

Here, the association between FANCD2 expression and SCE frequency has been established, however further investigation using siRNA technology would provide additional evidence for a causal link between the two phenotypes. From the evidence discussed above, we would postulate that knocking down FANCD2 in the FANCD2 complemented uveal melanoma cell line (196b-D2) would cause a reduction in spontaneous SCE to the phenotypically low level observed in these cells. As uveal melanoma is the only known disease state to exhibit reduced spontaneous SCE frequency, it would also be of interest to study the effect of knocking down FANCD2 expression in other cancer cell types such as WM793 or HCT116 to see if the same effect on SCE frequency is observed, or whether it is a phenomenon specific to uveal melanoma.

Chapter 5 –Characterisation of the Induced DNA Damage Response in Uveal Melanoma

5.1	Introduction.....	144
5.2	Uveal melanoma cell lines have increased resistance to thymidine (dT) and the ICL-inducing agents, MMC and cisplatin.....	145
5.3	FANCD2 is activated at a lower level in response to MMC treatment	150
5.4	HR is induced at a lower level in response to MMC treatment in uveal melanoma cell lines.....	154
5.5	MMC induces less DNA damage in uveal melanoma cell lines compared to WM793 and MRC5VA control cell lines	158
5.6	MMC induces fewer DNA ICLs in uveal melanoma cell lines.....	161
5.7	CYP450R required for MMC metabolism is reduced in uveal melanoma cell lines, thus causing the observed resistance to MMC.....	164
5.8	The defect in FANCD2 in uveal melanoma is not associated with the resistance to MMC	166
5.9	Discussion.....	172

List of Figures

Figure 5.1	Uveal melanoma cell lines are less sensitive to thymidine than WM793 and other control cell lines.....	147
Figure 5.2	Uveal melanoma cell lines and primary uveal melanoma tumour samples are less sensitive to the ICL-inducing agents MMC and cisplatin compared to control cell lines.....	149
Figure 5.3	FANCD2 is activated less in response to MMC induced damage in uveal melanoma cell lines compared to control cell lines.....	151

Figure 5.4 The induction of RAD51 foci formation following MMC treatment is reduced in uveal melanoma cell lines.....	155
Figure 5.5 MMC causes a significantly lower amount of damage in uveal melanoma cell lines compared to WM793.....	159
Figure 5.6 MMC does not cause G2 arrest in uveal melanoma cell lines.....	160
Figure 5.7 There is a decreased level of DNA ICLs formed following MMC treatment in uveal melanoma cells.....	162
Figure 5.8 Uveal melanoma cell lines and primary tumour samples have a decreased expression of CYP450R.....	164
Figure 5.9 Transient complementation of CYP450R in uveal melanoma cell lines increases sensitivity to MMC.....	166
Figure 5.10 Complementation of the uveal melanoma cell line, 196b with FANCD2 does not alter the resistance to MMC.....	167
Figure 5.11 FANCD2, RAD51 and γ H ₂ A.X foci formation was not induced to the same degree by MMC in a FANCD2 complemented uveal melanoma cell line compared to WM793 control cell line.....	168
Figure 5.12 Genome-wide demethylation, which affects the protein expression of FANCD2 in uveal melanoma cell lines, has no effect on the resistance to MMC.....	171
Figure 5.13 High doses of MMC increases γ H ₂ A.X foci formation in the uveal melanoma cell line 196b to similar levels observed for WM793 and MRC5VA controls.....	173

List of Tables

Table 5.1 The DNA damaging agents used for the sensitivity screen in uveal melanoma cell lines.....	146
--	-----

5.1 Introduction

So far, this thesis has examined spontaneous SCE and its association with FANCD2 expression in uveal melanoma. However, SCE is better understood as a response to exogenous DNA damage, and has been extensively used as a mutagenic screen. Interestingly, FA patient cells are characterised by a hypersensitivity to DNA ICL-inducing agents such as MMC, such agents are potent inducers of SCE. In FA patient cells, less SCEs are induced by ICLs. Taken together this data suggests that the FA pathway functions in the repair of ICL-induced damage, which in turn results in SCE, most likely as an end product of HR repairing the damage.

In mammalian cells the FA pathway is postulated to coordinate the NER, HR and TLS repair pathways to ensure the repair of ICL-induced damage (Mirchandani and D'Andrea, 2006). Indeed, the FA pathway been linked to all stages of ICL repair from the initial recognition of an ICL (Mosedale et al., 2005), to the promotion of HR in the repair of an ICL-generated DSB and in the bypass of the persisting ICL by TLS polymerases (Hinz et al., 2006; Mirchandani et al., 2008). As there is such strong evidence that SCEs are produced in response to DNA damage and that the FA proteins are particularly important in ICL repair leading to SCE, here the response of the uveal melanoma cell lines and FANCD2 complemented uveal melanoma cell lines to different DNA damaging agents was examined. As in Chapter 4, an example of the FA patient phenotype, the *FANCD2*^{-/-} patient cell line, PD20 and its FANCD2 complemented derivative (PD20-D2) has also been studied here.

Given the extreme sensitivity of FA patient cells to ICL-induced damage, the response of the uveal melanoma cell lines to ICL-inducing agents was particularly important. The natural anti-tumour antibiotic MMC, a potent inducer of SCE, is widely used to induce DNA damage and thus was used here to study the uveal melanoma DNA damage response to ICL-inducing agents. In addition to defects in the DNA damage response, such as the decrease in FANCD2 expression shown here, cellular metabolism can also affect MMC resistance. MMC requires reductive activation by various cellular reductases (Iyer and Szybalski, 1963) such as cytochrome P450 reductase (CYP450R) and DT-Diaphorase (DTD) (also known as NQO1) before it can interact with DNA causing the highly toxic lesions. The CYP450R and DTD reductases therefore play a

major role in the anti-cancer activity of MMC, and thus chemo-resistance to ICL-inducing agents as seen at the clinical level in uveal melanoma patients, could be the result of a defect in cellular metabolism and not just a result of defects in the DNA repair machinery.

5.2 Uveal melanoma cell lines have increased resistance to thymidine (dT) and the ICL-inducing agents, MMC and cisplatin

Although the FA pathway and thus FANCD2 has an important role endogenously and in ICL-induced repair, it is also activated by other DNA damaging agents such as IR, UV, camptothecin (CPT) and hydroxyurea (HU) (Howlett et al., 2005) suggesting a role for FANCD2 in the response to other types of damage besides ICL-inducing agents. To evaluate the effect that a lack of FANCD2 expression has on the uveal melanoma cellular survival following induced DNA damage, the cytotoxic response of the uveal melanoma cell lines 157d and 196b, to a wide range of DNA damaging agents was investigated (Table 5.1).

Each of the DNA damaging agents used was chosen to induce different types of DNA lesions, repaired by the different DNA repair pathways. UV for example was used to highlight defects in the NER pathway whereas H₂O₂ was used to study BER. There was no difference in the survival of the uveal melanoma cell lines compared to controls to HU, UV irradiation, IR, CPT, MMS or H₂O₂ (Figure 5.1 a – f). The uveal melanoma cell lines did however, show increased survival at 8 mM dT compared to WM793, MRC5VA and U2OS control cell lines (Figure 5.1 g). This was surprising as HR is required to overcome dT-induced replication stress and thus HR deficient cells have been shown to be sensitive to dT-induced damage (Lundin et al., 2002). In Chapter 3, uveal melanoma cell lines were also found to be deficient in endogenous HR as shown by reduced spontaneous RAD51 foci formation, thus this observed resistance may not be associated with the defect in repair studied here.

Cytotoxic agent	Mechanism of action	Dose
Camptothecin (CPT)	Inhibits topoisomerase I	0 – 15 nM
Cisplatin (CIS)	Forms intra- and interstrand DNA cross-links	0 – 2 μ M
Hydrogen Peroxide (H ₂ O ₂)	Causes oxidative stress	0 – 10 mM (for 2 h)
Hydroxyurea (HU)	Inhibits ribonucleotide reductase	0 – 0.6 mM
Ionising radiation (IR)	Causes double strand breaks	0 – 10 GY
Methyl methanesulfonate (MMS)	Alkylating agent that leads to methylation damage	0 – 3 mM (for 30 min)
Mitomycin C (MMC)	Alkylating agent that forms inter-strand DNA cross-links	0 – 200 nM
Thymidine (dT)	Suppresses synthesis of dCTP	0 – 8 mM
Ultraviolet irradiation (UV) (254 nm)	Forms intra-strand DNA cross-links	0 – 100 J/M ²

Table 5.1 The DNA damaging agents used for the sensitivity screen in uveal melanoma cell lines

Each cytotoxic agent used has a different mechanism of action (as listed above) to induce the various DNA repair pathways. Doses shown are for the continuous exposure over a period of 15 days, except for H₂O₂ and MMS where the agent was added to the cells for the stated period of time before being removed and replaced with fresh media.

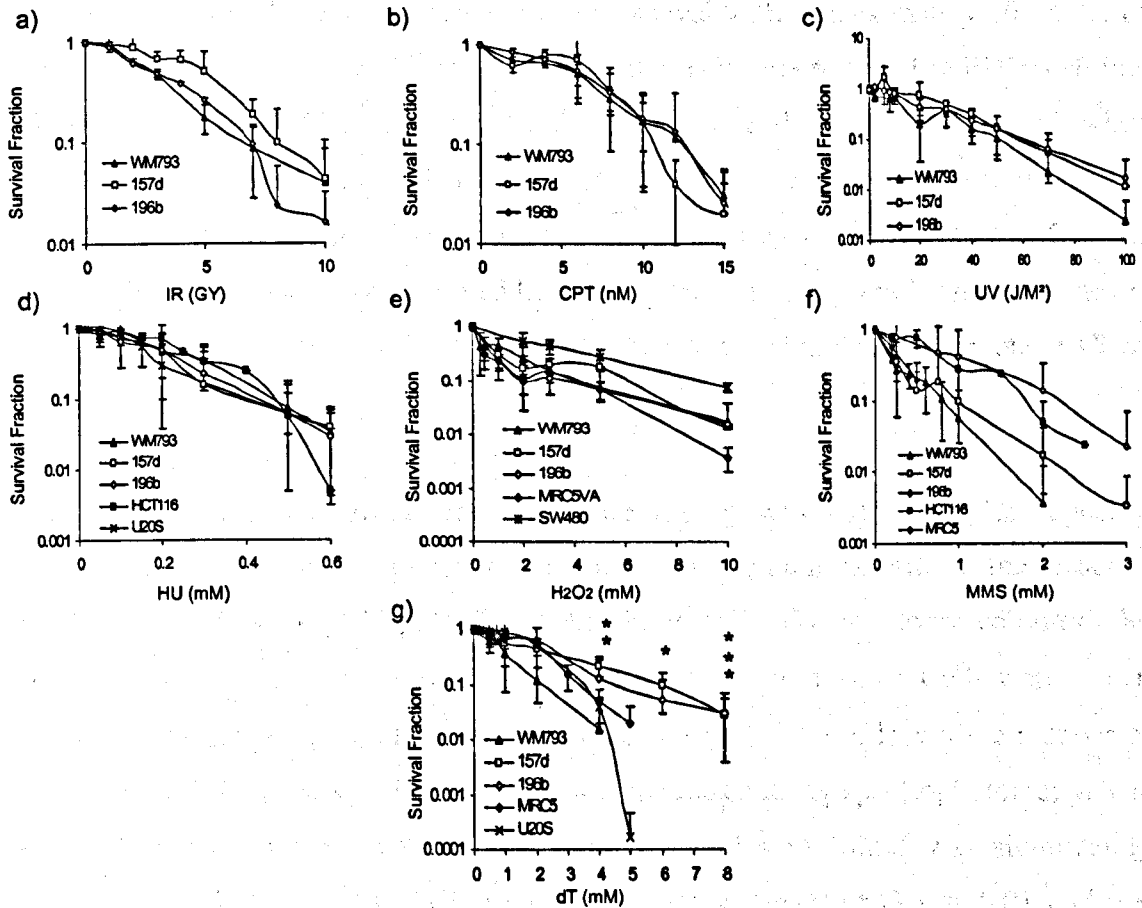


Figure 5.1 Uveal melanoma cell lines are less sensitive to thymidine than WM793 and other control cell lines

Toxicity assays for a range of DNA damaging agents in the uveal melanoma cell lines 157d and 196b, WM793 in all cases, MRC5VA in e), f) and g), HCT116 in d) and f), U2OS in d) and g), and finally SW480 in e). Data shown is the average of at least three separate experiments. Error bars represent standard deviations and statistical significance was calculated using the Student's T-test where $p < 0.05$ is indicated by *, $p < 0.01$ is indicated by ** and $p < 0.001$ is indicated by ***.

FA patient cells including the PD20 cell line used here are characterised by a hypersensitivity to DNA ICL-inducing agents. As the uveal melanoma cell lines also have a deficiency in the FA protein, FANCD2, it was of particular interest to study the survival of these cells following exposure to ICL-inducing agents. Figure 5.2 a) shows the survival of the uveal melanoma cell lines to MMC. At 200 nM MMC both uveal

melanoma cell lines have significantly greater survival with approximately 80 – 90% of cells surviving at this dose compared to all the other cell lines tested. The PD20 cell line was sensitive to MMC as reported in the literature and this was corrected when complemented with FANCD2 (Timmers et al., 2001) (Figure 5.2 b). It was postulated that the uveal melanoma cell lines would show a similar hypersensitivity to MMC as the PD20 cell line; the resistance observed here was therefore unexpected. The resistance is however, consistent with the chemo-resistant nature of uveal melanoma tumours (Albert et al., 1992).

To further confirm this result and to ensure that it was not a cell line specific phenomenon, the survival of primary uveal melanoma tumour samples in the presence of MMC was studied (Figure 5.2 c). As these cells do not form colonies, the proliferation rates were compared using an MTT proliferation assay. Cells were grown for 10 days in the presence of a range of MMC doses (0 – 50 nM) and the number of viable cells and thus the proliferation rate, was measured using spectrophotometry. The proliferation rate of the primary uveal tumour samples in MMC was significantly greater than in WM793 and SW480 control cell lines (for Mel533 $p = 0.01$ and $p = 0.005$, for Mel534 $p = 5 \times 10^{-5}$ and $p = 4 \times 10^{-5}$, for Mel537 $p = 5 \times 10^{-5}$ and $p = 7 \times 10^{-6}$, and for Mel538 $p = 0.007$ and $p = 0.001$, for WM793 and SW480 respectively). This is consistent with the result obtained using the uveal melanoma cell lines and is consistent with the high chemo-resistance observed at the clinical level.

To test whether this observed resistance was specific to MMC, the platinum-based ICL-inducing compound cisplatin, a commonly used chemotherapeutic agent, was also studied. Uveal melanoma cell lines showed a similarly low level of sensitivity to cisplatin by surviving at higher doses than all other human cell lines tested (Figure 5.2 d). This suggests that uveal melanoma cell lines are resistant to ICL-inducing agents. Due to the extensive use of MMC in FA studies, this agent was used for further experiments.

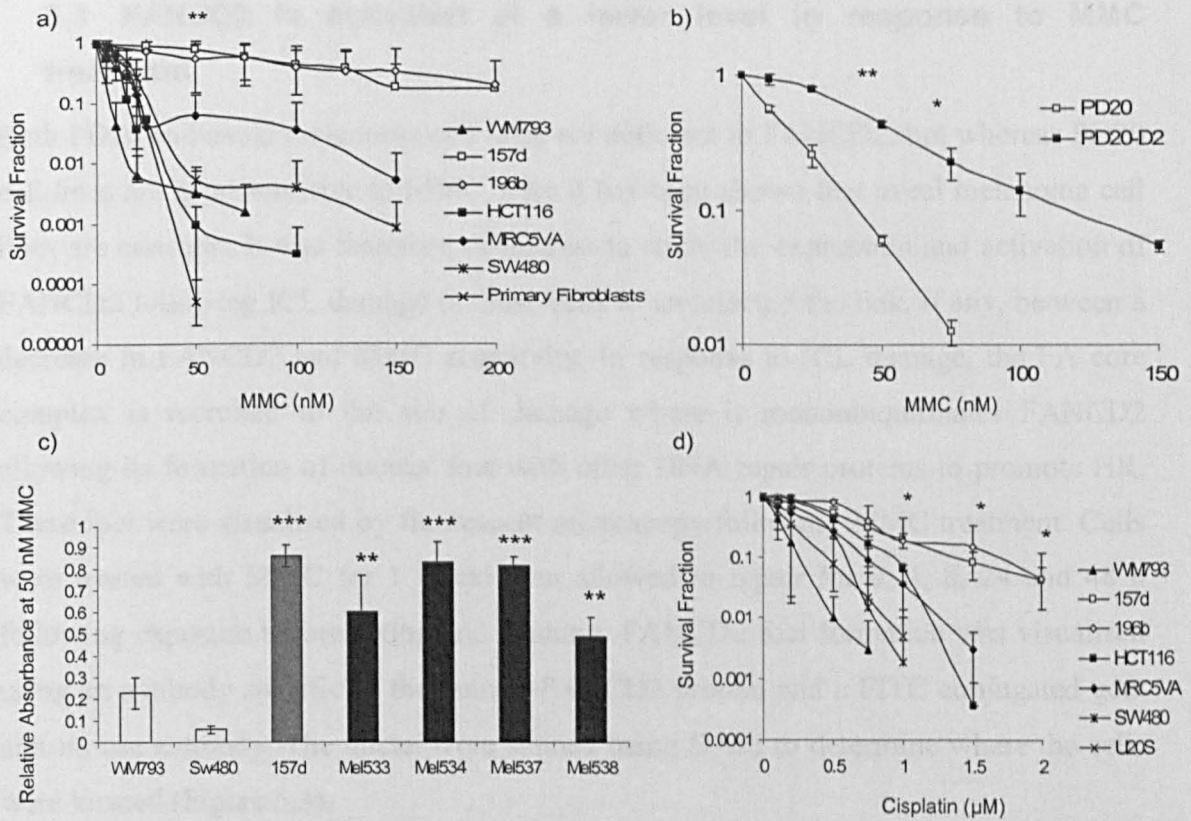


Figure 5.2 Uveal melanoma cell lines and primary uveal melanoma tumour samples are less sensitive to the ICL-inducing agents MMC and cisplatin compared to control cell lines

a) MMC toxicity assay for the uveal melanoma cell lines, 157d and 196b, in the WM793, HCT116, MRC5VA, SW480 control cell lines and primary human fibroblasts. b) MMC toxicity assay for PD20 and PD20-D2 cell lines. c) The proliferation of the uveal melanoma primary tumour samples, the 157d uveal melanoma cell line, and the WM793 and SW480 control cell lines at 50 nM MMC using an MTT assay. Absorbance (OD at 570 nm) at 50 nM MMC was calculated relative to the absorbance with no treatment. d) Cisplatin toxicity assay in the uveal melanoma cell lines, 157d and 196b, and in the WM793, HCT116, MRC5VA, SW480 and U2OS control cell lines. Data shown is the average of at least 3 experiments except for MEL524, 526 and 530 (c) where only one repeat was possible. Error bars represent standard deviations and significance was calculated for survival at 50 nM MMC (a), 50 and 75 nM MMC (b) and 1 – 2 μM cisplatin (d). Significance for primary tumour samples and 157d were calculated compared to WM793 and SW480 control cell lines. The Student's T-test was used where $p < 0.05$ is indicated by *, $p < 0.01$ is indicated by ** and $p < 0.001$ is indicated by ***.

5.3 FANCD2 is activated at a lower level in response to MMC treatment

Both PD20 and uveal melanoma cell lines are deficient in FANCD2, but whereas PD20 cell lines are hypersensitive to MMC, here it has been shown that uveal melanoma cell lines are resistant. It was therefore of interest to study the expression and activation of FANCD2 following ICL damage in these cells to understand the link, if any, between a decrease in FANCD2 and MMC sensitivity. In response to ICL damage, the FA core complex is recruited to the site of damage where it monoubiquitinates FANCD2 allowing its formation of nuclear foci with other DNA repair proteins to promote HR. These foci were visualised by fluorescent microscopy following MMC treatment. Cells were treated with MMC for 1 h and then allowed to repair for 0, 4, 8, 24 and 48 h following exposure before fixing and staining. FANCD2 foci formation was visualised using an antibody specific to the human FANCD2 protein and a FITC conjugated goat anti-mouse antibody. The nuclei were stained using DAPI to determine where the cells were located (Figure 5.3).

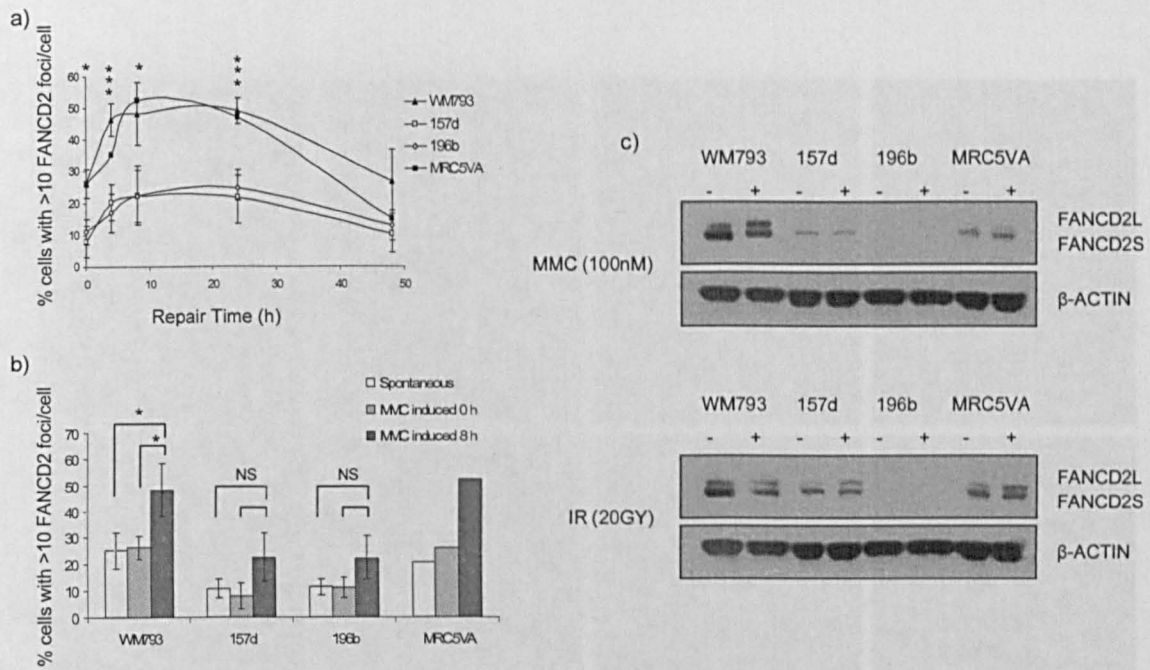
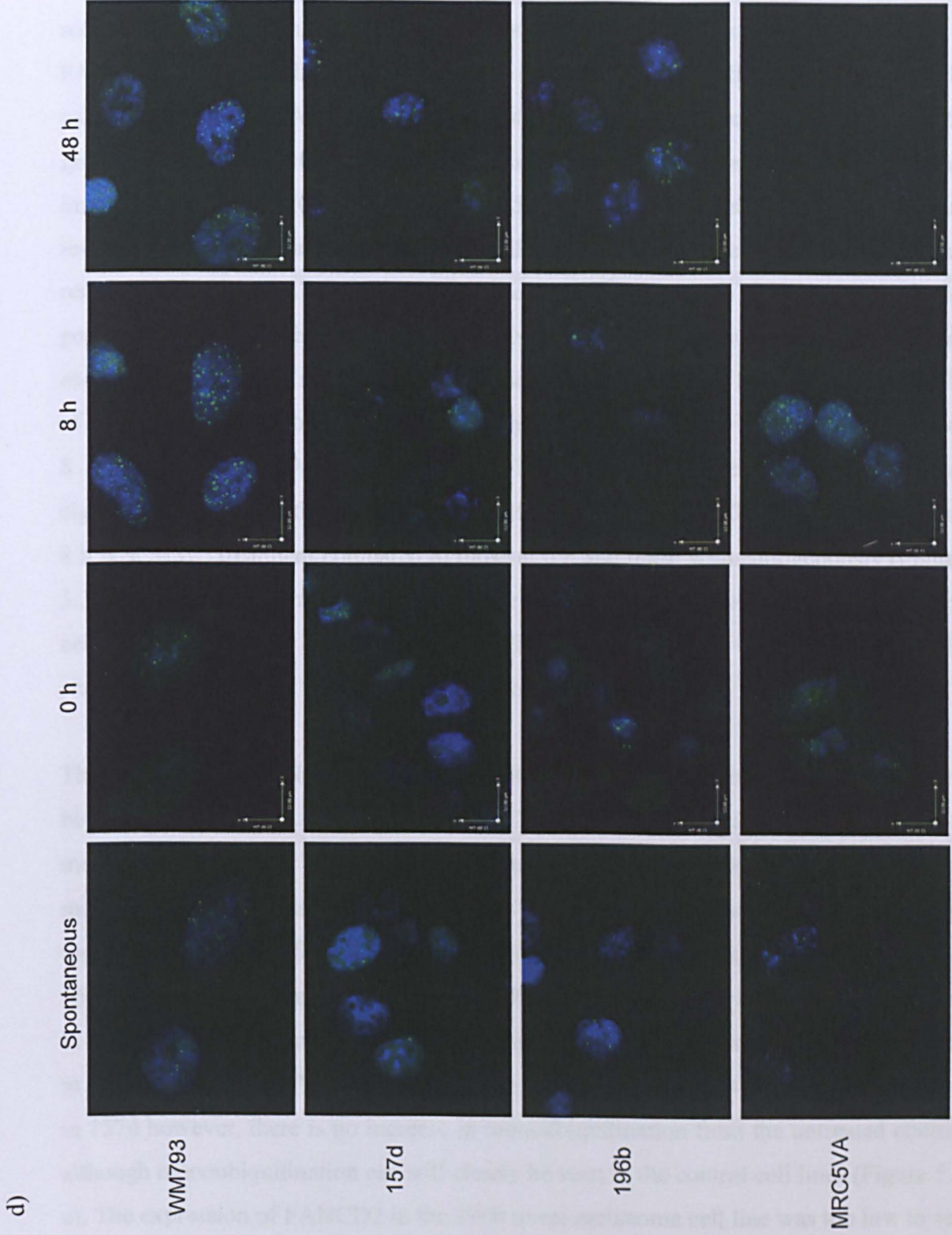


Figure 5.3 FANCD2 is activated less in response to MMC induced damage in uveal melanoma cell lines compared to control cell lines

FANCD2 foci formation visualised by fluorescent microscopy in the uveal melanoma cell lines, 157d and 196b, and in the WM793 and MRC5VA control cell lines (a and b). Cells were treated with MMC then allowed to repair for 0, 4, 8, 24 and 48 h, at which time the cells were fixed and stained. On each occasion, more than 50 cells were analysed and the % of cells with > 10 FANCD2 foci/cell was calculated. Data shown is the average from at least 3 separate experiments except for MRC5VA which was only carried out once. Error bars represent the standard deviations and significance was calculated using the Student's T-test where $p < 0.05$ is indicated by *, $p < 0.001$ is indicated by ***. a) Significance was calculated between WM793 and 196b and for b) significance between samples is indicated by brackets, where no significance is indicated by 'NS'. c) Western blot analysis showing the activation of FANCD2 following MMC and IR treatment in the uveal melanoma cell lines, 157d and 196b, and in the WM793 and MRC5VA control cell lines. The monoubiquitinated form of FANCD2 is shown as a shift from FANCD2S (155 kDa) to FANCD2L (166 kDa). Image is representative of at least 3 separate experiments and β -ACTIN is shown as a loading control where 30 μ g of protein was added. d) Representative images of FANCD2 foci formation (green) for each of the cell lines studied spontaneously and at 0, 8 and 48 h post MMC treatment, nuclei stained with DAPI (blue).

In the WM793 and MRC5VA control cell lines, PANCD2 localization was retained after 48 h of repair following exposure to H₂O₂ (Figure 5.3 a). PANCD2 localization



In the WM793 and MRC5VA control cell lines, FANCD2 foci formation was induced after 4 h of repair following exposure to MMC (Figure 5.3 a). FANCD2 foci formation reached a peak at 8 h with approximately 50% of cells containing greater than 10 FANCD2 foci/cell. Following this, there is a small decrease in the percentage of cells with greater than 10 FANCD2 foci/cell at 24 h and by 48 h the percentage of cells with greater than 10 FANCD2 foci/cell had returned to the levels seen at 0 h, i.e. immediately after MMC exposure (Figure 5.3 a and d) and those seen at endogenous levels (Figure 5.3 b and d). In both uveal melanoma cell lines, although the same response time for FANCD2 foci formation was observed as in the controls, the percentage of cells with greater than 10 FANCD2 foci/cell was significantly reduced at each of the time points rising from 10% of cells at 0 h post MMC treatment to only 20% of cells at 8 h post treatment ($p = 0.009$ and $p = 0.01$ at 0 h, and $p = 0.02$ and $p = 0.01$ at 8 h for 157d and 196b, respectively) (Figure 5.3 a). Furthermore, there was no significant increase in the percentage of cells with greater than 10 FANCD2 foci/cell at 8 h post MMC treatment compared to those at 0 h and those seen endogenously (Figure 5.3 b). This is in contrast to WM793 where a significant increase in the percentage of cells with greater than 10 FANCD2 foci/cell at 8 h compared to 0 h and endogenously was observed ($p = 0.02$ for both 0 h and endogenously).

The activation of FANCD2 following MMC treatment was also tested using western blot analysis (Figure 5.3 c). In order for FANCD2 to form nuclear foci, it must first be monoubiquitinated by the FA core complex (Garcia-Higuera et al., 2001). This monoubiquitination was visualised as a shift on a SDS-polyacrylamide gel moving from the short FANCD2 isoform (FANCD2S) at 155 kDa to the long isoform (FANCD2L) at 166 kDa. Using IR as a control, a clear shift from FANCD2S to FANCDL can be seen in the 157d uveal melanoma cell line, although at an overall lower expression level than in WM793 and MRC5VA cell lines (Figure 5.3 c). Following 24 h of MMC exposure, in 157d however, there is no increase in monoubiquitination from the untreated control although monoubiquitination can still clearly be seen in the control cell lines (Figure 5.3 c). The expression of FANCD2 in the 196b uveal melanoma cell line was too low to see any change at this exposure. The lack of FANCD2 activation as shown by a lack of monoubiquitination, suggests that at this dose of MMC (100 μ M) there is no response to MMC-induced damage compared to that seen in WM793 and from that observed

following IR-induced damage. From this and the fluorescent microscopy experiments, it is clear that the uveal melanoma cell lines have the capacity to monoubiquitinate FANCD2 through the FA core complex and thus can still form FANCD2 foci in response to DNA damage. However, following MMC induced damage this activation of FANCD2 is at a much reduced level. As FANCD2 activation is involved in the repair of ICL-induced damage this finding appears to contradict the resistance observed in uveal melanoma.

5.4 HR is induced at a lower level in response to MMC treatment in uveal melanoma cell lines

HR is one of the main pathways involved in the repair of ICL damage. Once the cross-link has been excised, a DSB occurs at this site. This is then repaired by one-ended HR. It was therefore of interest to study the formation of RAD51 foci, as a marker of HR, in response to ICL-induced DNA damage. RAD51 is an essential protein of the initial strand invasion step of HR and forms distinct nuclear foci upon DNA damage that can be visualised using fluorescent microscopy (Haaf et al., 1995). Cells were treated for 1 h with MMC and then allowed to repair for 0, 4, 8, 24 and 48 h before being fixed and stained. The nuclei of the cells were stained with DAPI so that the cells could be located (Figure 5.4).

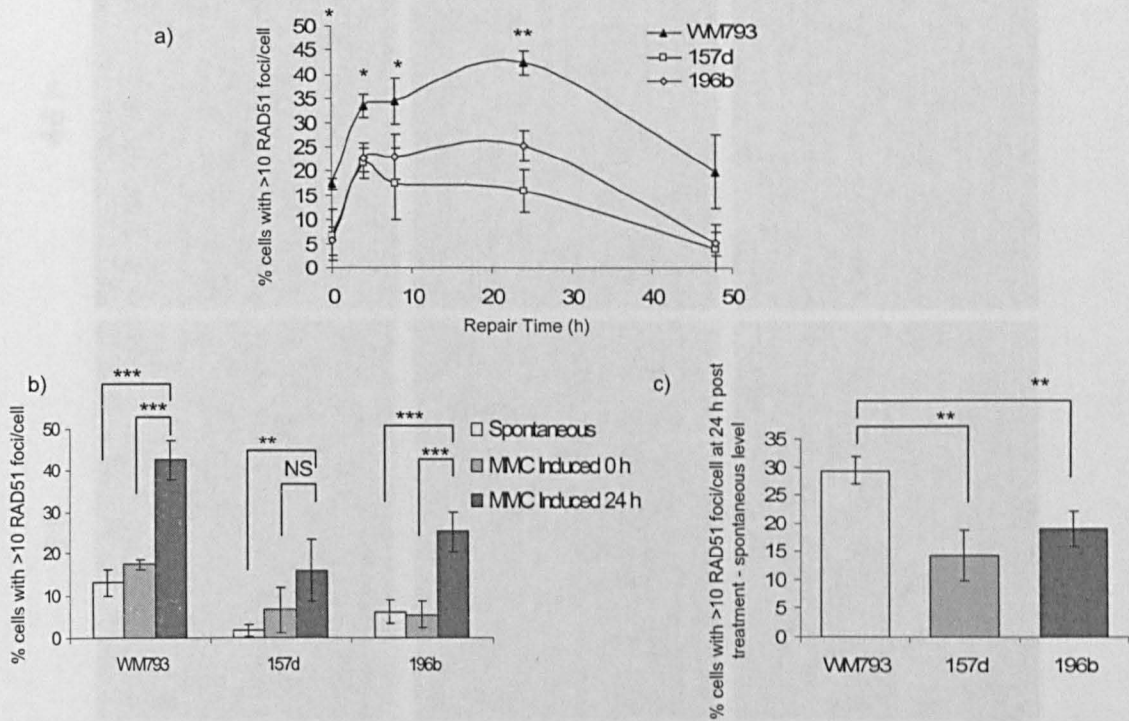


Figure 5.4 The induction of RAD51 foci formation following MMC treatment is reduced in uveal melanoma cell lines

RAD51 foci formation following MMC treatment visualised by fluorescent microscopy in the uveal melanoma cell line, 157d and 196b, and in the WM793 melanoma control cell line. a) Cells were treated with MMC then allowed to repair for the indicated times. 0 h represents cells that were immediately fixed following treatment. b) The induction of RAD51 foci formation after 24 h of repair compared to those at 0 h and endogenous levels. c) Induction of RAD51 foci formation in different cell lines. Data shown is the % cells with > 10 RAD51 foci/cell minus the background level of RAD51 foci formation (spontaneous levels). In all cases on each occasion, at least 50 cells were analysed and the % of cells with > 10 RAD51 foci/cell was calculated. Data shown represents the average of at least 3 experiments and error bars represent the standard deviations. Significance was calculated using the Student's T-test where $p < 0.05$ is indicated by *, $p < 0.01$ is indicated by ** and $p < 0.001$ is indicated by ***. Significance between samples is indicated by brackets where no significance is indicated by 'NS'. d) Representative images of the RAD51 foci formation (red) for each of the cell lines studied spontaneously and at 0, 8 and 48 h post MMC treatment, nuclei stained with DAPI (blue).

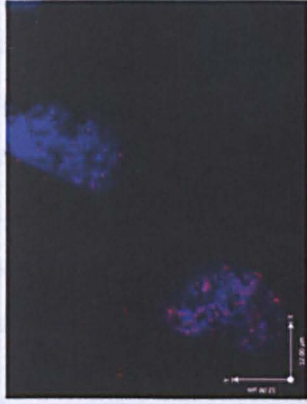
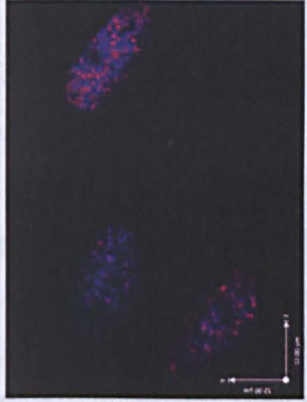
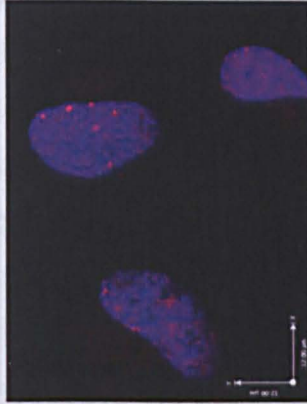
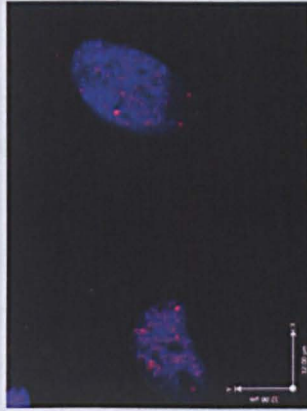
d)

Spontaneous

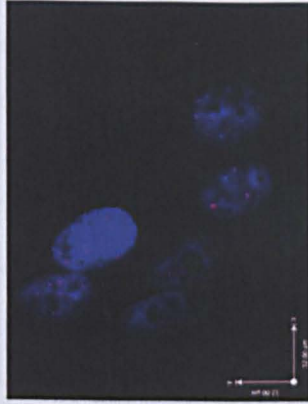
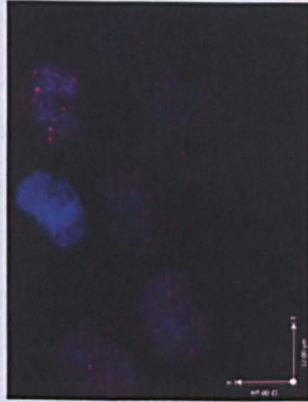
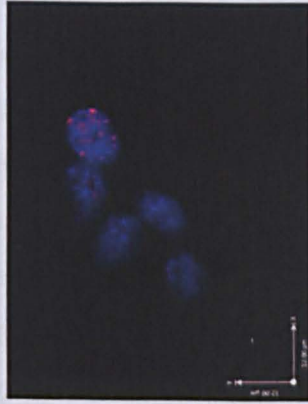
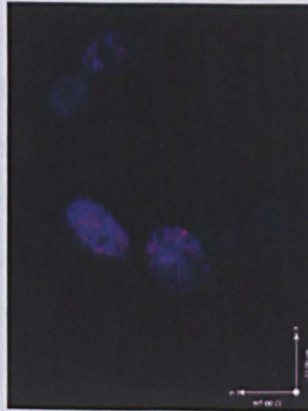
0 h

8 h

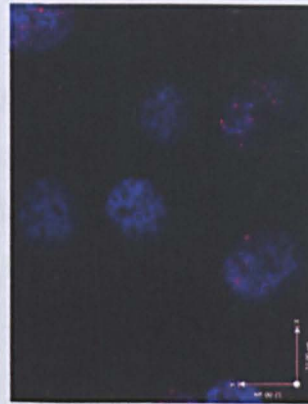
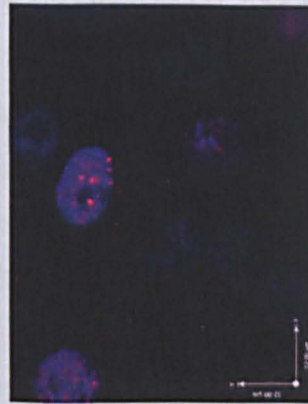
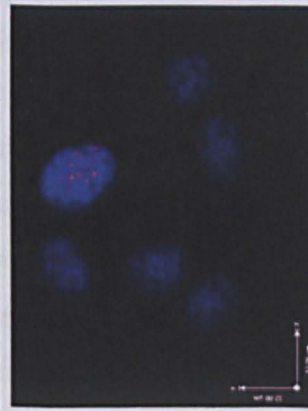
48 h



WM793



157d



196b

There is a significant difference in the level of RAD51 foci formation following MMC treatment in the uveal melanoma cell lines compared to WM793 at 0 to 24 h post treatment (Figure 5.4 a and c). Immediately following MMC exposure (0 h), approximately 20% of WM793 cells had greater than 10 RAD51 foci/cell. This increased to 35% at 4 h and was maintained until 24 h, decreasing to 16% 48 h post treatment. At each of the time points, uveal melanoma cells have significantly reduced RAD51 foci formation compared to WM793 (for 0 h $p = 0.02$ and $p = 4 \times 10^{-4}$, for 4 h $p = 0.02$ and $p = 0.006$, for 8 h $p = 0.01$ and $p = 0.007$, and for 24 h $p = 9 \times 10^{-4}$ and $p = 0.02$, for 157d and 196b respectively) (Figure 5.4 a). However despite this, at 4 h post treatment a small but significant increase in RAD51 foci formation was observed in MMC treated uveal melanoma cell lines compared to untreated uveal melanoma cell lines ($p = 0.003$ and $p = 4 \times 10^{-4}$ for 157d and 196b respectively) and was maintained until 24 h post treatment. Although there was a significant induction of RAD51 foci formation in 196b from 0 to 24 h ($p = 1.8 \times 10^{-5}$) (Figure 5.4 b), this was not observed in 157d. Both cell lines however exhibit a significant induction of RAD51 foci formation following MMC damage compared to endogenous levels ($p = 0.003$ and $p = 0.004$ for 157d and 196b respectively) (Figure 5.4 b), consistent with that observed for WM793 ($p = 6.6 \times 10^{-6}$). To ensure that only the difference in induced foci formation was compared, the percentage of cells with greater than 10 spontaneous RAD51 foci/cell was subtracted from the percentage of cells with greater than 10 RAD51 foci/cell at 24 h following MMC exposure (Figure 5.4 c). Significantly less RAD51 foci formation was observed in the uveal melanoma cell lines compared to WM793 ($p = 0.001$ and $p = 0.004$ for 157d and 196b respectively). This data suggests that uveal melanoma cell lines have the ability to form RAD51 foci in response to MMC damage and thus that HR can be activated following MMC exposure. The reduced level of RAD51 foci formation compared to the WM793 melanoma control cell line suggests that MMC does not induce the same level of response (HR) to this type of damage in uveal melanoma cell lines. This is consistent with the results obtained for FANCD2 foci formation induced by MMC, but again contradicts the resistance to ICL-damage in uveal melanoma.

5.5 MMC induces less DNA damage in uveal melanoma cell lines compared to WM793 and MRC5VA control cell lines

A decreased sensitivity to specific DNA damaging agents, suggests that cells have an increased ability to deal with this type of damage. Here however, uveal melanoma cell lines exhibit resistance to ICL-inducing agents but appear to have a reduced repair response to MMC-induced damage, as measured by a lack of FANCD2 and RAD51 foci induction following MMC treatment, and a reduced induction of SCE following MMC treatment (Hoh, 2007, unpublished data). The reduced repair response to MMC could be due to limited expression of FANCD2, leading to decreased HR. However, given the contradiction of this result with the resistance to MMC seen in uveal melanoma cell lines another possibility is that the MMC induces less damage due to defects in the metabolism of this compound.

To investigate the effect that MMC treatment has on uveal melanoma cell lines, $\gamma\text{H}_2\text{A.X}$ foci formation was studied using fluorescent microscopy. As $\gamma\text{H}_2\text{A.X}$ is a marker of DNA damage (Rogakou et al., 1998), $\gamma\text{H}_2\text{A.X}$ foci formation should be induced following MMC treatment. Cells were exposed to MMC for 1 h and then immediately fixed and stained for human $\gamma\text{H}_2\text{A.X}$. DAPI was used to stain the nuclei of the cells (Figure 5.5).

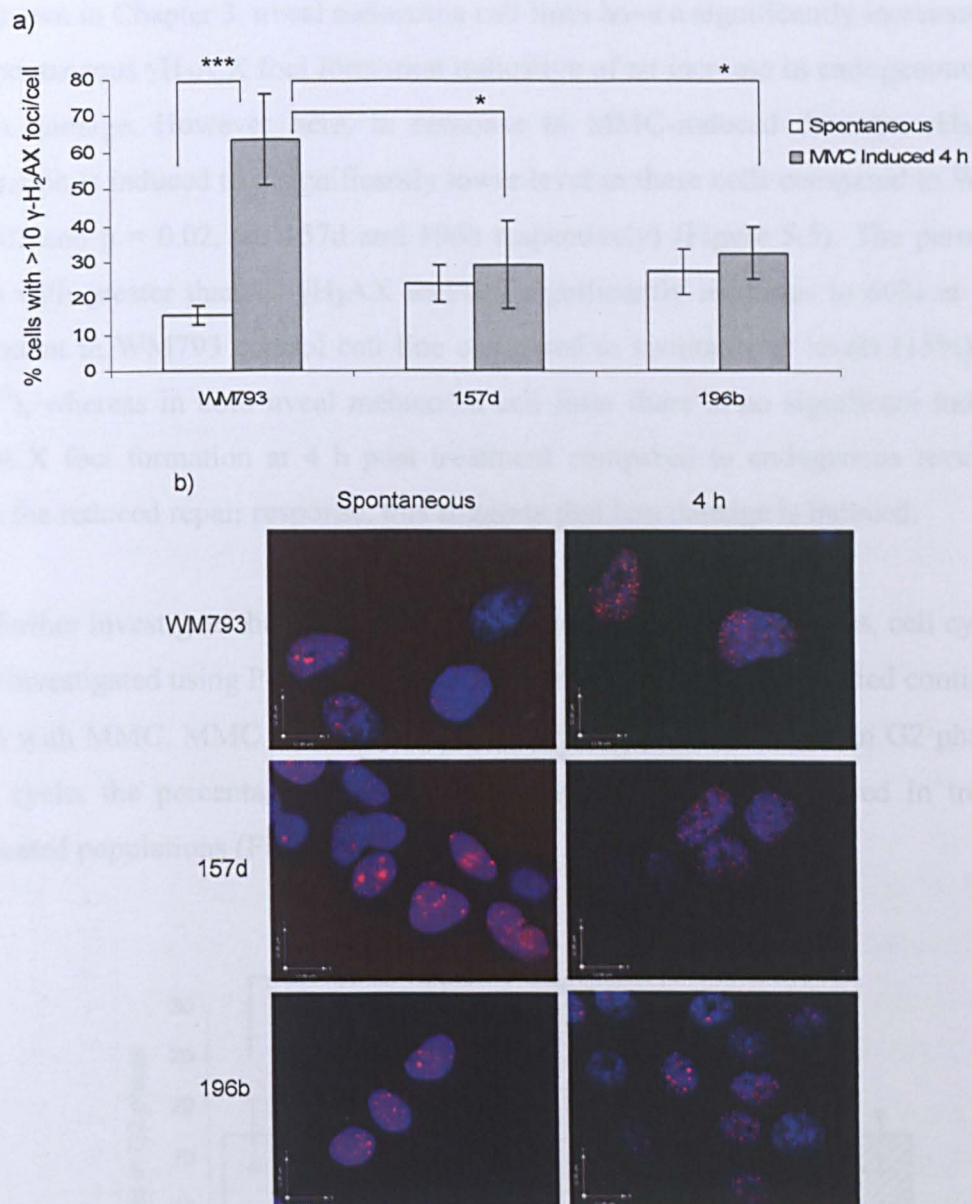


Figure 5.5 MMC causes a significantly lower amount of damage in uveal melanoma cell lines compared to WM793

a) γ H₂A.X foci formation visualised by fluorescent microscopy in the uveal melanoma cell lines 196b and 157d, and in the WM793 and MRC5VA control cell lines. On each occasion, at least 50 cells were analysed and the % of cells with >10 γ H₂A.X foci/cell was calculated. Cells were treated with MMC for 1 h and then allowed to repair for 4 h before being fixed and stained. Spontaneous data is also shown for comparison. Data represents the average from at least three separate experiments and error bars represent standard deviations. Significance was calculated using the Student's T-Test where $p < 0.05$ is indicated by * and $p < 0.001$ is indicated by ***. The significance between samples is indicated by brackets. c) Representative images of γ H₂A.X foci formation (red) in all cell lines studied spontaneously and at 4 h post MMC treatment, nuclei stained with DAPI (blue).

As shown in Chapter 3, uveal melanoma cell lines have a significantly increased amount of spontaneous $\gamma\text{H}_2\text{A.X}$ foci formation indicative of an increase in endogenous levels of DNA damage. However here, in response to MMC-induced damage, $\gamma\text{H}_2\text{A.X}$ foci formation is induced to a significantly lower level in these cells compared to WM793 ($p = 0.03$ and $p = 0.02$, for 157d and 196b respectively) (Figure 5.5). The percentage of cells with greater than 10 $\gamma\text{H}_2\text{A.X}$ foci/cell significantly increases to 60% at 4 h post-treatment in WM793 control cell line compared to spontaneous levels (15%) ($p = 2.5 \times 10^{-5}$), whereas in both uveal melanoma cell lines there is no significant induction of $\gamma\text{H}_2\text{A.X}$ foci formation at 4 h post treatment compared to endogenous levels. Taken with the reduced repair response, this suggests that less damage is induced.

To further investigate the effect of MMC in uveal melanoma cell lines, cell cycle status was investigated using PI staining and FACS analysis. Cells were treated continually for 24 h with MMC. MMC causes G2 arrest and thus cells accumulate in G2 phase of the cell cycle, the percentage of cells in G2 can therefore be compared in treated and untreated populations (Figure 5.6).

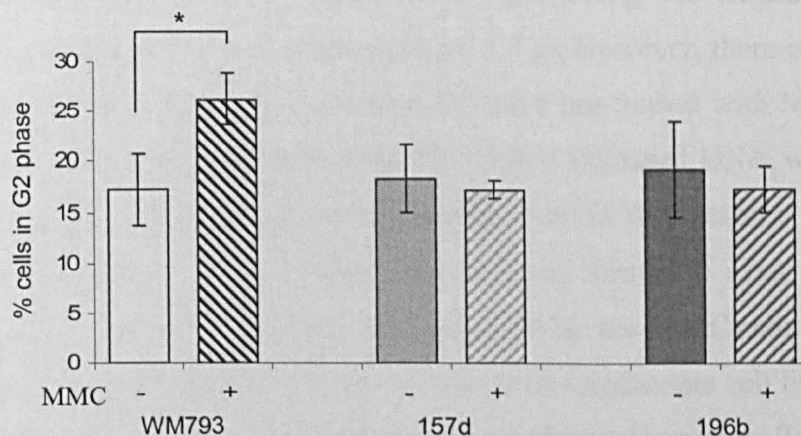


Figure 5.6 MMC does not cause G2 arrest in uveal melanoma cell lines

The % of cells in G2 as indicated by PI staining in the uveal melanoma cell lines, 157d and 196b and in the WM793 control cell line following either non-treated or continuously treated with MMC for 24 h. Data represents the average from at least two separate experiments and error bars represent standard deviations. Significance between non- and MMC treated samples for each cell line was calculated using the Student's T-test where $p < 0.05$ is indicated by *.

Figure 5.6 shows that there is no difference in the percentage of cells in G2 in treated or untreated uveal melanoma cell populations. This is in contrast to WM793 where there is a significant increase in the percentage of cells in G2 following MMC treatment ($p = 0.04$). Both the induced $\gamma\text{H}_2\text{A.X}$ foci formation and cell cycle data are consistent with both the resistance to ICL-inducing agents and the decreased repair response, and suggests that at the same dose, less damage is induced in uveal melanoma cell lines compared to control cell lines.

5.6 MMC induces fewer DNA ICLs in uveal melanoma cell lines

To confirm that MMC was causing a lower level of ICL damage in uveal melanoma cell lines, ICL formation was investigated. Once the cross-link has been recognised it is excised creating a SSB that collapses the replication fork forming a DSB. As the uveal melanoma cell lines show a reduced induction of $\gamma\text{H}_2\text{A.X}$ foci formation following MMC exposure, the formation of the initial ICL was investigated using a modified version of the comet assay technique.

In WM793, there is a significant reduction in TM when pre-treated with MMC ($p = 5 \times 10^{-4}$), suggesting that cross-links were formed, preventing the IR-induced damaged DNA from migrating out of the nucleus (Figure 5.7 a). However, there is no significant difference in TM between uveal melanoma cell lines pre-treated with MMC and those treated with IR alone, suggesting that the IR-induced damaged DNA was still able to migrate out of the nucleus during electrophoresis even in the presence of MMC. This suggests that at the same dose of MMC, less ICLs are formed in uveal melanoma cell lines compared to control cell lines. To confirm this, the MMC-induced percentage decrease in TM was calculated for each cell line, uveal melanoma cell lines were found to have a significantly reduced MMC-induced percentage decrease in TM compared to WM793 ($p = 0.04$ and $p = 0.03$ for 157d and 196b respectively) further suggesting that the formation of ICLs was decreased in uveal melanoma cell lines (Figure 5.7 b).

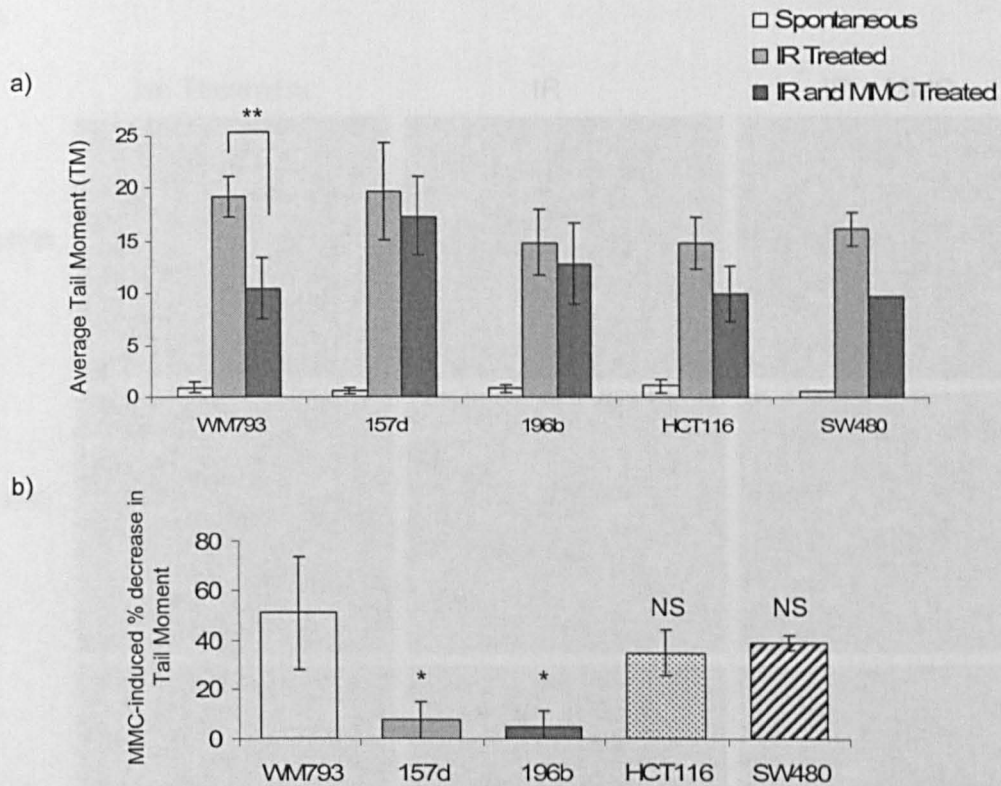
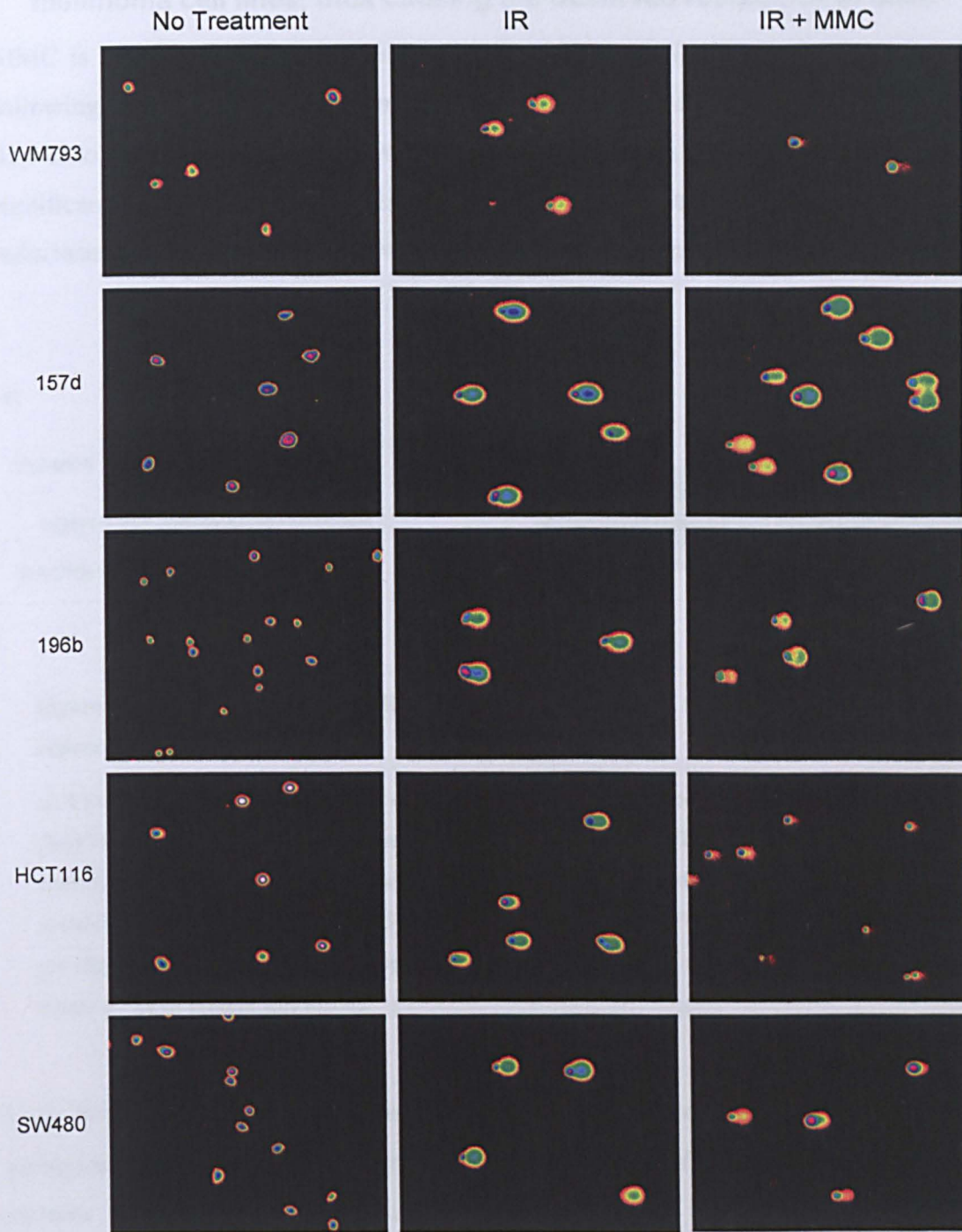


Figure 5.7 There is a lower level of DNA ICLs formed following MMC treatment in uveal melanoma cells

ICL induction by MMC in the uveal melanoma cell lines 157d and 196b, and in the WM793, HCT116 and SW480 control cell lines using a modified version of the comet assay. a) Cells were either untreated, treated with IR (10 GY) only, or pre-treated with MMC (15 μ M) for 1 h before being treated with IR, to induce DNA damage in each cell line. The average TM was calculated using CometScore™ software where at least 50 cells were analysed on each occasion. b) The MMC-induced % decrease in TM was calculated for each cell line where the decrease is directly proportional to the amount of ICLs formed. Data shown is the average from at least two experiments (except SW480, which was only done once as an extra control) and error bars represent standard deviations. Significance was determined using the Student's T-test where $p < 0.05$ is indicated by * and $p < 0.01$ is indicated by ** and calculated a) between MMC pre-treated and IR alone samples (as indicated by brackets) and b) compared to WM793. c) Representative comet assay images for each of the treatments, for each cell line. Images were obtained using the full spectrum function of the CometScore™ computer software. Cells were originally stained with SYBR Safe™ DNA gel stain.

c)



5.7 CYP450R required for MMC metabolism is reduced in uveal melanoma cell lines, thus causing the observed resistance to MMC

MMC is a potent inducer of ICLs however, its interaction with DNA can only occur following the reductive activation of MMC by various cellular reductases (Iyer and Szybalski, 1963) such as CYP450R and DTD (NQO1). As the formation of ICLs was significantly reduced in uveal melanoma cell lines, the protein expression of these two reductases was investigated using western blot analysis (Figure 5.9 a).

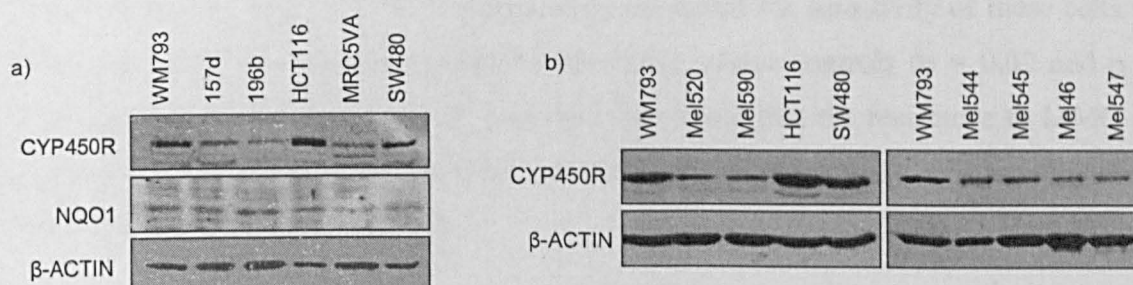


Figure 5.8 Uveal melanoma cell lines and primary tumour samples have a decreased expression of CYP450R

a) Western blot analysis to show the expression levels of the two reductases CYP450R and DTD (NQO1) in uveal melanoma cell lines compared to WM793, HCT116, MRC5VA and SW480 control cell lines. b) Western blot analysis to show the expression of CYP450R in primary uveal melanoma tumour samples compared to WM793, HCT116 and SW480 control cell lines. Images are representative of at least three separate experiments. β -ACTIN is shown as a loading control where 30 μ g of protein was loaded.

It was found that there was a decreased expression of the reductase CYP450R in uveal melanoma cell lines compared to WM793, HCT116 and SW480 control cell lines whereas NQO1 (DTD) expression was normal (Figure 5.8 a). This reduced expression was also confirmed in primary uveal melanoma tumour samples (Figure 5.8 b). Interestingly, MRC5VA also showed a reduced expression of this protein that may account for its lower sensitivity to MMC observed in Figure 5.2.

To investigate the association of the decrease in expression of CYP450R and MMC resistance, the bicistronic vector pEF-P450R-IRES-P (CYP450R) containing the human CYP450R cDNA sequence (Cowen et al., 2003), or an empty vector control was transiently expressed in 196b and WM793 cell lines using Lipofectamine™ 2000 reagent. A toxicity assay for MMC was performed 24 h following complementation and a western blot was carried out to confirm the complementation of CYP450R. Transiently complementing WM793 with the CYP450R plasmid did not affect the sensitivity of these cells to MMC (Figure 5.9 a). In 196b however, transient complementation with CYP450R significantly increased the sensitivity of these cells to MMC compared to non-complemented and empty vector controls ($p = 0.02$ and $p = 0.008$, respectively) (Figure 5.9 b). It is therefore likely that the resistance to MMC in uveal melanoma cell lines is caused by a defect in the ability of these cells to metabolise MMC rather than a defect in repair.

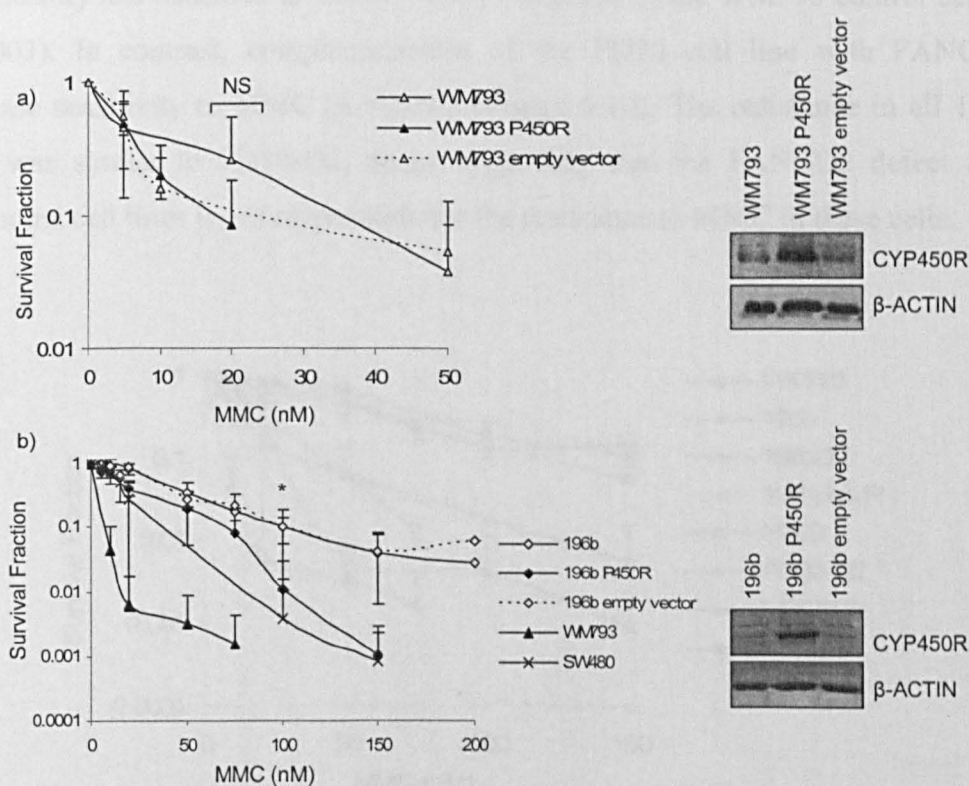


Figure 5.9 Transient complementation of CYP450R in uveal melanoma cell lines increases sensitivity to MMC

a) MMC toxicity assay following the transient complementation of the CYP450R plasmid into WM793 control cell line using lipofectamine 2000. Western blot analysis confirms the complementation of CYP450R. b) MMC toxicity assay and corresponding western blot image following the transient complementation of the CYP450R plasmid in the 196b uveal melanoma cell line. In each case the empty vector control is also shown. Data represents the average of at least three experiments and error bars show the standard deviations. Significance was calculated at 20 nM MMC for WM793 and 100 nM MMC for 196b using the Student's T-test where $p < 0.05$ is indicated by * and no significance is indicated by 'NS'.

5.8 The defect in FANCD2 in uveal melanoma is not associated with the resistance to MMC

To confirm that the resistance to MMC is caused by a defect in metabolism rather than a defect in DNA repair, the cytotoxic response to MMC was studied in the 196b uveal melanoma cell line retrovirally complemented with pMMP-empty (196b-pMMP) or pMMP-FANCD2 (196b-D2). The sensitivity to MMC was unchanged in the 196b-D2 cell line compared to 196b-pMMP and parental cell line 196b (Figure 5.10) and was

significantly less sensitive at 50 nM MMC compared to the WM793 control cell line ($p = 0.003$). In contrast, complementation of the PD20 cell line with FANCD2 did decrease sensitivity to MMC ($p = 0.04$) (Figure 5.10). The resistance in all 196b cell lines was similar to PD20-D2, again suggesting that the FANCD2 defect in uveal melanoma cell lines is not responsible for the resistance to MMC in these cells.

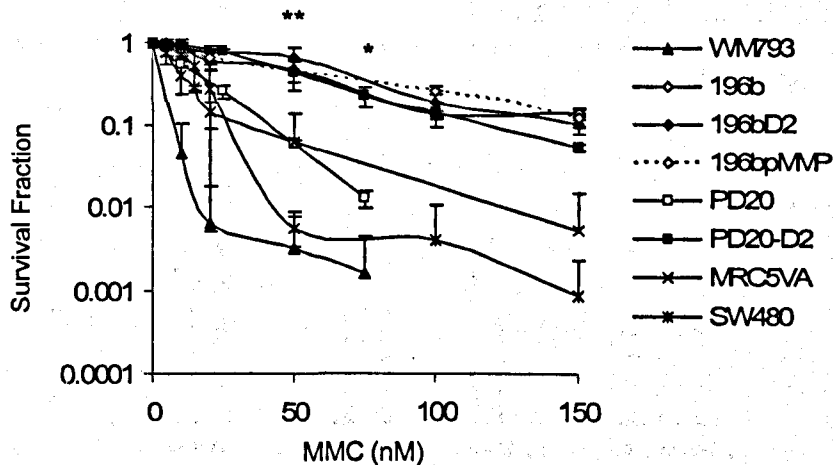


Figure 5.10 Complementation of the uveal melanoma cell line, 196b with FANCD2 does not alter the resistance to MMC

MMC toxicity assay in the uveal melanoma cell lines 196b, 196b-pMMP and 196b-D2, and in the WM793, PD20, PD20-D2, MRC5VA and SW480 control cell lines. Cells were continually exposed to a dose of MMC ranging from 0 – 150 nM for 15 days before being stained and counted for surviving colonies. Data shown is the average of at least two experiments and error bars represent standard deviations. Significance was calculated between PD20 and PD20-D2 at 75 nM MMC and between 196b-D2 and WM793 cell lines at 50 nM MMC. A Student's T-test was performed where $p < 0.05$ is indicated by * and $p < 0.01$ is indicated by **.

To further confirm that the resistance to MMC in uveal melanoma cell lines was due to a defect in metabolism rather than caused by a defect in DNA repair, MMC-induced FANCD2, RAD51 and γ H₂A.X foci formation were studied in 196b-pMMP and 196b-D2 cell lines. Cells were treated for 1 h with MMC and then allowed to repair up to 48 h post treatment before being fixed and stained with the appropriate antibody. Foci formation was visualised using fluorescent microscopy where DAPI was used to stain the nuclei of the cells (Figure 5.11).

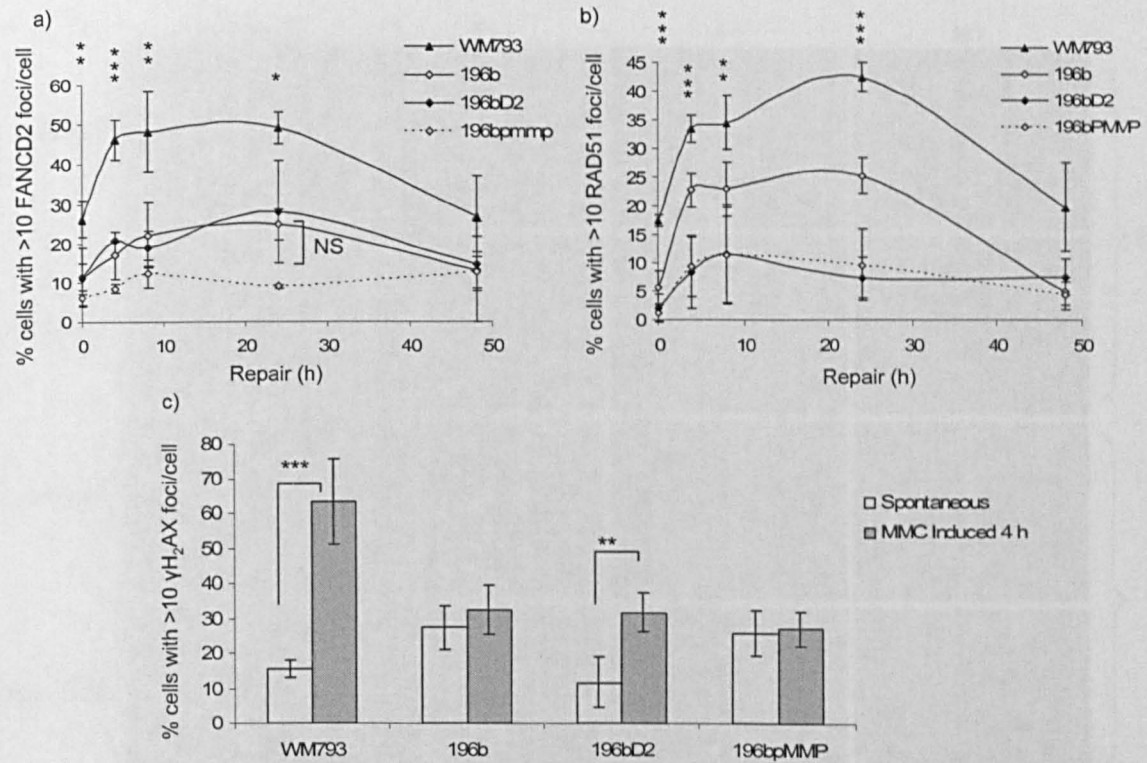
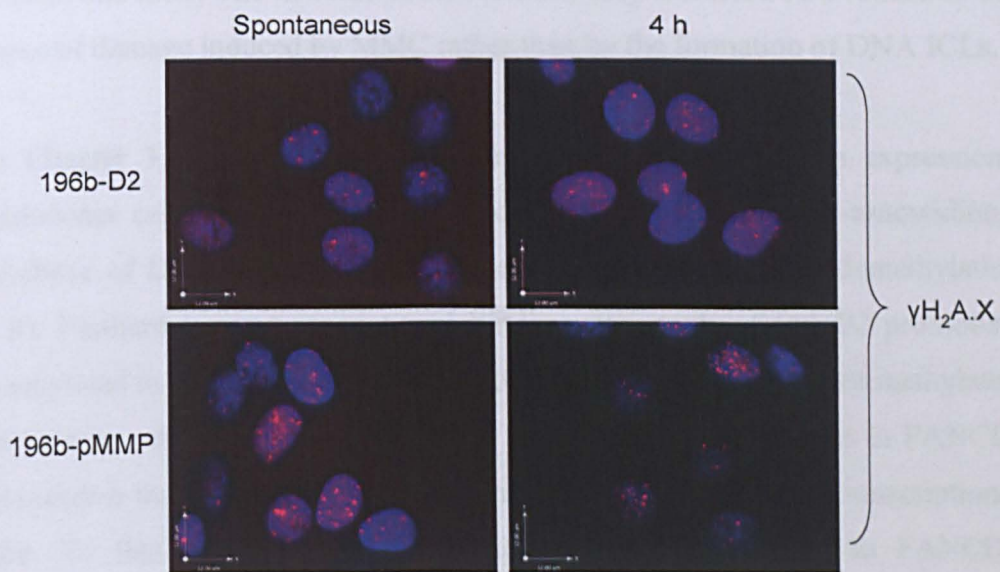
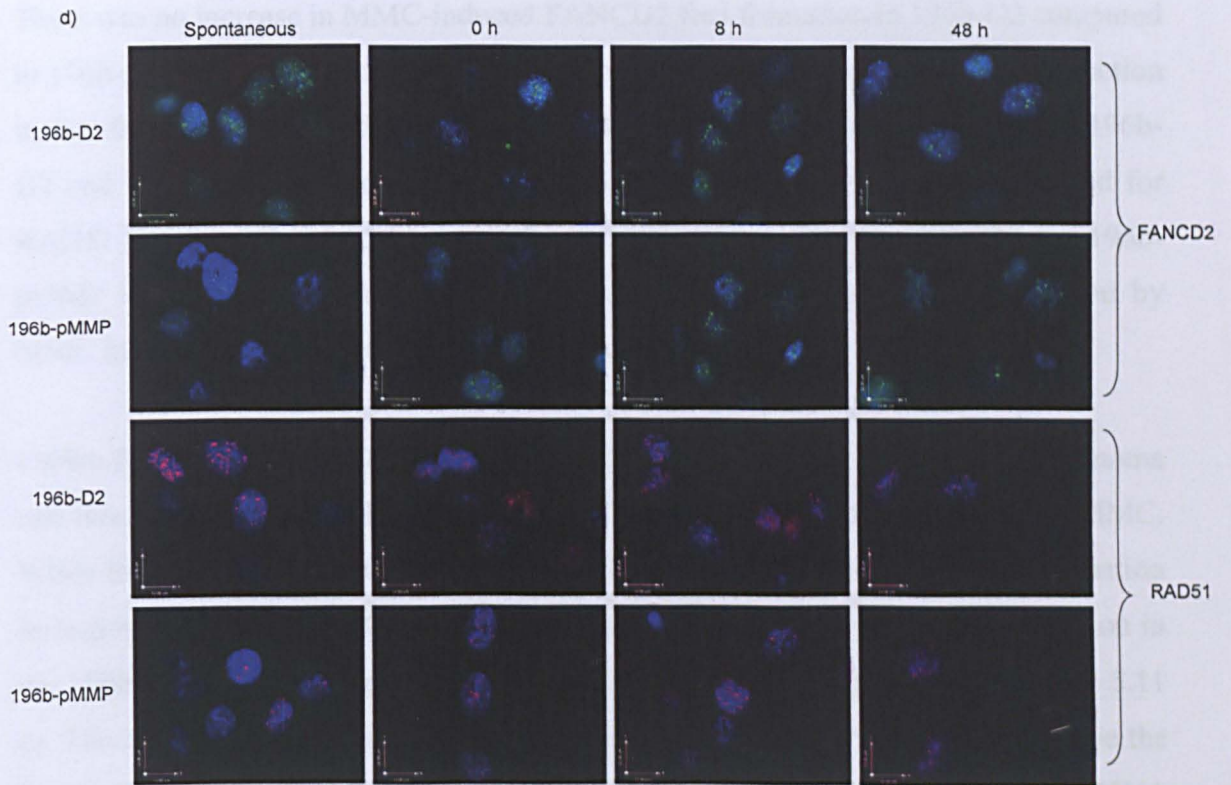


Figure 5.11 FANCD2, RAD51 and γ H₂A.X foci formation was not induced to the same degree by MMC in a FANCD2 complemented uveal melanoma cell line compared to WM793 control cell line

FANCD2, RAD51 and γ H₂A.X foci formation induced by MMC visualised by fluorescent microscopy in 196b-pMMP and 196b-D2 cell lines compared to 196b and WM793 control cell lines. On each occasion, at least 50 cells were analysed and the % of cells with > 10 foci/cell was calculated. a) and b) Cells were treated for 1 h with MMC and then allowed to repair for 0, 4, 8, 24 and 48 h, where 0 h represents immediate fixing. Significance was calculated for 196b-pMMP and 196b-D2 compared to WM793 at each of the time points. c) Cells were treated for 1 h with MMC and then left to repair for 4 h post treatment. γ H₂A.X foci formation induced at 4 h was compared to spontaneous levels for each cell line. Data shown is the average of at least three separate experiments and standard deviations are represented by error bars. Significance was calculated using the Student's T-test where $p < 0.05$ is indicated by *, $p < 0.01$ is indicated by ** and $p < 0.001$ is indicated by ***. Brackets indicate the significance calculated between samples where no significance is indicated by 'NS'. d) Representative images of FANCD2 (green) and RAD51 foci formation (red) at 0, 8 and 48 h post treatment, and γ H₂A.X foci formation (red) spontaneously and at 4 h post treatment for 196b-pMMP and 196bD2 cell lines, nuclei stained with DAPI (blue).



There was no increase in MMC-induced FANCD2 foci formation in 196b-D2 compared to 196b-pMMP and 196b cell lines, with both cell lines showing a significant reduction in foci formation compared to WM793 (at 24 h, $p = 0.02$ and $p = 1.4 \times 10^{-5}$, for 196b-D2 and 196b-pMMP respectively) (Figure 5.11 a). A similar result was obtained for RAD51 foci formation (at 24 h, $p = 6.5 \times 10^{-7}$ and $p = 2.4 \times 10^{-5}$ for 196b-D2 and 196b-pMMP respectively) (Figure 5.11 b), suggesting that HR was not being induced by MMC in these cells irrespective of FANCD2 expression.

Unlike FANCD2 and RAD51 foci formation, complementation of the uveal melanoma cell line 196b with FANCD2 did result in a change in the response of cells to MMC. While the non-complemented 196b cell line did not appear to induce $\gamma\text{H}_2\text{A.X}$ formation in response to MMC, MMC induced a significant increase in $\gamma\text{H}_2\text{A.X}$ foci formation in the 196b-D2 cell line compared to that seen in untreated cells ($p = 0.004$) (Figure 5.11 c). The complementation of these cells with FANCD2 has been shown to decrease the levels of endogenous $\gamma\text{H}_2\text{A.X}$ foci formation to that observed in WM793 and MRC5VA control cell lines. The increase observed here, may therefore be a reflection of the other types of damage induced by MMC rather than by the formation of DNA ICLs.

In Chapter 3, it was found that the reduced FANCD2 protein expression in uveal melanoma cell lines was further reduced by the addition of 5-azacytidine, a potent inhibitor of DNA methyltransferase that induces genome-wide demethylation (Figure 3.8). Furthermore, a transcriptional binding site on the *FANCD2* promoter that was methylated in the control cell lines, MRC5VA and SW480, was not methylated in uveal melanoma cell lines (Figure 3.9). This suggests that the decrease in FANCD2 protein expression may be controlled by the methylation status of this transcriptional binding site. To finally demonstrate that resistance was not related to FANCD2 protein expression level, cells were treated for 5 days with 5-azacytidine before MMC toxicity assays were performed. Cells were grown continually in the presence of MMC for 15 days before the survival fraction was calculated (Figure 5.12).

Inducing genome-wide demethylation in uveal melanoma cell lines did not affect resistance to MMC in these cells but interestingly neither did it have an effect on

WM793 and MRC5VA control cell lines (Figure 5.12). These results suggest that 5-azacytidine treatment does not affect MMC resistance in any cell line, even though FANCD2 protein expression is affected in all cell lines studied. This further supports the finding that MMC resistance in uveal melanoma cells is due to a defect in CYP450R required for the metabolism of the compound rather than the lack of FANCD2 expression that is associated with the reduced SCE phenotype in these cells.

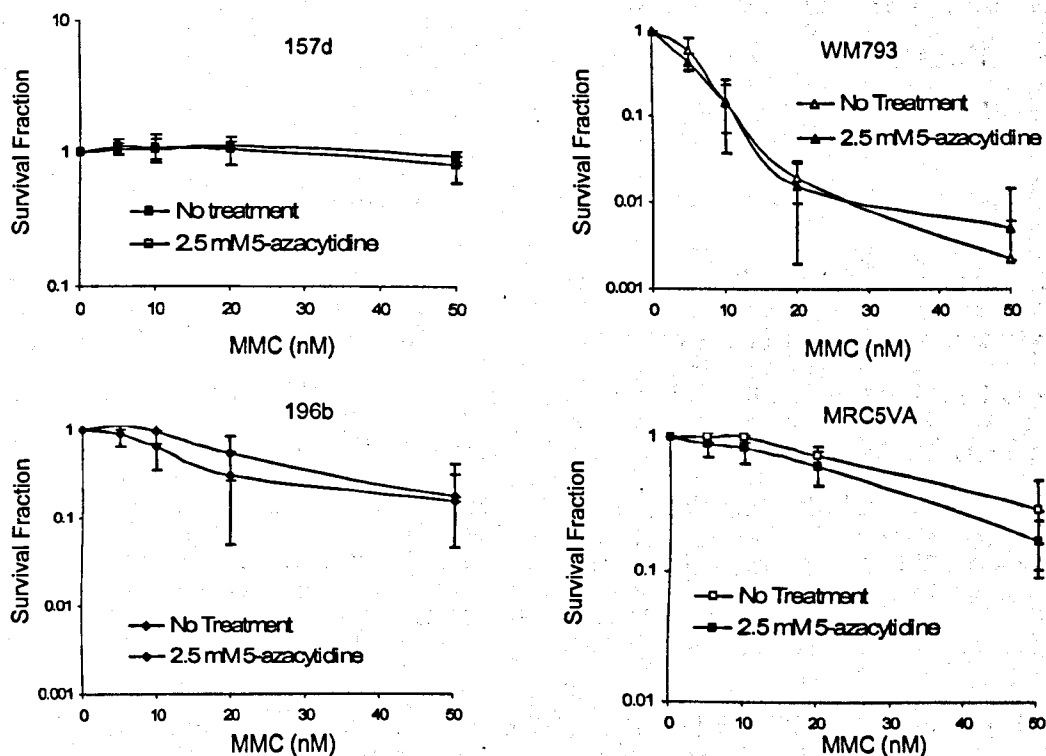


Figure 5.12 Genome-wide demethylation, which affects the protein expression of FANCD2 in uveal melanoma cell lines, has no effect on the resistance to MMC

MMC toxicity assays for the uveal melanoma cell lines, 157d and 196b, and for the WM793 and MRC5VA control cell lines following either no treatment or treatment with 2.5 mM 5-azacytidine for 5 consecutive days. Surviving colonies were counted after 15 days and the survival fraction calculated. Data shown represents the average from at least three experiments and error bars represent standard deviations.

5.9 Discussion

FA patient cells (including *FANCD2*^{-/-} patient cells) are characterised by normal levels of spontaneous SCE but a reduced induction of SCE by MMC; this is consistent with a defect in repair and their hypersensitivity to ICL-inducing agents. Complementation studies have shown that by complementing these cells with the missing FA protein hypersensitivity can be restored and thus, it is postulated that the FA pathway is essential to ICL repair. Here, it has been found that uveal melanoma cell lines are resistant to the ICL-inducing agents MMC and cisplatin. This resistance was not expected as the cell lines have a reduction in the expression of FANCD2 protein however it is consistent with the clinical phenotype of uveal melanoma (Albert et al., 1992).

Repair is promoted by the FA pathway, complementing the uveal melanoma cell lines with FANCD2 however, does not affect ICL resistance and it was subsequently found that the resistance to MMC was due to a reduced ability to form the initial cross-link between the strands of the DNA duplex (Figure 5.7). The potential effect of reduced expression of FANCD2 can therefore not be seen in the cellular response of uveal melanoma to MMC. Here, we have provided evidence to suggest that the resistance to ICL-inducing agents in uveal melanoma is not due to a defect in repair.

One difference between uveal melanoma cell lines and FA-D2 patient cells (PD20 cell line) is that PD20 cells have a mutation in the *FANCD2* gene that results in a severely truncated and non-functional FANCD2 protein whereas here, we postulate that the uveal melanoma cells have an intact *FANCD2* gene, but a reduced level of transcription and thus expression of functional FANCD2; although it is of note that point mutations have not been studied here. This suggests that although uveal melanoma cell lines have a reduced level of FANCD2 they may still have the ability to perform ICL repair, whereas FA patient cells cannot. This was confirmed by the ability of the uveal melanoma cell lines to form FANCD2 foci following MMC treatment. Subsequently, it has been found that in the uveal melanoma cell line 196b, a dose of 250 nM MMC can induce a similar level of γ H₂A.X foci formation to those seen in WM793 and MRC5VA cell lines at 90 nM MMC (Figure 5.13). This suggests that uveal melanoma cell lines are capable of ICL repair but at any given dose have a lower response to MMC-induced damage

compared to control cell lines, possibly due to a lower level of ICL induction. To investigate this hypothesis, studying the formation of ICLs in uveal melanoma cell lines at higher doses of MMC is required.

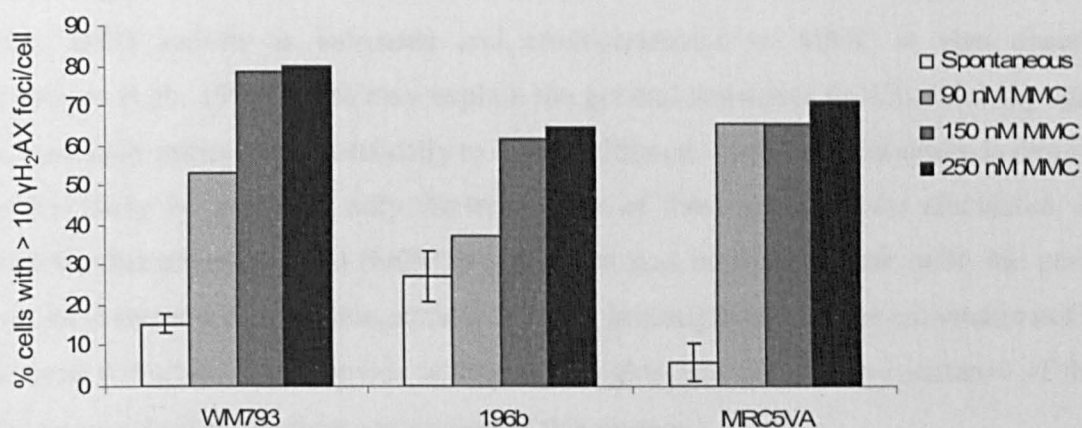


Figure 5.13 High doses of MMC increases $\gamma\text{H}_2\text{A.X}$ foci formation in the uveal melanoma cell line 196b to similar levels observed for WM793 and MRC5VA controls

MMC-induced $\gamma\text{H}_2\text{A.X}$ foci formation in the uveal melanoma cell line, 196b compared to WM793 and MRC5VA control cell lines. Cells were continually treated for 24 h with either no treatment, 90 nM MMC, 150 nM MMC or 250 mM MMC. Spontaneous $\gamma\text{H}_2\text{A.X}$ foci formation is also shown for comparison. Data shown is representative of only one experiment except for spontaneous data which is the average from at least three separate experiments and error bars represent standard deviations. On each occasion, at least 50 cells were analysed and the % of cells with $> 10 \gamma\text{H}_2\text{A.X}$ foci/cell was calculated.

MMC is an anti-tumour antibiotic that must first be reductively activated before it can bind to DNA causing the highly toxic lesions. The two major cellular reductases that act on this compound are CYP450R and DTD (NQO1). In uveal melanoma cell lines, CYP450R expression was found to be decreased, consistent with the reduced ICL formation and reduced induction of DNA damage by MMC in these cells. Subsequently, when complemented with CYP450R, the uveal melanoma cell line 196b gained sensitivity to the ICL-inducing agent. It is postulated that CYP450R and DTD act on MMC in competing pathways to produce different DNA lesions. Fast reductive activation of MMC by CYP450R promotes the formation of ICLs, DTD activation of MMC however, is slower and leads to the formation of the relatively nontoxic

metabolite 2, 7-diaminomitosenone (2, 7-DAM) (Suresh Kumar et al., 1997). Here, only CYP450R expression is reduced, it is therefore possible that the formation of 2, 7-DAM by DTD (NQO1) reductive activation may be upregulated in these cells. Furthermore, although reductive activation is not required for cisplatin to bind to DNA directly, interestingly, it has been shown that in cisplatin resistant human ovarian cancer cell lines, DTD activity is increased and cross-resistance to MMC is also observed (O'Dwyer et al., 1996). This may explain the general resistance to ICL-inducing agents in these cells rather than specifically to MMC, although further investigation is required. In this study for example, only the expression of these proteins was elucidated, it is possible that although DTD (NQO1) expression was normal in these cells, the protein may have increased enzymatic activity. Further investigation into the enzymatic activity of these reductases may provide additional insights into the chemo-resistance of these cell lines and aid in the future treatment of this disease.

The resistance to dT (Figure 5.1) was also unexpected as uveal melanoma cell lines were seen in Chapter 3 to be deficient in endogenous HR, and HR is required to overcome dT induced replication stress (Lundin et al., 2002). dT causes nucleotide pool imbalance and nucleotide metabolism has been shown to be altered in many cancers (De Korte et al., 1986) thus, perhaps the resistance to dT seen here is also unrelated to the defect in repair. Studying the effects of dT in PD20 and PD20-D2 cell lines may help to understand this additional resistance phenotype.

Chapter 6 – Discussion

6.1	Introduction	176
6.2	Decreased FANCD2 is associated with decreased spontaneous SCE frequency in uveal melanoma	176
6.3	Decreased levels of endogenous HR may be associated with decreased spontaneous SCE through the role of FANCD2 in the repair of endogenous damage	177
6.4	Types of endogenous DNA damage in uveal melanoma	180
6.5	Postulated involvement of NHEJ in the repair of endogenous DNA damage in uveal melanoma	181
6.6	Resistance to ICL-inducing agents in uveal melanoma is caused by a lack of CYP450R.....	183
6.7	Methylation events in uveal melanoma	186
6.8	How do uveal melanoma cells survive?	189

List of Figures

Figure 6.1	Proposed model for the spontaneous SCE phenotype in uveal melanoma.....	179
Figure 6.2	Proposed model of NHEJ in uveal melanoma compared to PD20 cell lines.....	182
Figure 6.3	Proposed endogenous DNA damage response in uveal melanoma.....	185
Figure 6.4	Possible mechanisms of inhibition of <i>FANCD2</i> expression in uveal melanoma.....	188
Figure 6.5	Proposed model for uveal melanoma survival.....	190

6.1 Introduction

Using uveal melanoma cell lines as a model system for SCE formation, work presented here suggests that there is an association between FANCD2 expression and spontaneous SCE. It was initially found that uveal melanoma cells have decreased levels of FANCD2, which upon complementation, corrected the reduced spontaneous SCE phenotype suggesting an association between the two. Furthermore, spontaneous HR levels were decreased supporting a role for HR in spontaneous SCE formation, which we postulate is due to the role of FANCD2. In addition, the resistance to ICL-inducing agents in uveal melanoma was found to be due to a lack of the cellular reductase, CYP450R, rather than a defect in repair.

6.2 Decreased FANCD2 is associated with decreased spontaneous SCE frequency in uveal melanoma

SCE can either occur spontaneously during S-phase or be induced by a wide range of mutagenic chemicals. Spontaneous SCE are considered to be a result of normal replication or repair of endogenous DNA damage, whereas induced SCE are a result of the DNA damage response, presumably as an end product of the DNA repair pathways (Nagasawa et al., 1983). Here, only spontaneously occurring SCEs will be discussed.

Published data on the association between FA proteins and SCE is conflicting. In *Fancc*^{-/-} and *Fancd2*^{-/-} chicken DT40 cell lines an increase in spontaneous SCE has been observed whereas in mammalian cell lines knocking out *Fancg* did not affect SCE formation (Niedziedz et al., 2004; Yamamoto et al., 2005). In humans, primary FA patient cells have also been shown to have normal levels of spontaneous SCE (Latt et al., 1975). Here, the FA patient cell line, PD20 (deficient in *FANCD2*) was found to have decreased spontaneous SCE compared to the PD20 complemented cell line (PD20-D2). Despite PD20 cell lines being continually used to study FANCD2 this decrease in SCE has not been reported previously. It suggests an association between FANCD2 and spontaneous SCE and is consistent with our data obtained for the uveal melanoma cell lines. However, whilst the spontaneous SCE frequency in the PD20 cell line was lower than its FANCD2 complemented derivative, the overall level of SCE was high compared to human primary fibroblasts and other human cancer cell lines. A possible reason for this is that upon immortalisation, the cells have adapted in culture and now

exhibit high SCE whereas primary FA patient cells still retain 'normal' SCE levels. However, there is no evidence to support this. Most importantly, the FANCD2 complemented PD20 cell line showed a further increase in spontaneous SCE, consistent with the results observed in the FANCD2 complemented uveal melanoma cell line.

The difference in spontaneous SCE levels between cell lines highlights the importance of using the correct control for this work. Although the WM793 melanoma cell line is derived from the same precursor cells as uveal melanoma and exhibit high spontaneous SCE, it is possible that normal melanocytes from the uveal tract have low SCE irrespective of melanoma. To ensure the observed phenotypes are not specific to cells of the eye, it would be of interest to study the SCE frequency and FANCD2 expression in normal uveal melanocytes. In addition, using SiRNA technology in other cell types would show whether the association between FANCD2 and SCE is a general phenotype or uveal melanoma specific.

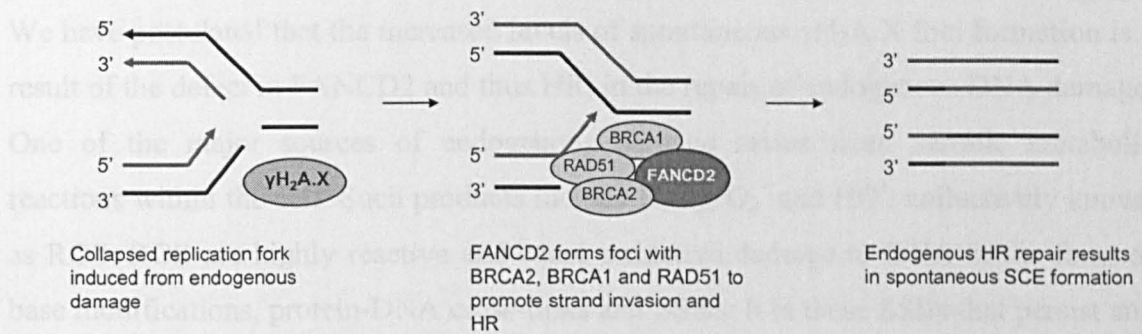
6.3 Decreased levels of endogenous HR may be associated with decreased spontaneous SCE through the role of FANCD2 in the repair of endogenous damage

Since its discovery over 50 years ago, there have been numerous theories of SCE formation. The most renowned was postulated by Kato (1977) and stated that SCE is a recombinational event involving double-stranded exchange and thus occurs during S-phase of the cell cycle. This double-strand exchange is now known as HR, and SCE is a known end-product of HR, particularly one-ended repair that is induced by persistent SSBs during replication (Saleh-Gohari et al., 2005). Furthermore, defects in DNA repair proteins associated with HR such as Rad51 in chicken DT40 cell lines, and Brca2 in mouse embryonic stem cells, have been found to decrease spontaneous SCE formation (Sonoda et al., 1999; Tutt et al., 2001) although this same decrease has not been observed in all biological systems studied (Kim et al., 2004). Here, we have found that reduced spontaneous SCE in uveal melanoma can be correlated with decreased FANCD2. As we also observed a decrease in spontaneous RAD51 foci formation we postulate that this is likely to be a result of aberrant HR repair of endogenous DNA damage (Figure 6.1).

During replication, persistent SSBs are converted to DSBs collapsing replication forks as a result of normal endogenous DNA damage (Saleh-Gohari et al., 2005). These lesions are a substrate for HR and, as only one-end is free for repair, result in SCE. In uveal melanoma cell lines, spontaneously occurring HR was reduced (as shown by reduced spontaneous RAD51 foci formation) suggesting that the collapsed replication forks arising from persistent SSBs during S-phase are not being repaired. This is consistent with our observation of the high levels of spontaneously formed γ H₂A.X foci. However, decreased repair and increased persistent damage are in contrast to cellular survival, which we do not see decreased in uveal melanoma. How uveal melanoma cells continue to survive will be discussed in Section 6.8.

The monoubiquitination of FANCD2 is highly regulated by the cell cycle and is required for normal cell cycle progression. During S-phase, monoubiquitinated FANCD2 colocalises with BRCA1 and RAD51 to form distinct nuclear foci (Taniguchi et al., 2002). It has therefore been postulated that FANCD2 has a role in promoting endogenous HR repair of collapsed replication forks. Although the exact role of FANCD2 in promoting HR is not known, it has been shown that *fancd2* depleted *Xenopus* extracts are unable to restart collapsed replication forks whereas replication restart following stalled forks is unaffected (Wang et al., 2008). This implies that FANCD2 has a specific role in the HR repair of collapsed replication forks during replication. Recently, using electrophoretic motility shift assays, it has been shown that FANCD2 has 3' to 5' exonuclease activity (Pace et al., 2010). A speculative role for FANCD2 could therefore be in the resectioning of ssDNA ends at the collapsed replication fork to ensure repair by HR. As we have found that uveal melanoma cell lines have high levels of spontaneous γ H₂A.X foci formation, indicative of high levels of endogenous DNA damage, reduced spontaneous FANCD2 protein expression, and reduced spontaneous RAD51 foci formation, our data support a role for FANCD2 in HR repair of collapsed replication forks during unperturbed replication and suggests that this FANCD2 function is conserved in humans. Our data are also consistent with the idea that endogenous lesions are collapsed forks, the repair of which by HR promotes SCE (Figure 6.1).

a) SCE formation from endogenous DNA damage



b) SCE formation from endogenous DNA damage when FANCD2 is reduced

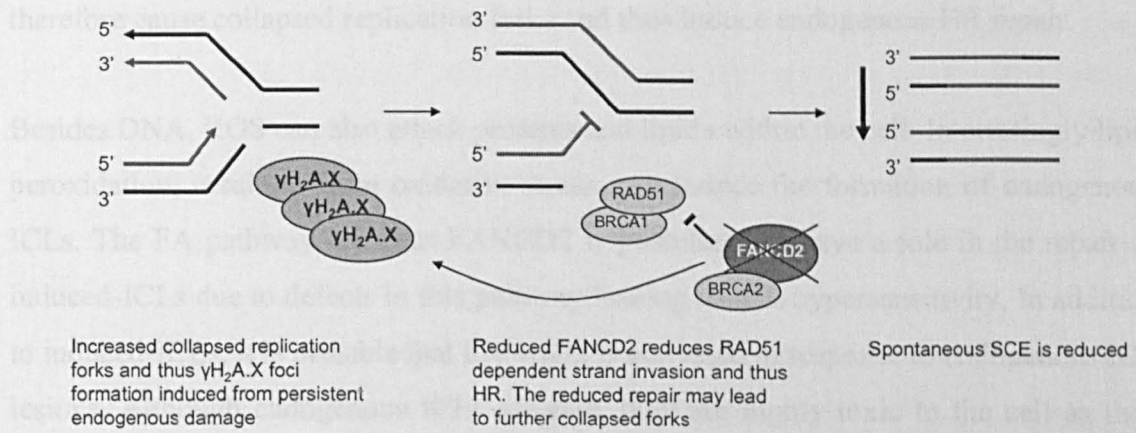


Figure 6.1 Proposed model for the spontaneous SCE phenotype in uveal melanoma

a) During replication collapsed forks are repaired by HR when persistent SSBs are converted to DSBs. $\gamma\text{H}_2\text{A.X}$ foci formation can be used as a marker of this endogenous damage as they accumulate at the site of the DNA damage and thus the collapsed replication forks. Upon DNA damage, FANCD2 forms foci with BRCA2, BRCA1 and RAD51 to promote its binding to the resected ssDNA overhang of the collapsed fork, to promote the initiation of strand invasion. Collapsed replication forks leave only one-end free for repair, thus only one Holliday junction forms that can be resolved in a single direction producing a SCE. b) A reduction in FANCD2 causes an increase in collapsed replication forks and thus high levels of $\gamma\text{H}_2\text{A.X}$ foci formation. Reduced FANCD2 reduces the ability of RAD51 to bind to ssDNA to initiate strand invasion, thus reducing endogenous HR repair. The decrease in HR repair results in less spontaneous SCE formation thus causing the reduced spontaneous SCE phenotype in uveal melanoma. A decrease in repair may also result in further collapsed replication forks and thus further increased levels of endogenous DNA damage.

6.4 Types of endogenous DNA damage in uveal melanoma

We have postulated that the increased levels of spontaneous γ H₂A.X foci formation is a result of the defect in FANCD2 and thus HR, in the repair of endogenous DNA damage. One of the major sources of endogenous damage arises from aerobic metabolic reactions within the cell. Such products include H₂O₂, O₂⁻ and HO[•], collectively known as ROS. ROS are highly reactive and cause oxidative damage to DNA in the form of base modifications, protein-DNA cross-links and SSBs. It is these SSBs that persist and are converted to DSBs during replication and are repaired by HR. ROS damage can therefore cause collapsed replication forks and thus induce endogenous HR repair.

Besides DNA, ROS can also attack proteins and lipids within the cell. Interestingly lipid peroxidation, resulting from oxidative stress, can induce the formation of endogenous ICLs. The FA pathway and thus FANCD2 is postulated to have a role in the repair of induced-ICLs due to defects in this pathway leading to ICL hypersensitivity. In addition to induced-ICLs, it is possible that FANCD2 is activated in response to endogenous ICL lesions. Although endogenous ICLs are rare, they are highly toxic to the cell as they form a covalent bond between the strands of the DNA duplex preventing unwinding and thus replication and transcription. Once the cross-link has been excised, a SSB is left that, upon continued replication is converted to a DSB collapsing the replication fork. FANCD2 is postulated to promote HR in response to these collapsed forks and thus as uveal melanoma cell lines are deficient in FANCD2 and HR, endogenous ICLs may be the persisting lesion causing increased collapsed forks and thus increased endogenous DNA damage. As ICL-inducing agents are potent inducers of SCE, the lack of repair of endogenous ICLs may also account for the reduced spontaneous SCE frequency and further supports an association between FANCD2 and SCE formation.

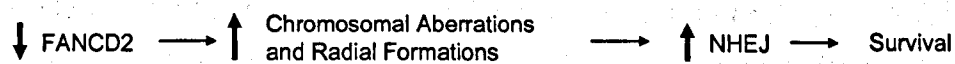
6.5 Postulated involvement of NHEJ in the repair of endogenous DNA damage in uveal melanoma

Repair of endogenous DNA damage is essential to ensure efficient replication and transcription, thus we cannot rule out the upregulation of other repair pathways, particularly NHEJ, in the repair of endogenous DNA damage in uveal melanoma, which would prevent cell death. This would after all account for similar survival rates.

DSBs are substrates for both HR and NHEJ although the exact factors that govern the use of each pathway are not fully understood. NHEJ is thought to primarily repair two-ended DSBs whereas HR repairs DSBs arising from collapsed forks during replication. Although two-ended DSBs are rare endogenous lesions, defective HR may force the cell to use NHEJ to repair persistent DSBs and ensure cell survival. Consistent with this, mammalian cells deficient in HR are still capable of repairing two-ended DSBs (Wang et al., 2001) and are able to survive. In addition, evidence for increased NHEJ in the absence of FANCD2 comes from FA patient cell lines (including the PD20 cell line) that are characterised by increased chromosomal aberrations and radial formations following MMC treatment, indicative of increased end-joining by NHEJ (Timmers et al., 2001). This increase in NHEJ presumably allows their survival. More recently, a role for the FA pathway in the suppression of NHEJ rather than promoting HR has been postulated (Adamo et al., 2010; Pace et al., 2010). Disruption of both FANCC and KU70 in human and chicken DT40 cells was found to suppress sensitivity to cross-linking agents, reduce chromosomal breaks, and reverse the defective HR (Pace et al., 2010). As FANCC is required for FANCD2 activation, it was further postulated that the role of FANCD2 was in the protection of the DNA ends against aberrant Ku70 binding at the break site. Consistent with this, in the PD20 cell line, DNA-PK_{CS} foci were found to be increased compared to wild-type human foreskin fibroblasts following replication stress (Adamo et al., 2010). This suggests that in the absence of the FA proteins including FANCD2, there is no control over initial NHEJ factors such as KU70 and DNA-PK_{CS} following DNA damage and thus NHEJ is upregulated and can carry out illegitimate repair causing the phenotypic traits of FA patient cells.

It is possible then, that in uveal melanoma, repair of endogenous DNA damage is carried out by NHEJ, sufficient to ensure survival but deficient enough to cause increased $\gamma\text{H}_2\text{A.X}$ foci formation (Figure 6.2). However, although uveal melanoma are characterised by gross chromosomal changes such as monosomy of chromosome 3 and are prone to chromosomal microdeletions, the radial formations and chromosomal aberrations have not been observed suggesting that NHEJ is not upregulated in uveal melanoma (Figure 6.2). The exact function of NHEJ in uveal melanoma is still to be elucidated and is the subject of a separate study.

a) In PD20 cells:



b) In uveal melanoma cells:

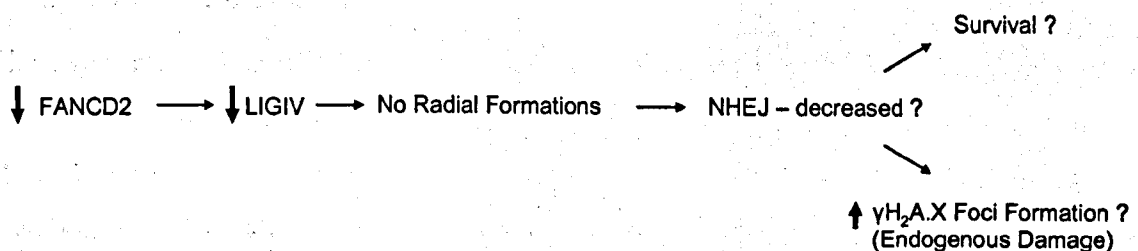


Figure 6.2 Proposed model of NHEJ in uveal melanoma compared to PD20 cell lines

a) PD20 cells deficient in FANCD2 are characterised by increased chromosomal aberrations and radial formations suggesting that NHEJ is upregulated in these cells, presumably accounting for their survival. b) Uveal melanoma cells are also deficient in FANCD2 but show few chromosomal aberrations and no radial formations. We have shown that these cells are also deficient in LIGIV suggesting that NHEJ may be decreased. Alternatively, NHEJ may be sufficient to ensure survival but deficient enough to cause the increased levels of $\gamma\text{H}_2\text{A.X}$ foci formation that are indicative of high levels of endogenous DNA damage.

The reduced expression of LIGIV in uveal melanoma is again consistent with no upregulation of NHEJ (Figure 6.2). It is more likely that repair of endogenous DNA damage in general is suppressed. As uveal melanoma cell lines and the PD20 cell line both have reduced FANCD2 expression, it would be of interest to study LIGIV expression in these FA patient cells. Although there is no evidence that these two proteins interact, it is possible that their expression is governed by the same factors (e.g. methylation) and that LIGIV expression is reduced to inhibit error-prone repair by NHEJ in the absence of HR. Furthermore, perhaps LIGIV and thus NHEJ are down-regulated in order for these cells to survive. In this case, it is possible that uveal melanoma cells are able to overcome cell cycle checkpoints and progress through the cell cycle without the need for endogenous repair (see Section 6.8). The role of aberrant methylation in this situation is discussed in Section 6.7 however, the role of point mutations effecting protein expression remains to be elucidated.

6.6 Resistance to ICL-inducing agents in uveal melanoma is caused by a lack of CYP450R

The uveal melanoma cell lines were found to be resistant to the ICL-inducing agents MMC and cisplatin, consistent with the high level of chemo-resistance observed at the clinical level. MMC is a bioreductive drug that must first be reduced to an active metabolite before it can bind to DNA and cause the ICL lesion. One of the main reductases involved in this metabolism is CYP450R. The formation of ICLs in uveal melanoma cell lines was reduced and it was subsequently found that this was due to the reduced expression of CYP450R. Because of this, it is not possible to study the effect that a defect in FANCD2 alone has on ICL repair and thus ICL-induced SCE; whether this defect is a consequence or a cause of the reduced CYP405R expression remains to be elucidated.

The ability to restore MMC sensitivity in uveal melanoma has therapeutic potential. Chemotherapy is rarely used in the treatment of uveal melanoma due to their high chemo-resistance and due to difficulties in the delivery of the drug to the tumour site (Albert et al., 1992). Current treatments such as plaque radiotherapy and enucleation are successful in treating the primary tumour, however it is the metastatic disease to the liver that causes mortality in over 50% of patients (Virgili et al., 2008). This is where

our finding may have the greatest potential. Using targeted-gene therapy, restoring the expression of CYP450R in these metastatic cells may increase the affinity of MMC to bind to DNA, thus increasing the formation of ICL lesions and the effectiveness of cross-linking chemotherapeutics in the treatment of this disease.

Although we have shown here that there is reduced RAD51 foci formation consistent with reduced HR repair of endogenous DNA damage, the lack of CYP450R suggests that uveal melanoma cell lines may have increased levels of endogenous DNA damage as a result of high levels of ROS rather than a defect in repair. The balance between the production and degradation of ROS maintains cellular homeostasis and thus an imbalance of metabolic enzymes can affect this dynamic. Such metabolic enzymes include the P450 enzymes that have been shown to be important for ROS production (Lewis and Pratt, 1998). Here, as CYP450R was found to be defective in uveal melanoma, it is possible that this defect causes an imbalance in the redox state of the cell producing more ROS, and thus endogenous DNA damage, as indicated by increased γ H₂A.X foci formation (Figure 6.3). Interestingly, FA patient cells exhibit high levels of 8-oxo-G modified bases, indicative of increased oxidative stress (Degan et al., 1995). Furthermore, in mammalian cells Fancc was found to interact and regulate the function of CYP450R (Kruyt et al., 1998), accounting for the sensitivity of the cells to H₂O₂ and the observed hypersensitivity to the ICL-inducing agent, MMC. Complementing the uveal melanoma cell line with FANCD2 increased HR repair and reduced spontaneously formed γ H₂A.X foci, it is likely then that a defect in repair and a defect in the metabolism of normal cellular processes may both contribute to the high levels of endogenous damage. However, the exact relationship between the two and whether the lack of FANCD2 is related to the reduced expression of CYP450R remains to be elucidated.

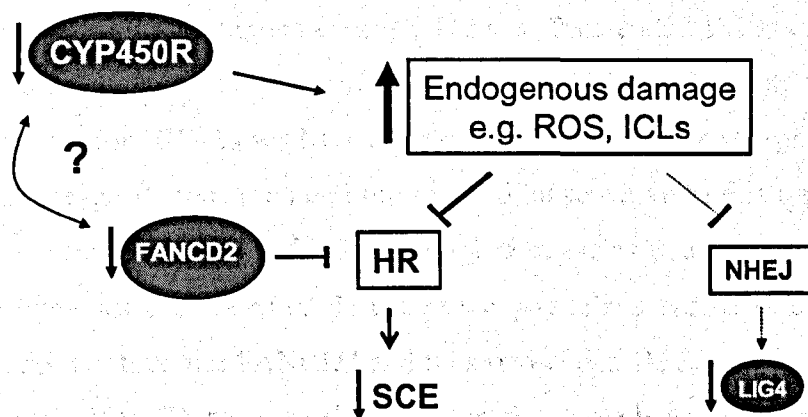


Figure 6.3 Proposed endogenous DNA damage response in uveal melanoma

Reduced expression of CYP450R may contribute to the high levels of endogenous DNA damage in uveal melanoma through the accumulation of ROS. In addition, the reduced FANCD2 expression may contribute to an accumulation of endogenous unrepaired ICLs, and thus reduced spontaneous SCE. Whether there is an association between reduced FANCD2 and reduced CYP450R remains to be elucidated.

The high levels of endogenous DNA damage and the reduced activation of the DNA repair pathways in response to this damage suggests that there is an abnormal equilibrium in uveal melanoma that allows these cells to proliferate and survive. As we observed a normal response to induced DNA damage, it is likely that the addition of such DNA damaging agents upsets this balance and thus activates the repair pathways resulting in a normal response to various DNA damaging agents. It may also indicate two separate responses to endogenous and induced DNA damage in uveal melanoma, possibly through differences in the lesions formed from endogenous or exogenous sources. Although we have postulated that the substrate for endogenous repair is similar to collapsed replication forks, these endogenously occurring lesions may be different, and thus are not recognised as damage and do not illicit a DNA damage response.

We have suggested that the DNA repair pathways HR and NHEJ are suppressed in response to endogenous DNA damage in uveal melanoma and that this accounts for the decrease in spontaneous SCE, however the response to induced DNA damage appears to be normal (with the exception of ICL-induced damage) compared to WM793

melanoma control and other human cancer cell lines. Two-ended DSBs can be induced by ionising radiation and are primarily repaired by NHEJ, although they are also possible substrates for HR. As we have shown defects in both these repair pathways it was expected that uveal melanoma cell lines would be sensitive to this type of damage. The normal response to two-ended DSBs therefore suggests that the induced repair of this damage bypasses the observed defects. One possible scenario is that two-ended repair by HR does not require *FANCD2* and thus two-ended DSBs can be repaired. This would be in contrast to FA patient cells however, that have been shown to be sensitive to IR (Nakanishi et al., 2002). Furthermore, this would not account for the normal response of uveal melanoma cell lines to camptothecin. In *Xenopus* extracts, *fancd2* has been shown to be important for replication restart following the collapse of replication forks induced by camptothecin (Wang et al., 2008). The normal response of uveal melanoma cell lines to this DNA damaging agent therefore contradicts the observed defect in HR although it is consistent with the idea that endogenous and induced lesions are different substrates of repair.

6.7 Methylation events in uveal melanoma

Epigenetic events that alter gene expression are important in the tumourigenesis of many sporadic cancers. In uveal melanoma, promoter methylation has been observed for *RASSF1a*, *p16* and *pRb* all of which are known tumour suppressor genes and have been shown to have a role in the tumour development of other human cancers (Edmunds et al., 2002; Maat et al., 2007; van der Velden et al., 2001). The methylation events that may affect DNA repair genes in uveal melanoma have not been studied. Here, we found that *FANCD2* gene expression was reduced and we postulated that this was due to the aberrant methylation status of a putative E2F transcriptional binding site within the promoter region. Aberrant methylation of *FANCD2* in human cancers has not been previously reported although polymorphisms in the *FANCD2* gene have been associated with increased sporadic breast cancer risk (Barroso et al., 2006).

Transcriptional regulation of *FA* gene expression, including *FANCD2* has been previously found to occur through the pRb/E2F pathway. This pathway is involved in G1/S cell cycle progression and is governed by the interaction between cyclin D and the cyclin dependent kinases, CDK4 and CDK6. When activated by cyclin D, CDK4/6

phosphorylates pRb leading to the activation of E2F and the subsequent expression of genes that are essential for cell cycle progression through G1/S phase (Weinberg, 1995). As the pRb/E2F pathway regulates the expression of *FANCD2*, this may explain the required activation of *FANCD2* for normal cell cycle progression. In uveal melanoma, loss of p16^{INK4a} expression through promoter hypermethylation has been observed in approximately half of uveal melanoma cell lines (van der Velden et al., 2001). p16^{INK4a} controls cell cycle proliferation during G1 by inhibiting the interaction between cyclin D and CDK4/6, thus inhibiting the phosphorylation of pRb and the subsequent activation of E2F (Serrano et al., 1993). This may therefore also contribute to the reduced *FANCD2* expression observed here (Figure 6.4). In addition, inducing genome-wide demethylation in uveal melanoma caused *FANCD2* protein expression to decrease further. The effect of demethylation on this regulatory pathway is unknown however, in conjunction with, or irrespective of the single methylation change observed here, changes in the methylation status of p16^{INK4a} and the pRb/E2F pathway provides a possible explanation for the further reduction in *FANCD2* protein expression seen following genome-wide demethylation and highlights the difficulties in studying single genes in complex cell systems.

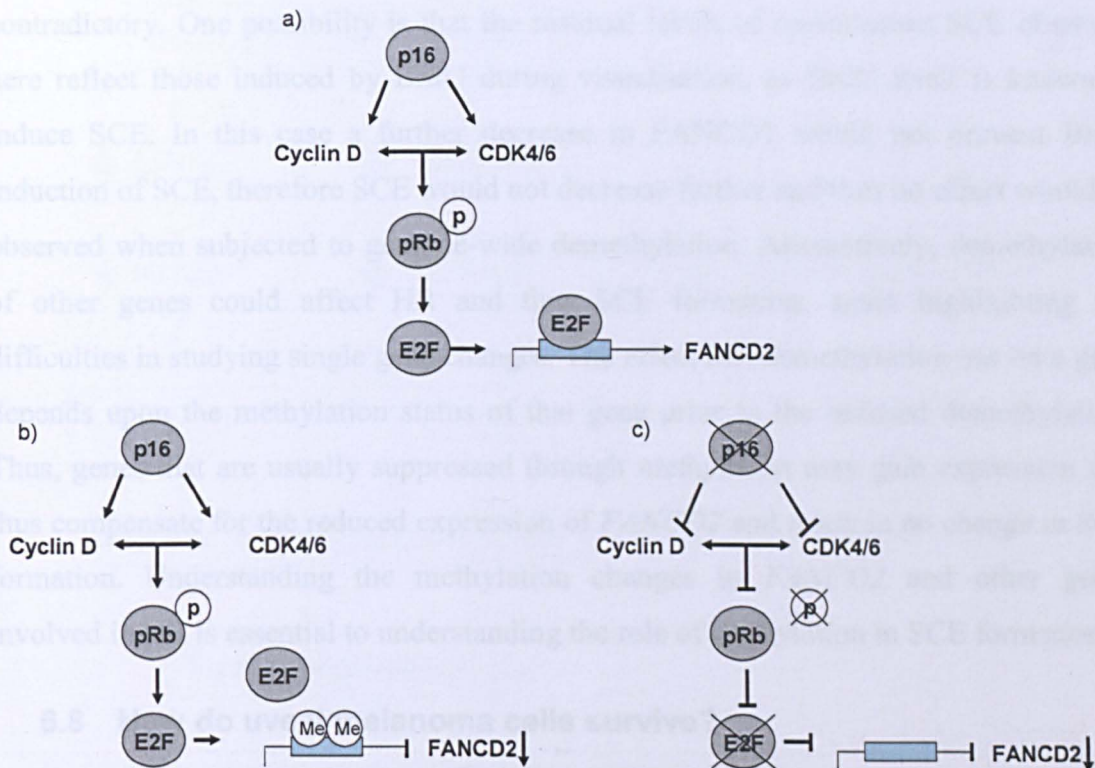


Figure 6.4 Possible mechanisms of inhibition of *FANCD2* expression in uveal melanoma

a) G1/S cell cycle progression is governed by p16^{INK4a} that controls the interaction of cyclin D and CDK4/6. When activated by cyclin D, CDK4/6 phosphorylates pRb leading to the activation of E2F. E2F then binds to the E2F transcriptional binding site of *FANCD2* causing the subsequent expression of *FANCD2* and normal cell cycle progression. b) Aberrant methylation at the E2F transcriptional binding site on *FANCD2* may block binding and result in reduced *FANCD2* expression. In this situation the upstream components of the pRb/E2F pathway are unaffected. c) Loss of expression of p16^{INK4a} through hypermethylation may inhibit the activation of CDK4/6 thus no phosphorylation of pRb would take place. This may lead to no activation of E2F, no E2F binding of *FANCD2* and thus reduced *FANCD2* expression. Similarly, methylation changes in pRb may inhibit phosphorylation by CDK4/6 and thus reducing E2F activation leading to reduced *FANCD2* expression.

Finally, SCE frequency was not affected by genome-wide demethylation and thus the reduced spontaneous SCE in uveal melanoma is unlikely to be a result of aberrant methylation. Given that *FANCD2* protein expression was decreased further following demethylation and given that we have shown an interaction between *FANCD2* expression and SCE frequency, the lack of an effect on SCE following demethylation is

contradictory. One possibility is that the residual levels of spontaneous SCE observed here reflect those induced by BrdU during visualisation, as BrdU itself is known to induce SCE. In this case a further decrease in *FANCD2* would not prevent BrdU induction of SCE, therefore SCE would not decrease further and thus no effect would be observed when subjected to genome-wide demethylation. Alternatively, demethylation of other genes could affect HR and thus SCE formation, again highlighting the difficulties in studying single gene changes. The effect that demethylation has on a gene depends upon the methylation status of that gene prior to the induced demethylation. Thus, genes that are usually suppressed through methylation may gain expression and thus compensate for the reduced expression of *FANCD2* and result in no change in SCE formation. Understanding the methylation changes in *FANCD2* and other genes involved in HR is essential to understanding the role of methylation in SCE formation.

6.8 How do uveal melanoma cells survive?

From this work, we have shown that uveal melanoma cells proliferate and survive in the presence of high levels of endogenous DNA damage. Defects in the major repair pathways involved in endogenous repair have also been identified, which may explain these high levels of damage. In patients, the suppression or redundancy of the endogenous DNA damage response may be beneficial to uveal melanoma cell survival and promoting tumourigenesis (Figure 6.5). One possible explanation for this is the loss of tumour suppressor genes such as $p16^{\text{INK4a}}$ and the pRb/E2F pathway as described above, which would promote tumour growth. $p16^{\text{INK4a}}$ inhibits the phosphorylation of pRb, controlling the progression of the cell from G1 into S phase and thus proliferation. A loss of $p16^{\text{INK4a}}$ or a methylation change as seen in approximately 50% of uveal melanoma tumours (van der Velden et al., 2001) would cause hyperphosphorylation of pRb and uncontrolled progression of the cell cycle and proliferation even in the presence of endogenous damage that would usually induce cell cycle arrest (Figure 6.5).

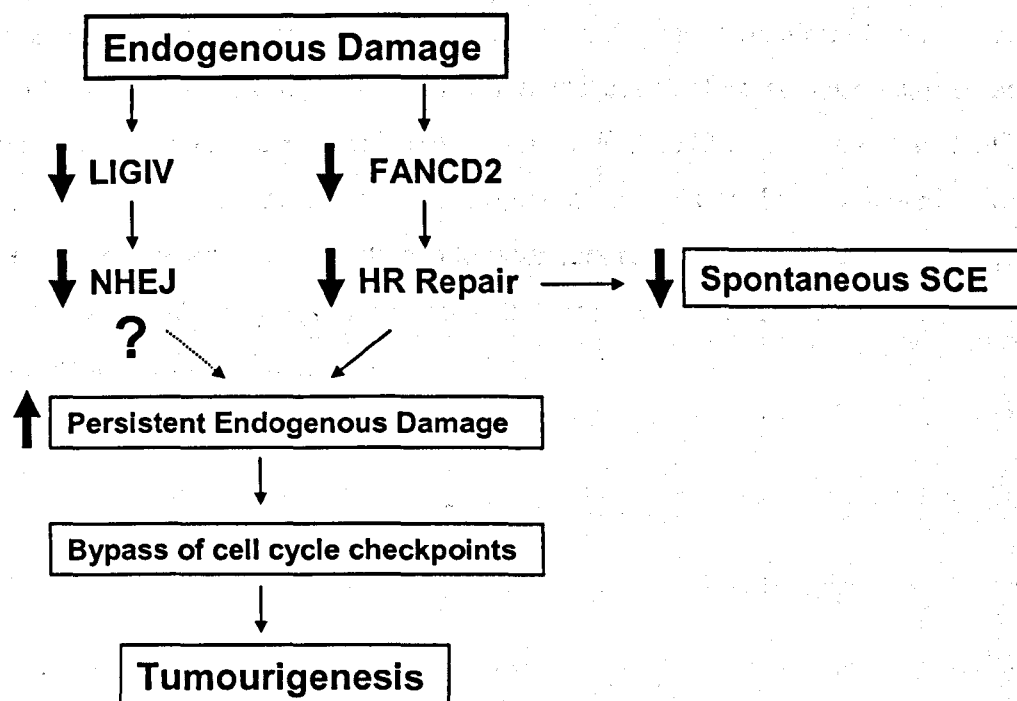


Figure 6.5 Proposed model for uveal melanoma survival

It is proposed that endogenous DNA damage is repaired by defective HR and NHEJ repair pathways in uveal melanoma. The reduced FANCD2 expression causes the decreased HR repair and the reduced spontaneous SCE phenotype of these cells. In addition, LIGIV protein expression is reduced suggesting that NHEJ is also suppressed, although its exact role remains to be elucidated. We propose that the reduced HR repair (and possibly the reduced NHEJ repair) of endogenous damage causes an increase in persistent endogenous DNA damage as indicated by the high levels of γ H₂A.X foci formation. As both repair pathways are suppressed, we propose that through the loss of expression or aberrant methylation of cell cycle regulators, uveal melanoma cells are able to bypass cell cycle checkpoints thus overcoming high levels of endogenous damage to promote tumourigenesis.

Monosomy of chromosome 3 is a common event in uveal melanoma and has been associated with metastatic development (Prescher et al., 1996). Partial deletions of chromosome 3 are also common events and thus it is thought that tumour suppressor genes involved in the tumourigenesis of uveal melanoma are located here. Interestingly, the tumour suppressor genes *Von Hippel-Lindau*, *FHIT* and *RASSF1a* are all located on chromosome 3p, however only *RASSF1a* located at 3p21.3, has been associated with the development of metastatic disease in uveal melanoma (Maat et al., 2007). As *FANCD2* is located at 3p25 it is possible that the loss of such tumour suppressor genes may be

responsible for the reduced *FANCD2*, deficient endogenous repair and thus the reduced SCE phenotype. Likewise, a loss of *FANCD2* may affect tumour suppressor gene expression. Whether the reduced expression of *FANCD2* and thus reduced SCE is a cause or consequence of tumour development remains to be elucidated. However, understanding the association between tumour suppressor genes located on chromosome 3 and *FANCD2* may provide insights into the metastatic development and tumourigenesis of uveal melanoma.

References

- Abraham, J., B. Lemmers, M.P. Hande, M.E. Moynahan, C. Chahwan, A. Ciccia, J. Essers, K. Hanada, R. Chahwan, A.K. Khaw, P. McPherson, A. Shehabeldin, R. Laister, C. Arrowsmith, R. Kanaar, S.C. West, M. Jasin, and R. Hakem. 2003. Emel is involved in DNA damage processing and maintenance of genomic stability in mammalian cells. *Embo J.* 22:6137-47.
- Adamo, A., S.J. Collis, C.A. Adelman, N. Silva, Z. Horejsi, J.D. Ward, E. Martinez-Perez, S.J. Boulton, and A. La Volpe. 2010. Preventing nonhomologous end joining suppresses DNA repair defects of Fanconi anemia. *Mol Cell.* 39:25-35.
- Ahmad, A., A.R. Robinson, A. Duensing, E. van Drunen, H.B. Beverloo, D.B. Weisberg, P. Hasty, J.H. Hoeijmakers, and L.J. Niedernhofer. 2008. ERCC1-XPF endonuclease facilitates DNA double-strand break repair. *Mol Cell Biol.* 28:5082-92.
- Akkari, Y.M., R.L. Bateman, C.A. Reifsteck, S.B. Olson, and M. Grompe. 2000. DNA replication is required To elicit cellular responses to psoralen-induced DNA interstrand cross-links. *Mol Cell Biol.* 20:8283-9.
- Albert, D.M., A.S. Niffenegger, and J.K. Willson. 1992. Treatment of metastatic uveal melanoma: review and recommendations. *Surv Ophthalmol.* 36:429-38.
- Alpi, A.F., P.E. Pace, M.M. Babu, and K.J. Patel. 2008. Mechanistic insight into site-restricted monoubiquitination of FANCD2 by Ube2t, FANCL, and FANCI. *Mol Cell.* 32:767-77.
- Andreassen, P.R., A.D. D'Andrea, and T. Taniguchi. 2004. ATR couples FANCD2 monoubiquitination to the DNA-damage response. *Genes Dev.* 18:1958-63.
- Aristei, C., F. Stracci, P. Guerrieri, P. Anselmo, R. Armellini, A. Rulli, F. Barberini, P. Latini, and A.R. Menghini. 2009. Frequency of sister chromatid exchanges and micronuclei monitored over time in patients with early-stage breast cancer: results of an observational study. *Cancer Genet Cytogenet.* 192:24-9.
- Arnaudeau, C., C. Lundin, and T. Helleday. 2001. DNA double-strand breaks associated with replication forks are predominantly repaired by homologous recombination involving an exchange mechanism in mammalian cells. *J Mol Biol.* 307:1235-45.
- Asami, S., H. Manabe, J. Miyake, Y. Tsurudome, T. Hirano, R. Yamaguchi, H. Itoh, and H. Kasai. 1997. Cigarette smoking induces an increase in oxidative DNA damage, 8-hydroxydeoxyguanosine, in a central site of the human lung. *Carcinogenesis.* 18:1763-6.

- Audebert, M., B. Salles, and P. Calsou. 2004. Involvement of poly(ADP-ribose) polymerase-1 and XRCC1/DNA ligase III in an alternative route for DNA double-strand breaks rejoining. *J Biol Chem.* 279:55117-26.
- Bailly, V., J. Lamb, P. Sung, S. Prakash, and L. Prakash. 1994. Specific complex formation between yeast RAD6 and RAD18 proteins: a potential mechanism for targeting RAD6 ubiquitin-conjugating activity to DNA damage sites. *Genes Dev.* 8:811-20.
- Bailly, V., S. Prakash, and L. Prakash. 1997. Domains required for dimerization of yeast Rad6 ubiquitin-conjugating enzyme and Rad18 DNA binding protein. *Mol Cell Biol.* 17:4536-43.
- Baltaci, V., F. Kayikcioglu, I. Alpas, H. Zeyneloglu, and A. Haberal. 2002. Sister chromatid exchange rate and alkaline comet assay scores in patients with ovarian cancer. *Gynecol Oncol.* 84:62-6.
- Barroso, E., R.L. Milne, L.P. Fernandez, P. Zamora, J.I. Arias, J. Benitez, and G. Ribas. 2006. FANCD2 associated with sporadic breast cancer risk. *Carcinogenesis.* 27:1930-7.
- Baumann, P., and S.C. West. 1998. Role of the human RAD51 protein in homologous recombination and double-stranded-break repair. *Trends Biochem Sci.* 23:247-51.
- Baumann, R.P., W.F. Hodnick, H.A. Seow, M.F. Belcourt, S. Rockwell, D.H. Sherman, and A.C. Sartorelli. 2001. Reversal of mitomycin C resistance by overexpression of bioreductive enzymes in Chinese hamster ovary cells. *Cancer Res.* 61:7770-6.
- Baylin, S.B., M. Esteller, M.R. Rountree, K.E. Bachman, K. Schuebel, and J.G. Herman. 2001. Aberrant patterns of DNA methylation, chromatin formation and gene expression in cancer. *Hum Mol Genet.* 10:687-92.
- Bender, M.A., H.G. Griggs, and J.S. Bedford. 1974. Recombinational DNA repair and sister chromatid exchanges. *Mutat Res.* 24:117-23.
- Berardini, M., P.L. Foster, and E.L. Loechler. 1999. DNA polymerase II (polB) is involved in a new DNA repair pathway for DNA interstrand cross-links in *Escherichia coli*. *J Bacteriol.* 181:2878-82.
- Bhagwat, N., A.L. Olsen, A.T. Wang, K. Hanada, P. Stuckert, R. Kanaar, A. D'Andrea, L.J. Niedernhofer, and P.J. McHugh. 2009. XPF-ERCC1 participates in the fanconi anemia pathway of cross-link repair. *Mol Cell Biol.* 29:6427-37.
- Bhattacharyya, N.P., A. Skandalis, A. Ganesh, J. Groden, and M. Meuth. 1994. Mutator phenotypes in human colorectal carcinoma cell lines. *Proc Natl Acad Sci U S A.* 91:6319-23.
- Bird, A. 1992. The essentials of DNA methylation. *Cell.* 70:5-8.

- Birnboim, H.C., and J. Doly. 1979. A rapid alkaline extraction procedure for screening recombinant plasmid DNA. *Nucleic Acids Res.* 7:1513-23.
- Bizanek, R., B.F. McGuinness, K. Nakanishi, and M. Tomasz. 1992. Isolation and structure of an intrastrand cross-link adduct of mitomycin C and DNA. *Biochemistry.* 31:3084-91.
- Blackwell, L.J., D. Martik, K.P. Bjornson, E.S. Bjornson, and P. Modrich. 1998. Nucleotide-promoted release of hMutSalpha from heteroduplex DNA is consistent with an ATP-dependent translocation mechanism. *J Biol Chem.* 273:32055-62.
- Bogliolo, M., A. Lyakhovich, E. Callen, M. Castella, E. Cappelli, M.J. Ramirez, A. Creus, R. Marcos, R. Kalb, K. Neveling, D. Schindler, and J. Surralles. 2007. Histone H2AX and Fanconi anemia FANCD2 function in the same pathway to maintain chromosome stability. *Embo J.* 26:1340-51.
- Brattain, M.G., W.D. Fine, F.M. Khaled, J. Thompson, and D.E. Brattain. 1981. Heterogeneity of malignant cells from a human colonic carcinoma. *Cancer Res.* 41:1751-6.
- Bridges, B.A., and S.G. Sedgwick. 1974. Effect of photoreactivation on the filling of gaps in deoxyribonucleic acid synthesized after exposure of Escherichia coli to ultraviolet light. *J Bacteriol.* 117:1077-81.
- Broomfield, S., T. Hryciw, and W. Xiao. 2001. DNA postreplication repair and mutagenesis in Saccharomyces cerevisiae. *Mutat Res.* 486:167-84.
- Cadet, J., T. Douki, D. Gasparutto, and J.L. Ravanat. 2003. Oxidative damage to DNA: formation, measurement and biochemical features. *Mutat Res.* 531:5-23.
- Caggana, M., and K.T. Kelsey. 1991. Sister chromatid exchange frequency in Hodgkin's disease patients with elevated in vivo hprt mutant frequencies. *Carcinogenesis.* 12:2141-5.
- Caldecott, K., and P. Jeggo. 1991. Cross-sensitivity of gamma-ray-sensitive hamster mutants to cross-linking agents. *Mutat Res.* 255:111-21.
- Caldecott, K.W., S. Aoufouchi, P. Johnson, and S. Shall. 1996. XRCC1 polypeptide interacts with DNA polymerase beta and possibly poly (ADP-ribose) polymerase, and DNA ligase III is a novel molecular 'nick-sensor' in vitro. *Nucleic Acids Res.* 24:4387-94.
- Calsou, P., P. Frit, O. Humbert, C. Muller, D.J. Chen, and B. Salles. 1999. The DNA-dependent protein kinase catalytic activity regulates DNA end processing by means of Ku entry into DNA. *J Biol Chem.* 274:7848-56.
- Carney, J.P., R.S. Maser, H. Olivares, E.M. Davis, M. Le Beau, J.R. Yates, 3rd, L. Hays, W.F. Morgan, and J.H. Petrini. 1998. The hMre11/hRad50 protein

- complex and Nijmegen breakage syndrome: linkage of double-strand break repair to the cellular DNA damage response. *Cell*. 93:477-86.
- Carrano, A.V., L.H. Thompson, P.A. Lindl, and J.L. Minkler. 1978. Sister chromatid exchange as an indicator of mutagenesis. *Nature*. 271:551-3.
- Chaganti, R.S., S. Schonberg, and J. German. 1974. A manyfold increase in sister chromatid exchanges in Bloom's syndrome lymphocytes. *Proc Natl Acad Sci U S A*. 71:4508-12.
- Chen, P.L., C.F. Chen, Y. Chen, J. Xiao, Z.D. Sharp, and W.H. Lee. 1998. The BRC repeats in BRCA2 are critical for RAD51 binding and resistance to methyl methanesulfonate treatment. *Proc Natl Acad Sci U S A*. 95:5287-92.
- Ciccia, A., A. Constantinou, and S.C. West. 2003. Identification and characterization of the human mus81-eme1 endonuclease. *J Biol Chem*. 278:25172-8.
- Ciccia, A., C. Ling, R. Coulthard, Z. Yan, Y. Xue, A.R. Meetei, H. Laghmani el, H. Joenje, N. McDonald, J.P. de Winter, W. Wang, and S.C. West. 2007. Identification of FAAP24, a Fanconi anemia core complex protein that interacts with FANCM. *Mol Cell*. 25:331-43.
- Cole, R.S. 1973. Repair of DNA containing interstrand crosslinks in *Escherichia coli*: sequential excision and recombination. *Proc Natl Acad Sci U S A*. 70:1064-8.
- Collins, N.B., J.B. Wilson, T. Bush, A. Thomashevski, K.J. Roberts, N.J. Jones, and G.M. Kupfer. 2009. ATR-dependent phosphorylation of FANCA on serine 1449 after DNA damage is important for FA pathway function. *Blood*. 113:2181-90.
- Cortes-Gutierrez, E.I., R.M. Cerda-Flores, and C.H. Leal-Garza. 2000. Sister chromatid exchanges in peripheral lymphocytes from women with carcinoma of the uterine cervix. *Cancer Genet Cytogenet*. 122:121-3.
- Costantini, S., L. Woodbine, L. Andreoli, P.A. Jeggo, and A. Vindigni. 2007. Interaction of the Ku heterodimer with the DNA ligase IV/Xrcc4 complex and its regulation by DNA-PK. *DNA Repair (Amst)*. 6:712-22.
- Cowen, R.L., A.V. Patterson, B.A. Telfer, R.E. Airley, S. Hobbs, R.M. Phillips, M. Jaffar, I.J. Stratford, and K.J. Williams. 2003. Viral delivery of P450 reductase recapitulates the ability of constitutive overexpression of reductase enzymes to potentiate the activity of mitomycin C in human breast cancer xenografts. *Mol Cancer Ther*. 2:901-9.
- Cross, N.A., A. Ganesh, M. Parpia, A.K. Murray, I.G. Rennie, and K. Sisley. 2006. Multiple locations on chromosome 3 are the targets of specific deletions in uveal melanoma. *Eye (Lond)*. 20:476-81.

- Cross, N.A., I.G. Rennie, A.K. Murray, and K. Sisley. 2005. The identification of chromosome abnormalities associated with the invasive phenotype of uveal melanoma in vitro. *Clin Exp Metastasis*. 22:107-13.
- Cunningham, R.P. 1997. DNA glycosylases. *Mutat Res*. 383:189-96.
- Davies, A.A., J.Y. Masson, M.J. McIlwraith, A.Z. Stasiak, A. Stasiak, A.R. Venkitaraman, and S.C. West. 2001. Role of BRCA2 in control of the RAD51 recombination and DNA repair protein. *Mol Cell*. 7:273-82.
- De Korte, D., W.A. Haverkort, D. Roos, H. Behrendt, and A.H. van Gennip. 1986. Imbalance in the ribonucleotide pools of lymphoid cells from acute lymphoblastic leukemia patients. *Leuk Res*. 10:389-96.
- de Laat, W.L., E. Appeldoorn, K. Sugawara, E. Weterings, N.G. Jaspers, and J.H. Hoeijmakers. 1998. DNA-binding polarity of human replication protein A positions nucleases in nucleotide excision repair. *Genes Dev*. 12:2598-609.
- de Laat, W.L., N.G. Jaspers, and J.H. Hoeijmakers. 1999. Molecular mechanism of nucleotide excision repair. *Genes Dev*. 13:768-85.
- de Murcia, J.M., C. Niedergang, C. Trucco, M. Ricoul, B. Dutrillaux, M. Mark, F.J. Oliver, M. Masson, A. Dierich, M. LeMeur, C. Walztinger, P. Chambon, and G. de Murcia. 1997. Requirement of poly(ADP-ribose) polymerase in recovery from DNA damage in mice and in cells. *Proc Natl Acad Sci U S A*. 94:7303-7.
- De Silva, I.U., P.J. McHugh, P.H. Clingen, and J.A. Hartley. 2000. Defining the roles of nucleotide excision repair and recombination in the repair of DNA interstrand cross-links in mammalian cells. *Mol Cell Biol*. 20:7980-90.
- Degan, P., S. Bonassi, M. De Caterina, L.G. Korkina, L. Pinto, F. Scopacasa, A. Zatterale, R. Calzone, and G. Pagano. 1995. In vivo accumulation of 8-hydroxy-2'-deoxyguanosine in DNA correlates with release of reactive oxygen species in Fanconi's anaemia families. *Carcinogenesis*. 16:735-41.
- Degrassi, F., R. De Salvia, C. Tanzarella, and F. Palitti. 1989. Induction of chromosomal aberrations and SCE by camptothecin, an inhibitor of mammalian topoisomerase I. *Mutat Res*. 211:125-30.
- Dillehay, L.E., D. Jacobson-Kram, and J.R. Williams. 1989. DNA topoisomerases and models of sister-chromatid exchange. *Mutat Res*. 215:15-23.
- Dominguez, I., N. Pastor, S. Mateos, and F. Cortes. 2001. Testing the SCE mechanism with non-poisoning topoisomerase II inhibitors. *Mutat Res*. 497:71-9.
- Dronkert, M.L., H.B. Beverloo, R.D. Johnson, J.H. Hoeijmakers, M. Jasin, and R. Kanaar. 2000. Mouse RAD54 affects DNA double-strand break repair and sister chromatid exchange. *Mol Cell Biol*. 20:3147-56.

- Drummond, J.T., G.M. Li, M.J. Longley, and P. Modrich. 1995. Isolation of an hMSH2-p160 heterodimer that restores DNA mismatch repair to tumor cells. *Science*. 268:1909-12.
- Edmunds, S.C., D.P. Kelsell, J.L. Hungerford, and I.A. Cree. 2002. Mutational analysis of selected genes in the TGFbeta, Wnt, pRb, and p53 pathways in primary uveal melanoma. *Invest Ophthalmol Vis Sci*. 43:2845-51.
- Ellis, N.A., J. Groden, T.Z. Ye, J. Straughen, D.J. Lennon, S. Ciocci, M. Proytcheva, and J. German. 1995. The Bloom's syndrome gene product is homologous to RecQ helicases. *Cell*. 83:655-66.
- Emi, N., T. Friedmann, and J.K. Yee. 1991. Pseudotype formation of murine leukemia virus with the G protein of vesicular stomatitis virus. *J Virol*. 65:1202-7.
- Evans, E., J.G. Moggs, J.R. Hwang, J.M. Egly, and R.D. Wood. 1997. Mechanism of open complex and dual incision formation by human nucleotide excision repair factors. *Embo J*. 16:6559-73.
- Fan, J., P.F. Wilson, H.K. Wong, S.S. Urbin, L.H. Thompson, and D.M. Wilson, 3rd. 2007. XRCC1 down-regulation in human cells leads to DNA-damaging agent hypersensitivity, elevated sister chromatid exchange, and reduced survival of BRCA2 mutant cells. *Environ Mol Mutagen*. 48:491-500.
- Fichtinger-Schepman, A.M., J.L. van der Veer, J.H. den Hartog, P.H. Lohman, and J. Reedijk. 1985. Adducts of the antitumor drug cis-diamminedichloroplatinum(II) with DNA: formation, identification, and quantitation. *Biochemistry*. 24:707-13.
- Fisher, L.A., M. Bessho, and T. Bessho. 2008. Processing of a psoralen DNA interstrand cross-link by XPF-ERCC1 complex in vitro. *J Biol Chem*. 283:1275-81.
- Fortini, P., E. Parlanti, O.M. Sidorkina, J. Laval, and E. Dogliotti. 1999. The type of DNA glycosylase determines the base excision repair pathway in mammalian cells. *J Biol Chem*. 274:15230-6.
- Friedberg, T., M.A. Grassow, and F. Oesch. 1990. Selective detection of mRNA forms encoding the major phenobarbital inducible cytochromes P450 and other members of the P450IIB family by the RNase A protection assay. *Arch Biochem Biophys*. 279:167-73.
- Fuller, L.F., and R.B. Painter. 1988. A Chinese hamster ovary cell line hypersensitive to ionizing radiation and deficient in repair replication. *Mutat Res*. 193:109-21.
- Gan, Y., Y. Mo, J.E. Kalns, J. Lu, K. Danenberg, P. Danenberg, M.G. Wientjes, and J.L. Au. 2001. Expression of DT-diaphorase and cytochrome P450 reductase correlates with mitomycin C activity in human bladder tumors. *Clin Cancer Res*. 7:1313-9.

- Garcia-Higuera, I., T. Taniguchi, S. Ganesan, M.S. Meyn, C. Timmers, J. Hejna, M. Grompe, and A.D. D'Andrea. 2001. Interaction of the Fanconi anemia proteins and BRCA1 in a common pathway. *Mol Cell*. 7:249-62.
- Genschel, J., and P. Modrich. 2003. Mechanism of 5'-directed excision in human mismatch repair. *Mol Cell*. 12:1077-86.
- Godthelp, B.C., F. Artwert, H. Joenje, and M.Z. Zdzienicka. 2002. Impaired DNA damage-induced nuclear Rad51 foci formation uniquely characterizes Fanconi anemia group D1. *Oncogene*. 21:5002-5.
- Godthelp, B.C., W.W. Wiegant, A. van Duijn-Goedhart, O.D. Scharer, P.P. van Buul, R. Kanaar, and M.Z. Zdzienicka. 2002. Mammalian Rad51C contributes to DNA cross-link resistance, sister chromatid cohesion and genomic stability. *Nucleic Acids Res*. 30:2172-82.
- Goyanes, V., J.L. Fernandez, S. Pereira, A. Campos, E. Rodriguez, M. Gonzalez, M. Rodriguez, O. Espido, and M. Garcia. 1994. Frequency of sister chromatid exchanges in humans at 14-16 week foetal stage and at birth. *Cytobios*. 77:67-72.
- Gradia, S., D. Subramanian, T. Wilson, S. Acharya, A. Makhov, J. Griffith, and R. Fishel. 1999. hMSH2-hMSH6 forms a hydrolysis-independent sliding clamp on mismatched DNA. *Mol Cell*. 3:255-61.
- Gragoudas, E.S., K.M. Egan, J.M. Seddon, R.J. Glynn, S.M. Walsh, S.M. Finn, J.E. Munzenrider, and M.D. Spar. 1991. Survival of patients with metastases from uveal melanoma. *Ophthalmology*. 98:383-9; discussion 390.
- Graham, F.L., J. Smiley, W.C. Russell, and R. Nairn. 1977. Characteristics of a human cell line transformed by DNA from human adenovirus type 5. *J Gen Virol*. 36:59-74.
- Grawunder, U., M. Wilm, X. Wu, P. Kulesza, T.E. Wilson, M. Mann, and M.R. Lieber. 1997. Activity of DNA ligase IV stimulated by complex formation with XRCC4 protein in mammalian cells. *Nature*. 388:492-5.
- Gu, L., Y. Hong, S. McCulloch, H. Watanabe, and G.M. Li. 1998. ATP-dependent interaction of human mismatch repair proteins and dual role of PCNA in mismatch repair. *Nucleic Acids Res*. 26:1173-8.
- Gupta, R., S. Sharma, J.A. Sommers, Z. Jin, S.B. Cantor, and R.M. Brosh, Jr. 2005. Analysis of the DNA substrate specificity of the human BACH1 helicase associated with breast cancer. *J Biol Chem*. 280:25450-60.
- Gupta, R., S. Sharma, J.A. Sommers, M.K. Kenny, S.B. Cantor, and R.M. Brosh, Jr. 2007. FANCF (BACH1) helicase forms DNA damage inducible foci with replication protein A and interacts physically and functionally with the single-stranded DNA-binding protein. *Blood*. 110:2390-8.

- Haaf, T., E.I. Golub, G. Reddy, C.M. Radding, and D.C. Ward. 1995. Nuclear foci of mammalian Rad51 recombination protein in somatic cells after DNA damage and its localization in synaptonemal complexes. *Proc Natl Acad Sci U S A*. 92:2298-302.
- Hanada, K., M. Budzowska, M. Modesti, A. Maas, C. Wyman, J. Essers, and R. Kanaar. 2006. The structure-specific endonuclease Mus81-Eme1 promotes conversion of interstrand DNA crosslinks into double-strands breaks. *Embo J*. 25:4921-32.
- Hazra, T.K., T. Izumi, L. Mardt, R.A. Floyd, and S. Mitra. 1998. The presence of two distinct 8-oxoguanine repair enzymes in human cells: their potential complementary roles in preventing mutation. *Nucleic Acids Res*. 26:5116-22.
- Heid, C.A., J. Stevens, K.J. Livak, and P.M. Williams. 1996. Real time quantitative PCR. *Genome Res*. 6:986-94.
- Helleday, T. 2003. Pathways for mitotic homologous recombination in mammalian cells. *Mutat Res*. 532:103-15.
- Hinz, J.M., P.B. Nham, E.P. Salazar, and L.H. Thompson. 2006. The Fanconi anemia pathway limits the severity of mutagenesis. *DNA Repair (Amst)*. 5:875-84.
- Hobbs, M.V., W.O. Weigle, D.J. Noonan, B.E. Torbett, R.J. McEvelly, R.J. Koch, G.J. Cardenas, and D.N. Ernst. 1993. Patterns of cytokine gene expression by CD4+ T cells from young and old mice. *J Immunol*. 150:3602-14.
- Hoegge, C., B. Pfander, G.L. Moldovan, G. Pyrowolakis, and S. Jentsch. 2002. RAD6-dependent DNA repair is linked to modification of PCNA by ubiquitin and SUMO. *Nature*. 419:135-41.
- Hoeijmakers, J.H.J. 2001. Genome maintenance mechanisms for preventing cancer. *Nature*. 411:366-374.
- Hoh, L. 2007. unpublished data.
- Hoskins, E.E., R.W. Gunawardena, K.B. Habash, T.M. Wise-Draper, M. Jansen, E.S. Knudsen, and S.I. Wells. 2008. Coordinate regulation of Fanconi anemia gene expression occurs through the Rb/E2F pathway. *Oncogene*. 27:4798-808.
- Houghtaling, S., C. Timmers, M. Noll, M.J. Finegold, S.N. Jones, M.S. Meyn, and M. Grompe. 2003. Epithelial cancer in Fanconi anemia complementation group D2 (Fancd2) knockout mice. *Genes Dev*. 17:2021-35.
- Howlett, N.G., J.A. Harney, M.A. Rego, F.W.t. Kolling, and T.W. Glover. 2009. Functional interaction between the Fanconi Anemia D2 protein and proliferating cell nuclear antigen (PCNA) via a conserved putative PCNA interaction motif. *J Biol Chem*. 284:28935-42.

- Howlett, N.G., T. Taniguchi, S.G. Durkin, A.D. D'Andrea, and T.W. Glover. 2005. The Fanconi anemia pathway is required for the DNA replication stress response and for the regulation of common fragile site stability. *Hum Mol Genet.* 14:693-701.
- Hsu, M.Y., Elder, D. E., Herlyn, M. 1999. Melanoma: The Wistar Institute (WM) cell lines. Kluwer Academic Publishers, Great Britain. 259 - 274 pp.
- Hussain, S., J.B. Wilson, A.L. Medhurst, J. Hejna, E. Witt, S. Ananth, A. Davies, J.Y. Masson, R. Moses, S.C. West, J.P. de Winter, A. Ashworth, N.J. Jones, and C.G. Mathew. 2004. Direct interaction of FANCD2 with BRCA2 in DNA damage response pathways. *Hum Mol Genet.* 13:1241-8.
- Illeni, M.T., D. Rovini, C. Grassi, C. Lombardo, M. Placucci, P. Squicciarini, N. Cascinelli, and A. Ghidoni. 1991. Sister chromatid exchange analysis in familial groups of malignant melanoma patients. *Cancer Genet Cytogenet.* 53:237-46.
- Ip, S.C., U. Rass, M.G. Blanco, H.R. Flynn, J.M. Skehel, and S.C. West. 2008. Identification of Holliday junction resolvases from humans and yeast. *Nature.* 456:357-61.
- Irizarry, R.A., C. Ladd-Acosta, B. Wen, Z. Wu, C. Montano, P. Onyango, H. Cui, K. Gabo, M. Rongione, M. Webster, H. Ji, J.B. Potash, S. Sabunciyan, and A.P. Feinberg. 2009. The human colon cancer methylome shows similar hypo- and hypermethylation at conserved tissue-specific CpG island shores. *Nat Genet.* 41:178-86.
- Ishiai, M., H. Kitao, A. Smogorzewska, J. Tomida, A. Kinomura, E. Uchida, A. Saberi, E. Kinoshita, E. Kinoshita-Kikuta, T. Koike, S. Tashiro, S.J. Elledge, and M. Takata. 2008. FANCI phosphorylation functions as a molecular switch to turn on the Fanconi anemia pathway. *Nat Struct Mol Biol.* 15:1138-46.
- Ishii, Y., and M.A. Bender. 1980. Effects of inhibitors of DNA synthesis on spontaneous and ultraviolet light-induced sister-chromatid exchanges in Chinese hamster cells. *Mutat Res.* 79:19-32.
- Iyer, V.N., and W. Szybalski. 1963. A Molecular Mechanism of Mitomycin Action: Linking of Complementary DNA Strands. *Proc Natl Acad Sci U S A.* 50:355-62.
- Jachymczyk, W.J., R.C. von Borstel, M.R. Mowat, and P.J. Hastings. 1981. Repair of interstrand cross-links in DNA of *Saccharomyces cerevisiae* requires two systems for DNA repair: the RAD3 system and the RAD51 system. *Mol Gen Genet.* 182:196-205.
- Jacobs, J.P., C.M. Jones, and J.P. Baille. 1970. Characteristics of a human diploid cell designated MRC-5. *Nature.* 227:168-70.
- Jansen, J.G., A. Tsaalbi-Shtylik, P. Langerak, F. Calleja, C.M. Meijers, H. Jacobs, and N. de Wind. 2005. The BRCT domain of mammalian Rev1 is involved in regulating DNA translesion synthesis. *Nucleic Acids Res.* 33:356-65.

- Jenner, T.J., C.M. deLara, P. O'Neill, and D.L. Stevens. 1993. Induction and rejoining of DNA double-strand breaks in V79-4 mammalian cells following gamma- and alpha-irradiation. *Int J Radiat Biol.* 64:265-73.
- Jung, E.G., E. Bohnert, and H. Boonen. 1986. Dysplastic nevus syndrome: ultraviolet hypermutability confirmed in vitro by elevated sister chromatid exchanges. *Dermatologica.* 173:297-300.
- Kannouche, P.L., and A.R. Lehmann. 2004. Ubiquitination of PCNA and the polymerase switch in human cells. *Cell Cycle.* 3:1011-3.
- Karow, J.K., A. Constantinou, J.L. Li, S.C. West, and I.D. Hickson. 2000. The Bloom's syndrome gene product promotes branch migration of holliday junctions. *Proc Natl Acad Sci U S A.* 97:6504-8.
- Kato, H. 1973. Induction of sister chromatid exchanges by UV light and its inhibition by caffeine. *Exp Cell Res.* 82:383-90.
- Kato, H. 1974. Possible role of DNA synthesis in formation of sister chromatid exchanges. *Nature.* 252:739-41.
- Kato, H. 1977. Spontaneous and induced sister chromatid exchanges as revealed by the BUdR-labeling method. *Int Rev Cytol.* 49:55-97.
- Kato, H., and H.F. Stich. 1976. Sister chromatid exchanges in ageing and repair-deficient human fibroblasts. *Nature.* 260:447-8.
- Kee, Y., J.M. Kim, and A.D. D'Andrea. 2009. Regulated degradation of FANCM in the Fanconi anemia pathway during mitosis. *Genes Dev.* 23:555-60.
- Kim, J.M., Y. Kee, A. Gurtan, and A.D. D'Andrea. 2008. Cell cycle-dependent chromatin loading of the Fanconi anemia core complex by FANCM/FAAP24. *Blood.* 111:5215-22.
- Kim, M.K., S. Zitzmann, F. Westermann, K. Arnold, S. Brouwers, M. Schwab, and L. Savelyeva. 2004. Increased rates of spontaneous sister chromatid exchange in lymphocytes of BRCA2 \pm carriers of familial breast cancer clusters. *Cancer Lett.* 210:85-94.
- Knees-Matzen, S., M. Roser, U. Reimers, U. Ehlert, M. Weichenthal, E.W. Breitbart, and H.W. Rudiger. 1991. Increased UV-induced sister-chromatid exchange in cultured fibroblasts of first-degree relatives of melanoma patients. *Cancer Genet Cytogenet.* 53:265-70.
- Kok, K., S.L. Naylor, and C.H. Buys. 1997. Deletions of the short arm of chromosome 3 in solid tumors and the search for suppressor genes. *Adv Cancer Res.* 71:27-92.

- Kokoska, R.J., L. Stefanovic, A.B. Buermeyer, R.M. Liskay, and T.D. Petes. 1999. A mutation of the yeast gene encoding PCNA destabilizes both microsatellite and minisatellite DNA sequences. *Genetics*. 151:511-9.
- Kolodner, R.D., and G.T. Marsischky. 1999. Eukaryotic DNA mismatch repair. *Curr Opin Genet Dev*. 9:89-96.
- Korenberg, J.R., and E.F. Freedlender. 1974. Giemsa technique for the detection of sister chromatid exchanges. *Chromosoma*. 48:355-60.
- Kruyt, F.A., T. Hoshino, J.M. Liu, P. Joseph, A.K. Jaiswal, and H. Youssoufian. 1998. Abnormal microsomal detoxification implicated in Fanconi anemia group C by interaction of the FAC protein with NADPH cytochrome P450 reductase. *Blood*. 92:3050-6.
- Kuluncsics, Z., D. Perdiz, E. Brulay, B. Muel, and E. Sage. 1999. Wavelength dependence of ultraviolet-induced DNA damage distribution: involvement of direct or indirect mechanisms and possible artefacts. *J Photochem Photobiol B*. 49:71-80.
- Kumaresan, K.R., M. Hwang, M.P. Thelen, and M.W. Lambert. 2002. Contribution of XPF functional domains to the 5' and 3' incisions produced at the site of a psoralen interstrand cross-link. *Biochemistry*. 41:890-6.
- Latt, S.A. 1973. Microfluorometric detection of deoxyribonucleic acid replication in human metaphase chromosomes. *Proc Natl Acad Sci U S A*. 70:3395-9.
- Latt, S.A., and R.R. Schreck. 1980. Sister chromatid exchange analysis. *Am J Hum Genet*. 32:297-313.
- Latt, S.A., G. Stetten, L.A. Juergens, G.R. Buchanan, and P.S. Gerald. 1975. Induction by alkylating agents of sister chromatid exchanges and chromatid breaks in Fanconi's anemia. *Proc Natl Acad Sci U S A*. 72:4066-70.
- Le Page, F., E.E. Kwoh, A. Avrutskaya, A. Gentil, S.A. Leadon, A. Sarasin, and P.K. Cooper. 2000. Transcription-coupled repair of 8-oxoguanine: requirement for XPG, TFIIF, and CSB and implications for Cockayne syndrome. *Cell*. 101:159-71.
- Lee, J.W., L. Blanco, T. Zhou, M. Garcia-Diaz, K. Bebenek, T.A. Kunkel, Z. Wang, and L.F. Povirk. 2004. Implication of DNA polymerase lambda in alignment-based gap filling for nonhomologous DNA end joining in human nuclear extracts. *J Biol Chem*. 279:805-11.
- Lewis, D.F., and J.M. Pratt. 1998. The P450 catalytic cycle and oxygenation mechanism. *Drug Metab Rev*. 30:739-86.

- Liang, F., M. Han, P.J. Romanienko, and M. Jasin. 1998. Homology-directed repair is a major double-strand break repair pathway in mammalian cells. *Proc Natl Acad Sci U S A.* 95:5172-7.
- Lindahl, T. 1979. DNA glycosylases, endonucleases for apurinic/aprimidinic sites, and base excision-repair. *Prog Nucleic Acid Res Mol Biol.* 22:135-92.
- Lindahl, T. 1993. Instability and decay of the primary structure of DNA. *Nature.* 362:709-15.
- Lindahl-Kiessling, K., I. Karlberg, and A.M. Olofsson. 1989. Induction of sister-chromatid exchanges by direct and indirect mutagens in human lymphocytes, co-cultured with intact rat liver cells. Effect of enzyme induction and preservation of the liver cells by freezing in liquid nitrogen. *Mutat Res.* 211:77-87.
- Ling, C., M. Ishiai, A.M. Ali, A.L. Medhurst, K. Neveling, R. Kalb, Z. Yan, Y. Xue, A.B. Oostra, A.D. Auerbach, M.E. Hoatlin, D. Schindler, H. Joenje, J.P. de Winter, M. Takata, A.R. Meetei, and W. Wang. 2007. FAAP100 is essential for activation of the Fanconi anemia-associated DNA damage response pathway. *Embo J.* 26:2104-14.
- Liu, L.F., T.C. Rowe, L. Yang, K.M. Tewey, and G.L. Chen. 1983. Cleavage of DNA by mammalian DNA topoisomerase II. *J Biol Chem.* 258:15365-70.
- Livak, K.J., and T.D. Schmittgen. 2001. Analysis of relative gene expression data using real-time quantitative PCR and the 2(-Delta Delta C(T)) Method. *Methods.* 25:402-8.
- Lundin, C., K. Erixon, C. Arnaudeau, N. Schultz, D. Jenssen, M. Meuth, and T. Helleday. 2002. Different roles for nonhomologous end joining and homologous recombination following replication arrest in mammalian cells. *Mol Cell Biol.* 22:5869-78.
- Luria, S.E., and M. Delbruck. 1943. Mutations of Bacteria from Virus Sensitivity to Virus Resistance. *Genetics.* 28:491-511.
- Ma, Y., U. Pannicke, K. Schwarz, and M.R. Lieber. 2002. Hairpin opening and overhang processing by an Artemis/DNA-dependent protein kinase complex in nonhomologous end joining and V(D)J recombination. *Cell.* 108:781-94.
- Maat, W., P.A. van der Velden, C. Out-Luiting, M. Plug, A. Dirks-Mulder, M.J. Jager, and N.A. Gruis. 2007. Epigenetic inactivation of RASSF1a in uveal melanoma. *Invest Ophthalmol Vis Sci.* 48:486-90.
- Machida, Y.J., Y. Machida, Y. Chen, A.M. Gurtan, G.M. Kupfer, A.D. D'Andrea, and A. Dutta. 2006. UBE2T is the E2 in the Fanconi anemia pathway and undergoes negative autoregulation. *Mol Cell.* 23:589-96.

- Mahajan, K.N., L. Gangi-Peterson, D.H. Sorscher, J. Wang, K.N. Gathy, N.P. Mahajan, W.H. Reeves, and B.S. Mitchell. 1999. Association of terminal deoxynucleotidyl transferase with Ku. *Proc Natl Acad Sci U S A.* 96:13926-31.
- Mahajan, K.N., S.A. Nick McElhinny, B.S. Mitchell, and D.A. Ramsden. 2002. Association of DNA polymerase mu (pol mu) with Ku and ligase IV: role for pol mu in end-joining double-strand break repair. *Mol Cell Biol.* 22:5194-202.
- Mari, P.O., B.I. Florea, S.P. Persengiev, N.S. Verkaik, H.T. Bruggenwirth, M. Modesti, G. Giglia-Mari, K. Bezstarosti, J.A. Demmers, T.M. Luider, A.B. Houtsmuller, and D.C. van Gent. 2006. Dynamic assembly of end-joining complexes requires interaction between Ku70/80 and XRCC4. *Proc Natl Acad Sci U S A.* 103:18597-602.
- McCabe, K.M., A. Hemphill, Y. Akkari, P.M. Jakobs, D. Pauw, S.B. Olson, R.E. Moses, and M. Grompe. 2008. ERCC1 is required for FANCD2 focus formation. *Mol Genet Metab.* 95:66-73.
- McLean, I.W., W.D. Foster, and L.E. Zimmerman. 1982. Uveal melanoma: location, size, cell type, and enucleation as risk factors in metastasis. *Hum Pathol.* 13:123-32.
- McPherson, J.P., B. Lemmers, R. Chahwan, A. Pamidi, E. Migon, E. Matysiak-Zablocki, M.E. Moynahan, J. Essers, K. Hanada, A. Poonepalli, O. Sanchez-Sweatman, R. Khokha, R. Kanaar, M. Jasin, M.P. Hande, and R. Hakem. 2004. Involvement of mammalian Mus81 in genome integrity and tumor suppression. *Science.* 304:1822-6.
- Medhurst, A.L., H. Laghmani el, J. Steltenpool, M. Ferrer, C. Fontaine, J. de Groot, M.A. Rooimans, R.J. Scheper, A.R. Meetei, W. Wang, H. Joenje, and J.P. de Winter. 2006. Evidence for subcomplexes in the Fanconi anemia pathway. *Blood.* 108:2072-80.
- Meek, K., P. Douglas, X. Cui, Q. Ding, and S.P. Lees-Miller. 2007. trans Autophosphorylation at DNA-dependent protein kinase's two major autophosphorylation site clusters facilitates end processing but not end joining. *Mol Cell Biol.* 27:3881-90.
- Meetei, A.R., J.P. de Winter, A.L. Medhurst, M. Wallisch, Q. Waisfisz, H.J. van de Vrugt, A.B. Oostra, Z. Yan, C. Ling, C.E. Bishop, M.E. Hoatlin, H. Joenje, and W. Wang. 2003. A novel ubiquitin ligase is deficient in Fanconi anemia. *Nat Genet.* 35:165-70.
- Meetei, A.R., A.L. Medhurst, C. Ling, Y. Xue, T.R. Singh, P. Bier, J. Steltenpool, S. Stone, I. Dokal, C.G. Mathew, M. Hoatlin, H. Joenje, J.P. de Winter, and W. Wang. 2005. A human ortholog of archaeal DNA repair protein Hef is defective in Fanconi anemia complementation group M. *Nat Genet.* 37:958-63.

- Mello Filho, A.C., and R. Meneghini. 1984. In vivo formation of single-strand breaks in DNA by hydrogen peroxide is mediated by the Haber-Weiss reaction. *Biochim Biophys Acta*. 781:56-63.
- Meschini, R., R. Bastianelli, and F. Palitti. 1996. The diplochromosome of endoreduplicated cells: a new approach to highlight the mechanism of sister chromatid exchange. *Chromosoma*. 105:50-4.
- Mimitou, E.P., and L.S. Symington. 2009. DNA end resection: many nucleases make light work. *DNA Repair (Amst)*. 8:983-95.
- Mimori, T., and J.A. Hardin. 1986. Mechanism of interaction between Ku protein and DNA. *J Biol Chem*. 261:10375-9.
- Miranda, M., C. Ligas, F. Amicarelli, E. D'Alessandro, F. Brisdelli, O. Zarivi, and A. Poma. 1997. Sister chromatid exchange (SCE) rates in human melanoma cells as an index of mutagenesis. *Mutagenesis*. 12:233-6.
- Mirchandani, K.D., and A.D. D'Andrea. 2006. The Fanconi anemia/BRCA pathway: a coordinator of cross-link repair. *Exp Cell Res*. 312:2647-53.
- Mirchandani, K.D., R.M. McCaffrey, and A.D. D'Andrea. 2008. The Fanconi anemia core complex is required for efficient point mutagenesis and Rev1 foci assembly. *DNA Repair (Amst)*. 7:902-11.
- Mitchell, D.L., C.A. Haipek, and J.M. Clarkson. 1985. (6-4)Photoproducts are removed from the DNA of UV-irradiated mammalian cells more efficiently than cyclobutane pyrimidine dimers. *Mutat Res*. 143:109-12.
- Modesti, M., J.E. Hesse, and M. Gellert. 1999. DNA binding of Xrcc4 protein is associated with V(D)J recombination but not with stimulation of DNA ligase IV activity. *Embo J*. 18:2008-18.
- Mohindra, A., L.E. Hays, E.N. Phillips, B.D. Preston, T. Helleday, and M. Meuth. 2002. Defects in homologous recombination repair in mismatch-repair-deficient tumour cell lines. *Hum Mol Genet*. 11:2189-200.
- Moldovan, G.L., and A.D. D'Andrea. 2009. How the Fanconi Anemia Pathway Guards the Genome. *Annu Rev Genet*.
- Moldovan, G.L., M.V. Madhavan, K.D. Mirchandani, R.M. McCaffrey, P. Vinciguerra, and A.D. D'Andrea. 2010. DNA polymerase POLN participates in cross-link repair and homologous recombination. *Mol Cell Biol*. 30:1088-96.
- Mosedale, G., W. Niedzwiedz, A. Alpi, F. Perrina, J.B. Pereira-Leal, M. Johnson, F. Langevin, P. Pace, and K.J. Patel. 2005. The vertebrate Hef ortholog is a component of the Fanconi anemia tumor-suppressor pathway. *Nat Struct Mol Biol*. 12:763-71.

- Moser, J., H. Kool, I. Giakzidis, K. Caldecott, L.H. Mullenders, and M.I. Fousteri. 2007. Sealing of chromosomal DNA nicks during nucleotide excision repair requires XRCC1 and DNA ligase III alpha in a cell-cycle-specific manner. *Mol Cell*. 27:311-23.
- Mulligan, R.C. 1993. The basic science of gene therapy. *Science*. 260:926-32.
- Nagasawa, H., D. Fornace, and J.B. Little. 1983. Induction of sister-chromatid exchanges by DNA-damaging agents and 12-O-tetradecanoyl-phorbol-13-acetate (TPA) in synchronous Chinese hamster ovary (CHO) cells. *Mutat Res*. 107:315-27.
- Nair, V., C.S. Cooper, D.E. Vietti, and G.A. Turner. 1986. The chemistry of lipid peroxidation metabolites: crosslinking reactions of malondialdehyde. *Lipids*. 21:6-10.
- Nakanishi, K., T. Taniguchi, V. Ranganathan, H.V. New, L.A. Moreau, M. Stotsky, C.G. Mathew, M.B. Kastan, D.T. Weaver, and A.D. D'Andrea. 2002. Interaction of FANCD2 and NBS1 in the DNA damage response. *Nat Cell Biol*. 4:913-20.
- Niedernhofer, L.J., J.S. Daniels, C.A. Rouzer, R.E. Greene, and L.J. Marnett. 2003. Malondialdehyde, a product of lipid peroxidation, is mutagenic in human cells. *J Biol Chem*. 278:31426-33.
- Niedzwiedz, W., G. Mosedale, M. Johnson, C.Y. Ong, P. Pace, and K.J. Patel. 2004. The Fanconi anaemia gene FANCC promotes homologous recombination and error-prone DNA repair. *Mol Cell*. 15:607-20.
- Nijman, S.M., T.T. Huang, A.M. Dirac, T.R. Brummelkamp, R.M. Kerkhoven, A.D. D'Andrea, and R. Bernards. 2005. The deubiquitinating enzyme USP1 regulates the Fanconi anemia pathway. *Mol Cell*. 17:331-9.
- Nimonkar, A.V., R.A. Sica, and S.C. Kowalczykowski. 2009. Rad52 promotes second-end DNA capture in double-stranded break repair to form complement-stabilized joint molecules. *Proc Natl Acad Sci U S A*. 106:3077-82.
- Norppa, H., S. Bonassi, I.L. Hansteen, L. Hagmar, U. Stromberg, P. Rossner, P. Boffetta, C. Lindholm, S. Gundy, J. Lazutka, A. Cebulska-Wasilewska, E. Fabianova, R.J. Sram, L.E. Knudsen, R. Barale, and A. Fucic. 2006. Chromosomal aberrations and SCEs as biomarkers of cancer risk. *Mutat Res*. 600:37-45.
- O'Dwyer, P.J., R.P. Perez, K.S. Yao, A.K. Godwin, and T.C. Hamilton. 1996. Increased DT-diaphorase expression and cross-resistance to mitomycin C in a series of cisplatin-resistant human ovarian cancer cell lines. *Biochem Pharmacol*. 52:21-7.
- Ohashi, A., M.Z. Zdzienicka, J. Chen, and F.J. Couch. 2005. Fanconi anemia complementation group D2 (FANCD2) functions independently of BRCA2- and

- RAD51-associated homologous recombination in response to DNA damage. *J Biol Chem.* 280:14877-83.
- Okada, T., E. Sonoda, M. Yoshimura, Y. Kawano, H. Saya, M. Kohzaki, and S. Takeda. 2005. Multiple roles of vertebrate REV genes in DNA repair and recombination. *Mol Cell Biol.* 25:6103-11.
- Olive, P.L., J.P. Banath, and R.E. Durand. 1990. Heterogeneity in radiation-induced DNA damage and repair in tumor and normal cells measured using the "comet" assay. *Radiat Res.* 122:86-94.
- Onken, M.D., J.P. Ehlers, L.A. Worley, J. Makita, Y. Yokota, and J.W. Harbour. 2006. Functional gene expression analysis uncovers phenotypic switch in aggressive uveal melanomas. *Cancer Res.* 66:4602-9.
- Ory, D.S., B.A. Neugeboren, and R.C. Mulligan. 1996. A stable human-derived packaging cell line for production of high titer retrovirus/vesicular stomatitis virus G pseudotypes. *Proc Natl Acad Sci U S A.* 93:11400-6.
- Ostling, O., and K.J. Johanson. 1984. Microelectrophoretic study of radiation-induced DNA damages in individual mammalian cells. *Biochem Biophys Res Commun.* 123:291-8.
- Pace, P., G. Mosedale, M.R. Hodskinson, I.V. Rosado, M. Sivasubramaniam, and K.J. Patel. 2010. Ku70 corrupts DNA repair in the absence of the Fanconi anemia pathway. *Science.* 329:219-23.
- Painter, R.B. 1980. A replication model for sister-chromatid exchange. *Mutat Res.* 70:337-41.
- Palombo, F., I. Iaccarino, E. Nakajima, M. Ikejima, T. Shimada, and J. Jiricny. 1996. hMutSbeta, a heterodimer of hMSH2 and hMSH3, binds to insertion/deletion loops in DNA. *Curr Biol.* 6:1181-4.
- Parrella, P., V.M. Fazio, A.P. Gallo, D. Sidransky, and S.L. Merbs. 2003. Fine mapping of chromosome 3 in uveal melanoma: identification of a minimal region of deletion on chromosomal arm 3p25.1-p25.2. *Cancer Res.* 63:8507-10.
- Paull, T.T., and M. Gellert. 1998. The 3' to 5' exonuclease activity of Mre 11 facilitates repair of DNA double-strand breaks. *Mol Cell.* 1:969-79.
- Paull, T.T., and J.H. Lee. 2005. The Mre11/Rad50/Nbs1 complex and its role as a DNA double-strand break sensor for ATM. *Cell Cycle.* 4:737-40.
- Perry, P., and H.J. Evans. 1975. Cytological detection of mutagen-carcinogen exposure by sister chromatid exchange. *Nature.* 258:121-5.
- Perry, P., and S. Wolff. 1974. New Giemsa method for the differential staining of sister chromatids. *Nature.* 251:156-8.

- Perticone, P., R. Cozzi, and B. Gustavino. 1987. Sister chromatid exchanges induced by DNA demethylating agents persist through several cell cycles in mammalian cells. *Carcinogenesis*. 8:1059-63.
- Petukhova, G., S. Stratton, and P. Sung. 1998. Catalysis of homologous DNA pairing by yeast Rad51 and Rad54 proteins. *Nature*. 393:91-4.
- Pichierri, P., D. Averbeck, and F. Rosselli. 2002. DNA cross-link-dependent RAD50/MRE11/NBS1 subnuclear assembly requires the Fanconi anemia C protein. *Hum Mol Genet*. 11:2531-46.
- Pichierri, P., and F. Rosselli. 2004. The DNA crosslink-induced S-phase checkpoint depends on ATR-CHK1 and ATR-NBS1-FANCD2 pathways. *Embo J*. 23:1178-87.
- Pommier, Y., L.A. Zwellung, C.S. Kao-Shan, J. Whang-Peng, and M.O. Bradley. 1985. Correlations between intercalator-induced DNA strand breaks and sister chromatid exchanges, mutations, and cytotoxicity in Chinese hamster cells. *Cancer Res*. 45:3143-9.
- Ponten, J., and E. Saksela. 1967. Two established in vitro cell lines from human mesenchymal tumours. *Int J Cancer*. 2:434-47.
- Prescher, G., N. Bornfeld, H. Hirche, B. Horsthemke, K.H. Jockel, and R. Becher. 1996. Prognostic implications of monosomy 3 in uveal melanoma. *Lancet*. 347:1222-5.
- Prescher, G., N. Bornfeld, B. Horsthemke, and R. Becher. 1992. Chromosomal aberrations defining uveal melanoma of poor prognosis. *Lancet*. 339:691-2.
- Puebla-Osorio, N., D.B. Lacey, F.W. Alt, and C. Zhu. 2006. Early embryonic lethality due to targeted inactivation of DNA ligase III. *Mol Cell Biol*. 26:3935-41.
- Qiao, F., J. Mi, J.B. Wilson, G. Zhi, N.R. Bucheimer, N.J. Jones, and G.M. Kupfer. 2004. Phosphorylation of fanconi anemia (FA) complementation group G protein, FANCG, at serine 7 is important for function of the FA pathway. *J Biol Chem*. 279:46035-45.
- Radman, M. 1975. SOS repair hypothesis: phenomenology of an inducible DNA repair which is accompanied by mutagenesis. *Basic Life Sci*. 5A:355-67.
- Ralf, C., I.D. Hickson, and L. Wu. 2006. The Bloom's syndrome helicase can promote the regression of a model replication fork. *J Biol Chem*. 281:22839-46.
- Ramilo, C., L. Gu, S. Guo, X. Zhang, S.M. Patrick, J.J. Turchi, and G.M. Li. 2002. Partial reconstitution of human DNA mismatch repair in vitro: characterization of the role of human replication protein A. *Mol Cell Biol*. 22:2037-46.

- Raschle, M., P. Knipscheer, M. Enoiu, T. Angelov, J. Sun, J.D. Griffith, T.E. Ellenberger, O.D. Scharer, and J.C. Walter. 2008. Mechanism of replication-coupled DNA interstrand crosslink repair. *Cell*. 134:969-80.
- Richardson, C., and M. Jasin. 2000. Coupled homologous and nonhomologous repair of a double-strand break preserves genomic integrity in mammalian cells. *Mol Cell Biol*. 20:9068-75.
- Robertson, K.D. 2002. DNA methylation and chromatin - unraveling the tangled web. *Oncogene*. 21:5361-79.
- Rogakou, E.P., D.R. Pilch, A.H. Orr, V.S. Ivanova, and W.M. Bonner. 1998. DNA double-stranded breaks induce histone H2AX phosphorylation on serine 139. *J Biol Chem*. 273:5858-68.
- Roy, S.K., A.H. Trivedi, S.R. Bakshi, R.K. Patel, P.H. Shukla, S.J. Patel, J.M. Bhatavdekar, D.D. Patel, and P.M. Shah. 2000. Spontaneous chromosomal instability in breast cancer families. *Cancer Genet Cytogenet*. 118:52-6.
- Rudland, P.S., A.M. Platt-Higgins, L.M. Davies, S. de Silva Rudland, J.B. Wilson, A. Aladwani, J.H. Winstanley, D.L. Barraclough, R. Barraclough, C.R. West, and N.J. Jones. 2010. Significance of the Fanconi Anemia FANCD2 Protein in Sporadic and Metastatic Human Breast Cancer. *Am J Pathol*. 176.
- Saiki, R.K., S. Scharf, F. Faloona, K.B. Mullis, G.T. Horn, H.A. Erlich, and N. Arnheim. 1985. Enzymatic amplification of beta-globin genomic sequences and restriction site analysis for diagnosis of sickle cell anemia. *Science*. 230:1350-4.
- Saleh-Gohari, N., H.E. Bryant, N. Schultz, K.M. Parker, T.N. Cassel, and T. Helleday. 2005. Spontaneous homologous recombination is induced by collapsed replication forks that are caused by endogenous DNA single-strand breaks. *Mol Cell Biol*. 25:7158-69.
- Sancar, A., and J.E. Hearst. 1993. Molecular matchmakers. *Science*. 259:1415-20.
- Sargent, R.G., M.A. Brenneman, and J.H. Wilson. 1997. Repair of site-specific double-strand breaks in a mammalian chromosome by homologous and illegitimate recombination. *Mol Cell Biol*. 17:267-77.
- Scotto, J., J.F. Fraumeni, Jr., and J.A. Lee. 1976. Melanomas of the eye and other noncutaneous sites: epidemiologic aspects. *J Natl Cancer Inst*. 56:489-91.
- Serrano, M., G.J. Hannon, and D. Beach. 1993. A new regulatory motif in cell-cycle control causing specific inhibition of cyclin D/CDK4. *Nature*. 366:704-7.
- Shafer, D.A. 1977. Replication bypass model of sister chromatid exchanges and implications for Bloom's syndrome and Fanconi's anemia. *Hum Genet*. 39:177-90.

- Shen, H.M., C.Y. Shi, Y. Shen, and C.N. Ong. 1996. Detection of elevated reactive oxygen species level in cultured rat hepatocytes treated with aflatoxin B1. *Free Radic Biol Med.* 21:139-46.
- Shields, C.L., J.A. Shields, M. Materin, E. Gershenbaum, A.D. Singh, and A. Smith. 2001. Iris melanoma: risk factors for metastasis in 169 consecutive patients. *Ophthalmology.* 108:172-8.
- Shields, J.A., C.L. Shields, and L.A. Donoso. 1991. Management of posterior uveal melanoma. *Surv Ophthalmol.* 36:161-95.
- Siegel, D., H. Beall, C. Senekowitsch, M. Kasai, H. Arai, N.W. Gibson, and D. Ross. 1992. Bioreductive activation of mitomycin C by DT-diaphorase. *Biochemistry.* 31:7879-85.
- Siegel, D., N.W. Gibson, P.C. Preusch, and D. Ross. 1990. Metabolism of mitomycin C by DT-diaphorase: role in mitomycin C-induced DNA damage and cytotoxicity in human colon carcinoma cells. *Cancer Res.* 50:7483-9.
- Siehler, S.Y., M. Schrauder, U. Gerischer, S. Cantor, G. Marra, and L. Wiesmuller. 2009. Human MutL-complexes monitor homologous recombination independently of mismatch repair. *DNA Repair (Amst).* 8:242-52.
- Simpson, L.J., and J.E. Sale. 2003. Rev1 is essential for DNA damage tolerance and non-templated immunoglobulin gene mutation in a vertebrate cell line. *Embo J.* 22:1654-64.
- Singh, A.D., and A. Topham. 2003. Incidence of uveal melanoma in the United States: 1973-1997. *Ophthalmology.* 110:956-61.
- Singh, A.D., and A. Topham. 2003. Survival rates with uveal melanoma in the United States: 1973-1997. *Ophthalmology.* 110:962-5.
- Singh, N.P., M.T. McCoy, R.R. Tice, and E.L. Schneider. 1988. A simple technique for quantitation of low levels of DNA damage in individual cells. *Exp Cell Res.* 175:184-91.
- Singleton, M.R., L.M. Wentzell, Y. Liu, S.C. West, and D.B. Wigley. 2002. Structure of the single-strand annealing domain of human RAD52 protein. *Proc Natl Acad Sci U S A.* 99:13492-7.
- Sisley, K. 1996. unpublished data.
- Sisley, K., M.A. Parsons, J. Garnham, A.M. Potter, D. Curtis, R.C. Rees, and I.G. Rennie. 2000. Association of specific chromosome alterations with tumour phenotype in posterior uveal melanoma. *Br J Cancer.* 82:330-8.

- Sisley, K., I.G. Rennie, D.W. Cottam, A.M. Potter, C.W. Potter, and R.C. Rees. 1990. Cytogenetic findings in six posterior uveal melanomas: involvement of chromosomes 3, 6, and 8. *Genes Chromosomes Cancer*. 2:205-9.
- Sisley, K., I.G. Rennie, M.A. Parsons, R. Jacques, D.W. Hammond, S.M. Bell, A.M. Potter, and R.C. Rees. 1997. Abnormalities of chromosomes 3 and 8 in posterior uveal melanoma correlate with prognosis. *Genes Chromosomes Cancer*. 19:22-8.
- Smiraldo, P.G., A.M. Gruver, J.C. Osborn, and D.L. Pittman. 2005. Extensive chromosomal instability in Rad51d-deficient mouse cells. *Cancer Res*. 65:2089-96.
- Smogorzewska, A., S. Matsuoka, P. Vinciguerra, E.R. McDonald, 3rd, K.E. Hurov, J. Luo, B.A. Ballif, S.P. Gygi, K. Hofmann, A.D. D'Andrea, and S.J. Elledge. 2007. Identification of the FANCI protein, a monoubiquitinated FANCD2 paralog required for DNA repair. *Cell*. 129:289-301.
- Sobol, R.W., J.K. Horton, R. Kuhn, H. Gu, R.K. Singhal, R. Prasad, K. Rajewsky, and S.H. Wilson. 1996. Requirement of mammalian DNA polymerase-beta in base-excision repair. *Nature*. 379:183-6.
- Sonoda, E., M.S. Sasaki, C. Morrison, Y. Yamaguchi-Iwai, M. Takata, and S. Takeda. 1999. Sister chromatid exchanges are mediated by homologous recombination in vertebrate cells. *Mol Cell Biol*. 19:5166-9.
- Stetka, D.G., Jr. 1979. Further analysis of the replication bypass model for sister chromatid exchange. *Hum Genet*. 49:63-9.
- Strathdee, C.A., H. Gavish, W.R. Shannon, and M. Buchwald. 1992. Cloning of cDNAs for Fanconi's anaemia by functional complementation. *Nature*. 356:763-7.
- Sugasawa, K., T. Okamoto, Y. Shimizu, C. Masutani, S. Iwai, and F. Hanaoka. 2001. A multistep damage recognition mechanism for global genomic nucleotide excision repair. *Genes Dev*. 15:507-21.
- Sugiyama, T., J.H. New, and S.C. Kowalczykowski. 1998. DNA annealing by RAD52 protein is stimulated by specific interaction with the complex of replication protein A and single-stranded DNA. *Proc Natl Acad Sci U S A*. 95:6049-54.
- Suresh Kumar, G., R. Lipman, J. Cummings, and M. Tomasz. 1997. Mitomycin C-DNA adducts generated by DT-diaphorase. Revised mechanism of the enzymatic reductive activation of mitomycin C. *Biochemistry*. 36:14128-36.
- Surtees, J.A., J.L. Argueso, and E. Alani. 2004. Mismatch repair proteins: key regulators of genetic recombination. *Cytogenet Genome Res*. 107:146-59.
- Takata, M., M.S. Sasaki, S. Tachiiri, T. Fukushima, E. Sonoda, D. Schild, L.H. Thompson, and S. Takeda. 2001. Chromosome instability and defective

- recombinational repair in knockout mutants of the five Rad51 paralogs. *Mol Cell Biol.* 21:2858-66.
- Taniguchi, T., I. Garcia-Higuera, P.R. Andreassen, R.C. Gregory, M. Grompe, and A.D. D'Andrea. 2002. S-phase-specific interaction of the Fanconi anemia protein, FANCD2, with BRCA1 and RAD51. *Blood.* 100:2414-20.
- Tateishi, S., H. Niwa, J. Miyazaki, S. Fujimoto, H. Inoue, and M. Yamaizumi. 2003. Enhanced genomic instability and defective postreplication repair in RAD18 knockout mouse embryonic stem cells. *Mol Cell Biol.* 23:474-81.
- Taylor, J.H. 1958. Sister Chromatid Exchanges in Tritium-Labeled Chromosomes. *Genetics.* 43:515-29.
- Tebbs, R.S., J.M. Hinz, N.A. Yamada, J.B. Wilson, E.P. Salazar, C.B. Thomas, I.M. Jones, N.J. Jones, and L.H. Thompson. 2005. New insights into the Fanconi anemia pathway from an isogenic FancG hamster CHO mutant. *DNA Repair (Amst).* 4:11-22.
- Thompson, L.H. 2005. Unraveling the Fanconi anemia-DNA repair connection. *Nat Genet.* 37:921-2.
- Thompson, L.H., K.W. Brookman, L.E. Dillehay, A.V. Carrano, J.A. Mazrimas, C.L. Mooney, and J.L. Minkler. 1982. A CHO-cell strain having hypersensitivity to mutagens, a defect in DNA strand-break repair, and an extraordinary baseline frequency of sister-chromatid exchange. *Mutat Res.* 95:427-40.
- Timmers, C., T. Taniguchi, J. Hejna, C. Reifsteck, L. Lucas, D. Bruun, M. Thayer, B. Cox, S. Olson, A.D. D'Andrea, R. Moses, and M. Grompe. 2001. Positional cloning of a novel Fanconi anemia gene, FANCD2. *Mol Cell.* 7:241-8.
- Tomasz, M., D. Chowdary, R. Lipman, S. Shimotakahara, D. Veiro, V. Walker, and G.L. Verdine. 1986. Reaction of DNA with chemically or enzymatically activated mitomycin C: isolation and structure of the major covalent adduct. *Proc Natl Acad Sci U S A.* 83:6702-6.
- Tomasz, M., and R. Lipman. 1981. Reductive metabolism and alkylating activity of mitomycin C induced by rat liver microsomes. *Biochemistry.* 20:5056-61.
- Tomasz, M., R. Lipman, D. Chowdary, J. Pawlak, G.L. Verdine, and K. Nakanishi. 1987. Isolation and structure of a covalent cross-link adduct between mitomycin C and DNA. *Science.* 235:1204-8.
- Tschentscher, F., G. Prescher, D.E. Horsman, V.A. White, H. Rieder, G. Anastassiou, H. Schilling, N. Bornfeld, K.U. Bartz-Schmidt, B. Horsthemke, D.R. Lohmann, and M. Zeschnek. 2001. Partial deletions of the long and short arm of chromosome 3 point to two tumor suppressor genes in uveal melanoma. *Cancer Res.* 61:3439-42.

- Tutt, A., D. Bertwistle, J. Valentine, A. Gabriel, S. Swift, G. Ross, C. Griffin, J. Thacker, and A. Ashworth. 2001. Mutation in Brca2 stimulates error-prone homology-directed repair of DNA double-strand breaks occurring between repeated sequences. *Embo J.* 20:4704-16.
- Urtishak, K.A., K.D. Smith, R.A. Chanoux, R.A. Greenberg, F.B. Johnson, and E.J. Brown. 2009. Timeless Maintains Genomic Stability and Suppresses Sister Chromatid Exchange during Unperturbed DNA Replication. *J Biol Chem.* 284:8777-85.
- van der Groep, P., M. Hoelzel, H. Buerger, H. Joenje, J.P. de Winter, and P.J. van Diest. 2008. Loss of expression of FANCD2 protein in sporadic and hereditary breast cancer. *Breast Cancer Res Treat.* 107:41-7.
- van der Velden, P.A., J.A. Metzelaar-Blok, W. Bergman, H. Monique, H. Hurks, R.R. Frants, N.A. Gruis, and M.J. Jager. 2001. Promoter hypermethylation: a common cause of reduced p16(INK4a) expression in uveal melanoma. *Cancer Res.* 61:5303-6.
- van Hoffen, A., J. Venema, R. Meschini, A.A. van Zeeland, and L.H. Mullenders. 1995. Transcription-coupled repair removes both cyclobutane pyrimidine dimers and 6-4 photoproducts with equal efficiency and in a sequential way from transcribed DNA in xeroderma pigmentosum group C fibroblasts. *Embo J.* 14:360-7.
- Virgili, G., G. Gatta, L. Ciccolallo, R. Capocaccia, A. Biggeri, E. Crocetti, J.M. Lutz, and E. Paci. 2008. Survival in patients with uveal melanoma in Europe. *Arch Ophthalmol.* 126:1413-8.
- Walker, J.R., R.A. Corpina, and J. Goldberg. 2001. Structure of the Ku heterodimer bound to DNA and its implications for double-strand break repair. *Nature.* 412:607-14.
- Wang, H., Z.C. Zeng, T.A. Bui, E. Sonoda, M. Takata, S. Takeda, and G. Iliakis. 2001. Efficient rejoining of radiation-induced DNA double-strand breaks in vertebrate cells deficient in genes of the RAD52 epistasis group. *Oncogene.* 20:2212-24.
- Wang, L.C., S. Stone, M.E. Hoatlin, and J. Gautier. 2008. Fanconi anemia proteins stabilize replication forks. *DNA Repair (Amst).* 7:1973-81.
- Wang, M., A. Mahrenholz, and S.H. Lee. 2000. RPA stabilizes the XPA-damaged DNA complex through protein-protein interaction. *Biochemistry.* 39:6433-9.
- Wang, R.Y., K.C. Kuo, C.W. Gehrke, L.H. Huang, and M. Ehrlich. 1982. Heat- and alkali-induced deamination of 5-methylcytosine and cytosine residues in DNA. *Biochim Biophys Acta.* 697:371-7.
- Wang, W. 2008. A major switch for the Fanconi anemia DNA damage-response pathway. *Nat Struct Mol Biol.* 15:1128-30.

- Wang, X., P.R. Andreassen, and A.D. D'Andrea. 2004. Functional interaction of monoubiquitinated FANCD2 and BRCA2/FANCD1 in chromatin. *Mol Cell Biol.* 24:5850-62.
- Wang, X., R.D. Kennedy, K. Ray, P. Stuckert, T. Ellenberger, and A.D. D'Andrea. 2007. Chk1-mediated phosphorylation of FANCE is required for the Fanconi anemia/BRCA pathway. *Mol Cell Biol.* 27:3098-108.
- Ward, I.M., and J. Chen. 2001. Histone H2AX is phosphorylated in an ATR-dependent manner in response to replicational stress. *J Biol Chem.* 276:47759-62.
- Watanabe, K., S. Tateishi, M. Kawasuji, T. Tsurimoto, H. Inoue, and M. Yamaizumi. 2004. Rad18 guides poleta to replication stalling sites through physical interaction and PCNA monoubiquitination. *Embo J.* 23:3886-96.
- Weinberg, R.A. 1995. The retinoblastoma protein and cell cycle control. *Cell.* 81:323-30.
- Weinfeld, M., M.A. Chaudhry, D. D'Amours, J.D. Pelletier, G.G. Poirier, L.F. Povirk, and S.P. Lees-Miller. 1997. Interaction of DNA-dependent protein kinase and poly(ADP-ribose) polymerase with radiation-induced DNA strand breaks. *Radiat Res.* 148:22-8.
- Weterings, E., and D.J. Chen. 2008. The endless tale of non-homologous end-joining. *Cell Res.* 18:114-24.
- Weterings, E., N.S. Verkaik, H.T. Bruggenwirth, J.H. Hoeijmakers, and D.C. van Gent. 2003. The role of DNA dependent protein kinase in synopsis of DNA ends. *Nucleic Acids Res.* 31:7238-46.
- Willers, H., L.A. Kachnic, C.M. Luo, L. Li, M. Purschke, K. Borgmann, K.D. Held, and S.N. Powell. 2008. Biomarkers and mechanisms of FANCD2 function. *J Biomed Biotechnol.* 2008:821529.
- Winer, J., C.K. Jung, I. Shackel, and P.M. Williams. 1999. Development and validation of real-time quantitative reverse transcriptase-polymerase chain reaction for monitoring gene expression in cardiac myocytes in vitro. *Anal Biochem.* 270:41-9.
- Wojcik, A., E. Bruckmann, and G. Obe. 2004. Insights into the mechanisms of sister chromatid exchange formation. *Cytogenet Genome Res.* 104:304-9.
- Wolff, S., J. Bodycote, G.H. Thomas, and J.E. Cleaver. 1975. Sister chromatid exchange in xeroderma pigmentosum cells that are defective in DNA excision repair or post-replication repair. *Genetics.* 81:349-55.
- Woodward, J.K., C.E. Nichols, I.G. Rennie, M.A. Parsons, A.K. Murray, and K. Sisley. 2002. An in vitro assay to assess uveal melanoma invasion across endothelial and basement membrane barriers. *Invest Ophthalmol Vis Sci.* 43:1708-14.

- Wu, L., and I.D. Hickson. 2003. The Bloom's syndrome helicase suppresses crossing over during homologous recombination. *Nature*. 426:870-4.
- Xia, B., Q. Sheng, K. Nakanishi, A. Ohashi, J. Wu, N. Christ, X. Liu, M. Jasin, F.J. Couch, and D.M. Livingston. 2006. Control of BRCA2 cellular and clinical functions by a nuclear partner, PALB2. *Mol Cell*. 22:719-29.
- Yamamoto, K., S. Hirano, M. Ishiai, K. Morishima, H. Kitao, K. Namikoshi, M. Kimura, N. Matsushita, H. Arakawa, J.M. Buerstedde, K. Komatsu, L.H. Thompson, and M. Takata. 2005. Fanconi anemia protein FANCD2 promotes immunoglobulin gene conversion and DNA repair through a mechanism related to homologous recombination. *Mol Cell Biol*. 25:34-43.
- Yamashita, Y.M., T. Okada, T. Matsusaka, E. Sonoda, G.Y. Zhao, K. Araki, S. Tateishi, M. Yamaizumi, and S. Takeda. 2002. RAD18 and RAD54 cooperatively contribute to maintenance of genomic stability in vertebrate cells. *Embo J*. 21:5558-66.
- Yang, H., P.D. Jeffrey, J. Miller, E. Kinnucan, Y. Sun, N.H. Thoma, N. Zheng, P.L. Chen, W.H. Lee, and N.P. Pavletich. 2002. BRCA2 function in DNA binding and recombination from a BRCA2-DSS1-ssDNA structure. *Science*. 297:1837-48.
- Yonetani, Y., H. Hohegger, E. Sonoda, S. Shinya, H. Yoshikawa, S. Takeda, and M. Yamazoe. 2005. Differential and collaborative actions of Rad51 paralog proteins in cellular response to DNA damage. *Nucleic Acids Res*. 33:4544-52.
- Yu, X., and J. Chen. 2004. DNA damage-induced cell cycle checkpoint control requires CtIP, a phosphorylation-dependent binding partner of BRCA1 C-terminal domains. *Mol Cell Biol*. 24:9478-86.
- Yun, M.H., and K. Hiom. 2009. CtIP-BRCA1 modulates the choice of DNA double-strand-break repair pathway throughout the cell cycle. *Nature*. 459:460-3.
- Zander, L., and M. Bemark. 2004. Immortalized mouse cell lines that lack a functional Rev3 gene are hypersensitive to UV irradiation and cisplatin treatment. *DNA Repair (Amst)*. 3:743-52.

Appendix 1

- Clinico-pathological details of the patients with primary uveal melanoma from which primary short-term cultures were obtained (Hoh, 2007, unpublished data).

Case Number	Patient sex ^a	Tumour location ^b	Cell type ^c	Mean tumour diameter (mm)
SOM 494	F	C	M	14.85
SOM 520	F	CB	S	-
SOM 521	F	C	E	18.6
SOM 524	F	CB	M	13.1
SOM 526	F	CB	M	8.3
SOM 537	M	CB/C	S	13.8
SOM 538	M	C	M	-
SOM 543	M	C	M	9.3
SOM 544	M	C	S	10.3
SOM 545	F	C	E	-
SOM 546	F	C	S	14.25
SOM 547	F	C	S	12.67
SOM 548	F	C	M	15.4
SOM 551	M	C	M	15.3

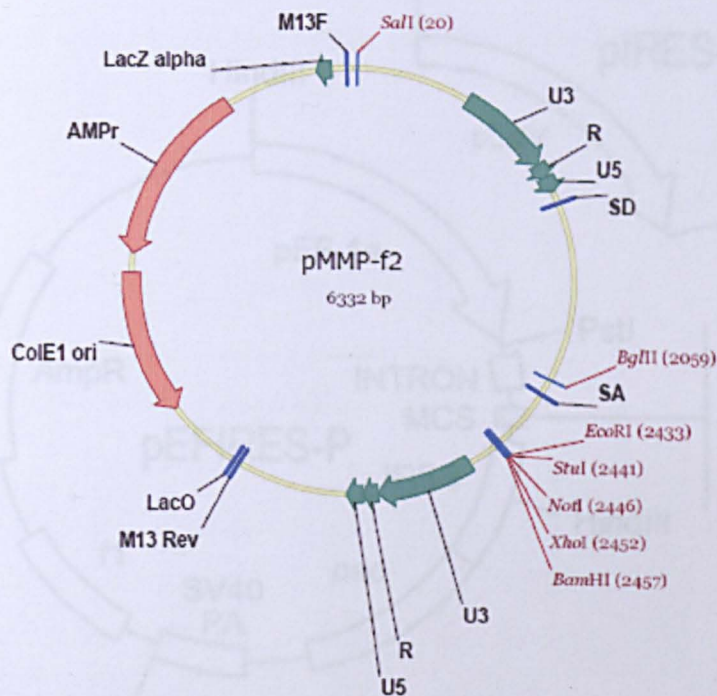
^a Patient sex indicates male (M) or female (F)

^b Tumour type indicates choroid (C) or ciliary body (CB)

^c Cell type indicates spindle (S), epithelioid (E) or mixed (M)

Appendix 2

- ◆ The pMMP-f2-FANCD2 vector with the human FANCD2 cDNA sequence cloned into the multiple cloning site (MCS). A kind gift from Dr. Alan D'Andrea at the Dana-Farber Cancer Institute, in Boston, Massachusetts.
- ◆ The pMMP-f2-empty (pMMP-f2) vector was also a kind gift from Dr. Alan D'Andrea at the Dana-Farber Cancer Institute, in Boston, Massachusetts.



MCS - multiple cloning site, unique restriction sites are indicated

M13 F - M13 forward primer site

M13 Rev - M13 reverse primer site

ColE1 ori - ColE1-type bacterial origin of replication

R - R viral promoter (part of LTR)

U5 - U5 viral promoter (part of LTR)

U3 - U3 viral promoter (part of LTR)

SD - splice donor site

SA - splice acceptor site

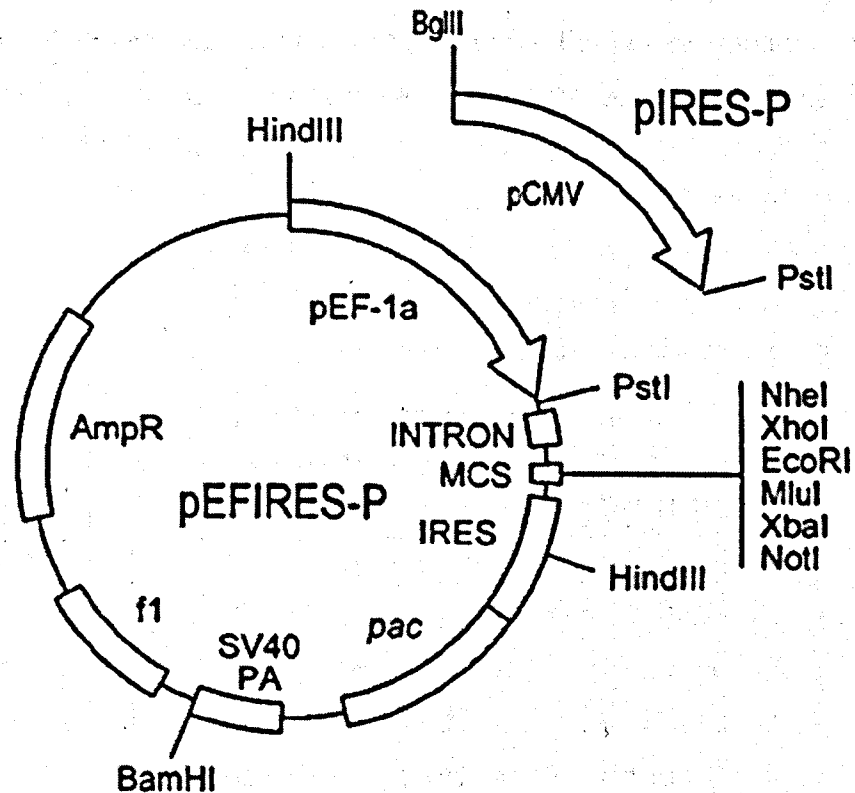
LacZ alpha - LacZ alpha fragment

AmpR - ampicillin resistance gene

LacO - LacO bacterial operon fragment

Appendix 3

- ♦ The pEF-P450R-IRES-P vector with the human CYP450R cDNA sequence cloned into the multiple cloning site (MCS). A kind gift from Dr. Kaye Williams at the School of Pharmacy and Pharmaceutical Sciences, University of Manchester, Manchester.



pEF-1a - human elongation factor 1a promoter

pCMV - cytomegalovirus immediate early enhancer/promoter

INTRON - chimaeric intron

MCS - multiple cloning site, unique restriction sites are indicated

IRES - EMC internal ribosome entry site from pCITE-1

pac - modified *pac* gene encoding puromycin N-acetyl transferase

SV40 PA - SV40 terminator/poly(A) signal

f1 - phage f1 origin

AmpR - bla ampicillin resistance gene

Appendix 4

- Apoptosis levels were no different in the uveal melanoma cell lines compared to the WM793 control as determined by Annexin-V staining. Annexin-V is an anticoagulant that binds to phosphatidylserine, a plasma-membrane phospholipid that gets flipped-out and exposed on the external side of the lipid bilayer during apoptosis. Annexin-V conjugated to FITC allows the identification of this change in the lipid bilayer and thus when co-stained with PI, the percentage of apoptotic cells can be determined using FACS.

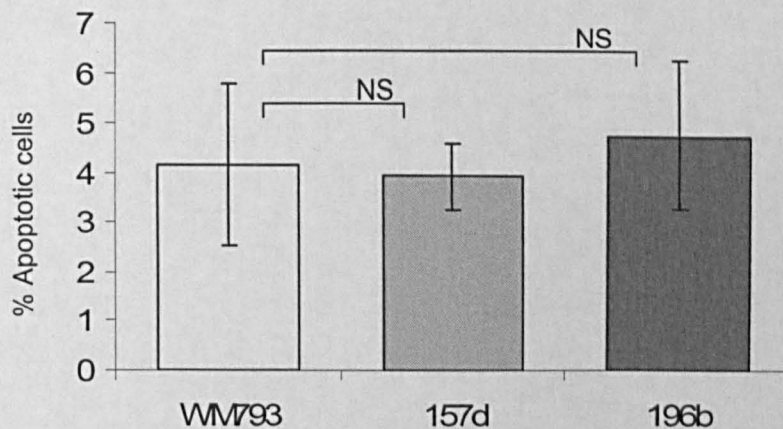


Figure 1 The percentage of apoptotic cells was no different in uveal melanoma cell lines compared to the WM793 cutaneous control.

Annexin-V and PI staining to determine the percentage of apoptotic cells in the uveal melanoma cell lines 157d and 196b compared to the control cell line WM93. Cells were stained with Annexin-V and PI before being analysed using FACS. The percentage of apoptotic cells was calculated as the percentage of cells that were positive for Annexin-V staining but negative for PI (not actively cycling). Data represents the average from at least 3 separate experiments and error bars represent standard deviations. Significance between samples as shown by brackets was calculated using the Student's T-Test where 'NS' represents no significance.